



**Optimization of Polymer Performance for Enhanced Oil Recovery  
(EOR) at Elevated Temperature and High Salinity using Polymers  
Integrated Technique**

**Uranta Kingsley Godwin**

A thesis submitted in partial fulfilment of the requirements of  
the Teesside University for the degree of Doctor of  
Philosophy

September 2019

***To God Almighty***

## ACKNOWLEDGEMENTS

Most importantly, my deepest appreciation goes to God almighty who bestowed upon me divine wisdom throughout this journey.

My special thanks goes to my supervisors: Dr. Sina Rezaei-Gomari, Dr. Paul Russell and Dr. Faik Hamad, through their encouragement, guidance and support this research saw light from the initial to the final level and that enabled me to develop a full understanding of this work. Accordingly, I have extremely benefited from your technical and professional advice and scientific support in positioning this research. I wouldn't forget Dr Reynal Anna the chemist who put me through the NMR analysis and application of topspin software, thanks so much.

I would also like to express my appreciation to the Petroleum Technology Development Fund (PTDF) in Nigeria for funding this project after scholarship pronouncement from Dr. Good luck Jonathan the then President of Federal republic of Nigeria on award after tireless and dedicated NYSC service year.

Thanks a million to my wonderful family: my lovely wife (Mrs Peace Uranta) and son (Cornerstone Uranta) for your prayers, encouragement and support in course of this journey. I do believe that I must have denied you a lot, thanks for your understanding. Thanks to Senibo Godwin Uranta my father and late Mrs Evelyn Ireogbu Uranta my mummy your prophecy before you left have become a reality and to my siblings: Architect Jackson Uranta, Alayim Uranta, Engr. Opuada Uranta, Mrs Gift Innocent Agwu and Miss Tamunomie, Amazing and Jessica Uranta and also to my step mother Mrs Nkechi Uranta. To my extended family and in-laws (Late Mr Dominic Ohalem and Mrs Priscilla Ohalem) thanks so much.

A special mention with sincere gratefulness goes to my pastor at Middlesbrough Pst Paul Oyani and Pst (Mrs) Dolapo Oyani and the entire BCF family and to friends and colleague who have in way or the other made a big change on my life by supporting and encouraging me throughout the studying years.

## ABSTRACT

The most common synthetic polymers used for enhanced oil recovery (EOR) are polyacrylamide (PAM) and partially hydrolysed polyacrylamide (HPAM). Improving the performance of these water-soluble polymers would involve satisfying various specifications, including good solubility in water, good injectivity, and the polymer solution's ability to maintain relatively optimum viscosity under the influence of challenging reservoir conditions such as high temperature, shearing and high water salinity during EOR polymer flooding applications.

The mechanisms of PAM performance and stability under reservoir conditions are not clearly understood. In addition, a satisfactory technique for laboratory to evaluate, optimise and enhance the polymer performance before EOR applications integrated from laboratory is still not available.

In recent times, the oil industry has shown increasing awareness towards maintaining optimum polymer selection and stability under reservoir conditions for the EOR applications through cost effective and better polymer design.

This thesis presents a new synthetic approach called the polymer integrated technique (PIT) which can predict impact of environment and operational conditions on polymer performance and improve stability of PAM from extensive laboratory measurements carried out on formation water and polymers.

In this study, the results of in-depth experimental research into polymer stability at elevated temperature, moderate and high salinity, different shear rates and ageing time and the relationships between them are presented. Correlation analysis was first conducted to determine the safe maximum temperature point (SMTP) for PAM in saline solution. It was found that different saline solutions like NaCl, CaCl<sub>2</sub> and NaHCO<sub>3</sub> possess different SMTPs. The proposed correlations provide a means of predicting the stability of PAM for reservoirs with different temperature, salinity and shear rates conditions. The effectiveness of the application of PAM in hydrocarbon reservoirs at different operational conditions was then investigated.

Polyvinylpyrrolidone (PVP) and 2-acrylamido-2-methylpropanesulphonic acid (AMPS) was incorporated at different stages into the optimized polymer solution to stabilize and improve performance of PAM solutions at high temperature and extremely high

water salinity. The Fourier transform infrared (FTIR) and Nuclear Magnetic Resonance (NMR) were utilised to determine the degree of hydrolysis of the integrated PAM, PVP and AMPS polymer solution. Fann model 35 Couette and a Cole Parmer, were utilized to measure solution viscosity at different shear rates.

A number of results are presented to illustrate how the new PIT can be used to characterize and optimise best fit mixture composition selection, evaluate polymer performance and stability. The PIT is useful as a design and analysis technique for EOR applications in the lab and in the field. Recommendations are also made for further work on this fascinating field of study based on polymer integrated technique developed in this research.

## LIST OF PUBLICATIONS

1. Uranta K.G., Gomari SR., Russell P., Hamad F. Determining Safe Maximum Temperature Point (SMTP) for Polyacrylamide Polymer (PAM) in Saline Solutions. *Journal of Oil, Gas and Petrochemical Sciences* (2018); 1(1):1 – 8p.
2. Uranta K.G., Gomari SR., Russell P., Hamad F. Studying the Effectiveness of Polyacrylamide (PAM) Application in Hydrocarbon Reservoirs at Different Operational Conditions. *Energies* (2018); 11(2201): 1 – 18p.
3. Uranta K.G., Gomari SR., Russell P., Hamad F. Application of Polymer Integration Technique for Enhancing Polyacrylamide (PAM) Performance in High Temperature and High Salinity Reservoirs. *Elsevier Heliyon* 2019. 5(02113): 1 – 14p
4. Uranta K.G., Gomari SR., Russell P., Hamad F. Modification of Polyacrylamide (PAM) at Harsh Reservoir Conditions with Optimised Polymer Integration Techniques (PIT). In proceeding of 81<sup>st</sup> European Association of Geoscientists and Engineers (EAGE) Annual Conference & Exhibition in London UK (2019) 3 – 6 June.

# TABLE OF CONTENTS

ACKNOWLEDGEMENTS .....	iii
ABSTRACT .....	iv
LIST OF PUBLICATIONS .....	vi
TABLE OF CONTENTS .....	vii
LIST OF FIGURES .....	x
NOMENCLATURE .....	xiv
CHAPTER 1: INTRODUCTION .....	1
1.1 Overview .....	1
1.2 Research Aims and Objectives .....	4
1.3 Contribution to Knowledge .....	4
1.4 Format of Thesis .....	6
CHAPTER 2: LITERATURE REVIEW .....	8
2.0 Crude Oil Extraction. ....	8
2.1 Secondary Oil Recovery .....	10
2.1.1 Water flooding .....	10
2.1.2 Water flooding .....	10
2.2 Efficiency Displacement of Oil by Water Flooding .....	11
2.2.1 Fractional flow for reservoir fluids .....	14
2.3 Problems Encountered in Displacement of Oil by Water .....	15
2.3.1 Reservoir Heterogeneity .....	16
2.3.2 Viscous Fingering (Unfavourable mobility ratio) .....	17
2.4 Enhanced Oil Recovery (EOR) Techniques .....	20
2.4.1 Thermal Recovery Technique .....	22
2.4.2 Miscible (Gas or CO <sub>2</sub> ) Injection Technique .....	23
2.4.3 Microbial Recovery Technique .....	24
2.4.4 Chemical Enhanced Oil Recovery (CEOR) Technique .....	26
2.5 Selection of polyacrylamide synthetic polymer .....	35
2.6 Polymer Solution Viscosity .....	35
2.7 Rheology Properties of polymers .....	36
2.7.1 Viscosity dependence on shear rate .....	36
2.7.2 Viscosity dependence on time .....	40
2.7.3 Viscosity dependence on Temperature .....	41
2.7.4 Viscosity dependence on Salinity and Concentration .....	42
2.7.5 Viscosity dependence on molecular weight .....	44
2.8 Polymer Rheology Behaviour in Porous Media .....	44

2.9 Mobility Control with Polymer Solutions .....	46
2.10 Polymer stability.....	47
2.10.1 Chemical degradation .....	48
2.10.2 Mechanical degradation .....	50
2.10.3 Thermal Degradation .....	52
2.11 Resultant Effect of High Temperature and Salinity .....	57
2.11.1 Polymer Syneresis .....	57
2.11.2 Polymer Precipitation .....	58
2.12 Control of Polyacrylamide (PAM) degradation .....	59
CHAPTER 3: MATERIALS AND METHOD .....	60
3.1 Materials .....	60
3.2 Research Methods.....	63
3.3 Safe Maximum Temperature Point (SMTP) Method.....	63
3.3.1 Correlation of temperature on the degree of hydrolysis (DH) of PAM.....	63
3.4 Synthetic Experimental method.....	64
3.4.1 Sample preparation for Rheology (viscosity) testing .....	64
3.4.2 Viscometer Technique .....	65
3.4.3 FTIR AND NMR Techniques.....	69
3.5 Modification of PAM with PVP for High Temperature Reservoirs Application .....	74
3.5.1 PAM AND PVP Mix Sample Preparation .....	74
3.6 Modification optimised PAM: PVP Mix with (AMPS) for High Salinity Reservoir. ....	76
3.6.1 PAM, PVP and AMPS Mix Sample Preparation.....	76
CHAPTER 4: ESTIMATION OF SAFE MAXIMUM TEMPERATURE POINT (SMTP) FOR PAM IN SALINE SOLUTION .....	78
4.1. Correlation of temperature on the degree of hydrolysis (DH) of PAM.....	79
4.2. Correlation of temperature on the viscosity of PAM .....	84
CHAPTER 5: STUDYING THE EFFECTIVENESS OF POLYACRYLAMIDE (PAM) FOR EOR APPLICATION AT DIFFERENT OPERATIONAL CONDITIONS. ....	89
5.1 Hydrolysis of PAM in thermally aged samples. ....	89
5.1.1 FTIR Analysis for PAM Amide group Hydrolysis. ....	90
5.1.2 NMR measurements on time zero samples.....	96
5.2 Effect of temperature and brine on hydrolysis of PAM solution .....	99
5.3 Rheological Behaviour of PAM Solution.....	101
5.3.1 Time–dependent effects on thermal stability of PAM viscosity. ....	101
5.3.2 Percentage change in viscosity of PAM solution. ....	107
5.3.3. Efficiency of PAM performance .....	109
5.3.4 Shear degradation on PAM solution.....	110



CHAPTER 6: INTEGRATION AND OPTIMIZATION OF PAM PERFORMANCE IN HIGH TEMPERATURE RESERVOIRS .....	115
6.1 Hydrolysis of PAM and PVP mix polymer at 90°C aged samples.....	115
6.1.1 FTIR analysis of PAM and PVP mix polymer .....	116
6.1.3 NMR analysis of PAM and PVP mix polymer hydrolysis.....	121
6.2 Stability of PAM and PVP integrated polymer.....	126
6.3 Optimization of PAM and PVP mix solution at High temperature .....	128
6.4 Impact of Salinity on high temperature optimized PAM and PVP integration.....	130
CHAPTER 7: APPLICATION OF PIT TO OPTIMIZE PAM PERFORMANCE AT HIGH TEMPERATURE AND HIGH SALINITY MEDIUM.....	132
7.1 Hydrolysis of the PIT solution.....	132
7.1.1 FTIR Analysis of PIT solution .....	133
7.1.2 NMR Analysis of PIT solution .....	137
7.2 Stability of integrated polymers extreme reservoir conditions .....	140
7.3 Optimized integrated polymer solution at extreme reservoir conditions .....	142
7.4 PIT shear behaviour.....	144
7.5 Stability of PIT.....	146
CHAPTER 8: CONCLUSIONS AND RECOMMENDATIONS .....	148
8.1 Conclusions .....	148
8.2 Recommendations .....	151
References:.....	152
APPENDICES .....	164
Appendix A: NMR Techniques .....	164
Appendix B: Integration and Optimization of PAM Performance in High Temperature Reservoirs.....	164
Appendix B: Application of PIT to Optimize PAM Performance at High Temperature and High Salinity Medium.....	167
Appendix C: Verification of Lab results for Comparative Simulation and Modelling on Polymer Flooding ...	169
8.2 Corey equation for estimating the endpoint modified Relative permeabilities. ....	169
8.3 Equation for estimating the endpoint correlated Relative permeabilities. ....	170

# LIST OF FIGURES

Figure1: Extending polyacrylamide (PAM) in harsh reservoir conditions of temperature of 90°C and salinity up of 200,000 ppm (TDS).....	3
Figure 2.1 Improved and enhanced oil recovery system.....	8
Figure 2.2. Process of water flooding operation for secondary oil recovery.....	11
Figure 2.3 Sketches on macroscopic and microscopic sweep efficiency.....	12
Figure 2.3a Fractional flow curve with its water saturation derivative.....	15
Figure 2.4 Reservoir heterogeneity behavior.....	16
Figure 2.5 Viscous fingering instability during displacement of oil by water.....	19
Figure 2.6 General sketches on enhanced oil recovery.....	21
Figure 2.7 Molecular Structure of Xanthan gum.....	31
Figure 2.8 Chemical structure HPAM.....	33
Figure 2.9 Viscoelastic fluid flow behavior [17].....	37
Figure 2.10a Rheology of a power law of time – independent fluid [98].....	38
Figure 2.10b Rheology of an Ellis model on time independent fluid.....	39
Figure 2.10c Rheology of a Carreau model on time independent fluid.....	40
Figure 2.11 Viscosity dependence on time.....	41
Figure 2.12 Viscosity dependence on polymer concentration at different salinities [100].... <b>Error! Bookmark not defined.</b>	
Figure 2.13 Viscosity versus polymer concentration and versus Molecular weight.....	44
Figure 2.14 Stages of Polymer stability [105].....	48
Figure 2.15 Effect of shear degradation on polyacrylamide with different molecular weight and NaCl Concentration.....	51
Figure 2.16. Various water-soluble polymer gels with maximum safe temperatures [84].....	54
Figure 2.17. Effect of elevated temperature in hydrolyzing PAM.....	55
Figure 2.18. Effect of Ca <sup>2+</sup> or Mg <sup>2+</sup> on hydrolyzed PAM.....	56
Figure 3.0. Partial structure of water soluble polymer polyacrylamide (PAM).....	61
Figure 3.1: Sequential order of this work research methods.....	62
Figure 3.2. Two Rotational Viscometers (a) Cole Parmer [143] and (b) Fann 35A Couette utilised in measuring viscosity [96].....	66
Figure 3.3. Sequence of rheological (Viscosity testing) and Analysis of polymers.....	68
Figure 3.4. Sequence of FTIR and NMR testing and analysis of degree of hydrolysis.....	69
Figure 3.5a. NMR equipment for polymers degree of hydrolysis testing.....	71
Figure 3.6: FTIR equipment for measuring change in absorbance of amide functional group hydrolysis in polymers.....	73
Figure 3.4. The Molecular structure of copolymer of Poly (acrylamide and vinyl Pyrrolidone).....	75
Figure 3.3 The Molecular structure of PAM, PVP and AMPS.....	77

Figure 4 (a). Effect of temperature on hydrolysis of PAM in the presence of 5% NaCl .....	81
Figure 4 (b). Effect of temperature on hydrolysis of PAM in the presence of 9% NaCl -1% CaCl <sub>2</sub> .....	81
Figure 4 (c). Effect of temperature on hydrolysis of PAM in the presence of 3% NaCl -1% NaHCO <sub>3</sub> .....	82
Figure 4.1. Graphically determination of safe maximum temperature point (SMTP) from the gradient $\partial H/\partial t$ (degree of hydrolysis with ageing time) against temperature for PAM solution in the presence of 5% NaCl, 9% NaCl - 1% CaCl <sub>2</sub> , and 3% NaCl-1% NaHCO <sub>3</sub> . .....	83
Figure 4.2. (a) Effect of temperature on viscosity of PAM against ageing time (b) absolute viscosity gradient of 9% NaCl and 1% CaCl <sub>2</sub> 30 rev/min .....	85
Figure 4.3. Effect of temperature on viscosity of PAM against ageing times 9 % NaCl + 1 % CaCl <sub>2</sub> for (a) 60 rev/min and (b) 12 rev/min .....	86
Figure 4.4. The absolute viscosity gradient against temperature in the presence of 9% NaCl and 1% CaCl <sub>2</sub> at 12, 30, and 60 rev/min. ....	87
Figure 5.0: FT-IR Spectra of PAM in pure water (a) and brine (b).....	92
Figure 5.1a: FT-IR Spectra absorbance of PAM at 50°C in pure water. ....	93
Figure 5.1b: FT-IR Spectra absorbance of PAM at 50°C in brine.....	93
Figure 5.2a: Percentage change in absorbance in PAM solution in presence of and without brine at 50°C. ....	94
Figure 5.2b: Percentage change in absorbance in PAM solution in presence of and without brine at 70°C. ....	95
Figure 5.2c: Percentage change in absorbance in PAM solution in presence of and without brine at 90°C.....	95
(b) PAM dissolved in brine.....	97
Figure 5.3: ( <sup>1</sup> H NMR) spectra: (a) PAM dissolved in pure water (b) PAM dissolved in brine.....	97
Figure 5.4a: Degree of hydrolysis of PAM in pure water at temperature of 50, 70 and 90°C.....	100
Figure 5.4b: Degree of hydrolysis of PAM in brine at temperature of 50, 70 and 90°C.....	100
Figure 5.5: Thixotropic behavior of PAM at 50°C at low rotational speeds of (a) 10 rpm and (b) 30 rpm, as well as at a high rotational speed of (c) 600 rpm.....	103
Figure 5.6: Thixotropic behavior of PAM at 70°C at low rotational speeds of (a) 10 rpm and (b) 30 rpm as well as (c) at a high rotational speed of 600 rpm.....	105
Figure 5.7: Thixotropic behavior of PAM at 90°C at low rotational speeds of (a) 10 rpm and (b) 30 rpm as well as at (c) a high rotational speed of 600 rpm.....	106
Figure 5.8: Percentage loss of viscosity of PAM in pure water and in the presence of brine at temperatures of 50, 70 and 90°C at rotational speeds of (a) 10 rpm, and (b) 30 r.p.m.....	108
Figure 5.9: Evaluated viscosity retention of PAM solutions at 50°C (a), 70°C (b), and 90°C (c).....	110
Figure 5.10: shear degradation of PAM presented as viscosity versus shear rate at 50°C: (a) in the absence of brine; and (b) with the presence of brine.....	112
Figure 5.11: shear degradation of PAM presented as viscosity versus shear rate at 70°C: (a) in the absence of brine; and (b) in the presence of brine.....	113
Figure 5.12: shear degradation of PAM presented as viscosity versus shear rate at 90°C: (a) in the absence of brine; and (b) in the presence of brine.....	113

Figure 6.0: FT-IR absorbance spectra (6a) pure PAM, (6b) pure PVP and (6c) PAM and (6c) Comparative PAM and PVP mix samples at time 0 and 30 days after aging at 90°C.....	120
Figure 6.1: Percentage change in amide absorbance of PAM, PVP and integrated polymers at 90 °C and 43,280 ppm TDS.....	121
Figure 6.2a: <sup>1</sup> H NMR spectra for integrated polymers of PAM: PVP at 90°C and TDS 43,280 ppm. ....	122
Figure 6.3: Extent of degree of hydrolysis of PAM: PVP solutions at different PAM: PVP weight ratios with respect to ageing time at 90°C and salinity of 43,280 ppm.....	125
Figure 6.4: Viscosity of PAM and different weight ratios of integrated polymer at 90°C and 43280 ppm TDS for a rotational speed of 10 r.p.m. ....	127
Figure 6.5: Stability of PAM and different weight ratios of integrated polymer at 90°C and 43280 ppm TDS for a rotational speed of 30 r.p.m.....	127
Figure 6.6: Determination of optimum concentration of PVP in integrated polymers of PAM: PVP at 90°C and a salinity of 43,280 ppm for a rotational speed of 10 rpm.....	129
Figure 6.7: Determination of optimum concentration of PVP in integrated polymers of PAM: PVP at 90°C and a salinity of 43,280 ppm for a rotational speed of 30 rpm.....	129
Figure 6.8: Effect of salinity concentration on optimized integration of 20 wt % PAM and 80 wt % PVP .....	130
Figure 7.0: FT-IR absorbance spectra for (7a) PAM, PVP and AMPS (7b) Comparative PAM, PVP and AMPS mix samples at time 0 and 30 days .....	134
Figure 7.1: Percentage change in amide absorbance of PAM and integrated (PAM: PVP polymers at 90 °C and 200,000 ppm TDS.....	136
Figure 7.2a: <sup>1</sup> H NMR spectra for integrated polymers of PAM: PVP (20:80) and different weight ratios of PAM: PVP: AMPS at 90°C and salinity 200,000 ppm. ....	138
Figure 7.3: Extent of degree of hydrolysis of 20:80 PAM: PVP and different weight ratios of PAM: PVP: AMPS at 90°C and 200,000 ppm salinity. ....	140
Figure 7.4: The viscosity of PAM: PVP: AMPS at 90°C in salinity of 200,000 ppm TDS at (a) 10 rpm and (b) 30 rpm and (c) 600 rpm.....	142
Figure 7.5: Optimized weight proportion of PAM: PVP: AMPS at 90°C and 200,000 ppm TDS.....	143
Figure 7.6: PIT Shearing at the salinity of 200000 ppm TDS and 90°C.....	145
Figure 7.7: Shearing and mechanical degradation at different PAM and salinity concentration. ....	146
Figure 6.2b: <sup>1</sup> H NMR spectra for integrated polymers of PAM: PVP at 90°C and TDS 43,280 ppm. ....	167
Figure 7.2b: <sup>1</sup> H NMR spectra for integrated polymers of PAM: PVP (20:80) and different weight ratios of PAM: PVP: AMPS at 90°C and salinity 200,000 ppm. ....	168

## **LIST OF TABLES**

<i>Table 2.1: Guide and characteristics of available for EOR techniques [1]</i> .....	21
<i>Table 3.1: Composition of the Synthetic Saline and Brine</i> .....	65
<i>Table 3.2 Constants for Viscosity calculations</i> .....	67
<i>Table 3.3: The weight composition of PAM:PVP</i> .....	76
<i>Table 3.4 The weight composition of PAM:PVP:AMPS</i> .....	77
<i>Table 5.0: Assignment of the FT – IR Characterization of bands of the PAM</i> .....	90
<i>Table 5.1: Initial degree of hydrolysis (DH<sub>i</sub>) for pure water and brine samples</i> .....	98
<i>Table 6.0: Assignment of FT-IR characterization bands ratio for pure PAM and pure PVP after ageing at 90oC</i> .....	118
<i>Table 6.1: Assignment of FT-IR characterization bands ratio for PAM: PVP</i> .....	118
<i>Table 6.2: Initial degree of hydrolysis (DH<sub>i</sub>) for time zero ageing and brine sample of 43,280 ppm salinity at 90°C</i> .....	124
<i>Table 7.0: FTIR Spectra or peak assignment for weight proportion of PAM: PVP: AMPS</i> .....	135
<i>Table 7.1: Peak assignment for 100 % AMPS at 200,000 ppm salinity</i> .....	135
<i>Table 7.3: Initial degree of hydrolysis (DH<sub>i</sub>) for brine samples of 200,000 ppm at 90°C</i> .....	139

## NOMENCLATURE

PAM	Polyacrylamides
HPAM	Hydrolysed Polyacrylamides
SMTp	Safe Maximum Temperature Point
PVP	Poly Vinyl Pyrrolidone
AMPS	2 Acrylamido -2-methylpropanesulphonic
PIT	Polymer Integration Technique
EOR	Enhanced Oil Recovery
IOR	Improved Oil Recovery
TDS	Total Dissolved Salts
DH <sub>i</sub>	Initial Degree of Hydrolysis
OOIP	Original oil in place
$E$	Overall Oil displacement efficiency
$E_v$	Macroscopic or volumetric displacement efficiency
$E_D$	Microscopic displacement efficiency
$k$	formation permeability
$K_{r_o}$	relative permeability to oil
$K_o$	effective permeability to oil
$f_w$	fractional flow of water
$K_w$	effective permeability to water
$K_{r_w}$	Relative permeability of water
$K_{r_o}$	Relative permeability of oil
$\mu_w$	water viscosity
$V_t$	total fluid velocity,

CO <sub>2</sub>	carbon dioxide
CH <sub>4</sub>	methane
CH	methine
CH <sub>2</sub>	Methylene
CH <sub>3</sub>	methyl
MEOR	microbial enhanced oil recovery
ASP	alkaline – surfactant polymer
COO-	carboxylic group
CONH <sub>2</sub>	amide group
$\tau$	Shear stress
$K$	flow reliability index or constants
$T_{ref}$	Reservoir temperature
R	Resistance factor
NaCl	Sodium Chloride
DH	Degree of hydrolysis
$DH_i$	Initial degree of hydrolysis
NMR	Neutron Magnetic Resonance
<sup>1</sup> H NMR	Proton nuclear magnetic resonance
FTIR	Fourier transform infrared
M	Mobility ratio
$\mu$	viscosity
$\rho_1$	Density





## CHAPTER 1: INTRODUCTION

### 1.1 Overview

In petroleum recovery, 67% of the original oil in place (OOIP) remains in reservoirs after application of conventional primary and secondary recovery processes [1]. This residual oil could be produced by application of chemically enhanced oil recovery (CEOR) technique. Polymer flooding is one of the principal chemical enhanced oil recovery (EOR) techniques currently being deployed to extract the residual oil as to meet the growing global demand for a continuous supply of energy [1 - 4].

Polymer EOR is an augmented water flooding technique introduced in the early 1960's [3]. In a water flooding technique, water is injected into the reservoir through injector wells to push oil towards production wells. The injection water could possess a low viscosity thereby acting as displacing fluid compare to oil with high viscosity. This causes the injection water to finger or channel towards the production well faster than oil, leading to production problems commonly known as viscous fingering and heterogeneity [5 - 9]. Mitigation of these problems is achieved by increasing the viscosity of injection water with high molecular weight water-soluble polymers. This will reduce the mobility ratio of the aqueous phase, enlarge the swept volume and consequently improve oil recovery efficiency.

Two most commonly used water-soluble polymers for mobility control in water floods are synthetic polymer (polyacrylamides (PAM) or hydrolysed PAM) and biopolymers (Xanthan gum) [3]. However, this work focuses on synthetic polymers precisely polyacrylamides (PAM) and HPAM because of their significance industrial impact of low cost, low risk, good solubility in water and strong viscosifying strength

[10 – 11, 18]. Historically, Polyacrylamides (PAM) was the first used polymer as thickening agent for aqueous solution [3]. From the 1970's onwards, researchers such as [12 - 16] identified that limiting conditions of polyacrylamides are due to its sensitivity to degradation.

Degradation of polyacrylamides occurs during dissolution and injection processes through three means; chemical, mechanical and thermal [18]. Chemical degradation occurs through oxidation or effect of ionic ions; accordingly, the amount of oxygen in the solution must be minimized using an oxygen scavenger [17]. Mechanical degradation arises through shearing of the fluid that occurs in the pipes, chokes, valves and pumps [18 - 19].

Thermal degradation depends on the reservoir temperature which results to hydrolysis [13 – 16, 18]. The mechanism of thermal degradation is described as when PAM is aged in moderate or high temperature of (50°C and > 75 °C) the amide group (CONH<sub>2</sub>) in the polyacrylamide structure hydrolyses to form a carboxylate group (COO<sup>-</sup>) [13 – 14, 16]. The presence of negative charges on the backbone of the polymers (carboxylate) could initially increase the viscosity because of charge repulsion but when anionicity increases above a critical level of 25% to 35%, the hydrolysed PAM become too sensitive on latter interaction to salinity (total dissolved solids TDS containing Mg<sup>2+</sup> and Ca<sup>2+</sup>) leading to a large effect on the rheological properties of the polymer solution and loss in solution viscosity [3, 11, 16].

Researchers has discovered that polyacrylamide applications in EOR operations is restricted to reservoir temperatures of about less than 75°C [11, 18], but successfully, PAM has been implemented for EOR applications in several oilfields

at low and moderate temperatures ( $< 50^{\circ}\text{C}$  and  $< 75^{\circ}\text{C}$ ) and salinity levels ( $< 30000$  ppm) [10].

Above  $75^{\circ}\text{C}$  temperature and high salinity ( $> 30,000$  ppm), stability limitations occurs in PAM or HPAM operation during EOR applications. Evidence of such was experienced in Class III reserve of Shengli Oilfield in China, where the temperature exceeds  $85^{\circ}\text{C}$  and the salinity (total dissolved solids (TDS)) is  $> 30,000$  ppm with the total amount of divalent cations being  $> 800$  ppm [11]

Lately, the oil industry has shown increasing cognizance towards maintaining optimum polymer selection and stability under harsh reservoir conditions of higher temperatures ( $>75^{\circ}\text{C}$ ) and higher salinity of  $30,000$  ppm even up to  $200,000$  ppm (TDS) [20 – 21]. It is clear that a research gap exist to address the stability limitations of PAM and HPAM gels used in reservoirs where the temperature is higher than  $75^{\circ}\text{C}$  precisely  $90^{\circ}\text{C}$  and beyond and higher salinity ( $>30,000$  ppm, even up to  $200,000$  ppm (TDS)) as shown in figure 1. Under these harsh reservoir conditions, this work focuses on facing these problems by maintaining optimum polymer mix selection that can stabilise the polymer gel for better design during EOR applications

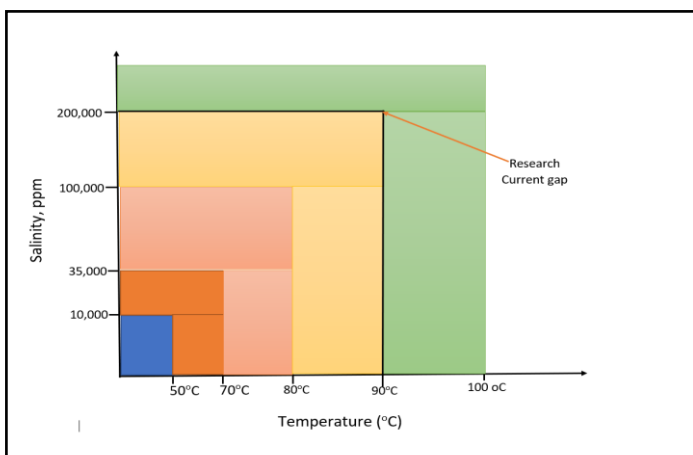


**Figure1:** Extending polyacrylamide (PAM) in harsh reservoir conditions of  $90^{\circ}\text{C}$  temperature and salinity up of  $200,000$  ppm (TDS).

## 1.2 Research Aims and Objectives

The principle aim of this work is to determine the optimum mix of copolymers that can extend the use of PAM/HPAM gels to high temperature ( $> 75\text{ }^{\circ}\text{C}$ ) and high salinity reservoirs ( $>30,000\text{ ppm}$ , even up to  $200,000\text{ ppm}$  (TDS)). It will be achieved by completion of the following objectives:

- Development of a correlation analysis on safe maximum temperature point (SMTP) for polyacrylamide (PAM) polymer in saline solutions.
- Characterisation of standard PAM gels under extreme conditions through:
  - Determination of the effectiveness of a standard polyacrylamide (PAM) application in Hydrocarbon reservoirs at different operational conditions.
- Examination and optimisation of the temperature stability of the polymer gel by addition of Poly Vinyl Pyrrolidone (PVP) to the polymer mix.
- Examination and optimisation of the temperature optimised mixture (PAM: PVP) for use at high salinity reservoir by addition of 2 – acrylamido-2-methylpropanesulphonic acid (AMPS) to the polymer mix.
- Verification of Laboratory results for comparative simulation and modelling on polymer flooding using Eclipse and petrel software.

## 1.3 Contribution to Knowledge

Significant industrial and research effort has been made to identify and develop a new synthetic polymers with improved stability and increases viscosity of injection water. The primary approach is to meet the criteria of inactivity or insensitivity to salt concentration containing divalent cations at high temperature and resistant to hydrolysis. The mechanisms of PAM performance and stability under reservoir conditions are not clearly understood. In addition, a satisfactory technique for

laboratory to evaluate, optimise and enhance the polymer performance before EOR applications integrated from laboratory is still not available. Although, alternative ideas to increase the polymer solution viscosity on harsh reservoir conditions such as high temperature and high salinity reservoirs have been studied over the last years.

This thesis presents a new synthetic approach called the polymer integrated technique (PIT), a chemical modifications which can predict impact of environment and operational conditions on polymer performance and improve stability of PAM from extensive laboratory measurements carried out on formation water and polymers, the essence is developing better polymers and optimizing to fit reservoirs with hostile conditions .

The synthetic approach screened polymers experimentally, a non-extant Polyvinylpyrrolidone (PVP) weight proportion of 80 wt % was found to be the optimum concentration of the composition resulting to overall optimum composition of copolymer PAM: PVP (20:80) wt % with low degree of hydrolysis of 29.9% for use in temperature of 90°C and high salinity of 43,280 ppm polymer flooding applications

In furtherance polymer integration technique (PIT) were extended to high salinity of 200,000 ppm TDS by adding AMPS to the temperature optimized polymer of 20 wt % PAM and 80 wt % PVP mixture. Accordingly, the polymer integration technique (PIT) favoured the specification criterion that is acceptable for polymer flooding application during EOR operation by reducing the initial degree of hydrolysis (DH<sub>i</sub>) to 22.2%. A novel AMPS weight proportion of 10 wt % was found to be the optimum concentration to overall optimum composition of 18:72:10 ter polymers of PAM: PVP: AMPS to enhance the performance of polymer application at temperature of 90°C and salinity of 200000 ppm.

According, this research also provided insights into the chemistry behind PAM degradation which could be helpful in predicting the maximum safe temperature point of polyacrylamide operations in the presence of brine and at any ageing time of interest during chemical IOR/EOR techniques.

#### **1.4 Format of Thesis**

This thesis adopted the following format and are structured into eight chapters:

Chapter 1: Introduction: An overview of polymer flooding during EOR applications and discussion of the challenges/limitations encountered when synthetic water-soluble polymers are applied is given. The identified research gap is presented along with the aim of the study, research objectives and proposed solution method.

Chapter 2: Literature review: crude oil extraction: focusing on secondary recovery precisely water flooding, oil displacement efficiency, fractional flow equation for reservoir fluid, factors affecting displacement efficiency, EOR classification, polymer – augment water flooding selection, rheology properties of PAM; viscosity dependence factors, polymer stability, factor affecting polymer stability, optimization of polymer for effective performance

Chapter 3: Methodology and approach used in studying the effectiveness of polyacrylamide (PAM) application in Hydrocarbon reservoirs at different operational conditions

Chapter 4: Correlation development on Safe Maximum Temperature Point (SMTP) for PAM from published data

Chapter 5: Results and discussion of studying the effectiveness of polyacrylamide (PAM) application in hydrocarbon reservoirs at different operational conditions.

Chapter 6: Modification and optimization of PAM with Polyvinylpyrrolidone (PVP) for use at high temperatures.

Chapter 7: Modification of integrated PAM: PVP performance with AMPS to face challenge of extreme high salinity conditions.

Chapter 8: Conclusions and Recommendation

## CHAPTER 2: LITERATURE REVIEW

### 2.0 Crude Oil Extraction.

Crude oil is recovered from underground porous sandstone or carbonate rock [19]. This recovery process take place in three stages (see figure 2.1): The first stage is primary recovery where natural energy prevailing in the reservoir is utilised to displace the oil from the reservoir through the wellbore and up to the surface production facilities [22 – 23]. This stage can only recover up to 30% of the original oil in place (OOIP) [2, 20 - 21]. Over time the natural pressure of the reservoir will fall leading to a drop in production. The second stage is supplementary or secondary oil recovery where additional energy is introduced into the reservoir e.g. water or gas to maintain its pressure and to displace the oil to the surface, during this stage the oil recovery increases to 50% of OOIP with 10 to 20% incremental recovery over secondary water flooding [24, - 25, 22]. The primary and secondary recovery stages are regarded as conventional recovery techniques.

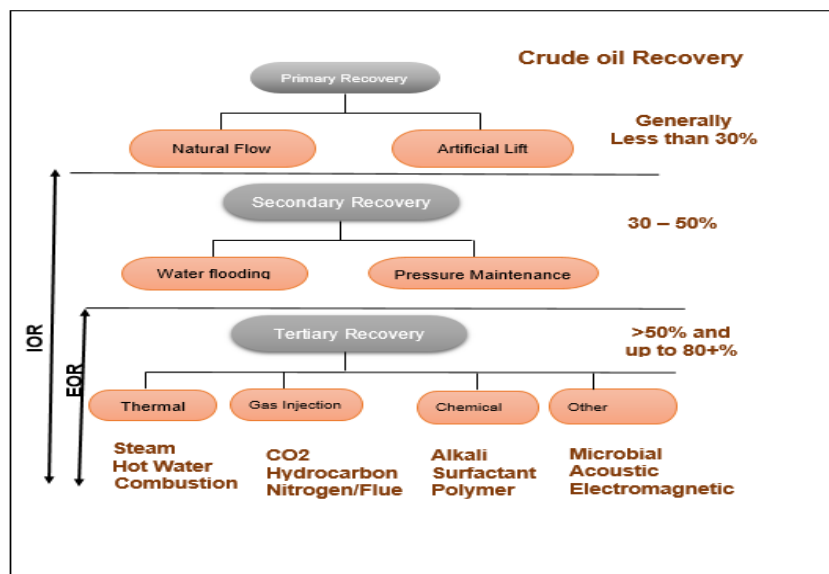


Figure 2.1 Improved and enhanced oil recovery system [2]



After conventional recovery techniques has reach their economical limits or has been exhausted. The next step in oil recovery is the enhanced oil recovery (EOR) also known as tertiary recovery techniques [1, 26]. The enhanced oil recovery (EOR) is when oil is recovered by injection of chemicals or gas and or thermal energy into the reservoir to improved oil recovery [27, 17]. Because the EOR definition focus on improving recovery, the technique could be regarded as a subgroup of the improved oil recovery (IOR). Accordingly, Improved Oil Recovery (IOR) could be defined as any processes which involves the addition of injection fluid to increase the recovery of oil from a hydrocarbon reservoir [28, 2]. This implies that improved oil recovery (IOR) apparently describes the secondary and tertiary recovery with exception to primary (natural) recovery. For instance, IOR processes includes the following: [27, 28]

- Water flooding (for pressure maintenance and oil sweep)
- Immiscible gas flood (dry gas, carbon dioxide, nitrogen, alternating injection with water)
- Miscible flooding with hydrocarbon (carbon dioxide or nitrogen as an injecting fluid solvent)
- Steam flood (including steam assisted gravity)
- In - situ combination – forward: dry, wet, huff and puff steam flood, hot water drive; electromagnetic
- Well simulation (acidizing and fracturing)
- Enhanced waterflood ( Surfactant, polymer and alkaline)

Because the Improved oil recovery (IOR) process is a supplement to primary recovery. However, more emphasis are placed on secondary oil recovery process precisely water flooding before proceeding to enhanced oil recovery (EOR).

## **2.1 Secondary Oil Recovery**

Secondary oil recovery is a process of oil recovery that is carried out through injection of external fluids such as water and or gas, mainly for the purpose of pressure maintenance and volumetric sweep efficiency [22]. There are two types of secondary recovery process – gas flooding and water flooding [5]. The gas flooding process in secondary recovery is when gas is injected into a zone of free gas (i.e. gas cap) to maximize recovery by gravity drainage. The injected gas is usually produced from natural gas within the reservoir in question [5]. In recent times, utilising gas injection is limited because of its low oil displacement effectiveness and often demand of gas for supplies in the global market [29]. Whereas, water flooding is the principal or most applied secondary recovery method. Accordingly, more emphasis are placed on water flooding technique in this research because it form the basic problem statement.

### **2.1.2 Water flooding**

Water flooding is a process used to inject water into an oil – bearing reservoir for pressure maintenance as well as for displacing and producing incremental oil after or sometimes before the economic production limit has been reached [22]. This technique is one of the most common IOR technology applied for recovering oil and has been in existence over 100 years. It became famous and significant in the 1950s when field applications increased production rates rapidly [30]. Traditionally, water flooding has been performed only on light oil reservoirs and even screening criteria indicated that water flooding is most efficient in reservoirs with oil viscosity that is less than 30 mPa.s [31]. The mode of water flooding operation is that water is injected into an oil-bearing reservoir through the injection well, to push and

displace some of the residual non-produced oil to surface production facilities as shown in **figure 2.2**. The amount of oil recovery through displacement of oil by water flooding determine the efficiency of the technique because recovery efficiency is the fraction of the oil in place (OOIP) that can be economically recovered.

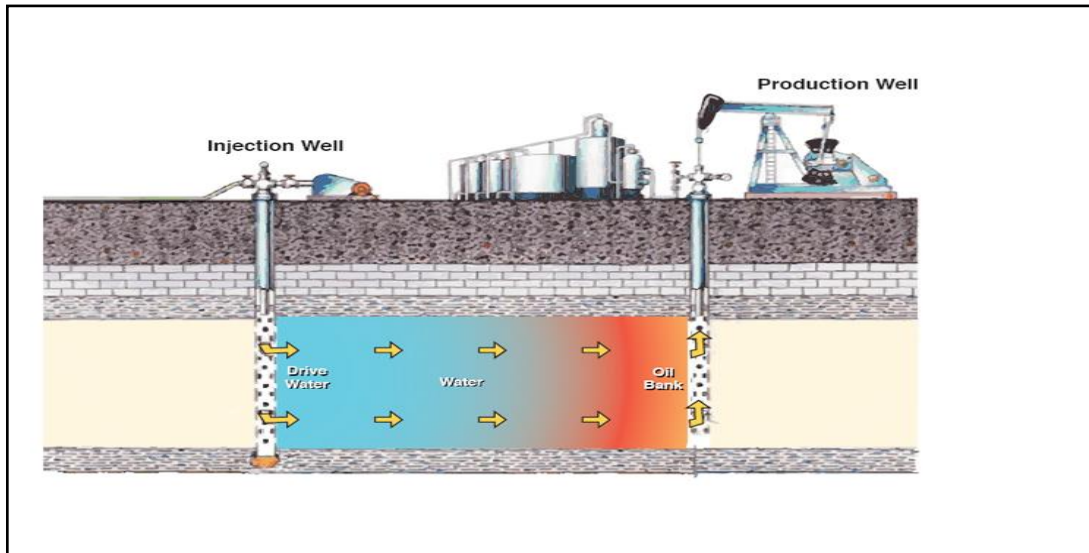


**Figure 2.2.** Process of water flooding operation for secondary oil recovery [32]

## 2.2 Efficiency Displacement of Oil by Water Flooding

In water flooding technique, oil displacement efficiency is termed as the percentage or volume of initial oil in place (OOIP) that injection water could sweeps from a bank of reservoir [33]. The crucial targets is to increase the overall oil displacement efficiency ( $E$ ). This depend on the efficiency of the macroscopic or volumetric displacement efficiency ( $E_v$ ) and the microscopic displacement efficiency ( $E_D$ ) [34, 5]. Macroscopic (volumetric) displacement efficiency is defined as the volume of oil that an injected fluid or displacing fluid are able to sweep or recover when in contact with reservoir. whereas the microscopic displacement efficiency measure effectiveness of the injected fluid or displacing fluids in mobilizing the residual oil trapped at pore scale by capillary forces once the fluid has contact [3, 34, 23]. The microscopic efficiency is affected by: interfacial and surface tension, wettability,

capillary pressure and relative permeability. While macroscopic displacement efficiency is affected by: heterogeneities and the mobility ratio of the displacing fluids (water or brine) compared with the displaced fluids (oil). The overall displacement efficiency in a waterflood or any supplementary processes could be defined as the product of the macroscopic or volumetric displacement efficiency ( $E_v$ ) and the microscopic efficiency ( $E_D$ ) as written in equation 2.1a.

$$E = E_v E_D, \quad 2.1a$$

Where  $E$  is the overall hydrocarbon displacement efficiency, the volume of hydrocarbon displaced divided by the volume of hydrocarbon in place at the start of the process measured at the same conditions of pressure and temperature;  $E_v$  macroscopic (volumetric) displacement efficiency; and  $E_D$  is microscopic hydrocarbon displacement efficiency.

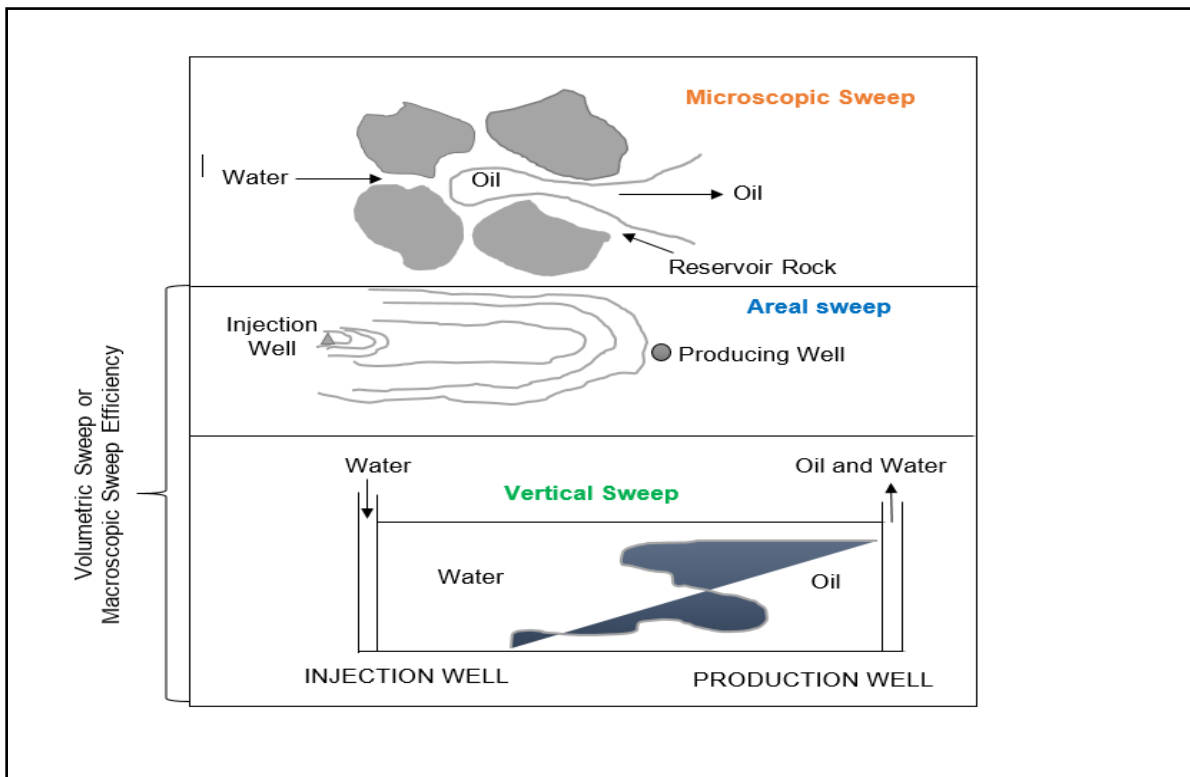


**Figure 2.3** Sketches on macroscopic and microscopic sweep efficiency [35]

In furtherance, the macroscopic or volumetric displacement are sub grouped into two different means: the areal sweep  $E_s$  efficiency and the vertical  $E_i$  sweep efficiency as seen in figure 2.3. The areal sweep efficiency represent the fraction of the reservoir area that the water will contact [3]. It depends primarily upon the relative flow properties of oil and water; accordingly, both the injection and the production well take place at a particular point. This points lead to the development of pressure distributions and corresponding streamlines between the injection and production well [33]. Whereas vertical sweep efficiency is defined as the cross sectional area contacted by the injected fluid divided by the cross sectional area enclosed in all layers behind the injected fluid front [36]. Descriptively, the injected fluid will move as an irregular front; however, in more permeable portions of the reservoir, the injected water will travel rapidly and in the less permeable portions it will move slowly. Accordingly, the volumetric efficiency ( $E_v$ ) measure the three – dimensional effect of reservoir heterogeneities and it could be equivalent to the product of the pattern areal sweep efficiency ( $E_p$ ) and the vertical sweep efficiency ( $E_i$ ) as in equation 2.1b.

$$E_v = E_p \times E_i \quad \mathbf{2.1b}$$

It is more emphasizing that the volumetric sweep efficiency is placed in frontline. Because it explain a detailed approach during which the displacing fluids (water) is injected at one corner in the reservoir and the displaced fluids (oil) are produced at another corner. This mechanisms is based on the relative permeabilities and the fluid viscosities which determine the manner in which oil is displaced by water. More understanding on the displacement efficiencies and the behaviour of fluids within the reservoir can be achieve through a basis concept of fractional flow or frontal advance method by Buckley - Leverett.

### 2.2.1 Fractional flow for reservoir fluids

In 1941 Leverett [37] pioneered a concept on fractional flow equation for water and oil as written in equation 2.1c. The concept monitored the knowledge behind the change in reservoir properties of permeability to oil, permeability to water, water viscosity and oil viscosity even to their respective change in water saturation. Basically, it could connote that the fractional flow of water ( $f_w$ ) for given set of rock, reservoir formation and flooding conditions is a function of water saturation alone.

$$f_w = \frac{1 + \frac{k k_{ro}}{u_t u_o} \left( \frac{\partial P_c}{\partial L} - g \Delta \rho \sin \alpha_d \right)}{1 + \frac{u_w k_o}{u_o k_w}} \quad 2.1c$$

Where  $f_w$  = fraction of the water flowing in the flowing stream passing at any point in the rock (i.e. water cut),  $k$  = formation permeability,  $K_{ro}$  = relative permeability to oil,  $K_o$  = effective permeability to oil,  $K_w$  = effective permeability to water,  $\mu_o$  = oil viscosity,  $\mu_w$  = water viscosity,  $V_t$  = total fluid velocity,  $P_c$  = capillary pressure =  $p_o - p_w$  = pressure in oil phase minus pressure in water phase,  $L$  = distance along direction of movement,  $g$  = acceleration due to gravity,  $\Delta \rho$  = water – oil density differences =  $p_w - p_o$ ,  $\alpha_d$  = angle of the formation dip to the horizontal. For practical usage, the fractional flow under capillary pressure in equation 2.1c is converted to equation 2.2

$$f_w = \frac{1 + 0.001127 \frac{k k_{ro}}{u_t u_o} \frac{A}{q_t} \left( \frac{\partial P_c}{\partial L} - 0.433 \Delta \rho \sin \alpha_d \right)}{1 + \frac{u_w k_o}{u_o k_w}} \quad 2.2$$

And for the horizontal displacement of oil by water, equation 2.2 was simplified into equation 2.3.

$$f_w = \frac{1 - \frac{k k_{rO}}{u_t u_o} (g \Delta \rho \sin \alpha_d)}{1 + \frac{u_w k_o}{u_o k_w}} \quad 2.3$$

$$f_w = \frac{1}{1 + \frac{u_w k_{rO}}{u_o k_{rW}}} \quad 2.4$$

Based on the initial work of [37 - 38] presented what is recognized as the basic equation for describing two - phase, immiscible displacement in a linear system. However, for incompressible displacement, the velocity of a plane shape of constant water saturation travelling through a linear system is given in equation 2.4a and also is the fractional flow plot against the reservoir saturation as seen in figure 2.3a

$$v = \frac{q}{A \phi} \left( \frac{\partial f_w}{\partial S_w} \right) \quad 2.4a$$

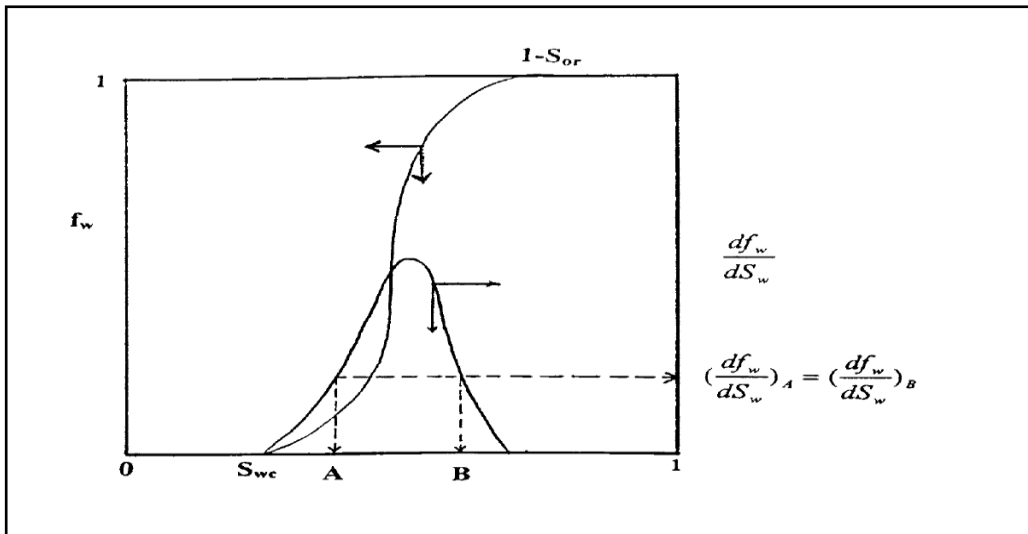


**Figure 2.3a** Fractional flow curve with its water saturation derivative [39]

### 2.3 Problems Encountered in Displacement of Oil by Water

The overall displacement efficiency were discussed in section 2.2. Displacement of oil by water flooding through the macroscopic or volumetric are controlled by some factors that is dependence on the areal or pattern sweep efficiency and vertical or

invasion sweep efficiency. The areal sweep efficiency depend primarily upon two factors: the flooding pattern, reservoir heterogeneity and mobility of the fluids in the reservoir whereas the vertical or invasion sweep efficiency depend upon the heterogeneities (distribution of the permeabilities within the reservoir) and mobility of the fluids [5]. Apparently, the reservoir heterogeneities and fluid mobility control are the challenging factors that contribute to the overall process efficiency.

### 2.3.1 Reservoir Heterogeneity

The amount of oil recovered by water flooding are reduced due to the heterogeneous nature of the reservoir rock. In heterogeneous reservoir, the displacing fluid (water) entering a rock system will preferentially flow faster through high permeability zone than that of the low permeability zone as seen in figure 2.4. This implies that high permeability zone exhibit very low resistance to flow [40]. This channelling through high permeability layers and gravity segregation of the injected water below target oil may lead in oil being bypassed where more injected fluid (water) is produced from the wellbore to the surface facilities [41]

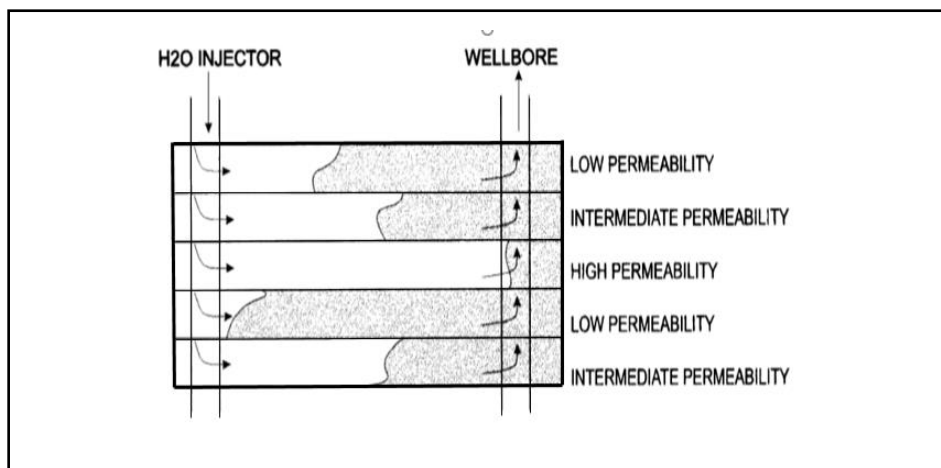


**Figure 2.4** Reservoir heterogeneity behavior [41]

The displacement of a viscous oil by a less viscous solvent is fundamentally unstable, even when the porous medium is homogenous, basically the reservoir



rocks are rarely homogeneous, though variations could occur in permeability and porosity of the reservoir [42]. Reservoir geologic heterogeneities may cause a large volume of mobile oil to be bypassed and remain within a field. This is a result of poor sweep efficiency when injected displacement water moves preferentially through higher permeability zones toward the production well [1].

### 2.3.2 Viscous Fingering (Unfavourable mobility ratio)

In displacement of oil by water, a problem could be encountered due to viscosity difference between both fluids. The mobility challenges arises when a less viscous fluid displace a more viscous fluid inside a porous media and resulting to instabilities. Accordingly, the process were simulated into a model system by Saffman and Taylor in 1958 and it was done in a thin linear channel or Hele – shaw cell [43 - 47]. Moreover, the interface between the less and more viscous fluid develops an instability leading to the formation of finger – like patterns called viscous fingering [48 - 49]. The viscous fingering instability during displacement of oil by water, is shown in **figure 2.5**. According to **Homsy [50]** to understand the basic mechanism of viscous fingering instability. He considered a displacement in a homogeneous porous media, characterized by a constant permeability  $K$ . The flow involve the displacement of a fluid of viscosity  $\mu_1$  and density  $\rho_1$  by a second of viscosity  $\mu_2$  and density  $\rho_2$  and velocity  $U$  under gravity  $g$ . The flow may be taken to satisfy Darcy's law, in a one – dimensional steady flow as written in equation 2.5a

$$\frac{\partial p}{\partial x} = \mu U/K + \rho g \quad \mathbf{2.5a}$$

Because the interface or boundary of the fluid density, viscosity and solute concentration changes rapidly. Accordingly change is driven by the pressure force

$(\rho_2 - \rho_1)$  on the displaced fluid as a result of a virtual displacement  $\partial x$  on the interface and is given in equation 2.5b

$$\partial \rho = (\rho_2 - \rho_1) = [(\mu_1 - \mu_2)U/K + (\rho_2 - \rho_1)g] \partial x \quad \mathbf{2.5b}$$

Assuming the net pressure force is positive, then any little displacement will increase, leading to an instability. Though, we see a combination of unfavourable density and/ or viscosity ratios and flow direction can conspire to render the displacement unstable. For instance, for downward vertical displacement of a dense, viscous fluid by a lighter and less viscous is equal to  $(\mu_1 - \mu_2) > 0, (\rho_2 - \rho_1) < 0$  and  $U > 0$ . However, gravity is a stabilizing force, while viscosity is destabilizing, leading to a critical velocity  $U_c$  above which there is instability as in equation 2.5c

$$U_c = \frac{(\rho_1 - \rho_2)gK}{\mu_1 - \mu_2} \quad \mathbf{2.5c}$$

An easier statement could be made when the gravity force is absent, for instance in a horizontal displacement of oil by water. In this case, instability always results when a bigger viscous fluid is displaced by a lighter viscous one, since the lighter viscous fluid has the bigger mobility. The mobility ratio (M) is defined as the ratio of the mobility of the displacing fluid (water) and the mobility of the displaced fluid (oil) where the mobility of the fluid ( $\lambda$ ) is the ratio of effective fluid permeability (K) to fluid viscosity ( $\mu$ ) [51]. This is shown in equation 25d:

$$M = \frac{\lambda_D}{\lambda_d} = \frac{K_{rw}}{\mu_w} / \frac{K_{ro}}{\mu_o} \quad \mathbf{2.5 d}$$

Where  $\lambda_D$  = mobility of the displacing fluid phase and  $\lambda_d$  = mobility of the displaced fluid phase,  $M$  = mobility ratio and is dimensionless,  $K_{rw}$  relative permeability of water,  $\mu_w$  viscosity of water,  $K_{ro}$  is the relative permeability of oil,  $\mu_o$  viscosity of oil.

Mobility ratio is extremely important parameter in any displacement process. It affects areal and vertical sweep efficiency as discussed in section 2.2. Both areal and vertical sweep efficiency sweep decreases as  $M$  increases for a given volume of fluid injected.  $M$  affects the stability of the displacement process with flow becoming unstable when  $M > 1.0$ . At this point the injected water is much less viscous than the oil it is meant to displace, the water could begin to finger or channel through the reservoir.

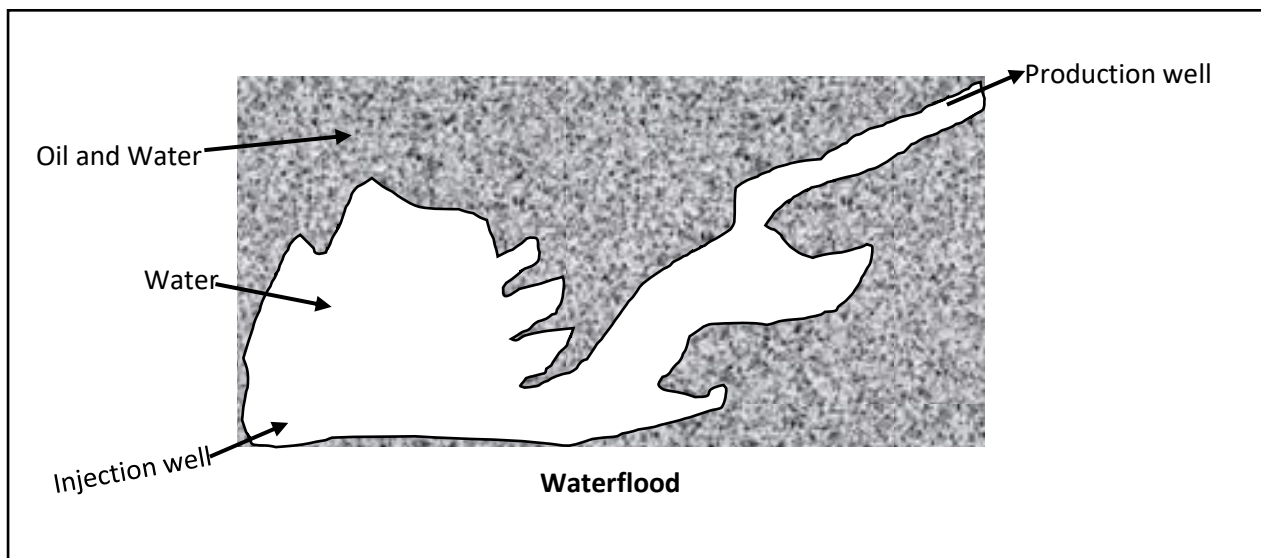


**Figure 2.5** Viscous fingering instability during displacement of oil by water [23]

In a summary, the limitations of water flooding due to instability are incurred from viscous fingering (unfavourable mobility ratio) and reservoir heterogeneity which could lead to significant bypassing of residual oil and lower flooding efficiencies. The solution to this problems is to modify the properties of the water flooding by applying enhanced oil recovery (EOR) technique that could in particular increase

the viscosity of the injection water as to reduce or control the mobility ratio and its behaviour in the reservoir.

## **2.4 Enhanced Oil Recovery (EOR) Techniques**

Enhanced oil recovery (EOR) is the third stage in oil recovery process. The process is used after secondary oil recovery technique (water or gas flooding) becomes uneconomical. The technique involves the injection of fluids such as gas, steam, surfactants, polymers or other chemicals into the reservoir to improve reservoir productivity [52 - 53]. The injected fluids and injection processes supplement the natural energy present in the reservoir to displace oil to a producing well [26, 23, 52]. Detailed explanation of EOR technique is seen in figure 2.6. The EOR process are categorized into four types namely: chemicals, miscible gases, thermal energy and other process such as microbial [23, 5]. Chemical EOR process includes; polymer, micellar polymer, alkaline flooding and microbial flooding. Thermal process include hot water, steam cycling, steam drive and in situ combustion. Whereas the miscible displacement includes carbon dioxide (CO<sub>2</sub>) and gas injection. Thermal process are applicable in reservoirs containing heavy crude oils whereas for chemical and miscible displacement process are suitable for reservoirs containing light crude oils. In **Table 2.1** give a descriptive unique areas of application of various EOR techniques and its characteristic or mechanism during operation.

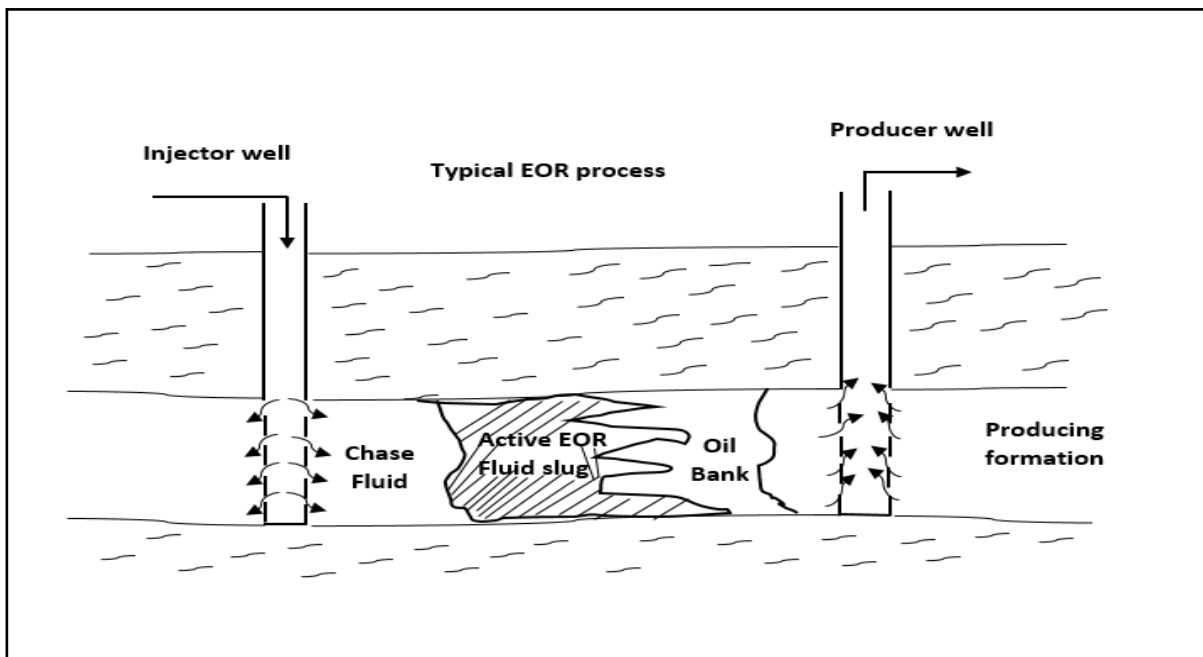


**Figure 2.6** General sketches on enhanced oil recovery [54]

**Table 2.1:** Guide and characteristics of available for EOR techniques [1]

<b>EOR Technique</b>	<b>Working Principle</b>	<b>Outcome/Results</b>	<b>When to Use</b>
Gas Injection	Injecting gas or nitrogen (immiscible)	Push out crude or thins it, reduce rock - oil surface tension	Follow - up to water injection development (WAG - water Alternating Gas injection)
Thermal Injection	Heat is injected to the reservoir to reduce the viscosity of the oil	Oil becomes lighter and flows more easily	Heavy crude fields
Chemical Injection	Different type of chemicals (polymers, surfactants and others)	* Increase flooded water viscosity * Reduce interfacial tension	Follows waterflood to capture residual oil; Sandstone, carbonate and less limestone
CO <sub>2</sub>	Injecting Carbon Dioxide (CO <sub>2</sub> )	CO <sub>2</sub> Swells oil and reduces viscosity	Follows waterflood to capture residual oil (generally used in Limestone reservoir)
Microbial EOR	Inoculated suitable bacteria and Nutrients , are injected	Formation of stable oil - water emulsions, mobilization of residual oil as to reduce interfacial tension.	Follows waterflood to capture residual oil; Sandstone, Carbonate

### 2.4.1 Thermal Recovery Technique

This technique is mostly used for recovery of heavy or viscous oils. Heavy oil is defined as crude oil which has a viscosity ranging from 100 to 10,000 cp and API gravities less than 20 [2]. Conversely, primary and secondary oil production from reservoirs containing heavy, low gravity crude oils is usually a very small fraction of the initial oil in place (OOIP). This is due to the fact that these types of oils are very thick and viscous and as a result, do not migrate easily to the producing wells [5]. In such cases the viscosity ratio can be drastically reduced by increasing the temperature. It could be reasonable to increase the temperature of a crude oil in the reservoir from 100°F to 200°F over the normal reservoir temperature, the oil viscosity will be reduced significantly and will flow much more easily to the wellbore down to the surface production facilities. This is achieved by one of the following methods (a) hot water injection (b) steam injection and in-situ combustion. However, according to Selby et al., [55] thermal recovery methods precisely steam or hot water injection and in-situ combustion are best for recovering moderately viscous or heavy oils provided the reservoir conditions are favourable, basically such conditions are; thin reservoir formation of less than 10 m, and large depth of greater than 1000 m and low formation permeability, low oil saturation and porosity. Under such conditions, non-thermal recovery methods considered are: miscible and immiscible carbon flooding, solvent flooding, improved water floods, polymer flooding, surfactant, caustic and other chemical floods. Accordingly, they are discussed in the next sections.

#### 2.4.2 Miscible (Gas or CO<sub>2</sub>) Injection Technique

Miscible injection technique is a process of mixing of two fluids – for instance, oil and a solvent such as carbon dioxide (CO<sub>2</sub>) into a single phase fluid and it could be a continuity between the oil and injected gas, due to a multiphase transition zone between the two fluids [1]. Basically, the miscible flooding process focuses on mobilizing the light oil components, reduction of oil viscosity, vaporization and swelling of the oil, and the lowering of the interfacial tension [56]. The displacing fluid and residual oil mix form one phase due to the dissolved injected CO<sub>2</sub> that spread on the crude oil phase at the minimum miscibility pressure (MMP) [57]. When the reservoir pressure is above the MMP, miscibility between CO<sub>2</sub> and reservoir oil is achieved through multiple – contact or dynamic miscibility, where intermediate and higher molecular weight hydrocarbon from the oil vaporize into the CO<sub>2</sub> [56]. It is preferable in microscopic displacement efficiency because it play a function of interfacial acting between the rocks and the displacing fluid [58 - 59]. In general, there are two types of miscible process [58 – 59].

The first type is referred to as the single – contact miscible process and involves the injection of fluids such as liquefied petroleum gases (LPG) nitrogen, CO<sub>2</sub>, flue gas (mainly nitrogen and CO<sub>2</sub>) and alcohols [26, 5]. These solvents are miscible with residual oil immediately on contact to overcome capillary forces and increase oil mobility. Conversely, Carbon dioxide is a special case of high pressure miscible recovery is injected into the selected oil reservoir either as continuous gas or as water – alternating gas injection also known as WAG, however, all reservoirs may not be suitable for CO<sub>2</sub> EOR but there are certain criteria that could be encouraging base on proper screening on factors such as reservoir geology, oil gravity, minimum miscibility pressure and viscosity to identify the most likely candidates for miscible

CO<sub>2</sub> [60]. This gas is highly soluble in crude oil, swelling the oil and reducing its viscosity, while simultaneously extracting lighter hydrocarbon by vaporization. The problem associated with miscible gas flood EOR is that a low viscosity fluid is being used to displace a higher one. Under these conditions a Saffman-Taylor instability occurs as discussed in subsection 2.3.2, the interface of the two fluids tend to allows viscous fingers to form and propagate through the displaced fluid, leaving much of the hydrocarbon behind [61]. The primary means of attacking this problem is the water – alternating – gas (WAG) technique. In this process, water flood and gas flood are alternated, with the design parameters being timing and the ratio of water to gas. The second type is the multiple – contact or dynamic miscible process. The injection fluid in this phase are usually methane (CH<sub>4</sub>), inert fluids, or an enriched methane gas supplemented with a C<sub>1</sub> – C<sub>6</sub> fraction. This fraction of alkanes has the unique ability to behave like a liquid or a gas at many reservoir conditions. However, the injected fluid and oil are usually not miscible on first contact but obviously rely on a process of chemical exchange between the two phases for miscibility to occur [5]

#### **2.4.3 Microbial Recovery Technique**

The microbial enhanced oil recovery (MEOR) flooding involves the injection of microorganism that react with reservoir fluids to assist in the production of residual oil [62]. MEOR process is divided into two types. Firstly, is those microorganism that react with reservoir fluids to generate surfactants and the second is those microorganism that react with reservoir fluids to generate polymers. MEOR have same mechanism as obtained from other chemical enhanced oil recovery (CEOR) although it possess an advantage that indicate that microbial metabolites are produced within the reservoir rock formation [63]



For those microorganism that react with reservoir fluids to generate either surfactant or polymers in the reservoir. Once either the surfactant or polymer has been produced, mobilizing and recovery of the residual oil becomes similar to those of the chemical flooding [5]. For instance a microorganism could be injected along with a nutrient usually molasses. This nutrients and suitable bacteria grows under anaerobic reservoir conditions and are injected into the reservoir. The microbes feed on the oil and microbial metabolic products that include bio surfactants, biopolymers, acids, solvents, gases and enzymes, modify the properties of the oil to form polymers [64]. The injected solution will enter high permeability zones and react to form the polymers that will then act as a permeability reducing agent. Equally, the solution microorganisms can react with the residual crude oil to form surfactant. The surfactant is to reduce the interfacial tension of the brine – water system, which thereby mobilizes the residual oil.

The resultant reaction of the microorganism with the reservoir fluids may also produces gases, such as CO<sub>2</sub>, N<sub>2</sub> H<sub>2</sub> and CH<sub>4</sub> [5]. The production of these gases will result in an increase in reservoir pressure, which will thereby enhance the reservoir energy. In MEOR heterogeneous issues may occur, it is advisable to generate polymer in situ, which could be used to divert fluid flow from high to low permeability channels and carefulness should be taken to avoid reservoir brine inhibiting the growth of the microorganisms. According to Craft and Hawkins [5] MEOR project has been applied in reservoir brines up to less than 100,000 ppm, rock permeabilities greater than 75 md and depth less than 6800ft and temperature of 75°C on light crude of API gravities between 30 and 40.

#### **2.4.4 Chemical Enhanced Oil Recovery (CEOR) Technique**

Chemical recovery processes entails the addition of one or more chemical substance as an augmented injected fluid either to reduce the interfacial tension between the reservoir oil or to improve the sweep efficiency of the injected fluid through increasing the viscosity and improving the mobility ratio. Accordingly, chemical recovery technique comprises of four types; Alkaline flooding, surfactant flooding, polymer flooding and alkaline – surfactant polymer (ASP) flooding [65]. Firstly, is the polymer flooding where high molecular weight molecules is used to increase the displacing fluid (water) viscosity. The process bring leads to improved sweep efficiency of the reservoir. The next two methods are micellar (Surfactant) polymer flooding and alkaline flooding. This two methods make use of chemicals that reduce the interfacial tension between oil and a displacing fluid. More recently Nano fluids or liquid suspensions of nanoparticles dispersed in distilled water or brine have recently been investigated and considered as Chemical EOR [66].

##### **2.4.4.1 Micellar (surfactant) flooding for chemical EOR**

This polymer flooding uses a surfactant as augmented injection fluid to lower the interfacial tension between the injection fluids (water) and the reservoir oil. A surfactant is a product of soap and detergent, which is liken to surface – active agent that contains a hydrophobic (dislikes water) as part of the molecule composition and a hydrophilic (water like) [65]. The surfactant migrates to the interface between the oil and water phases and could help make the two phase more miscible. As the interfacial tension between an oil phase and a water phase is reduced, the capacity of the aqueous phase to displace the trapped oil phase from the pores of the rock matrix increases [65]. The reduction of the interfacial tensions results in a shifting of the relative permeability curves so that the oil will

flow more readily at lower oil saturations. The micellar solution exist when surfactants is above a critical saturation in water – oil system. Accordingly, micellar (surfactant) polymer process are made up of two types namely; low concentration surfactant solution (less than 2.5 wt%) but large injected volume (50% Pore volume) and high concentration surfactant solution (5 to 12 wt%) and a small injected volume (5% to 15% pore volume), however both process has potential of achieving low interfacial tensions with a wide variety of brine crude oil systems [5].

#### **2.4.4.2 Alkaline flooding for chemical EOR**

Alkaline flooding is a process that relies on a chemical reaction between the caustic and organic acids in the crude oil to produce in – situ surfactants that lower interfacial tension between water and oil [66]. The alkaline solution is injected into a reservoir, it reacts with the acid component of the crude oil and a surfactant commonly known as soap and it is generated from the in situ. The alkaline solution includes sodium hydroxide (NaOH), sodium orthosilicate, sodium metasilicate, sodium carbonate, ammonia and ammonium hydroxide and the mechanism is that they are mixed with certain crude oils to form a surfactant [67]. When the formation of the surfactant molecules occurs in situ, the interfacial tension between the brine and oil phases could be reduced [68, 69]. A lot of alkaline process mechanism has been identified as aid in oil recovery. They includes: lowering of interfacial tension, emulsification of oil and wettability changes the rock formation [68]. The emulsification mechanism has been suggested to work by either of two methods [66]. The first is by forming an emulsion which becomes mobile and later trapped in downstream pores. The emulsion could blocks the pores, which thereby diverts flow and increases the sweep efficiency. The second mechanism also form

emulsion, which becomes mobile and carries oil droplets that could be transported to downstream production facilities.

#### **2.4.4.3 Nano particles (fluid) enhanced oil recovery**

The nanoparticle are found as smart fluids containing Nano additives, and the systems occur in the form of suspensions or emulsions known as nanofluids, nano-catalyst suspension or micro emulsions [70 - 72, 52]. Accordingly, nanofluids flooding or nano flooding is a new chemical EOR technique whereby nanomaterial or nanocomposite fluids are injected into oil reservoirs to effect oil displacement or improve injectivity [72 – 73]. These fluids particles are considered appropriate for EOR due to their strong particle surface interaction with solvents, its helps to overcome density difference that enable materials to float or drop down in a system. These materials are classified into three: (a) materials with lumps three-dimensional separated by distances in the order of nanometers (b) porous materials with particle sizes in the nanometer range or nanometer sized metallic clusters dispersed within a porous matrix (c) polycrystalline materials with nanometer sized crystallites [70]. The nano- emulsions are emulsion that exhibit unique characteristics such as great stability in comparison to micro – emulations. Accordingly, **Poettman [74]**, claimed that emulsion shows a promising solution to recover a large fraction of residual oil left in the reservoir after water flooding and polymer. The efficiency of oil/water emulsion flooding can be successfully enhanced unless the stability of injected emulsion gets affected by the *in situ* reservoir conditions. The reservoir temperature and pressure can destabilize oil/water emulsion by increasing droplet size due to temperature and flocculation due to pressure resulting in unsuccessful penetration of the emulsion droplets into the oil reservoirs [52]

#### **2.4.4.4 Polymer flooding for chemical EOR**

Half of the global oil production is improved using water flooding [75]. But the technique causes poor effectiveness due to mobility control of the injection water. The process or technique is augmented by adding polymer to the injection water. Polymer flooding is a process of adding high molecular weight molecules water soluble polymer to injection water as to increase its viscosity for effective EOR operation. Increasing the viscosity of the injection water reduces the mobility ratio of the system as to overcome the problems associated with viscous fingering and reservoir heterogeneity described in section 2.4.2. Specifically polymer – augmented water flooding is used in two situations:

(a) When the mobility ratio of a waterflood is unfavourable ( $M > 1$ ) causing viscous fingering, continuous injection of polymer solution is used to increase the microscopic displacement efficiency at a particular oil/water ratio and increases the macroscopic or volumetric efficiency in the reservoir

(b) Even when the mobility ratio is favourable ( $M, < 1$ ), reservoir heterogeneity precisely where the reservoir is stratified in the vertical direction causing poor volumetric sweep efficiencies. In this case, polymer augmented water flooding maybe used to reduce the water mobility in the high permeability layers, so that oil can be displaced from the lower – permeability layers [23].

Two types of polymer are used in enhancing oil recovery: natural biopolymers for example xanthan gum and synthetic polymers for example polyacrylamide (PAM) [25]

#### 2.4.4.4.1 Xanthan gum biopolymer

Biopolymers are polysaccharide based and produced commercially by microbial action of the organism *Xanthomonas campestris* on a carbohydrate feed stock [23]. The polymers act like a semi rigid rods to resist mechanical or shear degradation. Xanthan gum is the most commonly used biopolymer for EOR operation [76, 23]. The molecular structure of xanthan gum is given in figure 2.7. The molecular weights of xanthan gum range from 1 million to 15 million, depending on the method used to determine the molecular weight. Xanthan gum are susceptible to oxidative attack by dissolved oxygen in the injected water. The degradation is detected by the loss of solution viscosity with time. At low temperature, the reaction rate is slow and can go undetected in short tests. The degradation rate increases as temperature increases. Xanthan gum are prone to biological attack resulting in the loss of solution viscosity from the destruction of carbohydrate backbone. The advantages and disadvantages are given below:

The main advantages of Xanthan gum [77 – 78]:

The molecular structure gives a degree of rigidity or stiffness and it provides an excellent resistance to mechanical shear degradation

- High viscosity yield and resistance to salt water.
- High shear stability and resistance, when pumped at high flow rate it results in a slight increase in the well head pressure.

Disadvantages of Xanthan [77 – 78]:

- High cost, more expensive than synthetic polymers.
- Degradation by enzyme usually results in a decrease in the solution's viscosity

- Bacteria sensitivity (care must be taken to prevent bacteria attack)
- Degradation due to dissolved oxygen in reservoir
- Difficulty in preparation to achieve uniform solution [79]
- Greater potential wellbore plugging

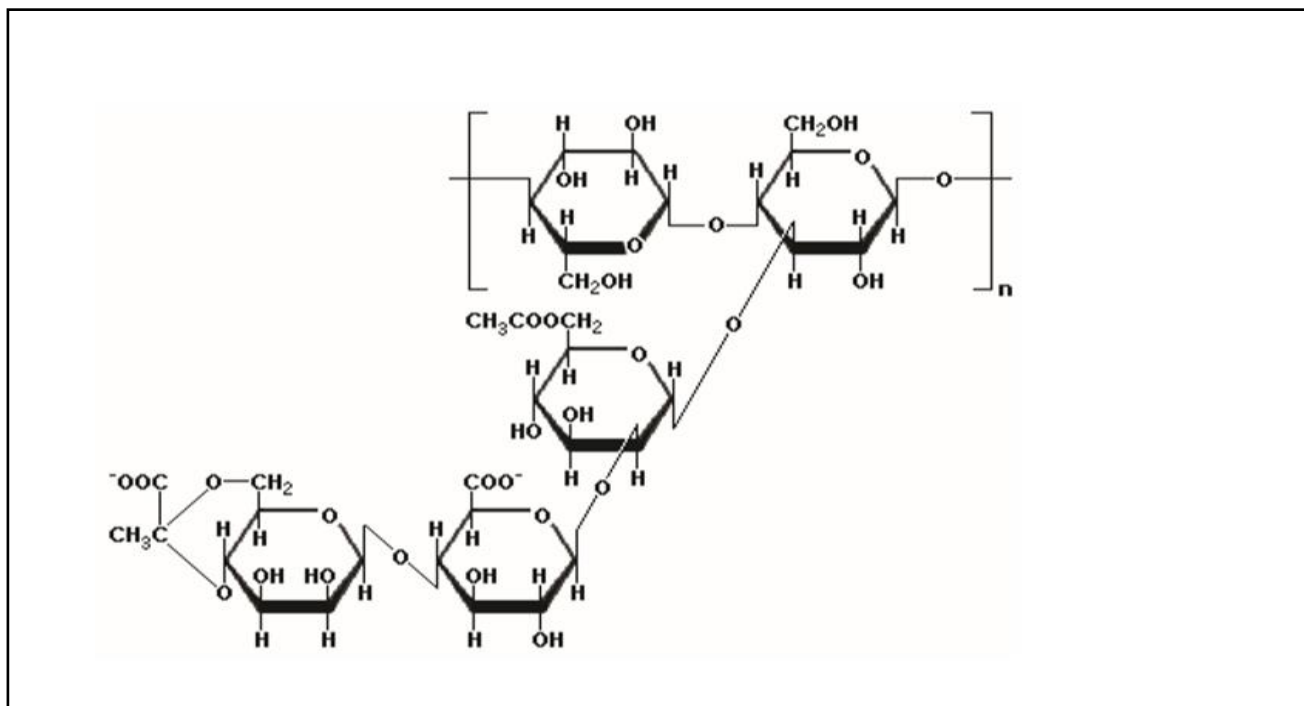


**Figure 2.7** Molecular Structure of Xanthan gum [19]

#### 2.4.4.4.2 Polyacrylamide synthetic polymers

In polymer flooding application, a high molecular weight synthetic polymer, polyacrylamide (PAM) or its derivative is added to thicken the viscosity of displacing fluid (water) so as to reduce the mobility of the aqueous phase, enlarge the swept volume and consequently improve oil recovery. Polyacrylamides are water soluble polymers obtained from synthetic linear co – polymers of acrylic acid and acrylamide (non-ionic) monomers used in polymer EOR [3, 79]. However, it undergo partial hydrolysis which introduces negatively charged carboxylic group (COO<sup>-</sup>) on the backbones of polymer chain. **Figure 2.6** is the structural representation of hydrolysed polyacrylamide (PAM). The basic mechanism during

the hydrolysis process is that some of the amide group (CONH<sub>2</sub>) would be replaced by negative charge carboxylate groups (COO<sup>-</sup>). The negative charges on the backbones of polymer chains have a large effects on the rheological properties [79 – 81]. The advantages and disadvantages are given below:

The main advantages of polyacrylamides

- High yield in normal water or fresh water because of its high molecular weight and could reduce viscous fingering
- Less cost compare to biopolymers
- More widely applied in the field operation than biopolymer as water mobility control agents
- Provides high injectivity
- Resistance to bacteria attack

Polyacrylamides have the following disadvantages:

- The hydrolysed polyacrylamide (HPAM) solution are sensitive to salts could dramatically reduce the viscosity of the properties
- The hydrolysed polyacrylamide (HPAM) solution is susceptible to the presence of oxygen, which is a source of instability and chemical degradation.
- The high temperature (> 70°C) causes the thermal degradation
- The hydrolysed PAM are sensitive to oxygen. However oxygen scavenger are need.
- Polyacrylamide are sensitive to shear which degrade the polymer into smaller into smaller molecules.



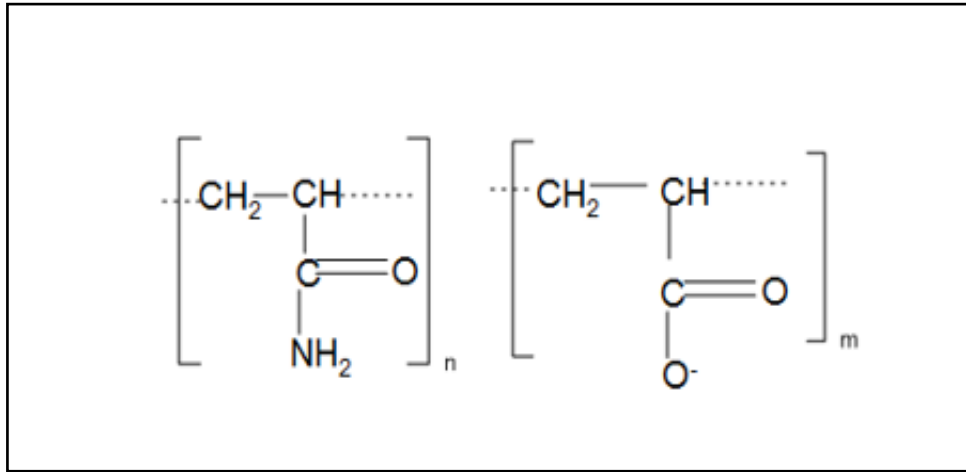


**Figure 2.8** Chemical structure HPAM [84]

### **Hydrolysed Polyacrylamide (HPAM)**

Hydrolysed polyacrylamide (PAM), is the most widely used polymer in EOR operations, shows strong viscosifying power in fresh water and at relatively low temperature (<75 °C) because of its extremely high molecular weight and synthetic linear copolymer of acrylic acid and acrylamide (non-ionic) monomers, with negative charges in the carboxylate groups [11]. HPAM molecules have long flexible chain structures and generally are long-winded coils in water solution and elastic deformation occurs in shear flow field [82]. Some amide groups (CONH<sub>2</sub>) would be replaced by carboxylate groups (COO<sup>-</sup>) during the hydrolysis process and thus, have strong interactions with cations. The degree of hydrolysis is the mole fraction of amide groups converted to carboxylate groups. Typical fresh injection water, the higher hydrolysed polyacrylamides of 15 - 35% produce the most viscous solutions [79]. The higher the present hydrolysis, the more polyacrylamides are affected by brines containing divalent ions and at 35% hydrolysis level may begin precipitate. In high brines containing divalent ion, a 15% or lower percentage hydrolysed polyacrylamide can produce greater solution viscosity [85]. Hydrolysis is faster at higher than moderate temperatures. PAM and HPAM polymer does not tolerant high temperature [83, 86]. Because hydrolysis is a function of viscosity,

hydrolysis of the PAM or (HPAM) polymer is regarded as necessary parameter which could be examined in polymer fluid rheology testing.

### **Other PAM Derived Polymers**

Other PAM derived polymer are synthetic water soluble polymers made from byproduct of acrylamide through integration process. Other PAM derived polymers used in EOR process include hydrophobically associating polymer, salinity – tolerant PAM (KYPAM) [87, 76] and 2 – Acrylamido -2 – methylpropanesulfonate (AMPS). It could be worth emphasizing that integration of other PAM derived polymers could presumed close connection between polymer stability under harsh reservoir conditions and polymer solution stability. This is because the stability limitation of PAM at high temperature in brines are consequence of hydrolysis of the amide functional groups, the primary approach followed has been that of substituting part of the acrylamide co-monomers with co-monomers meeting the criteria of inactivity toward divalent cations, resistance to hydrolysis [16]. Their advantages and disadvantages are given below:

The main advantages of other PAM derived polymers

- AMPS as part of the other PAM derived polymer contains sulfonated moieties that give it unique ability to tolerate high – salinity brines especially those containing divalent cations such as calcium ( $\text{Ca}^{2+}$ ) and magnesium ( $\text{Mg}^{2+}$ ) [4]
- High resistance to shear and excellent Injectivity

Disadvantages of other PAM derived polymers

- They are sensitivity to the presence of oxygen and could advisable to mitigate with oxygen scavenger.

## 2.5 Selection of polyacrylamide synthetic polymer

There are various criteria for candidate selection of PAM as water soluble polymer for reservoir flooding.

- Polyacrylamide and its derivative (HPAM) are advantageous for increasing or thickening the viscosity of injections water during water flooding.
- Polyacrylamide and its derivative (HPAM) are suitable at high mobility ratio ( $M > 1$ ) where viscous fingering occurs leading to poor sweep efficiencies
- Polyacrylamide and its derivative (HPAM) are suitable in heterogeneous reservoir, where the displacing fluid (water) entering a rock system will easily flow faster through high permeability zone than that of the low permeability zone
- Polyacrylamide and its derivative (HPAM) are cheap in price and have good solubility compared to Xanthan gum (biopolymer) [ 76, 17- 18, 25, 76, 88]

## 2.6 Polymer Solution Viscosity

The polymer solution viscosity is a key parameter to improve the mobility ratio between oil and water [11]. The polymer viscosity augment the water flooding to modify viscous instability [17, 76]. Amongst the water soluble polymer, polyacrylamide (PAM) happened to be the first polymer used as thickening agent for aqueous solutions [20]. The thickening ability of PAM dwell mainly in its high molecular weight [11, 83]. PAM is applied as the reference and preferred model polymer for EOR applications [20]. From partial hydrolysis of PAM, the HPAM could be obtained. The viscosity of polymer materials such as PAM and HPAM can be significantly affected by variables like shear rate, temperature, concentration, salinity and time of shearing and it is clearly important for us to highlight the way viscosity depends on such variables. To facilitate this, is to consider the shear rate,

from the rheological properties point of view, which is the most important influence on viscosity.

## **2.7 Rheology Properties of polymers**

Rheology is the study of fluid flow and deformation of materials as accepted when the American society of Rheology was founded in 1929 [89 – 90]. Studying fluid behaviour is to measure the internal friction of the fluid viscosity [91]. The fluid could be apparent when the layer of the fluid is made to move in the relation to another layer. The larger the friction, the larger the amount of force required to cause movement which is termed as shear. The shearing occurs whenever the fluid is physically moved or distributed, even as in pouring and mixing. Highly viscous fluids like high molecular weight water soluble polymers such as Polyacrylamides (PAM) fluids produce increase in viscosity and decrease in permeability. The viscosity could decrease as the shear rate increase such behave is known as non - Newtonian fluids. Accordingly, viscosity could be dependence on various properties such as (a) shear rate (b) time (c) temperature (d) salinity and polymer concentration (e) molecular weight.

### **2.7.1 Viscosity dependence on shear rate**

Shear rate dependence is one of the most important and defining characteristics of non – Newtonian fluids. Because Polyacrylamides (PAM) behave as non - Newtonian fluids and are pseudo plastic in viscosity behaviour [9]. Its means that the viscosity are strongly depends on the shear rate and other properties as previously mentioned in section 2.11. The evidence is seen in figure 2.7 on the log plot viscosity against shear rate. The polymer solution behaves like a pseudo plastic or shear thinning fluid leading to decrease in viscosity as shear rate increases. Dilatant fluid behaviour indicate that viscosity of fluids increases as the shear rate

increases. From the figure dilatant behaviour point of increase started at the second critical point by breaking the shear rate bond as to elongate the viscosity flow.

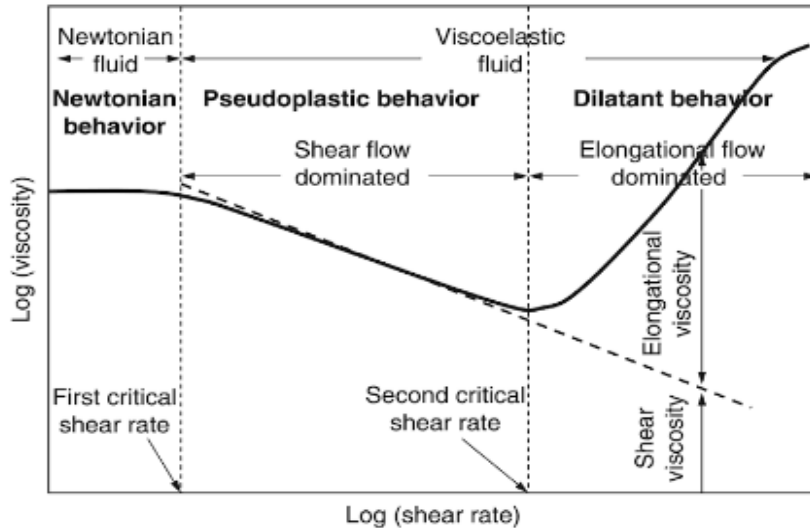


**Figure 2.9** Viscoelastic fluid flow behavior [17]

Newtonian fluid is a fluid which create a linearly proportionality between stress and viscosity in its corresponding shear rate. The viscosity is maintained stationary or constant before reaching the first critical shear rate. Between the first critical shear rate and the second critical shear rate is the non – Newtonian fluids, the shear rate varied and the shear stress don't vary in the same proportion however, considering that the shear rate varied, the viscosity of such fluids change. The change in viscosity is based on application of the shear stress against shear rate. Viscosity could be defined in equation 2.6. It connote that the change in viscosity is due to stress applied on the solution per unit shear rate. The stress causes molecules to align themselves with the shear field as to reduce internal friction.

$$\mu = \frac{\tau}{\dot{\gamma}}$$

**2.6**

Where  $\mu$  is the solution viscosity,  $\tau$  is the shear stress ( $\text{N/m}^2$ ),  $\gamma$  is the shear rate ( $\text{s}^{-1}$ ). Subsequently, time - independent fluids are function of shear rate, reduction in polymer solution viscosity possibly represent the rheological properties of a shear thinning fluid are classified into four fluids models of time – independent group: the power – law , Ellis, Carreau and Hershel – Bulkley [91 - 93, 97].

The power law is given in equation 2.7

$$\mu = k \gamma^{(n-1)} \quad \mathbf{2.7a}$$

Where  $\mu$  is the viscosity,  $K$  is the flow reliability index or constants that characterize the fluid,  $n$  is the flow behaviour index or power law exponent and  $\gamma$  is the shear rate. In the pseudo plastic region,  $n > 1$  is used to model shear thinning though it can also be used for modelling shear thickening as in figure 2.10a [97]. From the figure disadvantage exist in the power law model which is the absence of plateaux at low and even high shear rate. At different shear rate,  $n$  has little changes, but for a Newtonian fluid  $n = 1$  and  $K$  is simply the constant viscosity  $\mu$  [11].

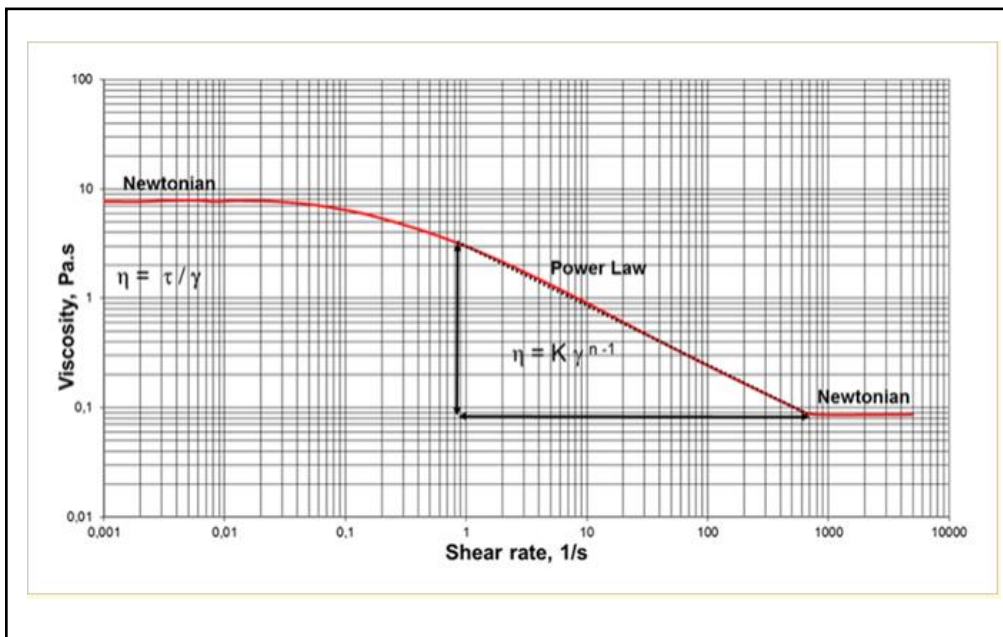


**Figure 2.10a** Rheology of a power law of time – independent fluid [98]

The absence of plateaux at low and even high shear rate of power law model brought about the Ellis model. The model became a substitute for the power law model and is appreciably better in matching experimental measurement [97, 99]. Ellis model is distinct from power law model by having Newtonian plateau at low shear rate without plateau at high shear rate as seen in figure 2.10b

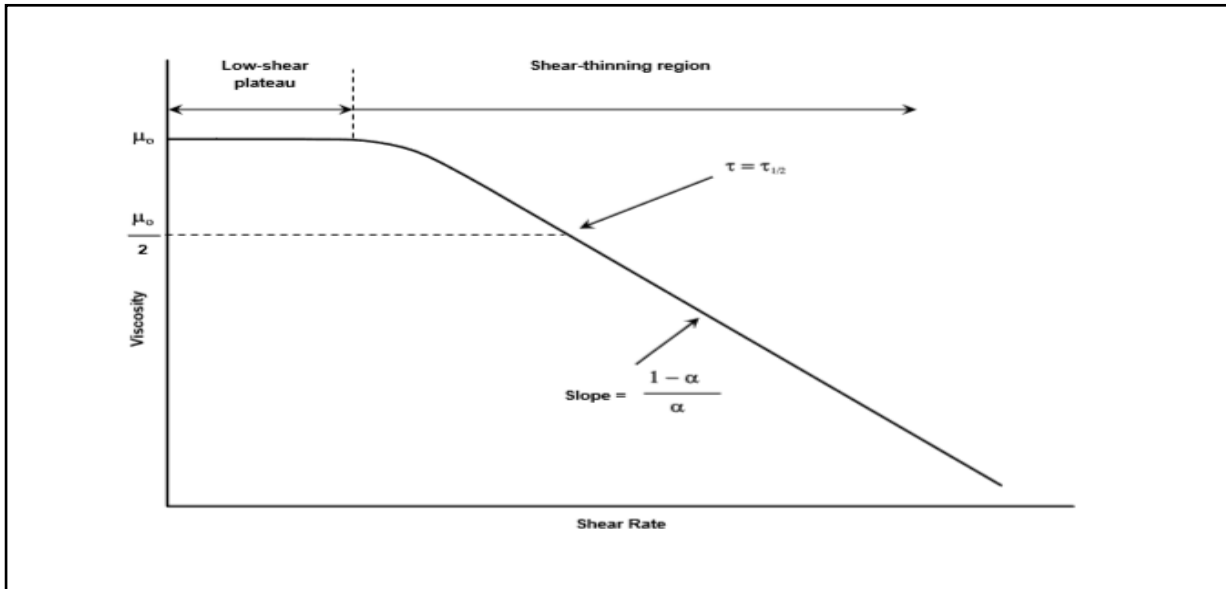


**Figure 2.10b** Rheology of an Ellis model on time independent fluid [97]

Accordingly, Ellis model, the fluid viscosity  $\mu$  is given in equation 2.7b

$$\mu = \frac{\mu_0}{1 + \left(\frac{\tau}{\tau_{\frac{1}{2}}}\right)^{\alpha-1}} \quad \mathbf{2.7b}$$

Where  $\mu_0$  is the low – shear viscosity,  $\tau$  is the shear stress  $\tau_{\frac{1}{2}}$  is the shear stress at which  $\mu = \frac{\mu_0}{2}$  and  $\alpha$  is an indices parameter related to the power index  $\alpha = \frac{1}{n}$ .

To have Newtonian plateau at low shear rate and plateau at high shear rate, a more general model is the Carreau model as seen in figure 2.10c [93, 90, 94]. Carreau equation is given in equation 2.8

$$\mu - \mu_{\infty} = (\mu_0 - \mu_{\infty}) [1 + (\lambda\dot{\gamma})^2]^{(n-1)/2} \quad \mathbf{2.8}$$

Where  $\mu_\infty$  is the limiting viscosity at high even approaching infinite shear limit and is generally taken as the water viscosity  $\mu_w$ ,  $\lambda$  and  $n$  are polymer – specific empirical constants: and  $\alpha$  is generally taken to be 2.  $\mu_0$  and  $\gamma$  are defined. Whereas,  $\mu$  and  $\mu_0$  are much larger than  $\mu_\infty$  and  $(\lambda\gamma)^2$  is much larger than 1. Thus equation 2.8 become the power law equation of the form  $\mu = \mu_0 (\lambda\gamma)^{n-1}$  which describes the viscosity at the intermediate and high shear rate regions. At the low shear rate region,  $\mu = \mu_0$

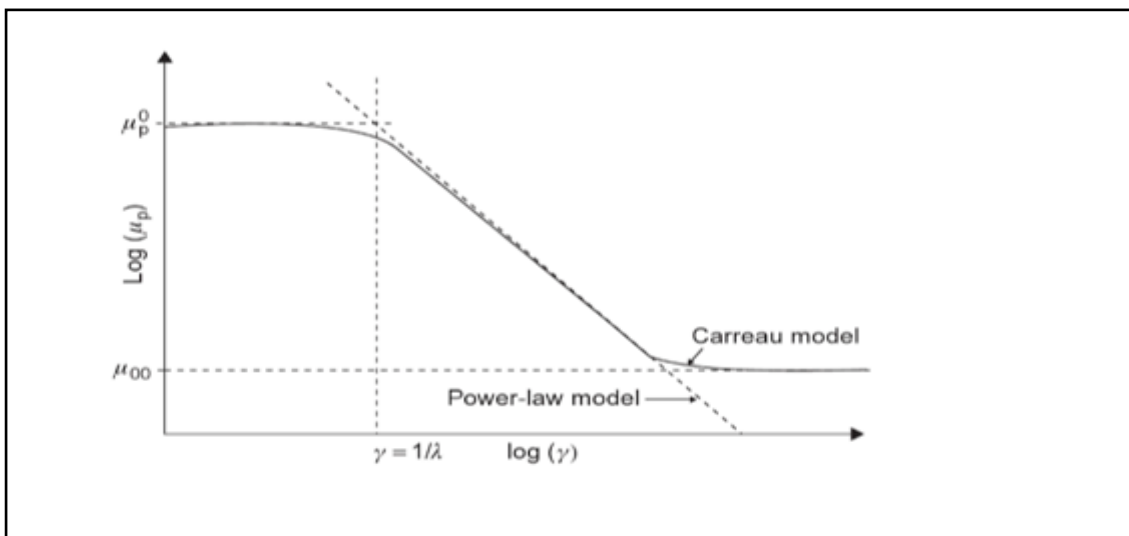


**Figure 2.10c** Rheology of a Carreau model on time independent fluid [17]

### 2.7.2 Viscosity dependence on time

The viscosity of Water soluble polymer such as polyacrylamide (PAM) is apparently dependence on time. The fluids will display a change in viscosity with time under conditions of constant shear rate. However, if the fluid undergoes a decrease in viscosity with time while it is subjected to a constant shear rate, it is known as thixotropic fluid behaviour whereas the rheopexy is the opposite thixotropic behaviour, in that the fluids viscosity increase with time at constant shear rate [17, 97]. As shown in the figure 2.11. In rheological investigation, time dependent shear effects are determined using constant shear measurement. This method would then



establish the independent effect of both shear rate and time on the viscosity behaviour of a given material.

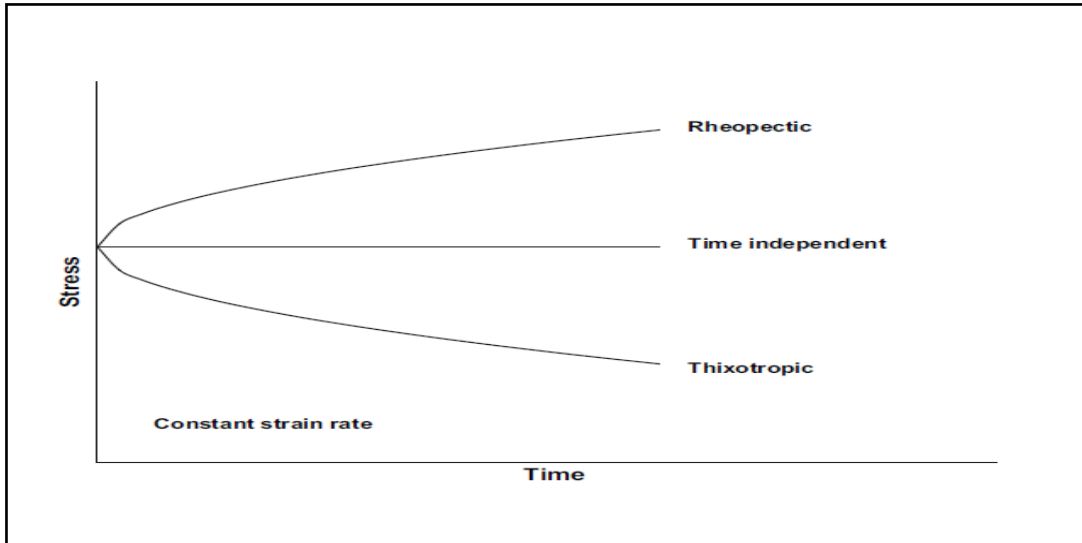


**Figure 2.11** Viscosity dependence on time [97]

### 2.7.3 Viscosity dependence on Temperature

The viscosity of a polymer solution is dependent on temperature. At low shear rate, the viscosity of the polymer solution decreases with temperature [76]. According to Meyer [95] temperature is dependent on viscosity and polymer viscosity could be found to follow the simple exponential relationship of the Arrhenius equation, as stated in equation 2.9.

$$\mu = Ae^{-\left(\frac{E_a}{RT}\right)} \quad 2.9$$

Where  $\mu_a$  is viscosity,  $E_a$  is the activation energy of the polymer solution (viscous flow) A is a constant, R is universal gas constant, and T is the temperature. This implies that the viscosity of PAM, its longevity (ageing time) and the thermal stability of the polymer solution depend on reservoir temperature [83]. Equation 2.9 shows that the viscosity decreases rapidly as the temperature increases. As the temperature increases, the activity of polymer chains and molecules is enhanced

and the friction between the molecules is reduced; thus, the flow resistance is reduced and the viscosity decrease.

Different polymers have different activated energy. Polymer with higher activated energy, the viscosity is more sensitive to temperature. According to **Sheng [17]** HPAM has two activated energy: when the temperature is less than 35°C, activated energy is low and the viscosity does not change too much as the temperature increases. When the temperature is higher than 35°C, activated energy is high and the viscosity is more sensitive to the variations in the temperature **[47, 76]**. Because temperature is dependence on kinetic rate coefficient of a polymer viscosity, the Arrhenius equation in 2.9 could be rewritten as equation 2.10 **[83, 68]**

$$\mu_a = \mu_{a,\text{ref}} \exp \left\{ E_a \left( \frac{1}{T} - \frac{1}{T_{\text{ref}}} \right) \right\} \quad \mathbf{2.10}$$

Where  $\mu_a$  is the apparent viscosity,  $\mu_{a,\text{ref}}$  is the viscosity at the reference temperature,  $T_{\text{ref}}$ , T is the reservoir temperature calculated from solving the energy balance equation,  $T_{\text{ref}}$  is the reference temperature assumed to be equal to the reservoir temperature,  $E_a$  is the activation energy of the apparent viscosity.

#### **2.7.4 Viscosity dependence on Salinity and Concentration**

Polymer solution viscosity is dependence on salinity and polymer concentration. Accordingly, Flory – Huggins equation which explained that at zero shear rate the polymer viscosity solution dependence on polymer concentration and brine salinity (**Flory 1953**). It is given in equation 2.11

$$\mu^0 = \mu_w \left( 1 + (A_{P1} C_P + A_{P2} C_P^2 + A_{P3} C_P^3) C_{Sep}^{S_P} \right) \quad \mathbf{2.11}$$

Where  $\mu^0$  the viscosity at zero shear rate,  $\mu_w$  is the water viscosity,  $C_P$  is the concentration in water (gmol/m<sup>3</sup>),  $A_{P1}, A_{P2}, A_{P3}$  and  $S_P$  the fitting constants and  $S_p$

the effective salinity for polymer (meq/ml). However, the factor  $C_{Sep}^{S_p}$  allow for dependence of polymer viscosity on salinity and hardness. According to **Sheng [17]** the effective salinity for polymer solution,  $C_{Sep}$  is given in equation 2.12

$$C_{Sep} = \frac{C_{51} + (\beta_p - 1)C_{61}}{C_{11}} \quad \mathbf{2.12}$$

Where  $C_{51}$ ,  $C_{61}$  and  $C_{11}$  are the anion, divalent and water concentration in an aqueous phase and  $\beta_p$  is measured in the laboratory which is about 10. The unit for  $C_{51}$  and  $C_{61}$  is meq/ml and the unit for  $C_{11}$  is water volume fraction in the aqueous phase. Accordingly, polymer solution concentration is an influencing factor during the course of polymer flooding. The higher the polymer concentration, the higher the viscosity of the solution and the higher the efficiency in performance. According to **Wang et al., [100]** higher polymer concentration cause greater reduction in water cut (percentage water production over the total production) and increases the enhanced oil recovery efficiency. Accordingly, figure 2.12 shows comparative plot of polymer viscosity against salinity concentration and polymer concentration, it demonstrated that viscosity is reduced as the salinity solution increases from 1000, 4000 and 7000 mg/l. even at lower solution polymer concentration of 200 mg/l the viscosity is low compare to 1000 mg/l.

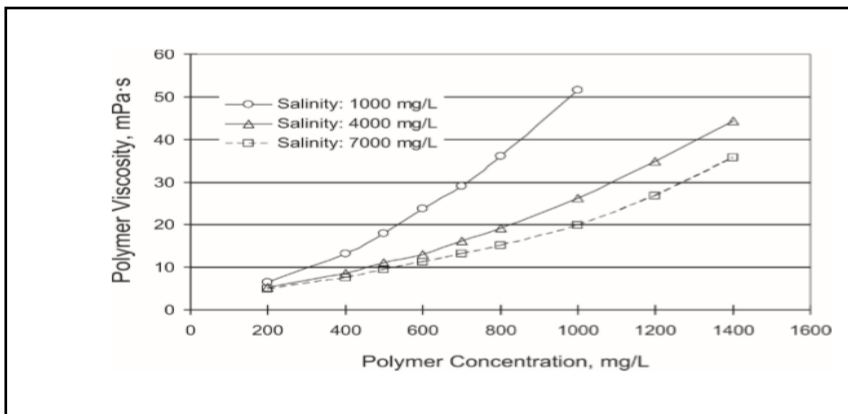
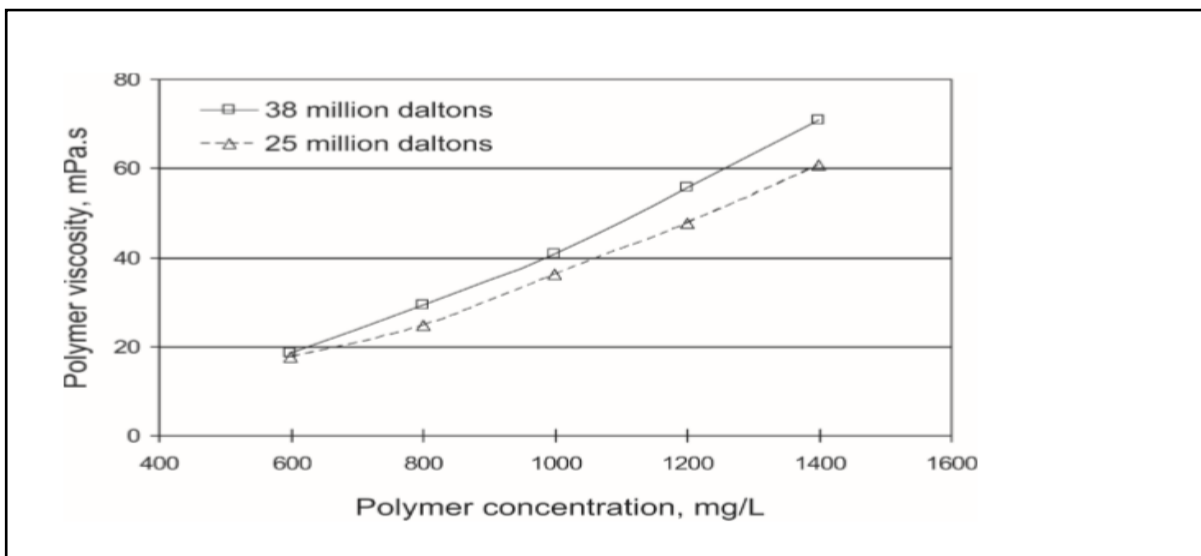


Figure 2.12 Viscosity dependence on polymer concentration at different salinities **[100]**

### 2.7.5 Viscosity dependence on molecular weight

Polymer molecular weight significantly affect the performance effectiveness. According to the **Wang et al., [100]** the polymer with higher molecular weight provide greater viscosity to the polymer with lower molecular weight as seen in figure 2.13. The molecular weight of 38 million Daltons have more viscosity compare to molecular weight of 25 million Daltons.



**Figure 2.13** Viscosity versus polymer concentration and versus Molecular weight [101]

In furtherance, **Xiaoqing et al., [101]** reported that polymer solutions with higher molecular weight have better absorption, higher resistance and residual resistance coefficient. This imply that to recover a given volume of oil, less polymer is needed when using a high molecular weight polymer than with a low molecular polymer.

### 2.8 Polymer Rheology Behaviour in Porous Media

The rheology behavior of polymer solution is a non-Newtonian fluid behaviors, such as shear thinning and shear thickening effects that leads to different viscosity properties as discussed in sub section 2.11.1. Basically, viscosity at any shear rate is important parameter for measurement of rheology. When a polymer solution

viscosity is injected into a reservoir from an injection well. The fluid flow velocity which is related to shear rate, will change from wellbore to in – depth of a reservoir; however the polymer solution viscosity will also change from near wellbore to in – depth of a reservoir [36, 103]. Earliest investigation studies have shown that rheological characteristics or viscosity fluid flow could be determined in the laboratory in two ways [6] (a) viscosity solution measurement using viscometer and (b) coreflood experimental analysis. Although, different nomenclature are used to recognize viscosity. Firstly, Bulk viscosity is measured in a viscometer whereas the in situ viscosity in porous media [17]. The in situ viscosity is not directly measured but instead it is calculated using coreflood experimental data according to the Darcy equation as seen in equation 2.13

$$\mu_{app} = k \frac{A\Delta P}{QL} \quad \mathbf{2.13}$$

Where Q is the liquid volume at designated time interval, A is the cross sectional area, L is the length of the sample in the macroscopic flow direction,  $\mu_{app}$  is the calculated viscosity of a fluid flowing through a porous media known as the apparent viscosity,  $\Delta P$  is the pressure drop across the porous media, k is the absolute permeability for porous media.

However, equation 2.13 is the apparent viscosity from Darcy's law used to describe the macroscopic rheology of a polymer fluid flow in a porous media whereas effective viscosity is from Poiseuille's law to describe polymer viscosity in a single capillary channel, which is in microscopic [79]. The effective viscosity is seen in equation 2.14

$$\mu_{eff} = \frac{\tau}{\gamma} \quad \mathbf{2.14}$$

Where  $\tau$  is the shear stress (N/m<sup>2</sup>) which represent the force per unit area,  $\gamma$  is the shear rate (s<sup>-1</sup>) representing the velocity change through the thickness,  $\mu_{eff}$  is the effective viscosity.

Most time the polymer solution viscosity in porous media cannot be directly measured, however is predictable from the Darcy equation if coreflood tests are conducted. At this process several coreflood tests need to be run and is reasonably expensive and preferably, it could be advisable to model polymer viscosities at different flow rates in porous media from the bulk solution viscosities at different shear rates [17]. However, to determine polymer solution viscosities at different flow rate using bulk solution viscosities at different shear rates, there is need to convert the flow rates into shear rates. The converted shear rates is known as equivalent shear rate which is equivalent to the viscosities of the bulk viscometer.

## 2.9 Mobility Control with Polymer Solutions

When the mobility ratio for water displacing oil is unfavorable as discussed in sub section 2.8.4. The injection water need to be improved to overcome the difficulty emanated by displacing fluid (water). To improve the displacement efficiency, water soluble polymer viscosity solution should be added to reduced Mobility ratio (M) from the value of 1 or less. Equation 2.5d is converted to equation 2.15

$$R = \frac{\lambda_w}{\lambda_o} / \frac{\lambda_p}{\lambda_o} = \frac{\lambda_w}{\lambda_p} \quad 2.15$$

$$R = \frac{k_w}{\mu_w} / \frac{k_p}{\mu_p} \quad 2.16$$

Where  $\lambda_w$  and  $\lambda_p$  refer to the mobility ratio of the water and polymer solution respectively, and  $\lambda_o$  mobility ratio of oil.

Resistance factor (R) is defined as the mobility ratio of the water or brine to the mobility ratio of the polymer solution at residual oil saturation [9, 11 102].  $k_w$  is the effective permeability of water or brine solution,  $k_p$  is the effective permeability of polymer solution,  $\mu_w$  is the viscosity of the water or brine and  $\mu_p$  is the viscosity of the polymer solution.

Equation 2.15 and 2.16 shows the mobility ratio of a polymer solution compared to the flow of the water or brine. It could be acceptable that the displacement of oil by polymer could be give mobility ratio less than 1 which is favorable for oil recovery. According to Seright (1983) resistance factors of polyacrylamide solutions are greater than viscosities, this suggests that polyacrylamides reduce water mobility both by increasing solution viscosity and reducing effective permeability to water. Measure of permeability reduction is retained after a polyacrylamide bank is displaced by brine. One method of assessing the degree of polymer solution (polyacrylamide) efficiency is to compare solution viscosities.

## 2.10 Polymer stability

Stability of polymer solution is essential requirement for EOR application. It is well established that in the presence of reservoir temperature and brine. Polymer can degrade under certain conditions leading to polymer instability. Polymer degradation is defined as any process that breaks down the molecular structure of macromolecules properties [104, 18]. Though, loss of solution viscosity with time is the major means to detect degradation [23]. Polymer degradation includes chemical, thermal, mechanical and biological [21, 23, 68]. But the Biological degradation is more prevalent in Biopolymer [23]. PAM and HPAM exhibit instability due to degradation such as chemical, thermal and mechanical. Figure 2.14 shows the plot evidence of different point of degradation from injection well point to the

wellbore. Mechanical degradation occurs at the injection point decreasing down the reservoir due to shearing. Chemical degradation occurs in the wellbore with exponential drop or slide decrease due to oxidation attack. Thermal degradation causes decrease in the reservoir. The decrease depends vividly on ageing time in the presence of reservoir temperature and salinity brine. It could be improve by controlling the degree of hydrolysis as to have polymer stability over long period.

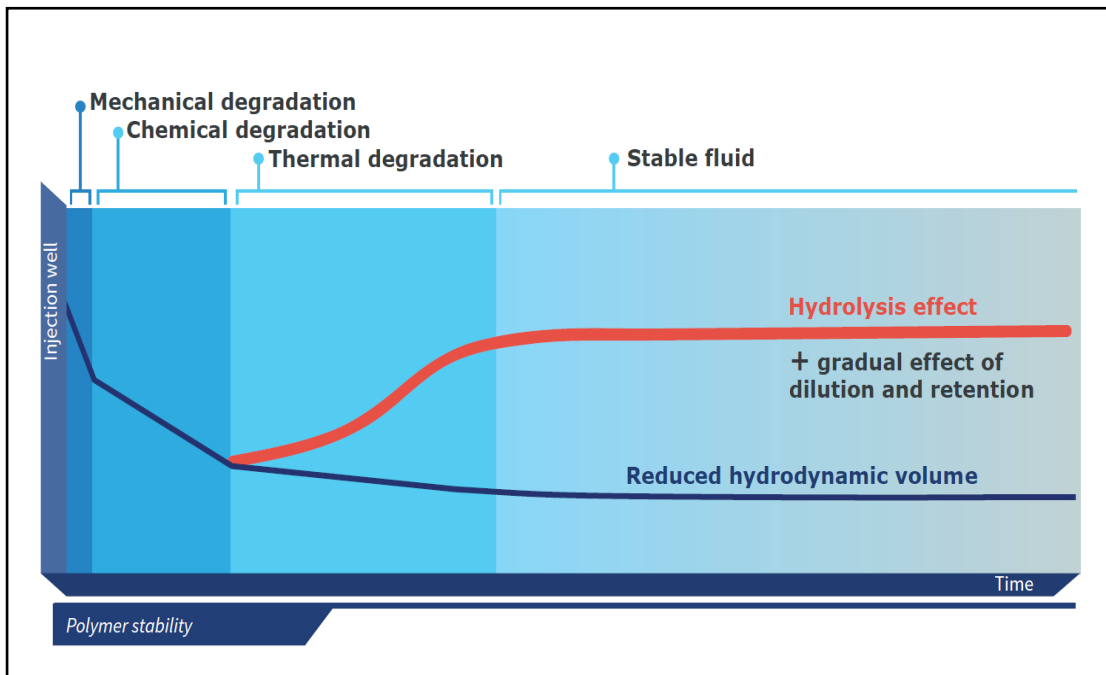


**Figure 2.14** Stages of Polymer stability [105]

### 2.10.1 Chemical degradation

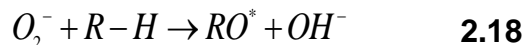
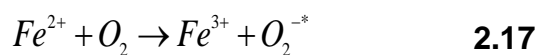
Chemical degradation is the breakdown of polymers molecules [66]. This breakdown are caused by factors; contaminants such as oxygen and iron and even long term attack on the molecular backbone by process of hydrolysis [104]. It is well established that both polyacrylamides and biopolymers are prone to oxidative attack by dissolved oxygen in the injected water. Many factors affects chemical degradation but two most important are oxygen and ferric ion.



### 2.10.1.1 Effect of oxygen and ferric ion on PAM stability

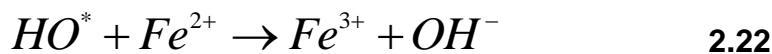
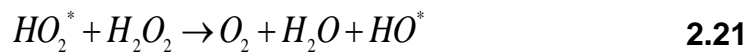
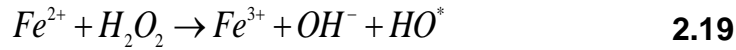
Polymer degrade chemically and the degradation are caused by oxygen which in turn could create a reaction with metals or metal ions [106]. The oxidative degradation reaction are catalysed by dissolved metal ions such as  $Fe^{3+}$ . In the oxidization reaction process, oxygen is a major means to accelerate the metal – induced degradation and more importance is the reaction that occurs between oxygen and ferrous ions to form radicals as shown in equation 2.17 and 2.18 which subsequently reacts with the polymer molecule to initiate a degradation chain reaction [107 – 108].

For instance, the oxidization of  $Fe^{2+}$  to  $Fe^{3+}$  produces a free radical  $O_2^-$ . Then the highly reactive oxygen-anion radical  $O_2^-$  may become attached to the polymer chain



to produce peroxide and break the backbone. Oxidization could also proceed via the free radical mechanism [104, 108]. According to **Fenton** [109], this mechanism occurs via a solution of hydrogen peroxide and an iron catalyst, and is use to oxidize contaminants or wastewater. The chemical reaction creates two different oxygen-radical species,  $H^+ + OH^-$ , with water as the by-product in the case of PAM. The active intermediate  $HO^*$  in equations 2.19 to 2.22 can react with ferrous iron, hydrogen peroxide or other components contained in the reaction mixture. As shown in equation 2, iron (II) oxidized by hydrogen peroxide to become iron (III), forming a hydroxyl radical and a hydroxide ion in the process. The iron (III) is then reduced back to iron (II) by another molecule of hydrogen peroxide forming a

hydroperoxyl radical and a proton, the step by step reaction are shown in equations **2.15 to 2.18** and it proposed by Haber and **[110]**.



Degradation by oxidative attack can be prevented or minimized by reducing the oxygen content of the water or brine to less than a few parts per billion. This is usually done by use of oxygen scavengers. For example, sodium dithonite used for stabilizing polyacrylamides. Even **Yang and Treiber [111]** provided guidelines for the use of oxygen scavengers to prevent degradation of polyacrylamides in field brines under simulated reservoirs conditions.

### **2.10.2 Mechanical degradation**

Mechanical degradation refers to the breakdown of macromolecules chain at high flow rate when fluid stresses are developed during deformation, or flow become large enough to break the polymer molecular chain **[76, 112]**. This occurs in pipes, through chokes, valves or pumps above a certain velocity or pressure drop as down hole through perforation **[18]**. Most viscosity loss occurred from the high pressure injection pumps and mixing system to the near wellbore. Drastically the reduction in polymer viscosity are due to the effect of shearing

### 2.10.2.1 Effect of Shear on PAM stability

Polyacrylamides (PAM) and HPAM are sensitive to shear degradation because of the flexible coil molecule [76, 86]. Shear degrades the polymer into smaller molecules. It is well established that the higher the molecular weight, the higher the sensitivity to mechanical degradation and the more viscosity loss. The rate of polymer chain rupture in high shear flow depends on the molecular weight. Larger molecules offer more resistance to flow, consequently experience larger shearing

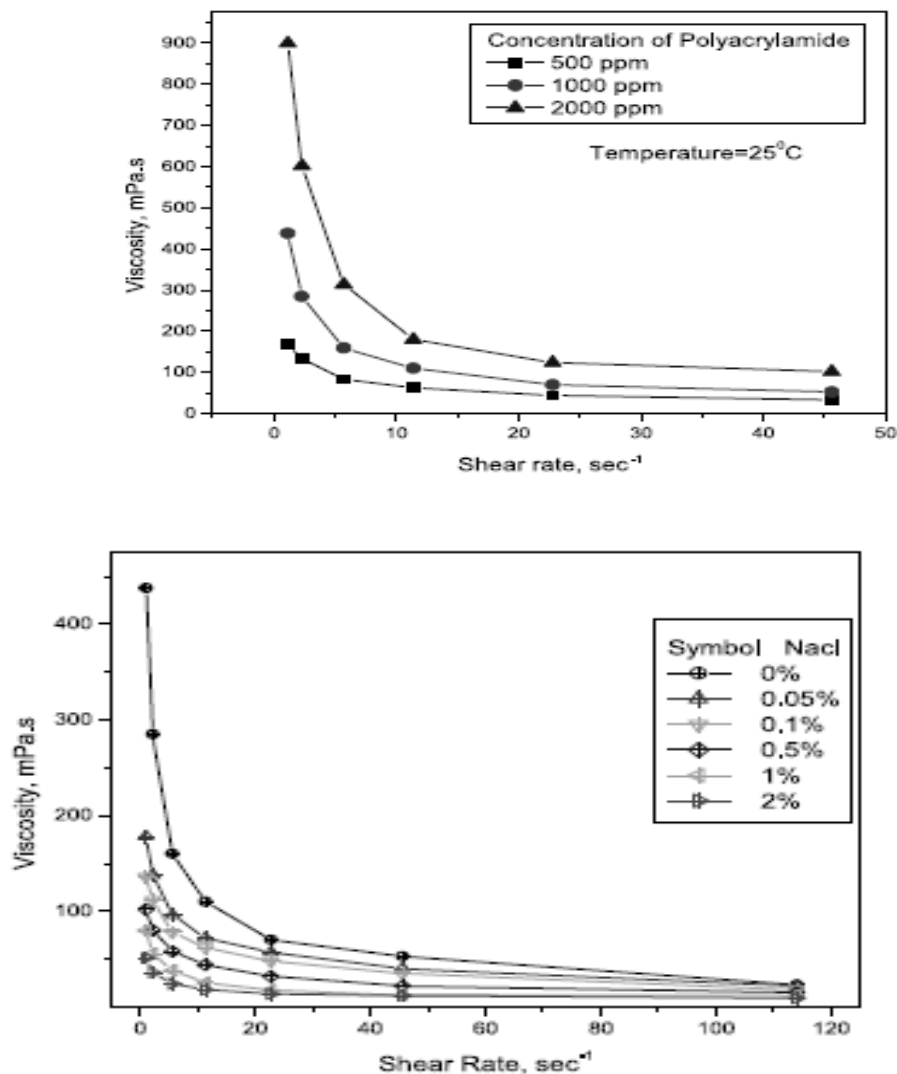


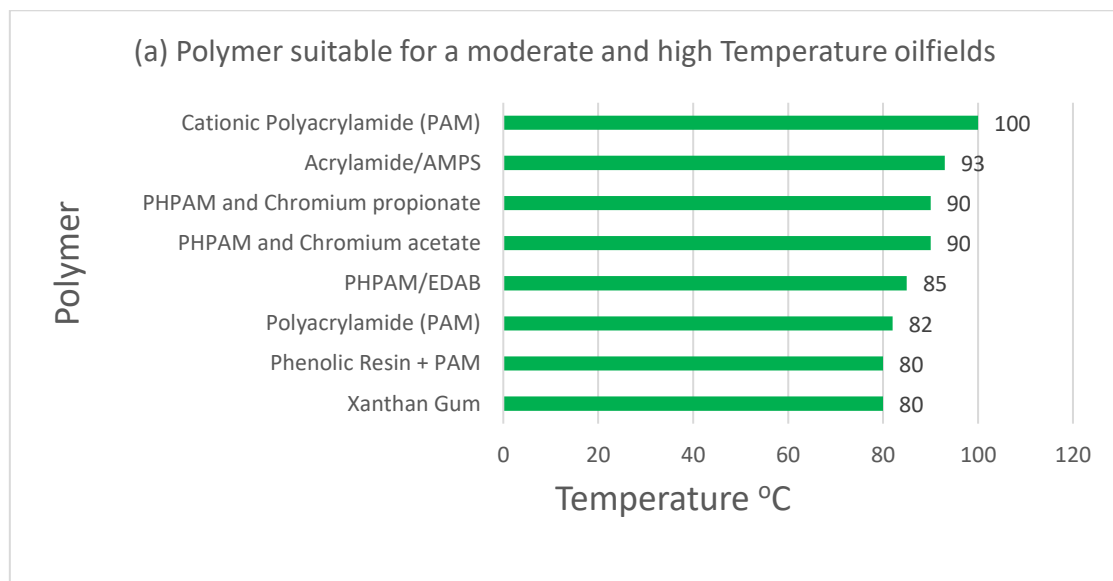
**Figure 2.15** Effect of shear degradation on polyacrylamide with different molecular weight and NaCl Concentration [113].

One method of assessing the degree of polymer mechanical degradation is to compare solution viscosities. However, **figure 2.15** is an experimental evidence on level of mechanical degradation on PAM where the apparent viscosity of PAM decreases with an increasing shear rate and to the brine solution, the higher NaCl brine concentration the more decrease in apparent viscosity as the shear rate increases. Accordingly, earlier experiment done by **Maerker [112]** found that the mechanical degradation of the polymer could be more severe in higher salinity brines and that the presence of calcium ions ( $\text{Ca}^{2+}$ ) had a particularly damaging effect over and above that expected from the simple increase in the solution's ionic strength.

### **2.10.3 Thermal Degradation**

Thermal degradation depends on reservoir temperature. Moreover, temperature is the determining factor for efficiency in performance of polyacrylamides (PAM) during polymer flooding application. Because temperature is a function of degree of hydrolysis. Degree of hydrolysis is defined as the degree of amide groups ( $\text{CONH}_2$ ) that are converted into carboxyl groups ( $\text{COO}^-$ ) **[76, 114]**. According to **Choi et al. [83]** the term hydrolysis was considered as different phenomenon from the chemical degradation which is sensitive to calcium ions. Chemical degradation should not be confused with acrylic backbone by radical mechanism which is referred as thermal degradation. In thermal degradation of polymer solution like polyacrylamide (PAM), the amide group ( $\text{CONH}_2$ ) hydrolyse at elevated temperature to form carboxylate groups ( $\text{COO}^-$ ) latter interaction with divalent ions  $\text{Ca}^{2+}$  and  $\text{Mg}^{2+}$  leads to a sharp reduction in polymer solution viscosity. **Albonico and Lockhart [16]** stated that the degree of hydrolysis at which PAM separate from solution depend directly proportional to salinity brine containing divalent ions and inversely proportional to

temperature. The aforementioned led to the recommendation of 70 – 82°C as safe maximum temperature (SMT) for the use of polyacrylamide in polymer flooding [13 – 15, 115]. Above the aforementioned temperature limit become elevated temperature. Elevated temperature is define as a temperature above the safe maximum reservoir temperature (SMRT) at which a particular polymer gel solution becomes unstable [84]. Various water soluble polymer have difference safe maximum temperatures (SMT) and they are categorised as low, high or ultra-high [116], as indicated in **Figure 2.16** which represents in plot (a) the low and moderate safe temperature range up to 82°C, in plot (b) the high safe temperature range between 90 - 150 °C, and in plot (c) ultra-high safe temperatures of above 150 °C.



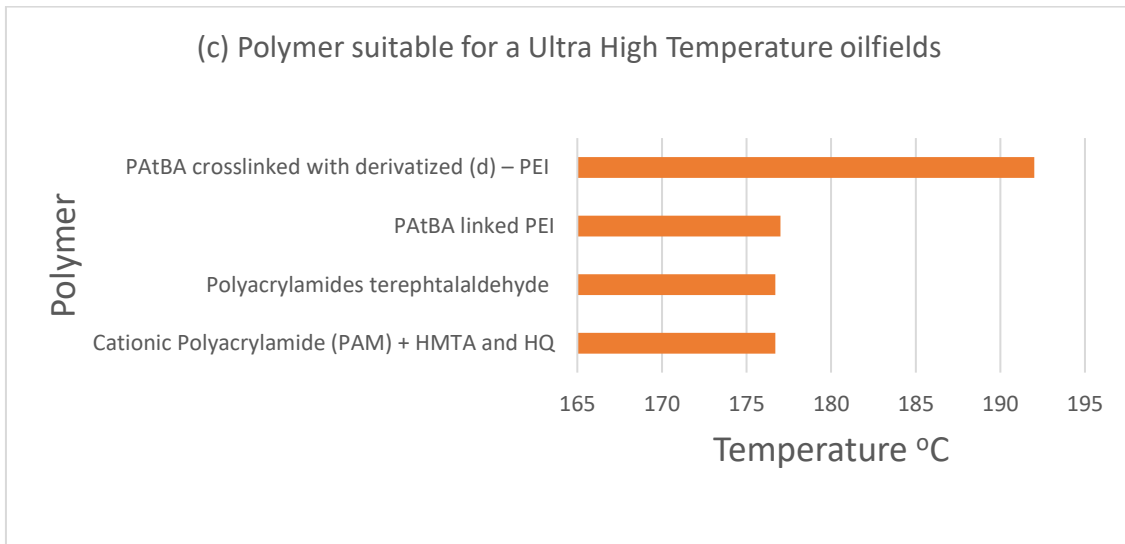
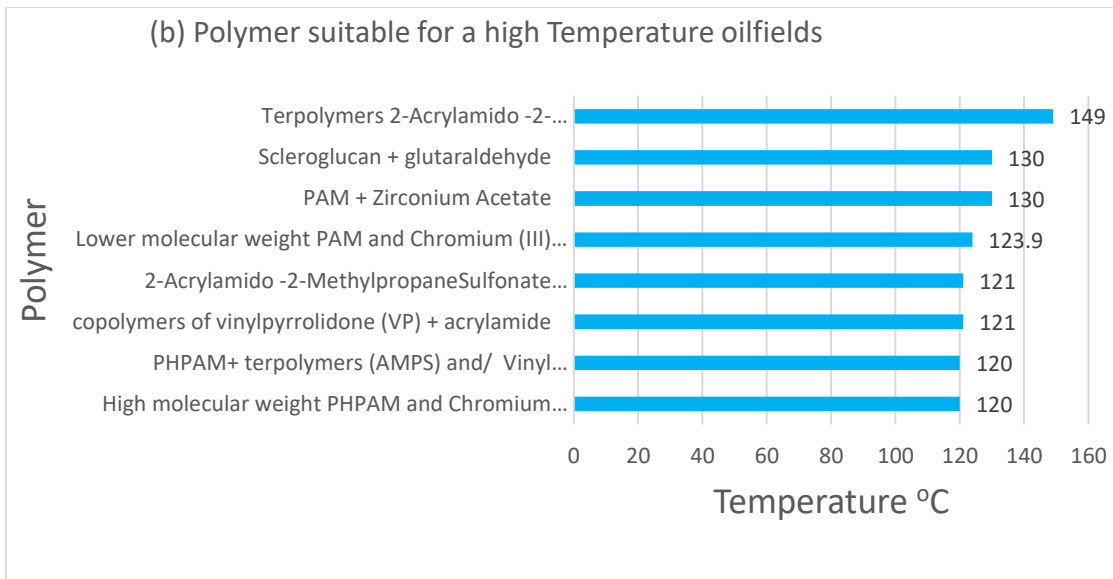


**Figure 2 16.** Various water-soluble polymer gels with maximum safe temperatures [84]

In commercial applications of polyacrylamide (PAM) suitable range of degree of hydrolysis are reported to be from 15 – 35% [36]. Because, when PAM is presence at temperature above moderate, the hydrolysis will increase faster and PAM may not be able to withstand high temperature [83]. Accordingly, **Ryle's** [15] experimental test confirmed that dissolved salinity brine had just less effect on hydrolysis rate however, the temperature is the main determining factor.

### 2.10.3.1 Effect of Temperature of Hydrolysis of PAM

Temperature has an influencing impact on polyacrylamide rheological properties. Because, polyacrylamide (PAM) as a synthetic water-soluble polymer in pure state are electrically neutral possessing a hydrogen bond [117]. But when mixed with water in presence of elevated temperatures, and its amide groups are converted into carboxylate groups [117 – 118] as shown in Figure 2.15. The hydrolysing nature basically depend on the elevated temperature. Because at elevated temperature gives a transformation into carboxylate group. The carboxylate group carries a negative charge and represents a reactive site, promoting ionic interaction with molecules such as monovalent and divalent cations. The mechanism of chemical transformation are in Figure 2.17

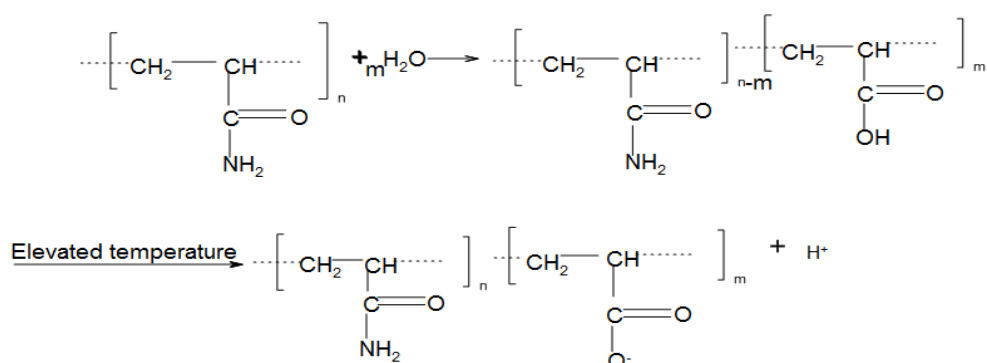
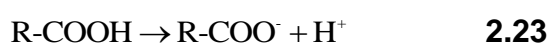


**Figure 2.17.** Effect of elevated temperature in hydrolyzing PAM [84].

In an understandable chemistry mechanism, for carboxylic group (RCOOH) to be converted into a carboxylate group (RCOO<sup>-</sup>), there must be a loss of a proton (H<sup>+</sup>), as shown in equation 2.23.



Making the carboxylate group (RCOO<sup>-</sup>) open for interaction with monovalent (NaCl) and multivalent ions, especially CaCl<sub>2</sub> and MgCl<sub>2</sub>, as shown in Figure 2.19. In furtherance, if the temperature increases, the negative charge on the rock surface is increased, resulting in higher electrostatic repulsion. Thus, the ionic polymer HPAM adsorption is reduced.

### 2.10.3.2 Effect of Formation Water Salinity on Hydrolysed PAM

Formation water salinity has a strong effect on polymer viscosity, especially for Hydrolysed PAM. Formation Water salinity is a measure of the total dissolved ions, such as Na<sup>+</sup>, K<sup>+</sup>, Ca<sup>2+</sup> and Mg<sup>2+</sup>, carried by water that naturally exist within the pores of a reservoir sedimentary rock. When water containing monovalent (NaCl) and multivalent ions (predominantly CaCl<sub>2</sub> and MgCl<sub>2</sub>) interact with hydrolysed PAM. The polymer viscosity decreases. However, the exact chemistry is in figure 2.16.

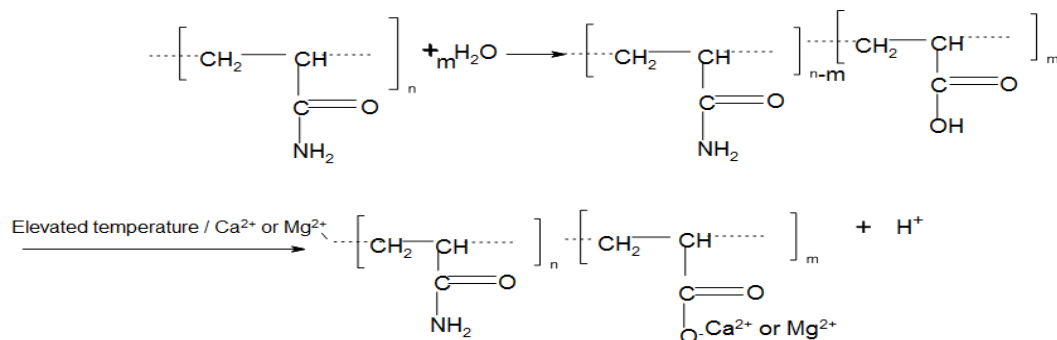


**Figure 2.18.** Effect of Ca<sup>2+</sup> or Mg<sup>2+</sup> on hydrolyzed PAM [84].

Apparently, reservoir containing high formation water salinity causes precipitation and decrease in the viscosity of polymer solution which could lead to poor mobility control. A clear evidence was a numerical simulation studies at Daqing oilfield China where oil recovery efficiency decreased from 30% to 50% when salinity increased from 2500 to 10,000 mg/l [100]



## 2.11 Resultant Effect of High Temperature and Salinity

Elevated temperatures and the presence of formation water salinity containing divalent cations ( $\text{Ca}^{2+}$  and  $\text{Mg}^{2+}$ ) have a strong effect on polyacrylamide during EOR applications. They cause polymer syneresis and precipitation.

### 2.11.1 Polymer Syneresis

Polymer syneresis is a phenomenon where the polymer gel structure collapses, expelling water and in turn resulting in contraction or shrinkage of the volume of the gel [84, 115, 119]. According to **Albonico and Lockhart [115]** it is reasonable to expect that severe syneresis could result in a reduction of 90% or more of the original gel volume, and this could have a significant impact on the performance of a gel within porous reservoir rock. However, the percentage of syneresis could be determined in laboratory by calculating the difference between the weights of a sealed vial containing polymer gel before placed in the oven and the weight of a vial in which syneresis has occurred, the difference are divided by the initial weight of the sealed vial containing polymer gel multiplied by one-hundred.

There are two ways in which syneresis may occur: (1) excessive cross-linking [120,121]; and (2) at elevated temperatures or in conditions of high salinity [122]. Excessive cross-linking, occurs during the transformation of polymer solution into gel via a chemical cross-linker. In this process, the cross-linker freely bonds the reactive groups to the polymer chains, and the effective molecular weight of the polymer increases. Consequently, if too much cross-linker is present in the vicinity, cross-linking may continue beyond the point of gelation, the polymer starts to contract in volume, and water is expelled [120].

**Karimi et al., [119]** demonstrated how excess cross-linker could lead to syneresis in an experiment using four different weight ratios of polymer to cross-linker with a polymer concentration of 11,000 ppm and at a temperature of 80°C. The polymer-to-cross-linker weight ratios were 10 to 20; no syneresis occurred after 150 days but with a ratio of 40 to 60, syneresis occurred and increased. It became obvious that once the cross-linker concentration exceeds a certain value, the rate of syneresis starts to increase.

Whereas in elevated temperature and in conditions of high salinity, syneresis could occur when the polyacrylamide solution with high salinity is placed in an oven over an extended period. The polyacrylamide solution experiences hydrolysis and the acrylamide groups on the polymer backbone converted into acrylate, further interaction with divalent cations leads to the syneresis of the polymer gel. According to **Karimi et al.'s [119]** experimental report, syneresis occurred when polyacrylamide (PAM) was placed in an oven for 6 months at temperatures of 80 and 100°C, but did not occur when it was placed in the oven at 30 or 60°C. The temperature increase from 30 and 60°C to 80 and 100°C respectively resulted in syneresis, with some degree of reduction in gel volume. This implies that, as the temperature increases, the percentage of syneresis increases. **Karimi et al., [119]** also showed that salinity has an effect on syneresis by adding NaCl, MgCl<sub>2</sub> and NaHCO<sub>3</sub>, however, reductions in the volume of the polymer gel were observed.

### **2.11.2 Polymer Precipitation**

Polymer precipitation is the result of interaction between the formation water salinity containing divalent cations (Ca<sup>2+</sup> and Mg<sup>2+</sup>) and the carboxylate groups (COO<sup>-</sup>) on the hydrolysed polymer **Zaitoun and Potie [13]**. This interaction implies that, as the percentage of carboxylate groups increases, solubility decreases. However, if this

happens to excess, it will eventually amount to precipitation and the polymer solution will not transform into polymer gel [14, 115, 13 121].

## **2.12 Control of Polyacrylamide (PAM) degradation**

The earlier researchers discovered that polymer flood projects are suitable to relatively ideal reservoirs with low temperature and low salinity but when applied in hostile reservoir conditions, such as high or elevated temperature and high salinity, the polymer suffer from degradation leading to substantial loses in polymer solution viscosity [12, - 16, 21]. The key mechanism of PAM degradation was found to be amide group hydrolysis. The rate of hydrolysis was found to vividly depend on temperature. Hydrolysis appears to be the key factor affecting polymer stability followed by precipitation in the phase of salinity containing multivalent ion ( $\text{CaCl}_2$  and  $\text{MgCl}_2$ ). The polymer degradation becomes more severe as temperatures increases, especially above  $70^\circ\text{C}$  [15, 21, 76]. Above  $75^\circ\text{C}$  PAM could give rise to extensive thermal hydrolysis up to 80 mole % [15]. Moreover, polymer flood project at different field globally is challenging because of high reservoir temperature and high salinity of formation water [86]. To withstand the news problems and limitations caused by high temperature and high salinity concentration. This study adopted and designed research materials and methods as discussed in Chapter 3. The purpose is to meet the criteria of inactivity or insensitivity to moderate and high salinity concentration at high temperature and resistance to hydrolysis. Firstly, before the synthetic experimental approaches followed a correlation analysis was conducted to determine the safe maximum temperature point (SMTP).

## CHAPTER 3: MATERIALS AND METHOD

Polyacrylamide (PAM) and its derivatives HPAM have been successfully implemented for EOR applications in several oilfields [86,123] at moderate temperatures and salinity levels to control the mobility ratio and improve the sweep efficiency. But the current challenges being faced in modern fields is that many oilfields tend to have higher temperatures ( $>75^{\circ}\text{C}$ ) and high salt concentrations  $>30000$  ppm TDS [2]. Facing these challenging reservoir conditions, materials and research methods were adopted as to fit in the existing technical gap and address the stability limitations of PAM.

### 3.1 Materials

A high molecular weight ( $5 - 6 \times 10^6$  Dalton) non-ionic water-soluble polymer of Polyacrylamide (PAM) as shown structurally in figure 3.0 were utilized as basic material for this work because it possesses thickening (viscosity) capacity for EOR applications based on its high molecular weight [20]. The challenging situation of PAM under EOR applications is that PAM is apparently unsuitable for use under harsh reservoir conditions of high temperature and high salinity. Facing the challenging high temperature situation, poly vinyl Pyrrolidone (PVP) of Mw - 55,000 Dalton were combined with PAM in saline solution of 43280 ppm. The molecular structural of PAM and PVP mix is shown in figure 3.2. The main purpose of PVP additive to PAM, is that PVP act as resistant to PAM degradation at high temperatures and it also exhibits a non toxic and environment – friendly behaviour [124 – 127]. In furtherance the optimised solution of PAM and PVP mix were extended to extreme salinity of 200000 ppm but the results showed that instability occurred. Facing extreme salinity of 200000 ppm, 2 – acrylamido-2-methylpropanesulphonic acid (AMPS) of Mw: 207.25 g/mole were added to the

optimised solution of PAM and PVP mix. AMPS were deployed because the polymer contain sulfonate groups that are expected to offer high stability in solution and can tolerate high salinity [88]. The molecular structural of PAM PVP and AMPS mix is shown in figure 3.3. To avoid substantial chemical degradation of polymers solutions in the presence of oxygen, Sodium thiosulphate ( $\text{Na}_2\text{S}_2\text{O}_3$ ) concentration were added to the polymers solution as an oxygen scavenger [106]. The three water soluble polymers PAM, PVP and AMPS were sourced from Sigma-Aldrich Company (St. Louis, USA).

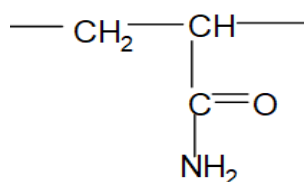


**Figure 3.0.** Partial structure of water soluble polymer polyacrylamide (PAM)

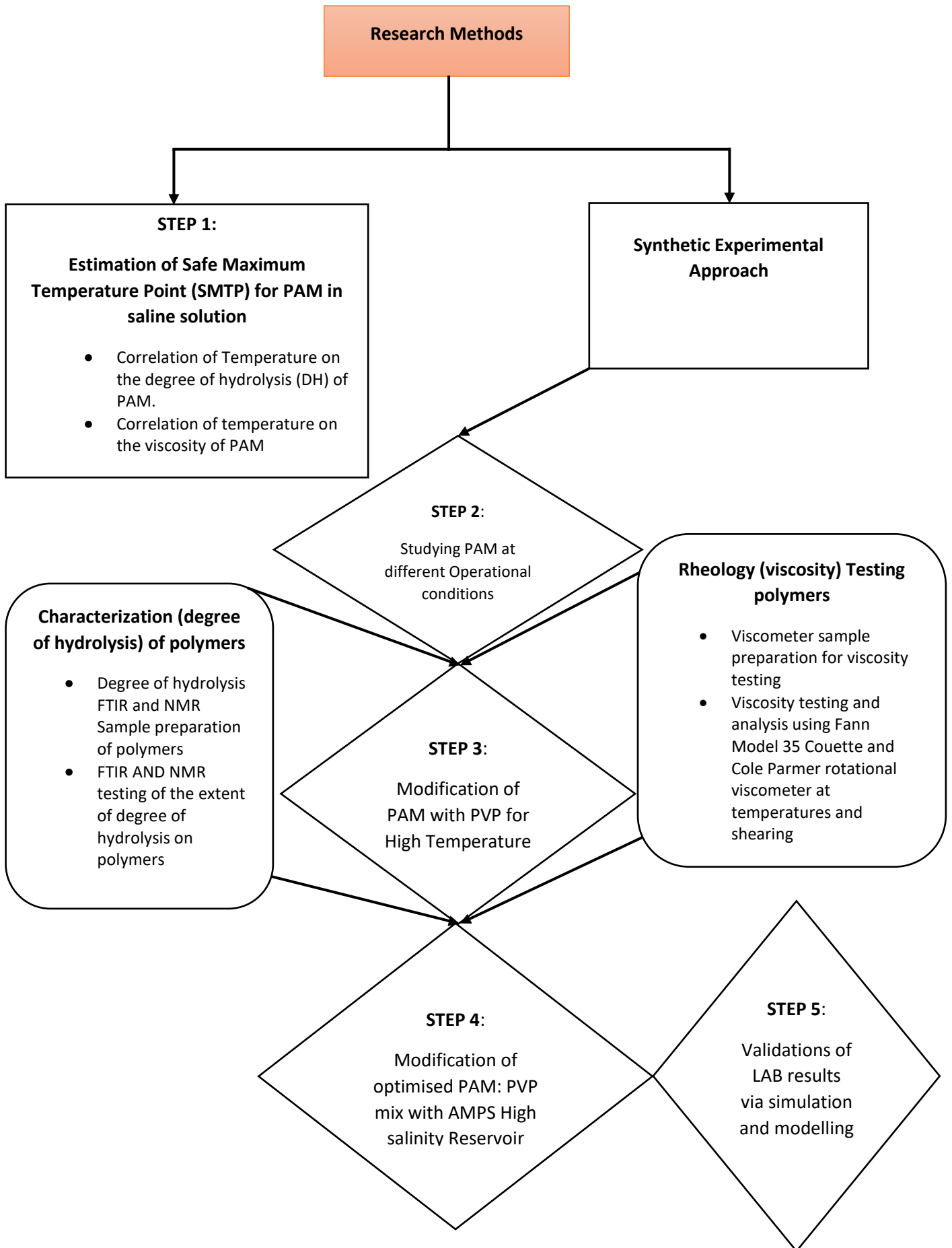


Figure 3.1: Sequential order of this work research methods

## **3.2 Research Methods**

This study adopted two research methods: first method, deduced safe maximum temperature points (SMTP) from published data(s) and second method conducted synthetic experiment on the polymers as to fit in the existing technical gap and address the stability limitations of PAM. The sequential order of the research method is shown in figure 3.1

### **3.3 Safe Maximum Temperature Point (SMTP) Method**

In determining the safe maximum temperature point (SMTP) of PAM under improved and enhanced oil recovery (IOR/EOR) applications. A correlation were deduced based on previously published data (s) on PAM studies and it is sectioned into two:

- Correlation of temperature on the degree of hydrolysis (DH) of PAM in saline concentration.
- Correlation of temperature on the viscosity of PAM in saline concentration

#### **3.3.1 Correlation of temperature on the degree of hydrolysis (DH) of PAM**

This approach involved two stages; firstly, plotting the degree of hydrolysis of PAM against ageing time in three different oilfield brines of (5% NaCl), (9% NaCl and 1% CaCl<sub>2</sub>), (3% NaCl and 1% NaHCO<sub>3</sub>) at temperature of 25 to 93°C made available from published data.

Secondly, plotting the gradient of the degree of hydrolysis against the temperature ranges in presence of the oilfield brines. This approach was repeated also in Correlation of temperature on the viscosity of PAM.

### **3.4 Synthetic Experimental method**

The synthetic experimental method is a quantitative research method designed to determine the limit of operational performance of PAM and effects of presumed causes of instability while in operation. The key chronological step includes: sample preparation, laboratory measurement with equipment such as Fann model 35 and Cole Parmer rotational viscometer for viscosity testing and Fourier transform infrared (FTIR) and neutron magnetic resonance (NMR) for testing the extent of degree hydrolysis and finally the results analysis before validations of results as shown in figure 3.1.

#### **3.4.1 Sample preparation for Rheology (viscosity) testing**

Studying the effectiveness of polyacrylamide at different operational conditions, a high molecular weight ( $5 - 6 \times 10^6$  Dalton) non-ionic water-soluble polymer of Polyacrylamide (PAM) was selected and sourced from Sigma–Aldrich. Two types of polymer solution were then prepared: type 1 using deionized water and type 2 synthesized formation water (hereafter called brine) mimicking the Draugen reservoir, North Sea, with total dissolved salts of 43,280 ppm [128]. The reservoir is of sandstone formation, Table 3.1 presents the composition of the synthesized saline and brine used in this research. The polymer solution with or without brine was prepared using a 1% (w/v) polymer (10g) concentration in a 1000 ml beaker mixed with an electric stirrer for 3 hours. To prevent polymer degradation due to the presence of oxygen, 1% (w/v) or 10g Sodium thiosulphate ( $\text{Na}_2\text{S}_2\text{O}_3$ ) concentration was added to 1000 mL of the solution as an oxygen scavenger.



**Table 3.1:** Composition of the Synthetic Saline and Brine

<b>Ion</b>	<b>Synthetic Saline (ppm)</b>	<b>Synthetic brine (ppm)</b>
NaCl	34700	170,000
CaCl <sub>2</sub> . 6H <sub>2</sub> O	4900	15000
MgCl <sub>2</sub> .6H <sub>2</sub> O	2700	10000
KCl	400	2500
NaHCO <sub>3</sub>	400	1500
SrCl <sub>2</sub> .6H <sub>2</sub> O	120	600
BaCl <sub>2</sub> .6H <sub>2</sub> O	60	400
<b>TDS</b>	<b>43,280</b>	<b>200,000</b>

To maintain high quality testing results the following steps have been followed:

1. Mix the required solution from the same chemical manufacturing batch for operational conditions.
2. Ensure that the quality control testing procedure has been applied.
3. Maintaining high quality control, the results presented for the viscosity of each solution at different conditions is the average of three measurements and the error calculated based on test repeatability.

### **3.4.2 Viscometer Technique**

Viscosity is the measurement of the internal friction to fluid flow [129] and is measured with an instrument known as viscometer. A viscometer is special type of rheometer (instrument for measuring rheological properties) which is limited to the measurement of viscosity [90 – 91]. Basically in polymer solution viscosity, two major viscometer are used: capillary viscometer and rotational viscometer. Capillary Viscometer measure viscosity by timing how long it takes for a transparent or

translucent fluid to flow between two points of capillary tube and its viscosities measurement is always at zero shear rate ( $\dot{\gamma}=0$ ) Whereas rotational viscometer use a torsion spring to measure the torque required to rotate a cone, plate and a spindle in the materials and its viscosities measurement is always at different speed rotational or shearing ( $\dot{\gamma}>0$ ). Because polymer viscosity measurement is based on internal friction, the fluid is meant to move from one layer in relation to another layer. The greater the friction, the greater the amount of force required to cause this movement, which is called shear. Shearing occurs whenever the fluid (polymer) is mixed and pumped and it physically moved or distributed from wellbore to a few or far hundred feet away from the bore; accordingly, the viscosity of the polymer solution will change [91]. This sudden rheological change is based on viscosity dependence on shear rate and shear degradation effect on fluid (polymer) as discussed in sub section 2.11.2 and 2.14.2. Moreover, effective shear degradation research studied cannot be observed or measured at only point zero. It need go beyond zero shearing, that imply that rotational viscometer is best suitable for this research measurement.

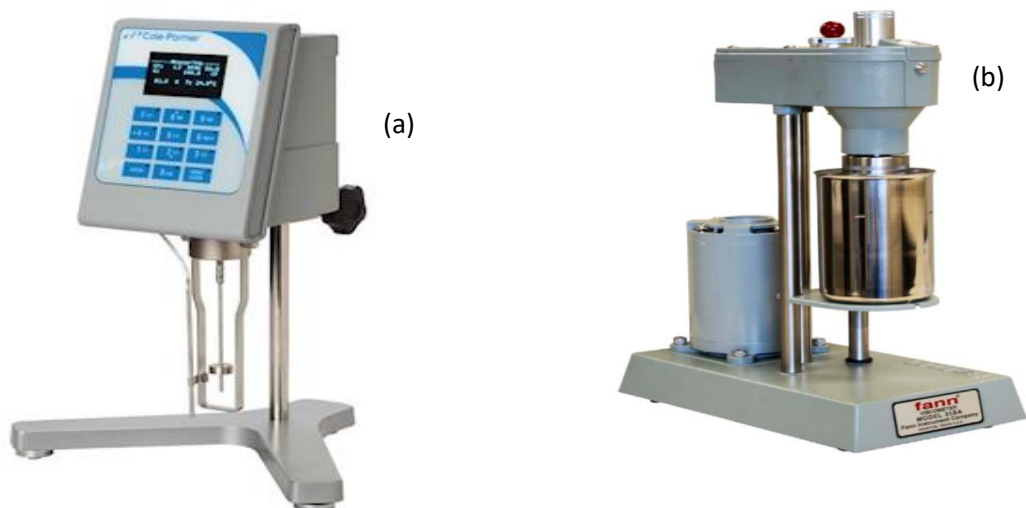


Figure 3.2. Two Rotational Viscometers (a) Cole Parmer [143] and (b) Fann 35A Couette utilised in measuring viscosity [96].

### 3.4.2.1 Viscosity testing and Analysis

Two different rotational viscometers namely; a Fann model 35 Couette and a Cole Parmer, were utilized to measure solution viscosity as shown in figure 3.2. Accordingly, the Fann viscometer system utilized concentric cylinder with rotor and bob radius of 1.8415 and 1.725 cm respectively, and also is Cole Parmer rotational viscometer with R<sub>2</sub> stainless steel spindle. The prepared PAM solutions were aged in an oven at temperatures of 50, 70 and 90°C for time intervals of 0, 1, 2, 4, 10, 20 and 30 days, where an ageing time of zero refers to any measurements immediately after PAM preparation. To assess the effect of shear rate and rheological test on PAM stability, viscosity was measured at rotational speeds of 3, 6, 10, 30, 100, 200, 300 and 600 rpm corresponding to shear rates of 5, 10, 17, 51, 170, 340, 510 and 1021 sec<sup>-1</sup> respectively. Accordingly, to analyse the measured viscosity test results for FANN viscometer, the rotor – bob combination (R1B1) were utilised as shown in **Table 3.2**.

**Table 3.2** Constants for Viscosity calculations

Constant	Rotor – Bob (RB) Combinations					
	R1B1	R2B1	R3B1	R1B2	R1B3	R1B4
Overall Instrument Constant, K Standard F1 Torsion Spring	300	94.18	1355	2672	7620	15200
Shear Rate Constant K3 (Sec-1 Per rpm)	1.7023	5.4225	0.377	0.377	0.268	0.268
Shear Stress Constant for Effective Bob Surface K2 (Cm <sup>-3</sup> )	0.01323	0.01323	0.01323	0.0261	0.0529	0.106

The shear viscosity of a fluid ( $\mu$ ) is calculated by dividing the shear stress ( $\tau$ ) to the shear rate  $\gamma$  as given in **equation 2.6**. Accordingly, for Newtonian fluids  $\mu$  is a

constant but for a non – Newtonian fluids it will be a function of the prevailing shear stress and shear rate put together as seen in **equation 3.0a** and **equation 3.0b** respectively. Hence the viscosity or effective viscosity is measured at any particular shear stress when divided by the shear rate and is expressed in **equation 3.1 and 3.2 [96]**. Accordingly, the sequence of rheological (viscosity testing) and analysis of polymers are given in figure 3.3

$$\text{Shear stress } (\tau) = 1 \text{ Fann} = 5.11 \text{ dynes/cm}^2 \quad \mathbf{3.0 a}$$

$$\text{Shear rate } \gamma = 1/\text{sec} = 1.7023 \text{ N} \quad \mathbf{3.0 b}$$

$$\text{The viscosity } (\mu) = \left( \frac{5.11 \theta}{1.7023N} \right) \times 100 \quad \mathbf{3.1}$$

$$\text{Effective Viscosity } (\mu_e) = 300 \times \left( \frac{\theta}{N} \right) \quad \mathbf{3.2}$$

Where N is revolution per minutes (rpm),  $\theta$  Fann dial reading

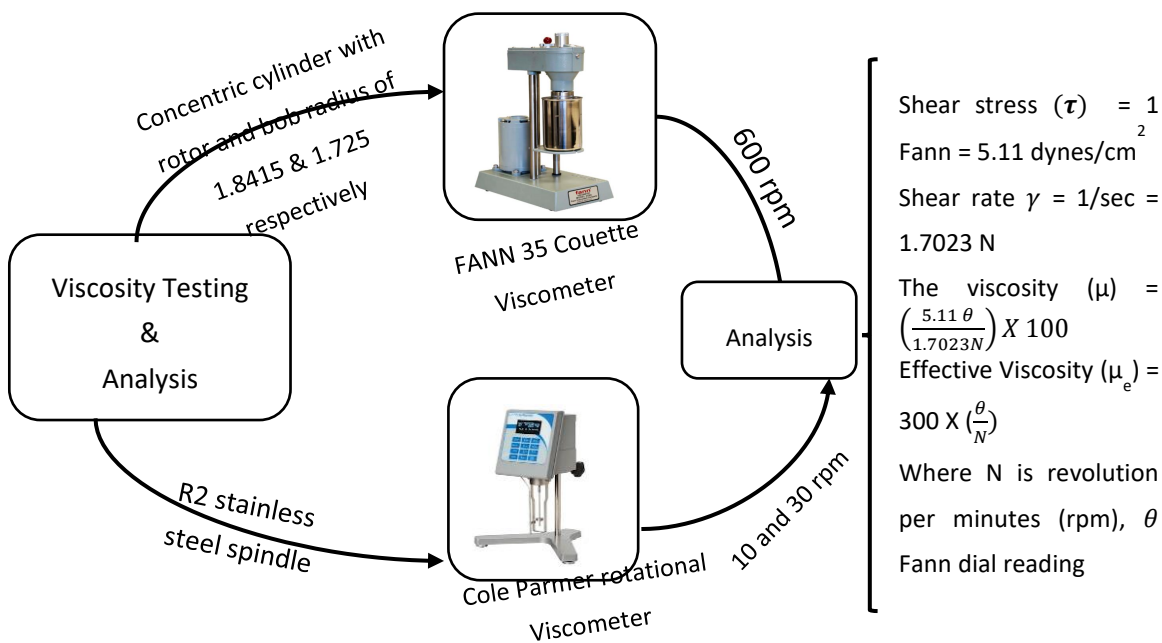


**Figure 3.3.** Sequence of rheological (Viscosity testing) and Analysis of polymers.

### 3.4.3 FTIR AND NMR Techniques

Measuring the degree of changes in hydrolysis gives a measure of the degradation of the polymer gel. This is due to the fact that primary mechanism of polyacrylamide degradation was found to be caused by amide functional group hydrolysis [15]. Accordingly, degree of hydrolysis is defined as the actual number of carboxylate ( $\text{COO}^-$ ) groups that could replace the amide group ( $\text{CONH}_2$ ) divided by the total number of amide and carboxylate groups [114, 117, 130]. To determine the degree of hydrolysis, two techniques were utilized proton nuclear magnetic resonance ( $^1\text{H}$  NMR) and Fourier transform infrared (FTIR) [12]. The Sequential operation FTIR and NMR testing and analysis in determination of degree of hydrolysis are given in figure 3.4

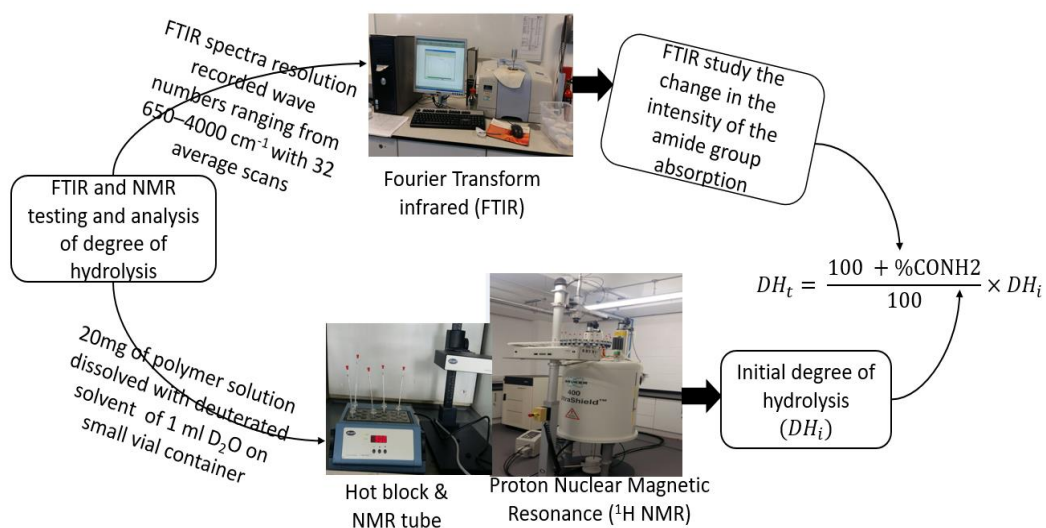


**Figure 3.4.** Sequence of FTIR and NMR testing and analysis of degree of hydrolysis

#### 3.4.3.1 NMR Technique

Basically, the **Nuclear Magnetic Resonance** NMR spectroscopy as given in figure 3.5 is used in determining the structures of molecules. But major application of NMR

spectroscopy in polymers is in study of chain configurations and microstructure. This is obtained by measuring, analysing and interpreting of spectra. NMR has an advantage in that it allows study of the motion and positions of protons, which are not readily detected by most other means [95]. The technique utilises the property of spin which is angular momentum and its associated magnetic moment possessed by nuclei whose atomic number and mass number are both even. Such nuclei include  $^1\text{H}$ ,  $^{13}\text{C}$ ,  $^{17}\text{O}$  and  $^{19}\text{F}$ . Oftentimes the nuclides that mainly utilised are the protons ( $^1\text{H}$ ) and carbon – 13 ( $^{13}\text{C}$ ) because their resonances are the most important for determining the structures of organic molecules [131]. They shows strong magnetic field to material containing such nuclei splits the energy levels into two, representing states with spin parallel and anti – parallel to the field. Measuring the displacement in resonance is termed as chemical shifts. The size of the chemical shift scale is measured with part per millions (ppm). Experimentally, deuterated solvents are often used as the solution solvent because they contribute no resonance. Considering the cost of the deuterated solvent.  $\text{D}_2\text{O}$  and  $\text{CDCl}_3$  are the most commonly used solvents because they are the cheapest and yield satisfactory results most of the time. In  $^1\text{H}$  NMR spectroscopy, the chemical shifts of protons are determined mainly by the diamagnetic shielding because hydrogen atom have one electron and other nuclei with spherically symmetric charge distribution [131]. The chemical shift ( $\delta$ ) is expressed in ppm and it shift range from 0 to 12 ppm. According, **Friebolin [131]** stated that 95% of  $^1\text{H}$  NMR shift in organic molecules lie within the narrow range of  $\delta = 0$  to 12. Whereas in carbon – 13 ( $^{13}\text{C}$ ) NMR spectroscopy shift range from 0 to 240 ppm and are determined by paramagnetic shielding to correct these discrepancies by taking into account the effect of the non – spherical charge distribution. Both the protons ( $^1\text{H}$ ) and carbon

–  $^{13}\text{C}$  NMR could identify the peak area as assigned to the functional group. Due to availability or accessibility this research utilised the protons ( $^1\text{H}$ ) NMR to identify the peak area, accordingly, the proton ( $^1\text{H}$ ) NMR structure – chemical shift assignments shown figure 3.5b.



**Figure 3.5a.** NMR equipment for polymers degree of hydrolysis testing [144]

### 3.4.3.2 NMR Sample Preparation and Analysis

Initial degree of hydrolysis ( $DH_i$ ) of polyacrylamide (PAM) samples collected at zero time were tested and analysed using proton nuclear magnetic resonance spectroscopy ( $^1\text{H}$  NMR). The  $^1\text{H}$  NMR detect the information about type of protons and the number of each type of proton area.

Accordingly, the NMR samples were prepared with 20 mg of the PAM solution dissolved with deuterated solvent of 1 ml of deuterium oxide ( $\text{D}_2\text{O}$ ) on a small vial container which was then placed at three different temperatures of 50, 70 and 90°C on a hot block for over 3 hours. The mixed solution after ageing was then transferred from the vial container to a NMR tube on sample level depth of 5.5 cm with a glass

Pasteur pipette. The NMR tube was inserted into the Bruker Advance III 400 MHz triple-NMR spectrometer with fast magnetic angle spinning (MAS) at 65 KHz and a rotor diameter between 1.3 and 4 mm to achieve the results. The results were analysed via identification of the peak area assigned to the functional group before further processing using Bruker Topspin 3.5 software. The Bruker topspin 3.5 software integrate the amount of H atoms within the integration. The integrating values indicate the amount of H atoms within the integration region by assessing the number of H atoms that give rise to the peak. This help to identify the carbon skeleton such as methine (CH), methylene (CH<sub>2</sub>) and methyl (CH<sub>3</sub>) or other equivalent H atoms.

#### **3.4.3.3 FTIR Technique**

Fourier transform infrared (FTIR) spectroscopy given in figure 3.6 is one of the important analytical technique for study of the molecular interaction. In water soluble polymers, it examine the change in the intensity of amide group absorption of water-soluble polymers. This technique mechanism is based on the vibrations of the atoms of a molecule. The spectrum is commonly obtained by passing infrared radiation through a sample and determining what fraction of the incident radiation is absorbed at a particular energy [132]. The spectrum and positions of peaks are sensitive to environmental changes in the conformations of the macromolecule as could be identified by the chemical interaction on the shifts band. Eventually, this change in the absorption bands of the functional groups occurs when molecules undergo transition between quantum states corresponding to two different internal energies; the frequency of the radiation emitted or absorbed by quantum. The peak in FTIR are represented in transmittance and absorbance against the wavelength. The spectrum peak when in transmittance (%T) could be converted to absorbance



(A). Moreover, the absorbance is equal to the difference between the logarithms of the intensity of the light entering the sample ( $I_0$ ) and the intensity of the light transmitted ( $I$ ) by the sample. The conversion from transmittance to absorbance are represented in equation 3.3 – 3.5.

$$A = \log I_0 - \log I = \log \left( \frac{I_0}{I} \right) \quad \mathbf{3.3}$$

Percentage transmittance (% $T$ )

$$\%T = 100 \times T \quad \mathbf{3.4}$$

$$A = - \log \frac{\%T}{100} \quad \mathbf{3.5}$$

In infrared absorption spectrum, there is always bands that appear can usually be assigned to particular parts of molecule according to functional group.



**Figure 3.6:** FTIR equipment for measuring change in absorbance of amide functional group hydrolysis in polymers [144]

#### 3.4.3.4 FTIR Testing

The Fourier transform infrared (FT-IR) analytical technique was used to measure the percentage change in absorbance of amide functional group hydrolysis after ageing. The aged PAM solutions, were cast into a watch glass and allowed to dry before being placed on a Perkin Elmer spectrum 100 FTIR – Attenuated total

reflectance (ATR) spectrometer sensor for recording. In Perkin Elmer spectrum 100 FTIR is an attached diamond ATR crystal material, where the samples is placed and an arm that is screw down onto the sample, to enhance a perfect contact to the diamond phase. Then the spectrum will begin to appear on the computer screen, continue screwing until good spectrum is obtain. The resolution of FTIR spectra recorded wave numbers ranging from 650–4000  $\text{cm}^{-1}$  with 32 average scans. The absolute measurement provided by the  $^1\text{HNMR}$  on the time zero samples was used as a calibration point for the change in absorbance measurements obtained from the FTIR to derive the absolute degree of hydrolysis of the aged polymer samples.

### **3.5 Modification of PAM with PVP for High Temperature Reservoirs Application**

Improving the performance of PAM focuses on two aspects. The challenging reservoir conditions such as high temperature and high salinity. Two stages were involved to achieve the improvement process. The first stage is to face high temperature challenge in a moderate salinity and the primary synthetic approach followed has been that of substituting part of the polyacrylamide (PAM) with Polyvinylpyrrolidone (PVP). PVP is non-toxic water soluble polymer that effectively protects the polyacrylamide or acrylamide group against extensive thermal hydrolysis [125 -127]. Whereas the second stage is to extend the optimised polymer of PAM and PVP mix to extreme high salinity solution.

#### **3.5.1 PAM AND PVP Mix Sample Preparation**

To face the challenge of high temperature reservoir, two stages in sample preparation approach were utilized. First stage, two water-soluble polymers (A high molecular  $5 - 6 \times 10^6$  Dalton non – ionic polyacrylamide (PAM) combined with Polyvinylpyrrolidone (PVP) of Mw ~ 55,000 Dalton) were utilized and which were

made available by Sigma-Aldrich Company (St. Louis, USA) and the molecular structure are presented in figure 3.2. The modified polymer solution overall composition was prepared with 1% (w/v) 10g concentration as seen in **Table 3.3** and are dissolved in 1000 ml beakers containing formation water with moderate salinity of 43280 ppm as presented in **Table 3.1** and mixed with electric stirrer for 3 hours. The prepared polymer solutions were aged in an oven at temperature 90°C for each time intervals of 0, 1, 2, 4, 10, 20 and 30 days.

Second stage, the optimised composition of PAM and PVP were extended to synthesized formation brine of TDS (200000 ppm) and the results proved that the degree of hydrolysis started increasing and the viscosity decreased. Values of weight ratio and synthesized formation water salinity are presented in **Tables 3.1** respectively. Accordingly, to prevent the degradation of the integrated polymer solution from the presence of oxygen, 1% (w/v) or 10g of Sodium thiosulphate ( $\text{Na}_2\text{S}_2\text{O}_3$ ) concentration were added to the polymer solution as an oxygen scavenger.

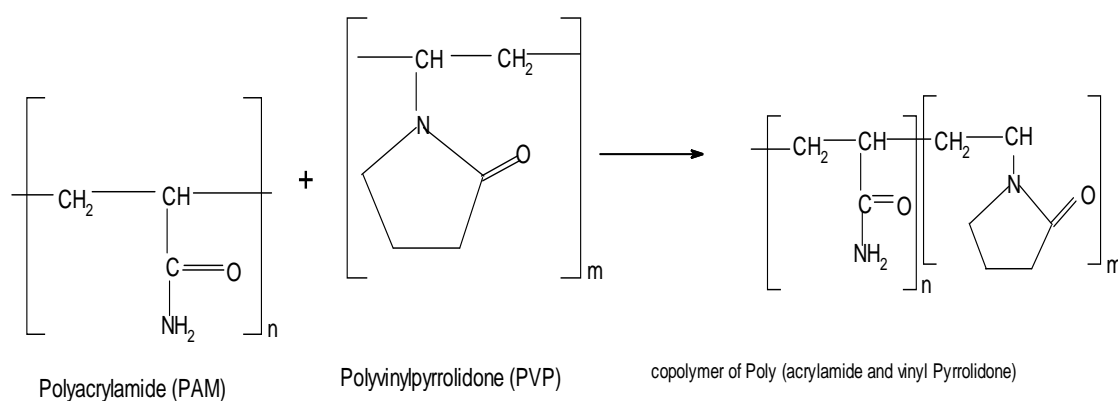


**Figure 3.4.** The Molecular structure of copolymer of Poly (acrylamide and vinyl Pyrrolidone)

**Table 3.3:** The weight composition of PAM:PVP

Sample No:	PAM wt (%)	PVP wt (%)
1	100	0
2	90	10
3	80	20
4	70	30
5	60	40
6	50	50
7	40	60
8	30	70
9	20	80
10	15	85
11	10	90
12	5	95
13	0	100

### **3.6 Modification optimised PAM: PVP Mix with (AMPS) for High Salinity Reservoir.**

The optimised composition of PAM and PVP were extended to synthesized formation salinity of 200000 ppm TDS and the results proved that the degree of hydrolysis started increasing and the viscosity decreased. Improving the optimised PAM and PVP with 2 – acrylamido-2-methylpropanesulphonic acid (AMPS). AMPS is a copolymer of acrylamide with sulfonated co-monomers which offer hydrogen bonding capability and polyelectrolyte behaviour in aqueous solution and in turn giving good stability in high salinity [88].

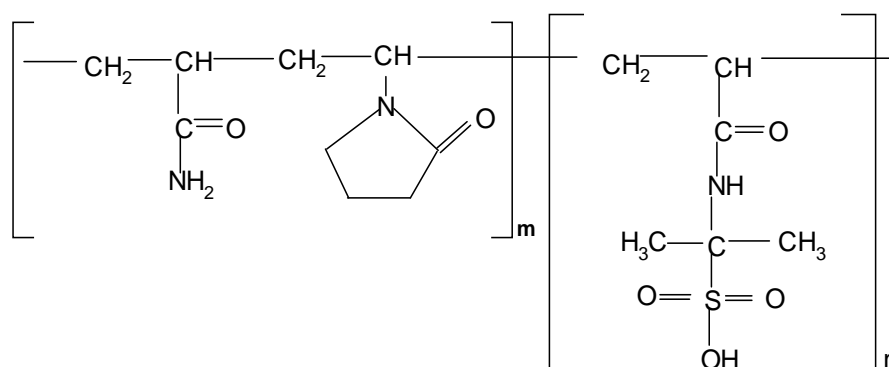
#### **3.6.1 PAM, PVP and AMPS Mix Sample Preparation**

To face the challenge of extreme high salinity with TDS 200,000 ppm, 2 – acrylamido-2-methylpropanesulphonic acid (AMPS) of Mw: 207.25 g/mole made available from Sigma-Aldrich Company (St. Louis, USA) were added to the optimised mixture of PAM and PVP solution. The modified polymer solution overall

composition was prepared with 1% (w/v) 10g concentration as indicated in **Table 3.4** in 1000 ml beakers containing formation water with extreme high salinity of 200000 ppm as seen in **Table 3.1** and mixed with electric stirrer for 3 hours. The prepared polymer solutions were aged in an oven at temperature of 90°C for time intervals of 0, 1, 2, 4, 10, 20 and 30 days. Figure 3.3 is the molecular structure of PAM, PVP and AMPS. Accordingly, to prevent the degradation of the integrated polymer solution(PAM, PVP and AMPS) from the presence of oxygen, 1% (w/v) or 10g of Sodium thiosulphate ( $\text{Na}_2\text{S}_2\text{O}_3$ ) concentration was added to the polymer solution as an oxygen scavenger.

**Table 3.4** The weight composition of PAM:PVP:AMPS

Sample No:	PAM wt (%)	PVP wt (%)	AMPS Wt (%)
1	20	90	0
2	19	76	5
3	18	72	10
4	10	40	50
5	2	8	90
6	0	0	100



copolymer of Poly (acrylamide and vinyl Pyrrolidone)

2 Acrylamido - 2 - methyl propane - sulfonic acid

**Figure 3.3** The Molecular structure of PAM, PVP and AMPS

## CHAPTER 4: ESTIMATION OF SAFE MAXIMUM TEMPERATURE POINT (SMTP) FOR PAM IN SALINE SOLUTION

Serious technical challenge exist when PAM and it derivative HPAM are applied in harsh reservoir conditions of elevated temperature and high salinity during polymer flooding enhanced oil recovery (EOR) operation however, they represent a powerful means of increasing the viscosity of injection water and most importantly, improving mobility ratio [11]. The selective criteria or screening requirement for industrial application of water soluble polymer polyacrylamide (PAM) during improved and enhanced oil recovery (IOR/EOR) is to ensure that the polymer does not degrade as it moves through the reservoir. Accordingly, **Ryles [15]** and **Albonico and Lockhart [16]** stated that the PAM degradation depend vividly on the hydrolysis of the amide functional group. The degree of hydrolysis at which PAM separate or degrade from solution depend directly on the salinity containing divalent cations concentration and inversely on temperature [14]. Such considerations have led to the recommendation of 70 – 82°C as the maximum safe temperature for the use of polyacrylamide in polymer flooding [13 – 16, 115]. Recent study have also claimed that gels produced with polyacrylamide and it derivatives (HPAM) used in (IOR/EOR) for treatment of reservoirs with temperature below 75°C [11]. To maintain a safe operation during PAM application in (IOR/EOR) operation, there is need to establish a correlate on safe maximum temperature in saline solution. Based on the aforementioned, this work through accessible published data on PAM's properties, draw correlations between temperature and saline concentration on the degree of hydrolysis, and the viscosity of PAM solutions. The correlation analysis were based on gradient of PAM hydrolysis and viscosity as a function of time, temperature (within the range of 25 to 93°C) and salinity, to determine the safe

maximum temperature point (SMTP) during improved and enhanced oil recovery (IOR/EOR) applications.

#### 4.1. Correlation of temperature on the degree of hydrolysis (DH) of PAM

According to **Borling et al., [117]**, the proportion of amide groups that convert to carboxylate are called the degree of hydrolysis (DH). The degree of hydrolysis varies from 0 to 60%, in this form the polymer is referred to as a partially hydrolysed polyacrylamide (HPAM). **Gao [86]** explained that the loss of solution viscosity in formation water or brines is the major problem encountered in the use of HPAM for improved oil recovery, due to the presence of monovalent ion and multivalent cations under elevated temperature.

The effect of elevated temperatures on the degree of hydrolysis of PAM was analysed in three different oilfield saline solution of: (5% NaCl), (9% NaCl and 1% CaCl<sub>2</sub>), (3% NaCl and 1% NaHCO<sub>3</sub>) **[14 -15, 11]** as to ascertain suitable safe maximum temperature (SMTP) of PAM in EOR application.

Figure. 4 (a, b, and c) shows the relationship between degree of hydrolysis (%) and ageing time (days) for PAM solutions at temperature ranges of 25 to 93°C in the presence of 5% NaCl (figure 4a) 9% NaCl -1% CaCl<sub>2</sub> (figure 4b) and 3% NaCl-1% NaHCO<sub>3</sub> (figure 4c), respectively. The plots are in two regimes, where first regime represents the linear and second regime non-linear curve. The degree of hydrolysis seen to be sensitive to temperature changes, where increases in temperature result in a higher degree of hydrolysis. Moreover, the hydrolysis is enhanced with addition of salt to the solution. For all cases in the first regime degree of hydrolysis ( $\partial H$ ) appears to be a linear relationship with time as shown in **equation**

**4:**

$$y = \frac{\partial H}{\partial t} x \quad (4)$$

Where  $\frac{\partial H}{\partial t}$  is the gradient of degree of hydrolysis against time

However, for all cases in second regime, degree of hydrolysis ( $\partial H$ ) shows a fit function in the increase form of exponential decay with time as in **equation 4.1**

$$y = \partial H_0 e^{kx} \quad (4.1)$$

Where  $\partial H_0$  is the intercept at the degree of hydrolysis,  $k$  is the gradient or slope

Comparing results from three different studies [14 -15, 11]. It can be concluded that as the temperature increases the gradient DH of PAM for both first regime and second regime increases hence the stability of polymer reduces. Furthermore, the higher the temperature, the more the degree of hydrolysis (DH) of PAM increases in presence of divalent ions ( $\text{CaCl}_2$ ) and monovalent salts (NaCl) and the lesser the ageing time. For instance, in figure 5b second regime, it is demonstrated that a percentage DH of PAM increased within 12 - 38% by 578 days of aging time at temperature of 50, 60 and 70°C, while at 90°C percentage DH increased to 58% with lesser ageing time of 154 days. It implies that at higher temperature like 90°C, the more hydrolyzed it become and the lesser the ageing time. This is also applicable to the first regime with linear relationship, the higher temperature, lesser the ageing time and lower the temperature, the higher the ageing time



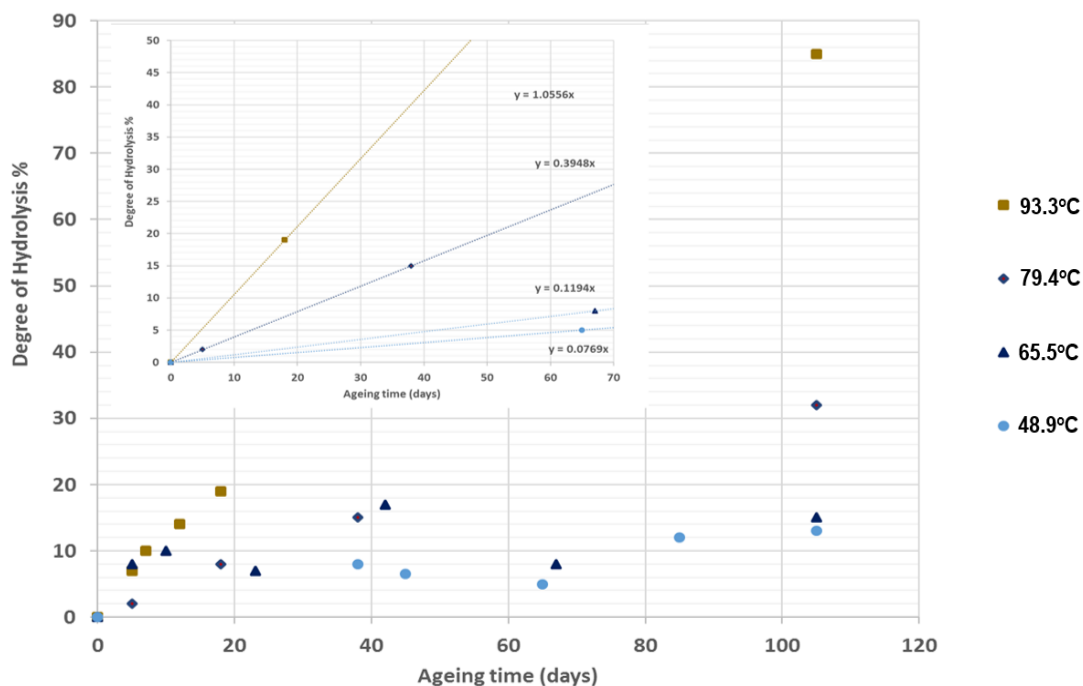


**Figure 4 (a).** Effect of temperature on hydrolysis of PAM in the presence of 5% NaCl [14].

The curve for each temperature can be divided in two regions where first region presents the linear and second region non-linear. The plot on the top of figure is related to the first region where the gradient was evaluated from.

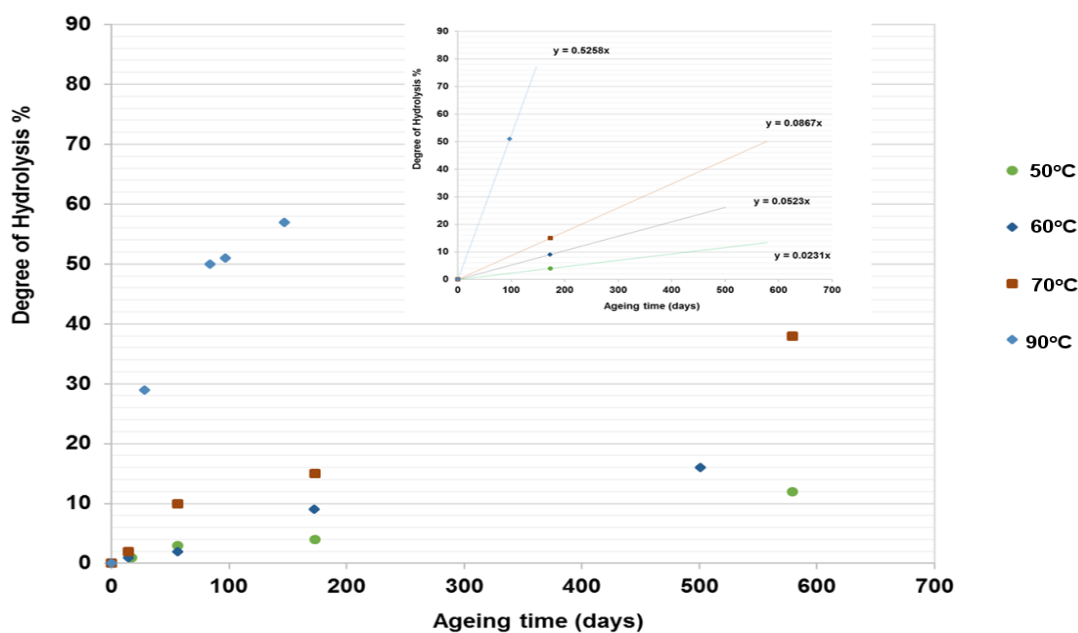


**Figure 4 (b).** Effect of temperature on hydrolysis of PAM in the presence of 9% NaCl -1% CaCl<sub>2</sub>. [15].

The curve for each temperature can be divided in two regions where first region presents the linear and second region non-linear. The plot on the top of figure is related to the first region where the gradient was evaluated from.

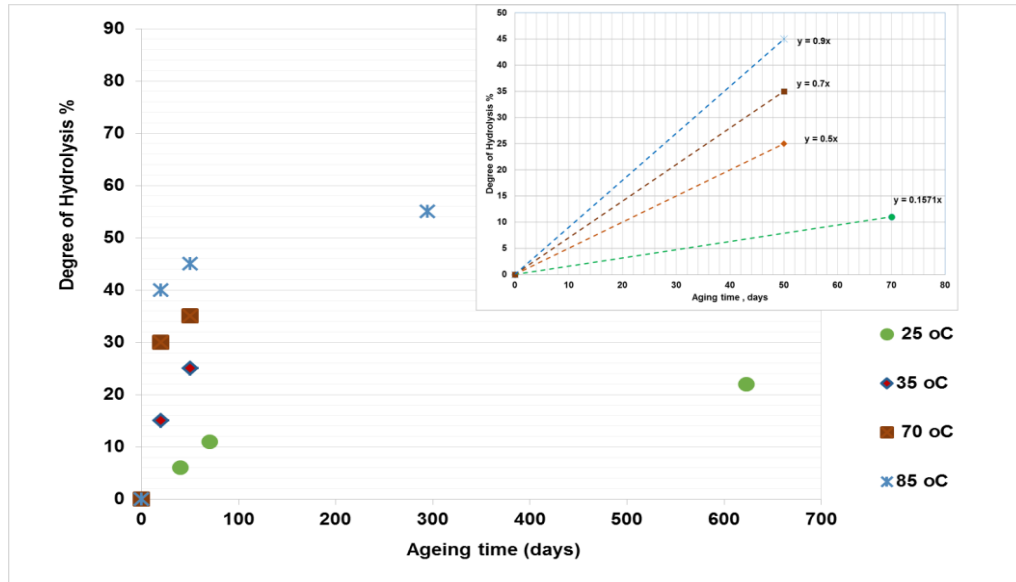


**Figure 4 (c).** Effect of temperature on hydrolysis of PAM in the presence of 3% NaCl -1% NaHCO<sub>3</sub> [108].

The curve for each temperature can be divided in two regions where first region presents the linear and second region non-linear. The plot on the top of figure is related to the first region where the gradient was evaluated from. To try to have better understanding on SMTP of PAM's hydrolysis in presence of saline solution, the next step involved plotting the gradient change of hydrolysis against temperature. The results are presented in **Figure 4.1**.

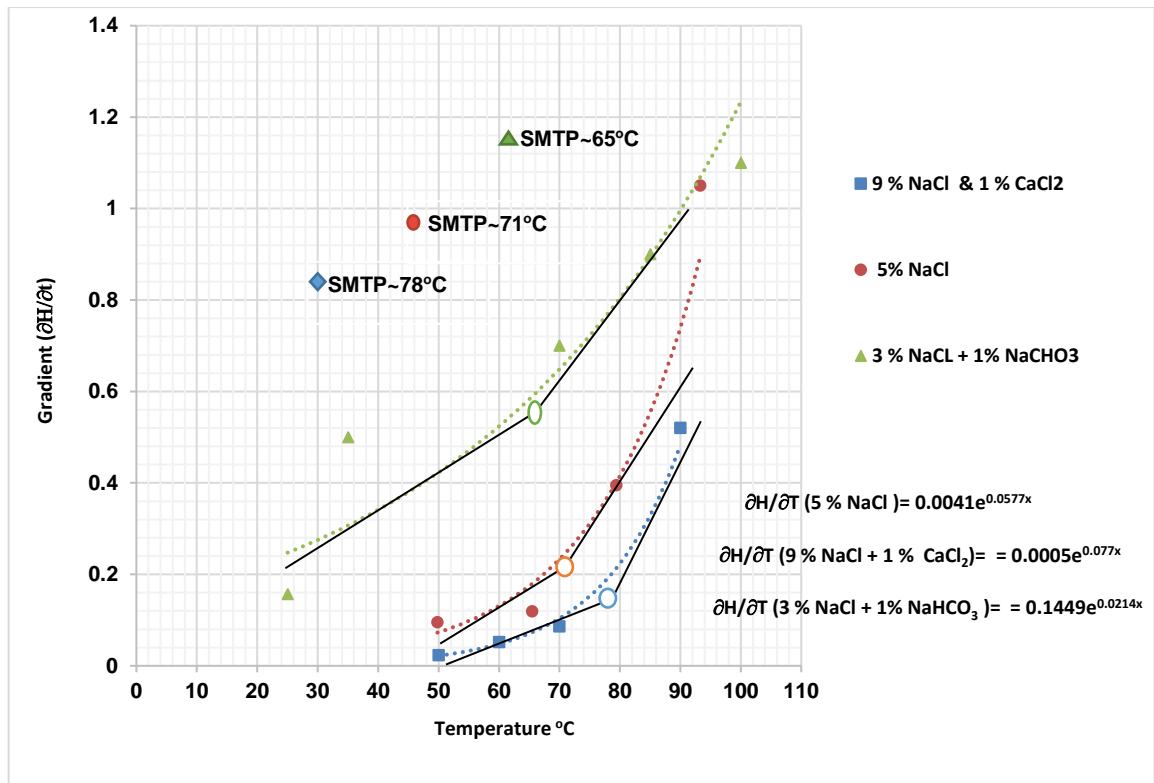


**Figure 4.1.** Graphically determination of safe maximum temperature point (SMTP) from the gradient  $\partial H/\partial t$  (degree of hydrolysis with ageing time) against temperature for PAM solution in the presence of 5% NaCl, 9% NaCl - 1%  $\text{CaCl}_2$ , and 3% NaCl- 1%  $\text{NaHCO}_3$ .

In **Figure 4.1**, there is a sharp shift from slow hydrolysis rate to high hydrolysis rate at a certain temperature. This temperature can be defined as safe maximum temperature point (SMTP), which varies as the ambient solution changes. In the presence of 9% NaCl and 1%  $\text{CaCl}_2$  this shift (SMTP) is observed at 74°C and the correlation on degree of hydrolysis ( $\partial H$ ) against temperature shows a fit function in the increase form of exponential decay with time as seen in equation 4.2a

$$\partial H/\partial T (9 \% \text{ NaCl} + 1 \% \text{ CaCl}_2) = 0.0005e^{0.077x} \quad 4.2a$$

Whereas for 5% NaCl and 3% NaCl and 1%  $\text{NaHCO}_3$  solutions it is observed at about 71°C and 65°C, respectively. Accordingly, 5% NaCl and 3% NaCl and 1%  $\text{NaHCO}_3$  correlations on degree of hydrolysis ( $\partial H$ ) against temperature shows a fit

function in the increase form of exponential decay with time as seen in equation 4.1b and 4.1c respectively

$$\partial H/\partial T (5 \% \text{ NaCl}) = 0.0041e^{0.0577x} \quad 4.2b$$

$$\partial H/\partial T (3 \% \text{ NaCl} + 1 \% \text{ NaHCO}_3) = 0.1449e^{0.0214x} \quad 4.2c$$

Based on this, it is clear that hydrolysis of PAM varies with salinity hence its stability. The abnormally low temperature of 65°C observed for 3% NaCl/1% NaHCO<sub>3</sub> is thought to be due to the increased alkalinity in this solution, which suppresses the SMTP.

#### 4.2. Correlation of temperature on the viscosity of PAM

The viscosity of polymer solution is known to vary widely with temperature. It is obvious that a change in polymer viscosity solution with temperature is associated with the concurrent change in the volume of the polymer. This is because as the temperature increases, the hydrolysed polymer solution opens to the anionic charge attached to the polymer backbone. According to Bill Meyer Jr. [95] temperature dependence of viscosity is found to follow the simple exponential relationship of Arrhenius equation as stated in equation 10.

$$\mu = Ae^{-(E/RT)} \quad (4.3)$$

Where  $\mu$  is viscosity in mPa.s, E is activation energy for viscous flow, A is a constant, R is gas constant and T is the temperature.

From the Arrhenius equation, the viscosity of the polymer solution ( $\mu$ ) depends directly on the ratio of the activated energy (E) of the viscous flow of polymer solution to the temperature. This implies that the viscosity of PAM solution or thermal stability of polymer solution depends on the reservoir temperature.

The effect of temperature on viscosity of PAM against ageing times is demonstrated in **Figure 4.2a** for the solution of 9% NaCl and 1% CaCl<sub>2</sub> at 30 rev/min. At 50°C the viscosity reduction is seen to drop linearly with time at lower rate, while at the higher temperatures of 70°C and 90°C a drastic shift in behaviour is seen where viscosity decreases at higher rate.

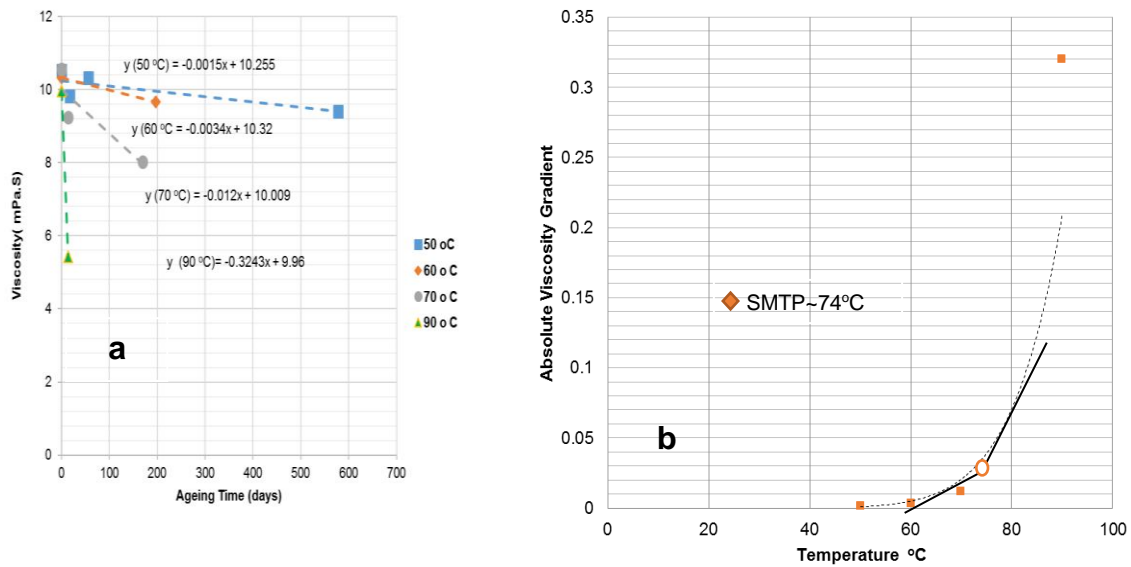


Figure 4.2. (a) Effect of temperature on viscosity of PAM against ageing time (b) absolute viscosity gradient of 9% NaCl and 1% CaCl<sub>2</sub> 30 rev/min [15].

This shift in polymer’s viscosity is illustrated in **Figure 4.2** by plotting the absolute value of viscosity gradients extracted from **Figure 4.2 a**. **Figure. 4.2b** can be used to obtain the safe maximum temperature point (SMTP) for the application of a polymer in a saline solution, in a similar approach to that obtained from the gradient of degree of hydrolysis. It is worth mentioning that the SMTP obtained from viscosity data is similar as the one obtained from hydrolysis data for the same solution which shows the accuracy of proposed method in obtaining the polymer SMTP for specific saline solution.

As it is reported by **Stahl and Schulz [81]** the polymer solutions used in an oilfield are non-Newtonian fluids which are usually affected by shear rate. As shear

rate is a function of viscosity, any changes in mechanical degradation which may occurs in pipes, through choke, valves or pumps above a certain velocity or pressure drop, can influence the solution’s properties. Accordingly, at a low shear rate the polymer fluid behaves as a Newtonian fluid and thus the viscosity does not vary with the shear rate. However, as the shear rate increases the polymer molecules deform and the viscosity decreases. Such a situation, where the polymer viscosity solution reversibly decreases with increasing shear rate is termed shear thinning. The effect of shear thinning on SMTP has been investigated by fitting data measured for a saline solution of 9% NaCl and 1% CaCl<sub>2</sub> at 60 and 12 revolutions per minutes (two and five times lower that the revolution speed for the data presented in figure 4.2. These data are presented in Figure 4.3 a, and b. As temperature increases viscosity decreases, hence the aging time decreases. It is also worth mentioning that following decrease in the rotational speed (rev/min) of the device, a decrease in shear rate impacted the viscosity results, especially for lower temperature, where higher rotational speed increased the viscosity in contrast to the lower rotation which shows normal and expected trend.

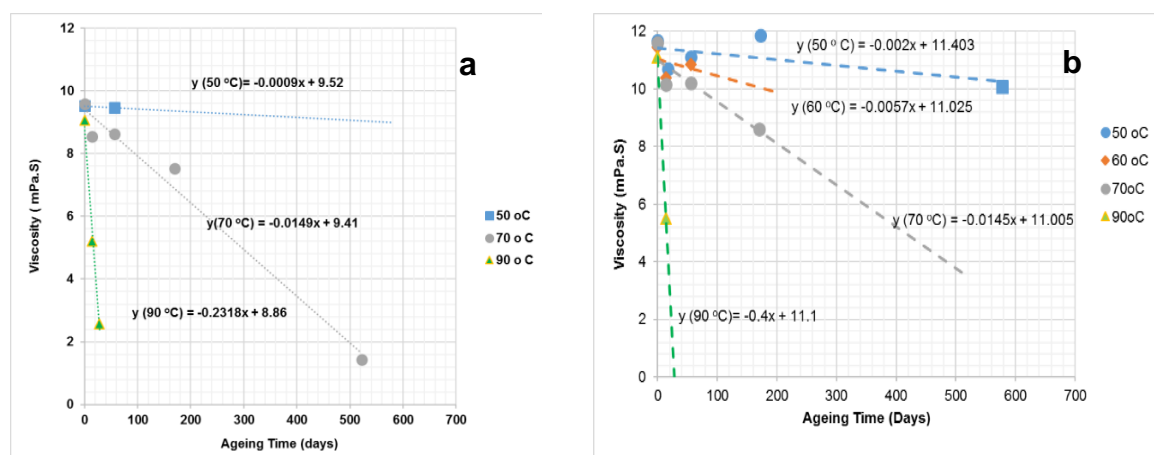
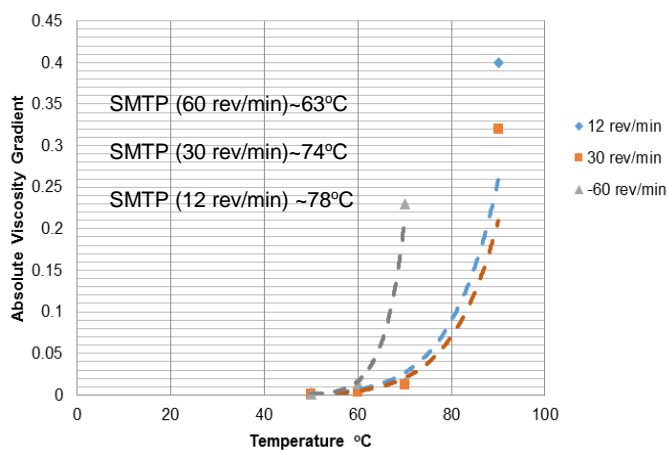


Figure 4.3. Effect of temperature on viscosity of PAM against ageing times 9 % NaCl + 1 % CaCl<sub>2</sub> for (a) 60 rev/min and (b) 12 rev/min [15].

The absolute values of a viscosity gradient for the data presented in Figures 4.2 a, b, and Figure 4.3 are plotted in Figure 4.4 as a function of temperature. The estimated SMTP values for these solutions at 30, 12 and 60 rev/min are 74, 78 and 63°C respectively in the presence of 9 % NaCl + 1 % CaCl<sub>2</sub>. Comparing these results, it is apparent that SMTP for higher share rate of 60° decreases about 25°C, which indicates that the polymer become instable in shorter aging time at higher shear compared to lower shear rate. Higher the shear rate, lower the SMTP value



**Figure 4.4.** The absolute viscosity gradient against temperature in the presence of 9% NaCl and 1% CaCl<sub>2</sub> at 12, 30, and 60 rev/min.

In summary, PAM degradation in the presence of brine containing divalent cations depends on the extent of degree of hydrolysis which is caused by temperature [14]. Such considerations have led to the recommendation of 70 – 82°C as the maximum safe temperature for the use of polyacrylamide in polymer flooding [13 – 16, 115]. Recent study have also claimed that gels produced with polyacrylamide and its derivatives (HPAM) used in (IOR/EOR) for treatment of reservoirs with temperature below 75°C [11]. To maintain a safe operation during PAM application in (IOR/EOR) operation, correlate on safe maximum temperature in saline solution have been established.

The results obtained from SMTP correlation analysis proved that different saline solution like NaCl, CaCl<sub>2</sub> and NaHCO<sub>3</sub> contain different SMTP. Accordingly, at 5% NaCl, the SMTP was about 71°C, while a combined saline solution containing 9% NaCl and 1% CaCl<sub>2</sub>, the SMTP was 78°C and 65°C at 3% NaCl and 1% NaHCO<sub>3</sub>. It is worth mentioning that the SMTP obtained from viscosity data is similar as the one obtained from hydrolysis data for the same solution which shows the accuracy of proposed method in obtaining the polymer SMTP for specific saline solution. The proposed correlations provide a means of predicting the stability of PAM for reservoirs with different temperature, salinity and shear rates conditions.

The correlations provided an insight in the experimental studies on the effectiveness of PAM application in hydrocarbon reservoirs at different operational conditions of moderate and high temperature, shear rate and moderate salinity of 43,280 ppm discussed in Chapter 5.



## **CHAPTER 5: STUDYING THE EFFECTIVENESS OF POLYACRYLAMIDE (PAM) FOR EOR APPLICATION AT DIFFERENT OPERATIONAL CONDITIONS.**

Degradation of polymer solution (PAM) is determined by measuring the solution viscosity as discussed in chapter 2. However, this implies that the polymer solution viscosity plays an important role in successful polymer flooding projects during EOR operation. The specification for application of polymer solution such hydrolyzed PAM in EOR tertiary recovery must maintain a relatively apparent viscosity ( $\geq 11.5$  mPa.s) under the influences of moderate and high temperatures, shearing and formation water salinity [10]. Accordingly, in studying the extent of polymer solution (PAM) performance under the influence of the aforementioned variables, it is facilitated through a detailed practical investigation ranges from degree of hydrolysis in temperature aged sample to the viscosity change observed on shearing time and in depth shear rate, which is view from rheological behavior.

### **5.1 Hydrolysis of PAM in thermally aged samples.**

The rate of hydrolysis of amide groups has been found to be the primary mechanism behind polyacrylamide (PAM) degradation. Later interaction between the hydrolysed polyacrylamide and saline solutions containing monovalent salt (NaCl) and multivalent salts ( $MgCl_2$  and  $CaCl_2$ ) could cause significant losses in solution viscosity. However, the rate of hydrolysis was found to depend mostly on temperature; apparently, the higher the temperature, the higher the degree of hydrolysis [15]. The more increase in the amide group hydrolysis, the more changes in solution properties and rheology of polyacrylamide solution is affected. To study the characteristic or rheological behaviour of polyacrylamide and determine the extent of hydrolysis at moderate and high temperature of 50, 70 and 90°C. FTIR

and NMR spectroscopy were utilised and the experimental approach are discussed in chapter 3.

### 5.1.1 FTIR Analysis for PAM Amide group Hydrolysis.

Previous studies by [114, 117, 130] have proposed that the proportion of amide (CONH<sub>2</sub>) groups that is converted to carboxylate (COO<sup>-</sup>) is termed as the degree of hydrolysis (DH). FTIR can be used to monitor the change in absorbance associated with the stretching of the secondary amide (CONH<sub>2</sub>) C=O to give a measure of the change in degree of hydrolysis of the amide functional group. Emission or absorption spectra arise when PAM molecules undergo transitions between quantum states corresponding to the internal energy. In infrared spectroscopy, the presence of different functional groups results in the absorption of energy at specific wavelengths and its re-transmission results in the formation of peaks. **Table 5.0** shows the assignment of the FT-IR characterization of the bands and spectra of PAM.

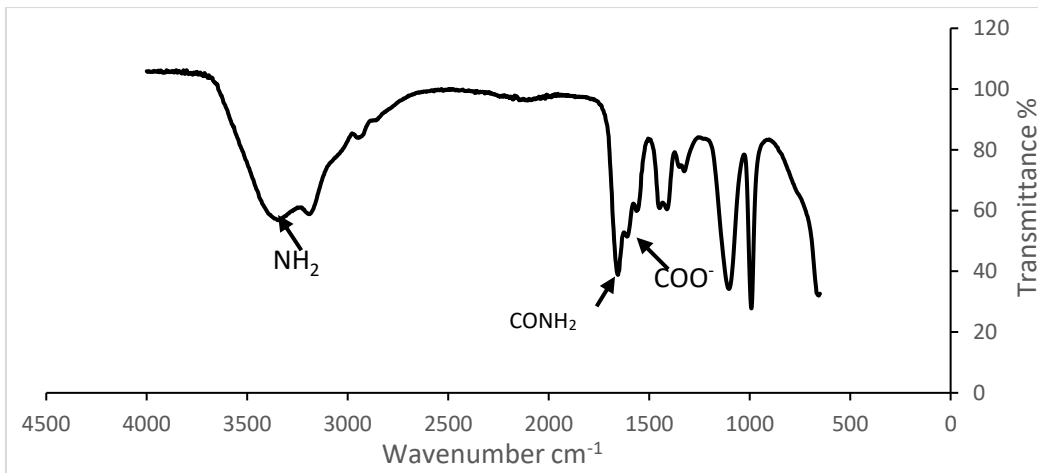
**Table 5.0:** Assignment of the FT – IR Characterization of bands of the PAM

Frequency	Assignment
3340 – 3332	Primary amide NH <sub>2</sub> asymmetric stretching
3300 – 3250	Secondary amide N – H stretching
3190 – 3170	Primary amide NH <sub>2</sub> symmetric stretching
3100 – 3060	Secondary amide II overtone
1680 – 1630	Primary amide C = O stretching
1630 – 1603	Secondary amide C = O stretching
<b>Carbonyl containing compound</b>	
The major bands which appear in the infrared spectra of carboxylic acids (which contain the COOH group) summarized below:	

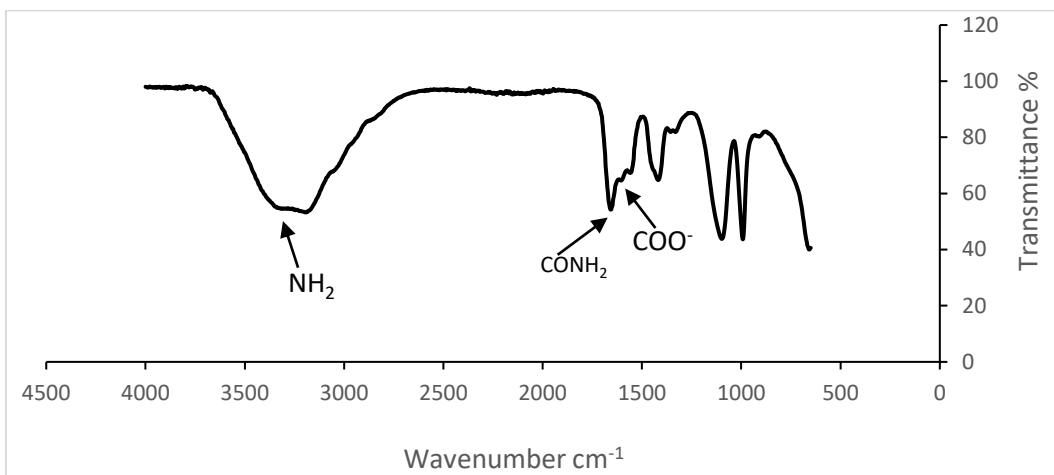
1603 – 1330	COO <sup>-</sup> stretching
1330 – 1300	C – O stretching
1300 - 1000	C – O – H in plane bending
900 - 992	C – O – H out of plane bending

Primary amide NH<sub>2</sub> symmetric stretching occurred at 3190–3170 cm<sup>-1</sup> and the asymmetric stretching band of NH<sub>2</sub> appeared at 3340–3332 cm<sup>-1</sup>. A combination of these two peaks was used to determine the transmittance of the amide group. Secondary amide N–H stretching was observed at 3300–3250 cm<sup>-1</sup> with a corresponding secondary amide II overtone. The primary amide C=O stretching (CONH<sub>2</sub>) was assigned in a shift range of 1680–1630 cm<sup>-1</sup>. The vibrational modes of amide groups may be affected due to hydrogen bonding. Therefore, the secondary amide C=O stretching (CONH<sub>2</sub>) was assigned at a point between 1630–1603 cm<sup>-1</sup>.

Four significant peaks for carboxylate groups were observed at 1330-1600 cm<sup>-1</sup> due to stretching of acrylate. The vibration on the band shifted at C–O stretching at around 1200–1300 cm<sup>-1</sup>; the vibrations also existed in plane bending around 1000–1300 cm<sup>-1</sup> and out-of-plane bending at 900–992 cm<sup>-1</sup>. **Figures 5.0** presents the percentage transmittance versus wave-number for PAM solutions in pure water and brine respectively.



a) PAM in pure water



b) PAM in brine

**Figure 5.0:** FT-IR Spectra of PAM in pure water (a) and brine (b)

For relevance in application, the value of transmittance is converted into absorbance using **equation 3.3 [132]**. The amide group content of the hydrolysed polyacrylamide was determined from the intensities of the absorbance in the amide group ( $\text{CONH}_2$ ). In water soluble polymers like polyacrylamide, the absorption spectrum is often surprisingly consider as the large number of atoms involved in the normal vibrations of same frequency and therefore appear in the spectrum as one absorption band. The absorption band wavelengths arising from the functional

group and atomic vibrations. These results are presented in **Figure 5.1a** and **Figure 5.1b**.

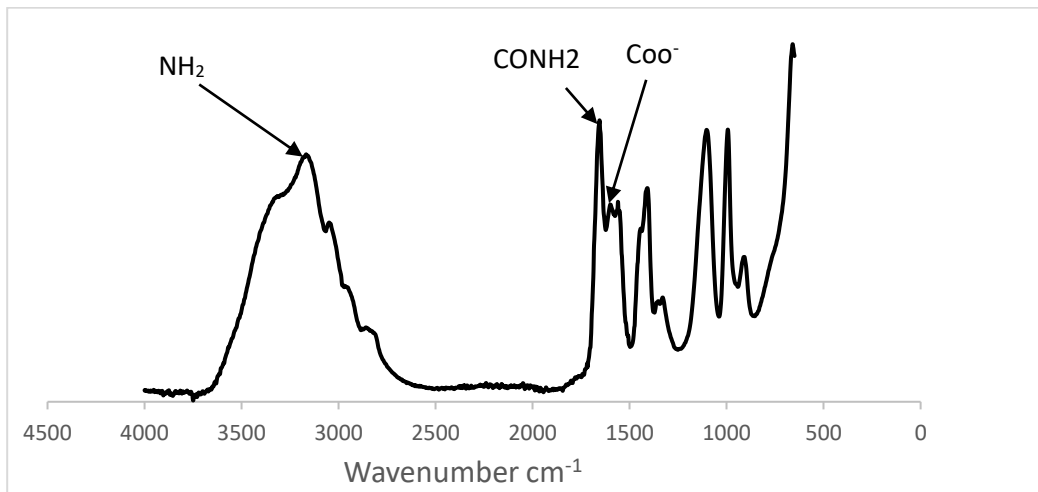
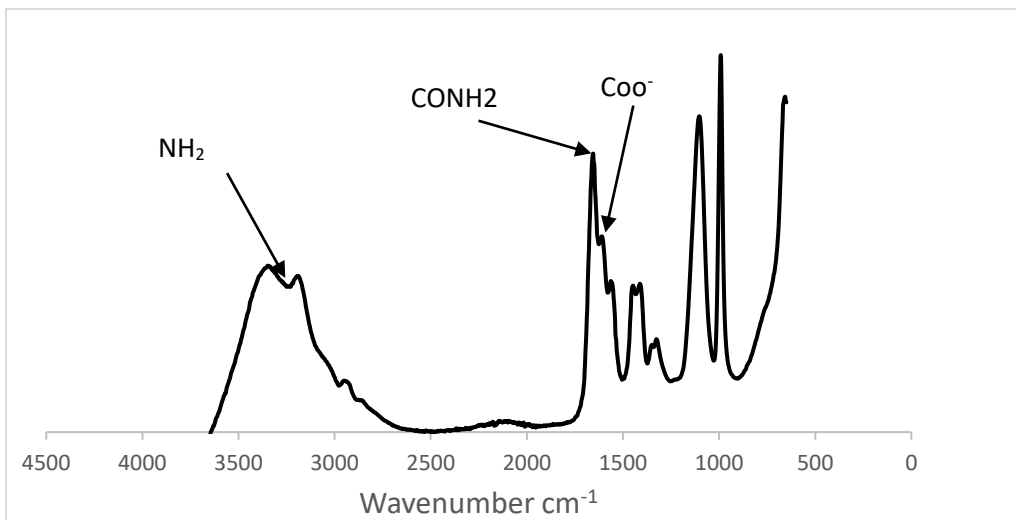


Figure 5.1a: FT-IR Spectra absorbance of PAM at 50°C in pure water.



**Figure 5.1b:** FT-IR Spectra absorbance of PAM at 50°C in brine.

The percentage increase in amide absorbance is equal to the difference between the initial amide absorbance at day zero ( $A_0$ ) and each amide absorbance at the designated ageing times ( $A_{0, 1, 2, 4...30}$ ) over the initial amide absorbance expressed as a percentage, as shown in equation 4.0:

$$\text{Percentage change in Absorbance (\%)} = \frac{A_{0,1,2,4\dots,30} - A_0}{A_0} \times 100 \quad \mathbf{4.0}$$

**Figures 5.2a, b and c** present the percentage change in absorbance of amide groups (CONH<sub>2</sub>) against ageing time in days at 50, 70 and 90°C for both PAM in pure water and PAM mix with brine. As shown in these figures, the percentage of amides absorbance at 50, 70 and 90°C increases from 18 to 30%, from 33 to 57%, and from 48 to 57% at the different temperatures. It is also noticed that the more the ageing time, the more the percentage amides absorbance increases at the designated temperature.

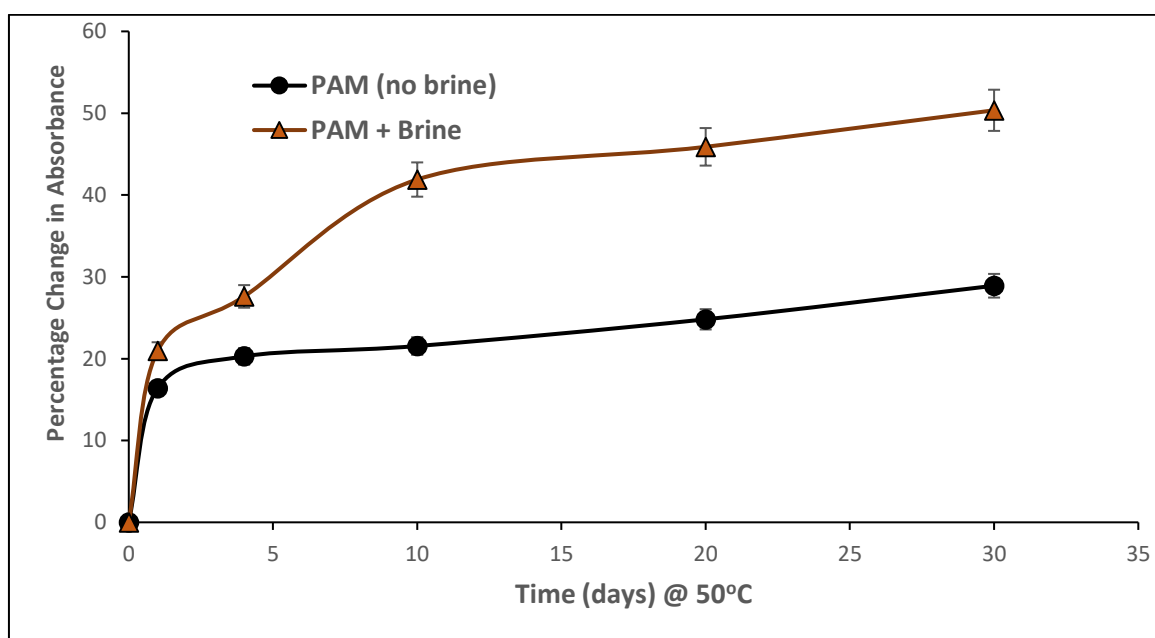


**Figure 5.2a:** Percentage change in absorbance in PAM solution in presence of and without brine at 50°C.

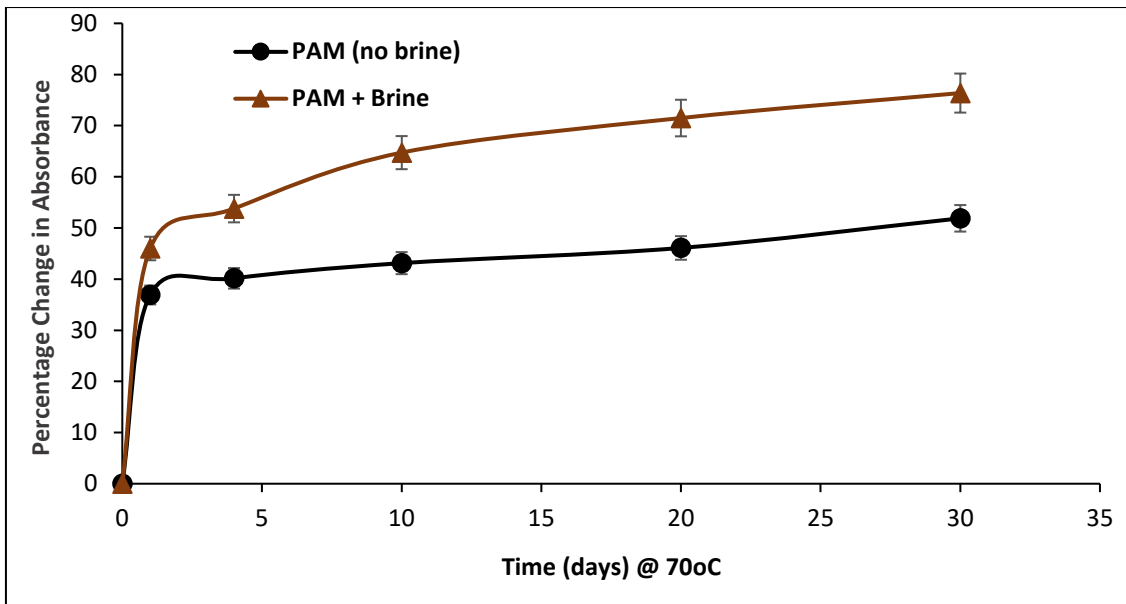


**Figure 5.2b:** Percentage change in absorbance in PAM solution in presence of and without brine at 70°C.

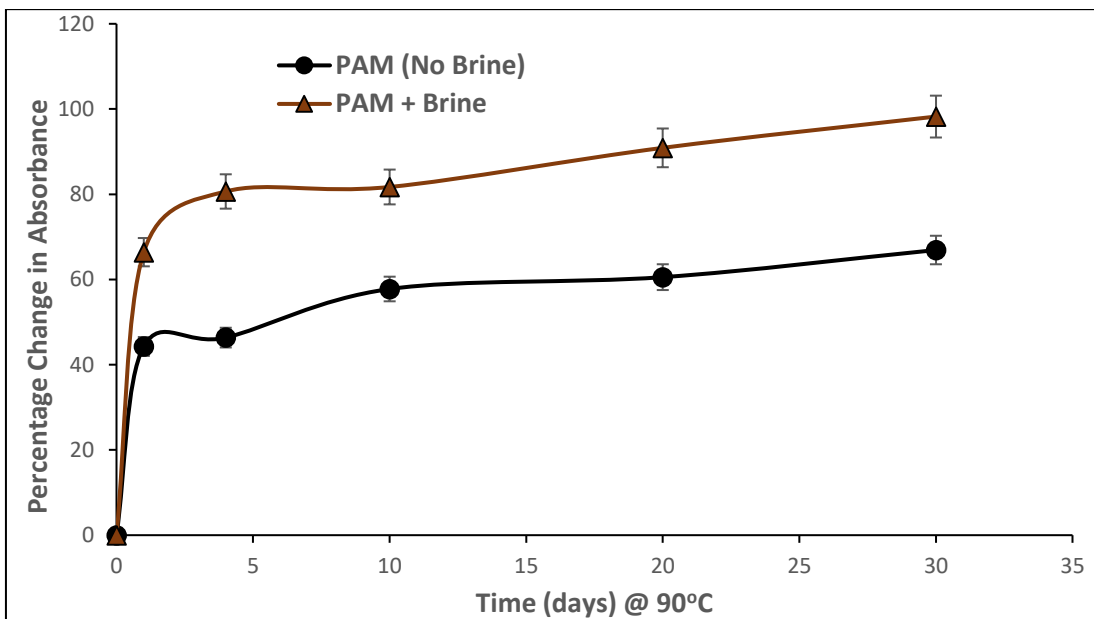


**Figure 5.2c:** Percentage change in absorbance in PAM solution in presence of and without brine at 90°C.

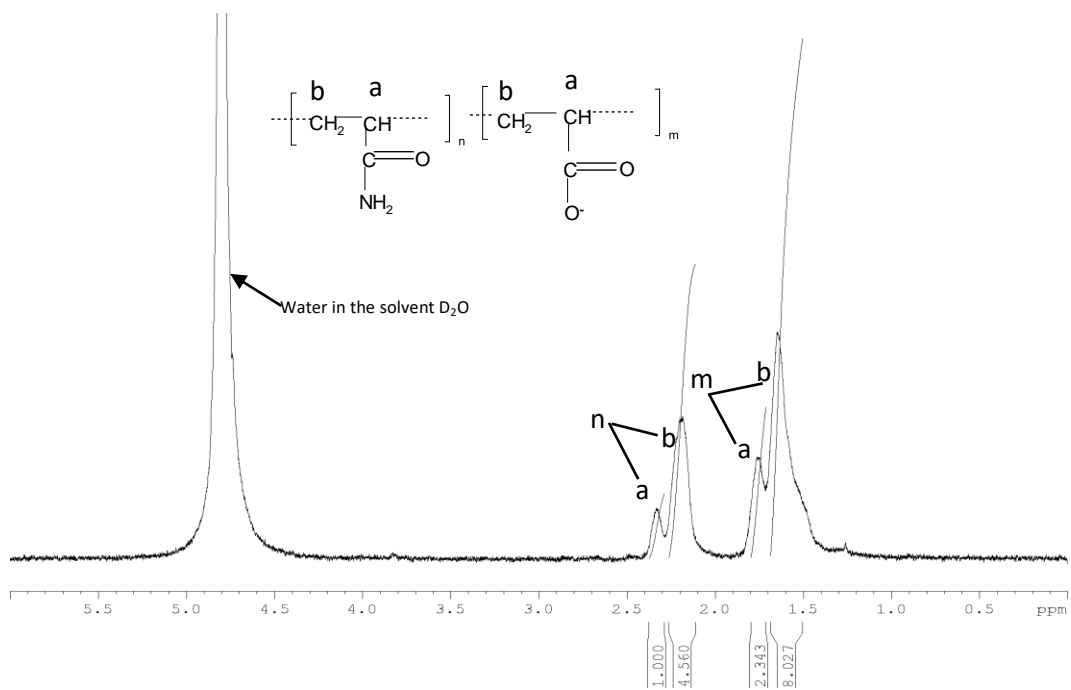
These results prove that the percentage change in the absorbance of amide groups present in PAM increases as the temperature increases, indicating that temperature is the major driving force for the degradation of PAM. In the presence of brine, the

amide group in PAM is further hydrolysed, where at the same temperature conditions as in the absence of brine the percentage of amide groups increased from 25 to 61%, from 38 to 75% and from 62 to 88%, at the three different temperatures. Therefore, the interaction of PAM with brine at 50, 70 and 90°C shows greater percentage increases in amide groups in the solutions than when brine is not present. It also shows that percentage absorbance of amide functional group hydrolysis is quite rapid at 90°C compare to 50 and 70°C both for PAM (no brine) and PAM with brine additive.

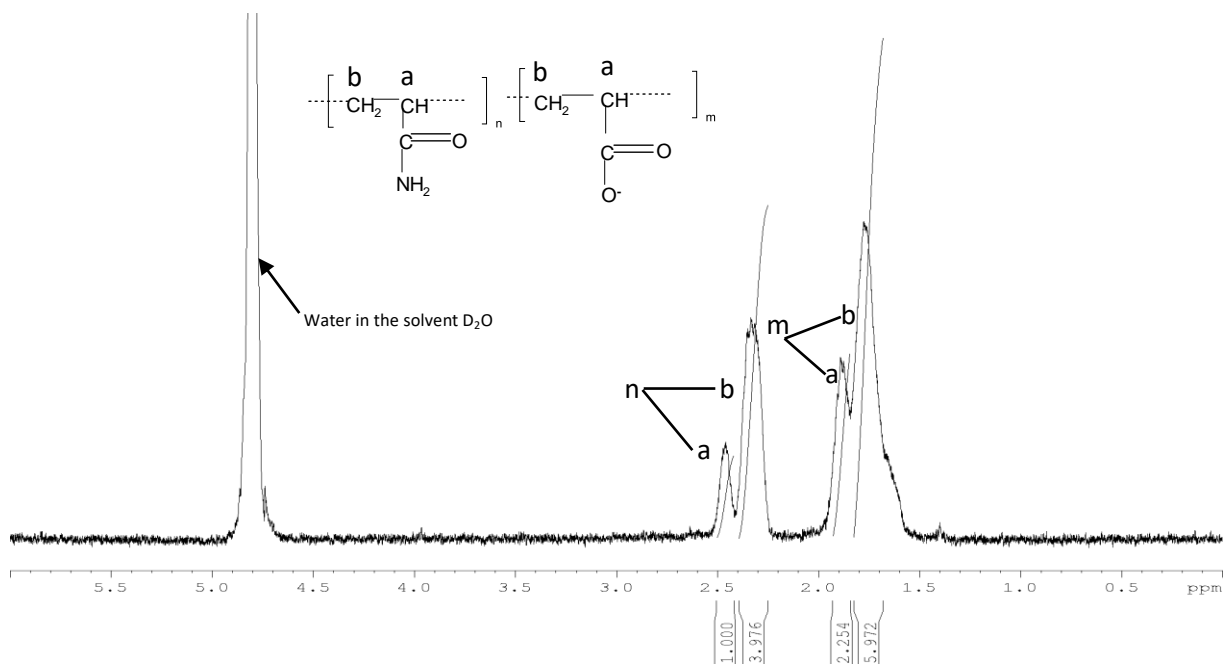
### **5.1.2 NMR measurements on time zero samples**

In the section 4.1.1, the FITR was utilised to determine the percentage amide group absorbance which is a step to amide functional group hydrolysis. Nevertheless,  $^1\text{H}$  NMR in this section is used in determining the degree of hydrolysis. The analysis of the degree of hydrolysis was performed by processing the calibration axis and integration of the peak area using Bruker topspin 3.5 software. In Bruker topspin 3.5 software, the integral values from the peak area indicate the total amount of hydrogen (H) atoms within the molecular structure, and this could help in identifying the functional groups such as methine (CH), methylene ( $\text{CH}_2$ ) and methyl ( $\text{CH}_3$ ) that contain the amide ( $\text{CONH}_2$ ) and carboxylate ( $\text{COO}^-$ ) groups. **Figure 5.3** illustrates the  $^1\text{H}$  NMR spectra for PAM dissolved in pure water and brine.





(a) PAM dissolved in pure water



(b) PAM dissolved in brine

**Figure 5.3:** (<sup>1</sup>H NMR) spectra: (a) PAM dissolved in pure water (b) PAM dissolved in brine.

The first peak in these two scans positioned at 4.8 ppm represents water content in the deuterium oxide solvent. The peaks measured at 2.20 - 2.40 and 1.60 -1.80 ppm represent hydrogen (H) atom in functioning group of methine (CH) attached to amide (CONH<sub>2</sub>) and carboxylate (COO<sup>-</sup>) groups, respectively. The degree of hydrolysis (DH) was calculated using equation 5.1.

$$DH (\%) = \frac{n_a}{m_a + n_a} \times 100 \quad 5.1$$

Where  $n_a$  is the position of the amide groups (CONH<sub>2</sub>) on the peak shift as assigned by the hydrogen atom in methine (CH),  $m_a$  is the position of the Carboxylate group (COO<sup>-</sup>) in the peak shift as assigned by the Hydrogen atom in methine (CH).

The degrees of hydrolysis of the initial samples for PAM dissolved in both pure water and brine are recorded in **Table 5.1**.

**Table 5.1:** Initial degree of hydrolysis ( $DH_i$ ) for pure water and brine samples

Temperature	$DH_i$ (pure water)	$DH_i$ (Brine)
50°C	30%	34%
70°C	31%	37%
90°C	33%	38%

For the initial samples at time zero, it is clear that the initial degree of hydrolysis ( $DH_i$ ) rises with temperature for both sets of samples. The initial degree of hydrolysis for the brine dataset is systematically higher than that for the samples prepared in pure water.

To convert the percentage absorbance change into the degree of hydrolysis, the percentage increase in amide groups and the initial degree of hydrolysis (DH) are combined and the final equation is expressed in **equation 5.3**.

$$DH_t = \frac{100 + \%CONH_2}{100} \times DH_i \quad \mathbf{5.3}$$

Where  $DH_t$  is the degree of hydrolysis, at each designated time,  $DH_i$  is the initial degree of hydrolysis at day zero from the  $^1H$  NMR analysis and  $\%CONH_2$  is the percentage change in absorbance.

Apparently, it is a necessity to determine the initial degree of hydrolysis of each temperature reservoir so that the peak viscosity of PAM solution can quickly be reached before the beginning point of degradation.

## **5.2 Effect of temperature and brine on hydrolysis of PAM solution**

Temperature is behind the extensive amide group hydrolysis of PAM and brings about significant changes in solution properties, rheological and phase behaviour. According to Albonico and Lockhart [16] the degree of hydrolysis at which PAM separates from solution depends directly on the brine concentration and inversely proportional to the temperature. From **figure 5.4a and 5.4b** is an evidence that temperature and brine solution plotted as a function of ageing time is the determining factor on amide functional group hydrolysis. PAM in pure water demonstrated that, the higher the temperature, the faster the rate of hydrolysis.

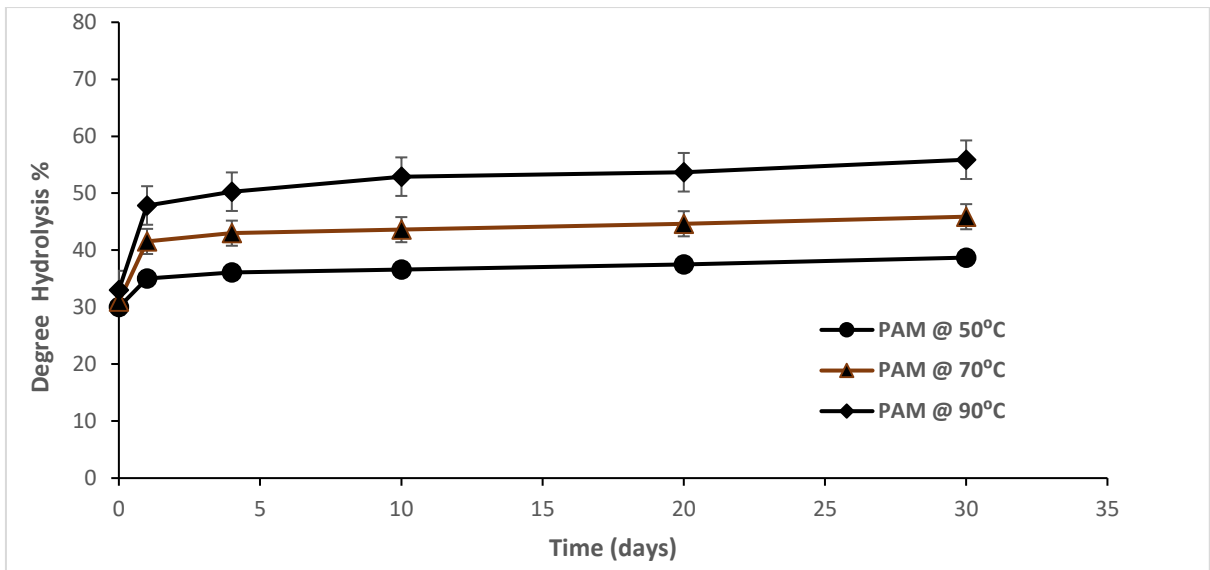


**Figure 5.4a:** Degree of hydrolysis of PAM in pure water at temperature of 50, 70 and 90°C.

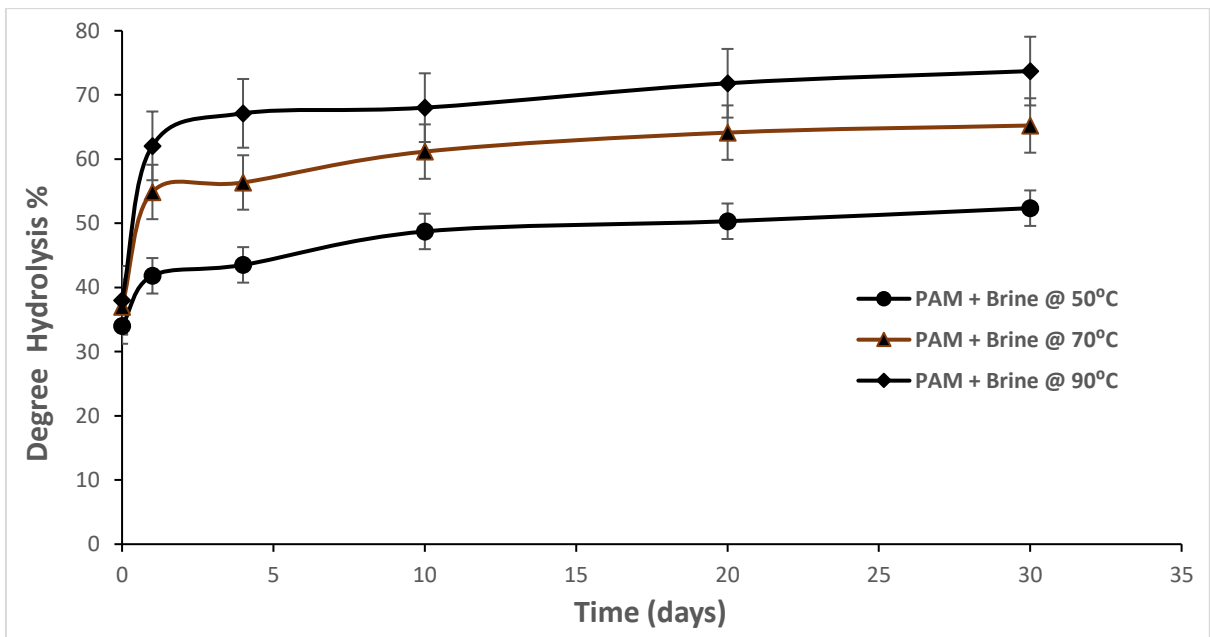


**Figure 5.4b:** Degree of hydrolysis of PAM in brine at temperature of 50, 70 and 90°C.

**Figure 5.4 (a)** provides evidence of the degree of hydrolysis against ageing time for PAM mixed in pure state. As seen in this figure, temperature and ageing time

are the main factors determining the increasing degree of hydrolysis. All samples demonstrate an increase in hydrolysis with temperature.

Using a similar approach, the degrees of hydrolysis of PAM in the presence of salts or brine against ageing time for the temperatures studied are demonstrated in **figure 5.4(b)**. The degree of hydrolysis in the brine solutions is systematically higher than that observed in the samples prepared in pure water. For instance, degrees of hydrolysis of about 39%, 46% and 56 % at 50°C, 70°C and 90°C for PAM solution in pure water increased after ageing up to 30 days to values of about 52%, 65%, and 74% respectively in brine solution. All records show two dissimilar phases of hydrolysis. In phase one (0 -1 day) the degree of hydrolysis rises very quickly. In phase two, the rate of change in degree of hydrolysis is reduced significantly and the trend takes a linear form.

### **5.3 Rheological Behaviour of PAM Solution.**

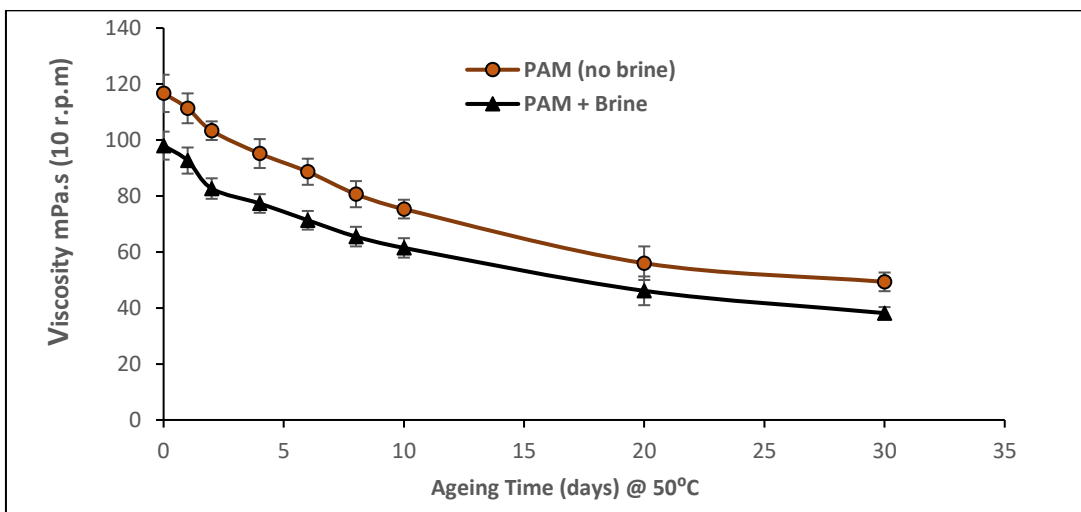
The viscosity of the displacing fluid is a necessary criterion for screening an injection fluid during chemical flooding, because an optimal viscosity of the displacing fluid is required to ensure favourable mobility as to achieve better oil recovery with good injectivity at lower cost [11]. The viscous behaviour of PAM at different temperatures and salinities was measured in terms of its thermal stability, where the estimation detected two types of rheological behaviour: thixotropic (a change in polymer viscosity with time under constant shear rate) and pseudo-plastic (where viscosity decrease with increase in shear rate).

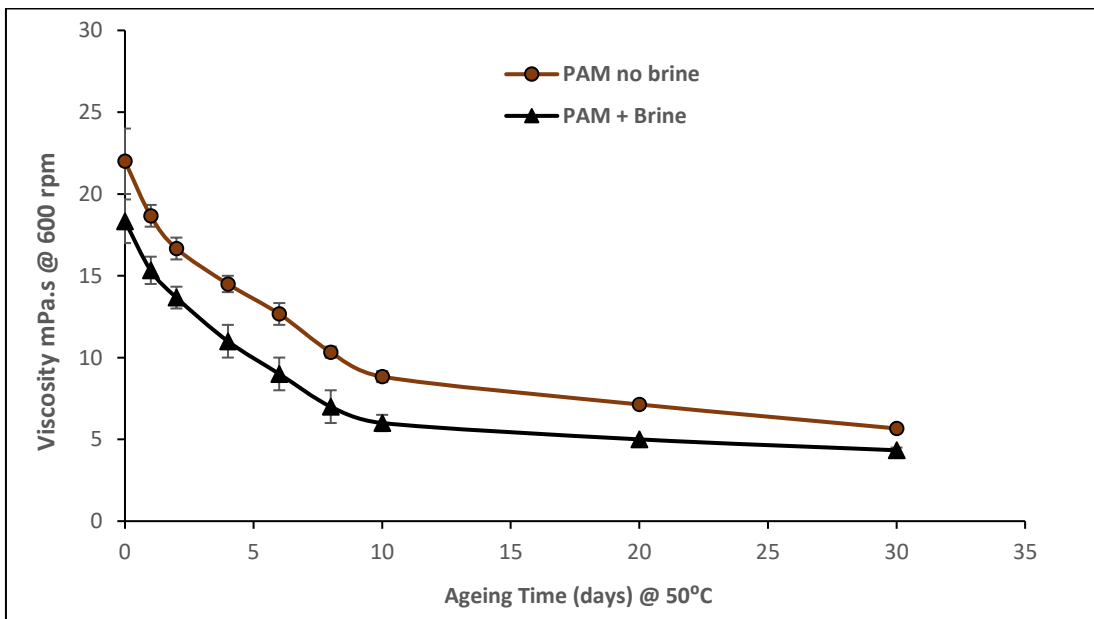
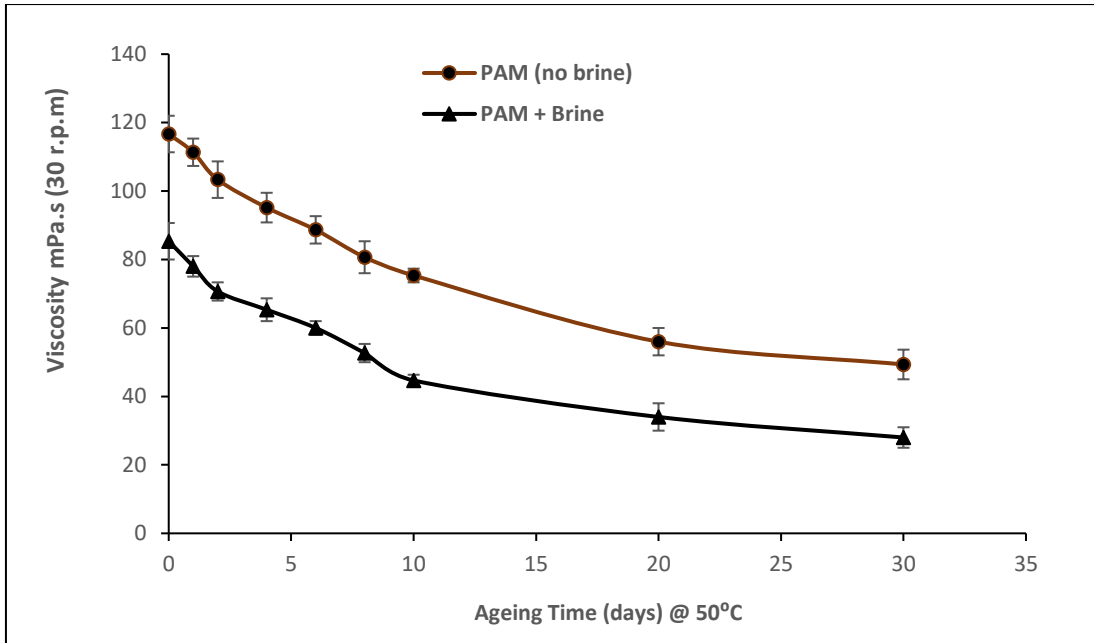
#### **5.3.1 Time–dependent effects on thermal stability of PAM viscosity.**

As discussed in section 5.4 a and b above, PAM solutions at high temperature experience a higher degree of hydrolysis, leading to an increase in the anionicity of

PAM solution that could result in instability in the behaviour of the gel. When the degree of hydrolysis is above 33%, polymer degradation or precipitation may occur at high temperature [13]. PAM exhibits thixotropic behaviour where solution viscosity tend to decrease at constant shear rate during some extended test period [89]. This implies that if shear rate is maintained. The measured shear stress and hence the viscosity, can either increase or decrease with time of shearing and such changes can be reversible or irreversible.

**Figure 5.5** presents the measured viscosity levels of PAM solution at 50°C in the presence and absence of brine for constant low shear rates of 10 and 30 rpm and constant high shear rates of 600 rpm, the viscosity test for each weight temperature and shear rate was conducted three times and the mean of the three viscosity measurement presented as the final viscosity and error bars calculated based on test repeatability. The results show a steady decrease in viscosity for a constant lower shear rates while the decrease is sharper for constant higher shear rates. It is worth mentioning that, at constant higher shear rates, much decrease in viscosity occurred after 10 days of ageing and, after that, no significant change in viscosity was observed.

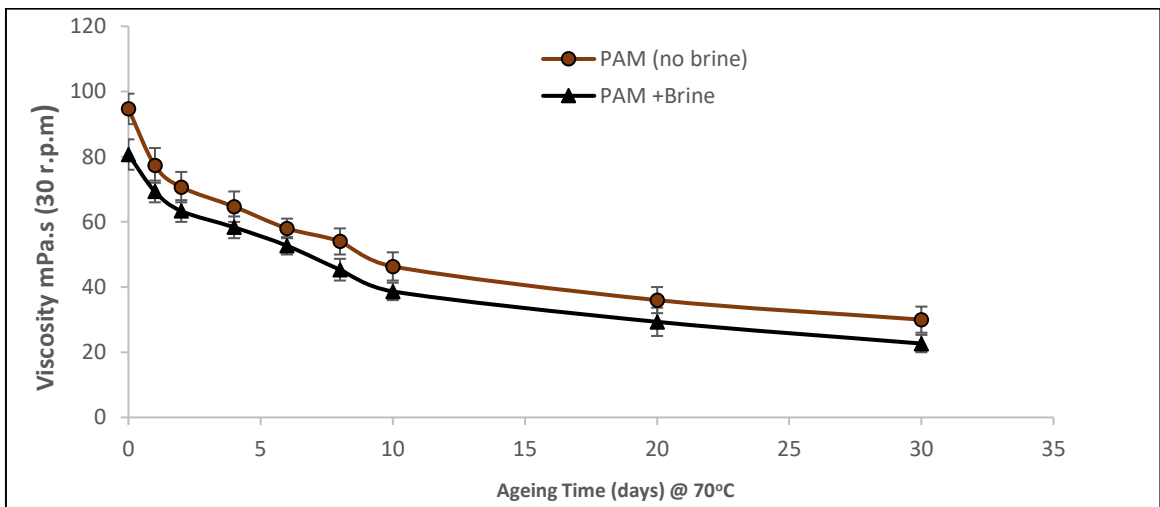
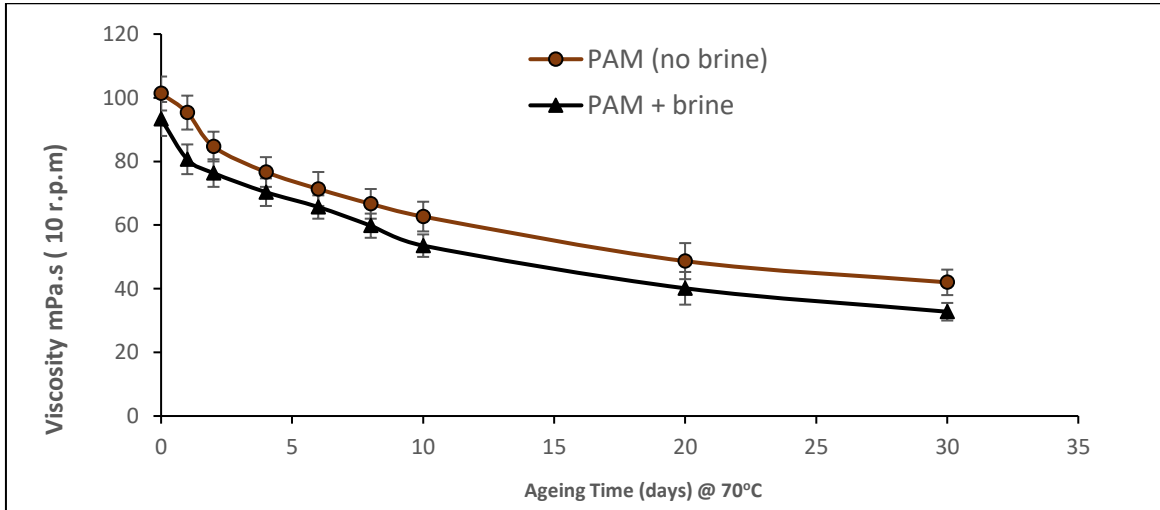




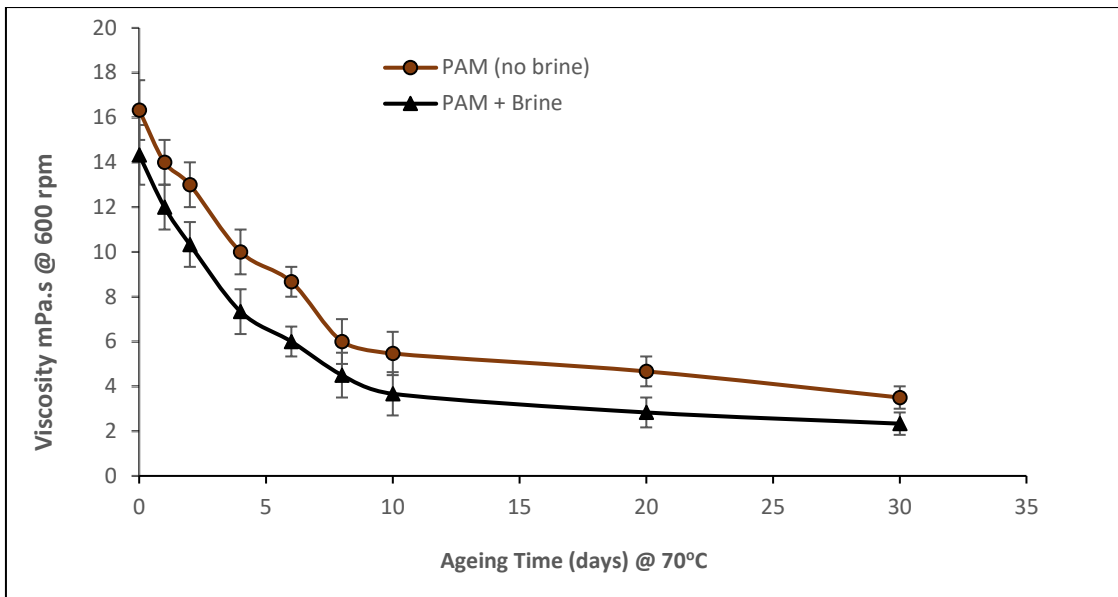
**Figure 5.5:** Thixotropic behavior of PAM at 50°C at low rotational speeds of (a) 10 rpm and (b) 30 rpm, as well as at a high rotational speed of (c) 600 rpm.

The constant low shear rate at 10 rpm leads to a steady fall in viscosity over the time, while at 30 rpm a similar trend is observed but with a slightly higher fall in viscosity. The high shear rate at 600 rpm gives a much larger overall fall in viscosity, which seems to take place in two stages. Accordingly, in stage 1 a rapid fall over the first 10 days starts to level off over the remaining time, and this is suggestive of

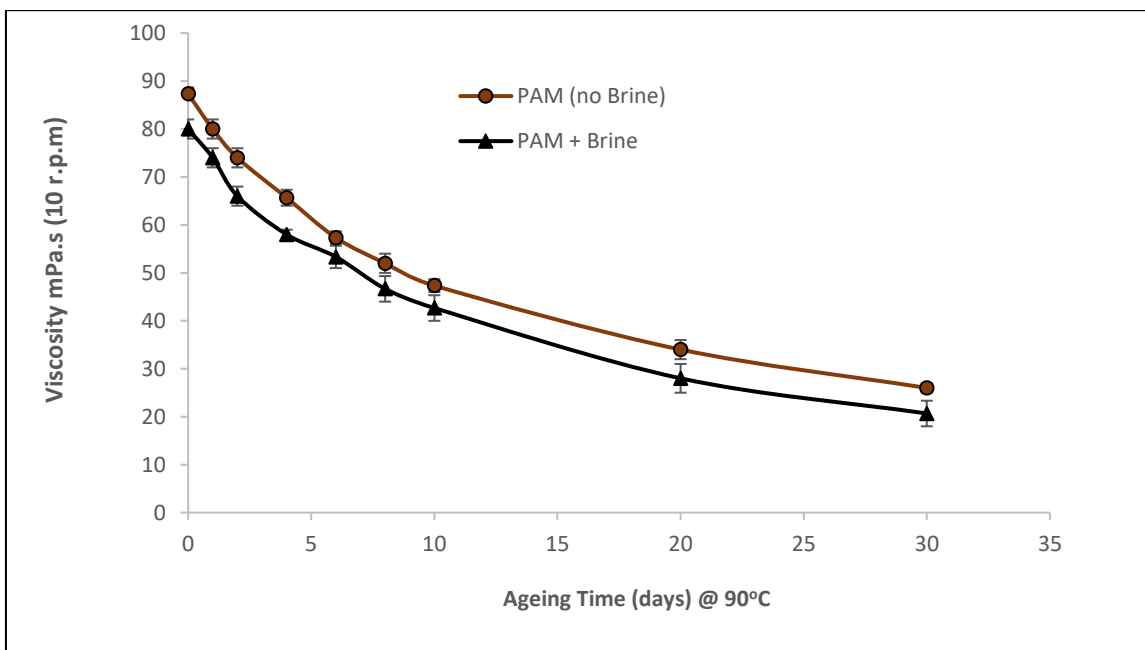
shear thinning Behaviour and the collapse of the gel structure. The same approach was adopted for the higher temperatures and the data are reported in figures 5.6 and 5.8







**Figure 5.6:** Thixotropic behavior of PAM at 70°C at low rotational speeds of (a) 10 rpm and (b) 30 rpm as well as (c) at a high rotational speed of 600 rpm.



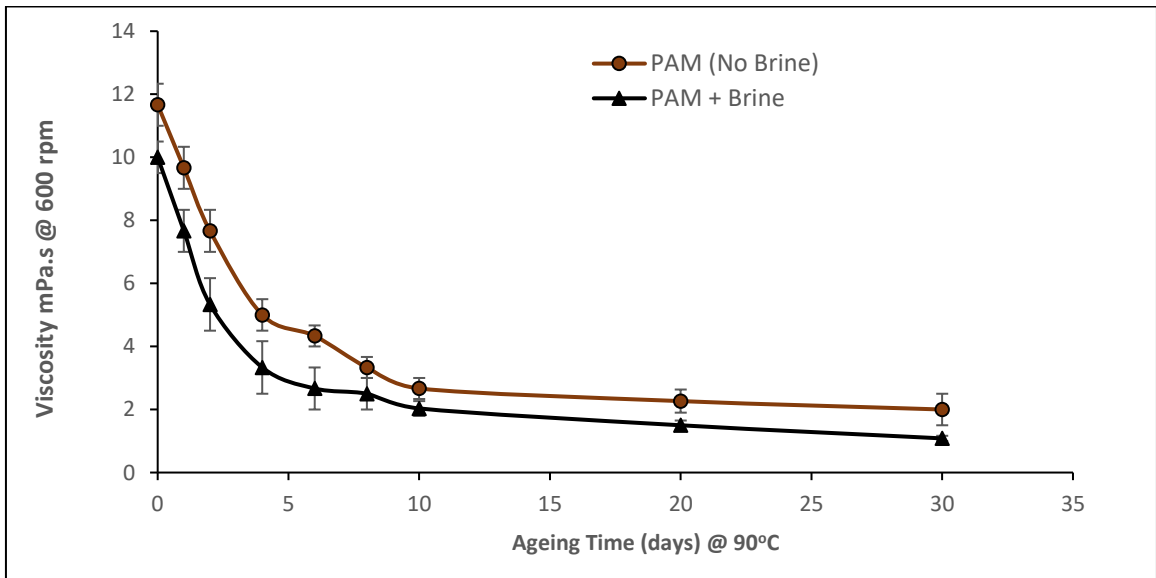
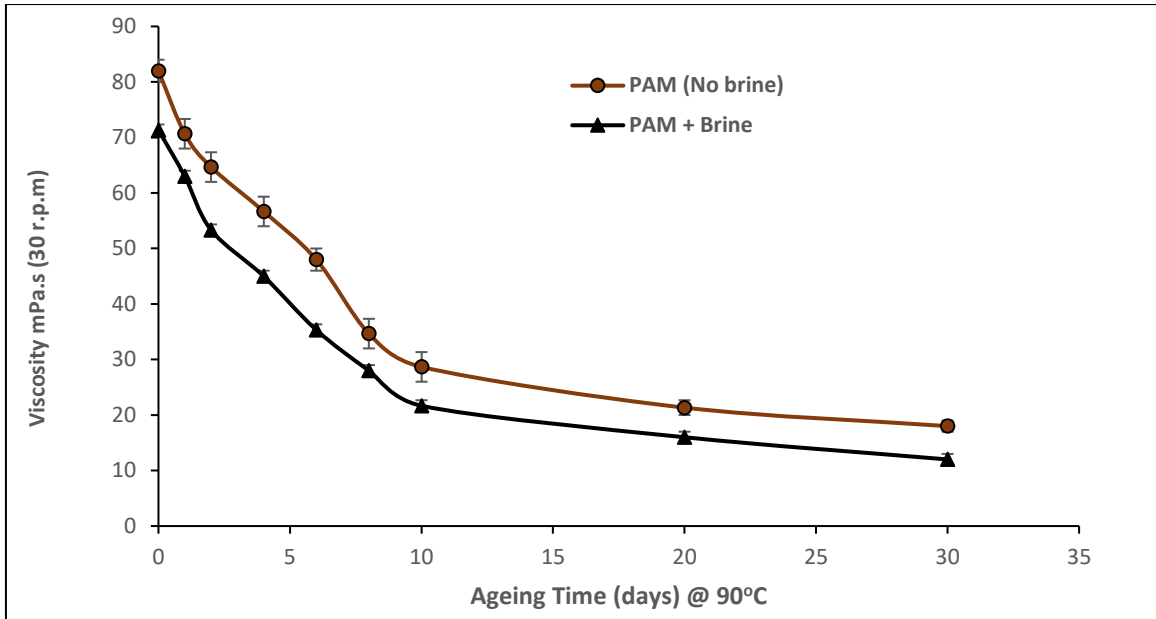


**Figure 5.7:** Thixotropic behavior of PAM at 90°C at low rotational speeds of (a) 10 rpm and (b) 30 rpm as well as at (c) a high rotational speed of 600 rpm.

Evidences from **Figures 5.5 – 5.7**, shows that the rate of fall in viscosity increased with temperature specifically for the PAM solutions in presence of brine. At 90°C, the transition to stage 2 behaviour has occurred at 30 rpm, indicating that gel

collapse is accelerated at higher temperature and constant lower rotational speeds or shear rate.

### 5.3.2 Percentage change in viscosity of PAM solution.

In the application of polyacrylamide in oilfields, it is of primary importance to ensure that the polymer solutions remain effective over long periods at different temperatures. To determine loss of viscosity of the PAM solution, combined operational conditions of shear rate, time, brines and temperature (50°C, 70°C and 90°C) were analysed using **equation 5.4**.

$$\text{Loss of viscosity (\%)} \text{ of PAM solution} = \frac{V_0 - V_n}{V_0} \times 100. \quad \mathbf{5.4}$$

where  $V_0$  is the initial polymer solution viscosity before ageing in oven, and  $V_n$  is viscosity at different ageing time.

These results are shown in detail in **Figure 5.8**. At all temperatures and rotational speeds, it was observed that the longer the ageing time of PAM solution in either pure water or brine, the greater the loss of PAM viscosity. For instance, at higher temperature of 90°C and 30 days of aging, the loss of viscosity was between 84-78 % and 77-71 % for PAM mixed in brine and PAM mixed in pure water,

respectively. While, at lower temperature of 50°C, the loss of viscosity was 69-66% and 61-58%, respectively.

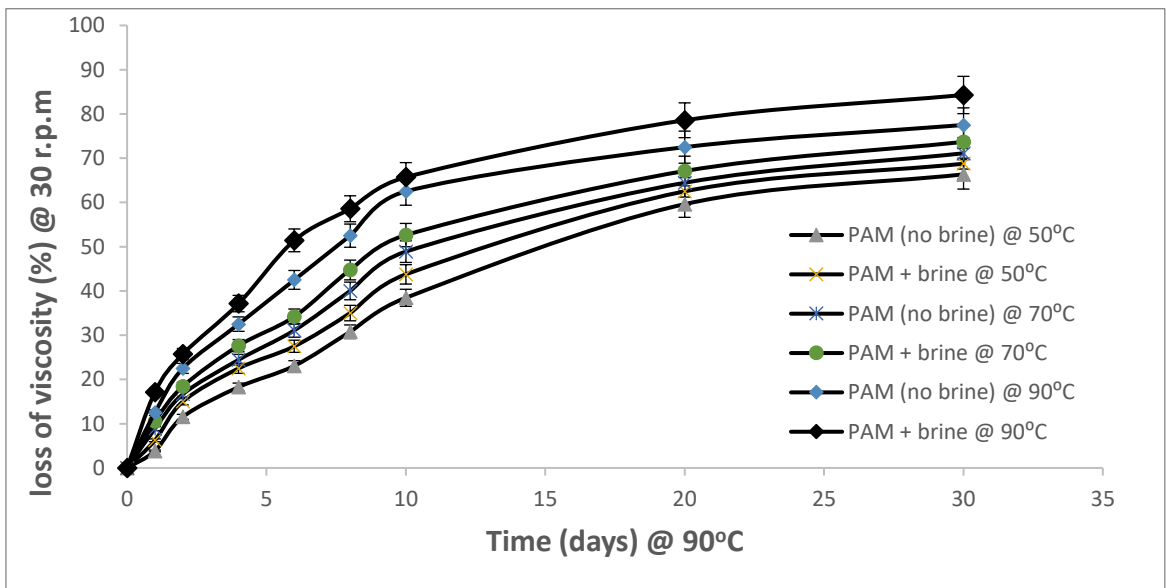
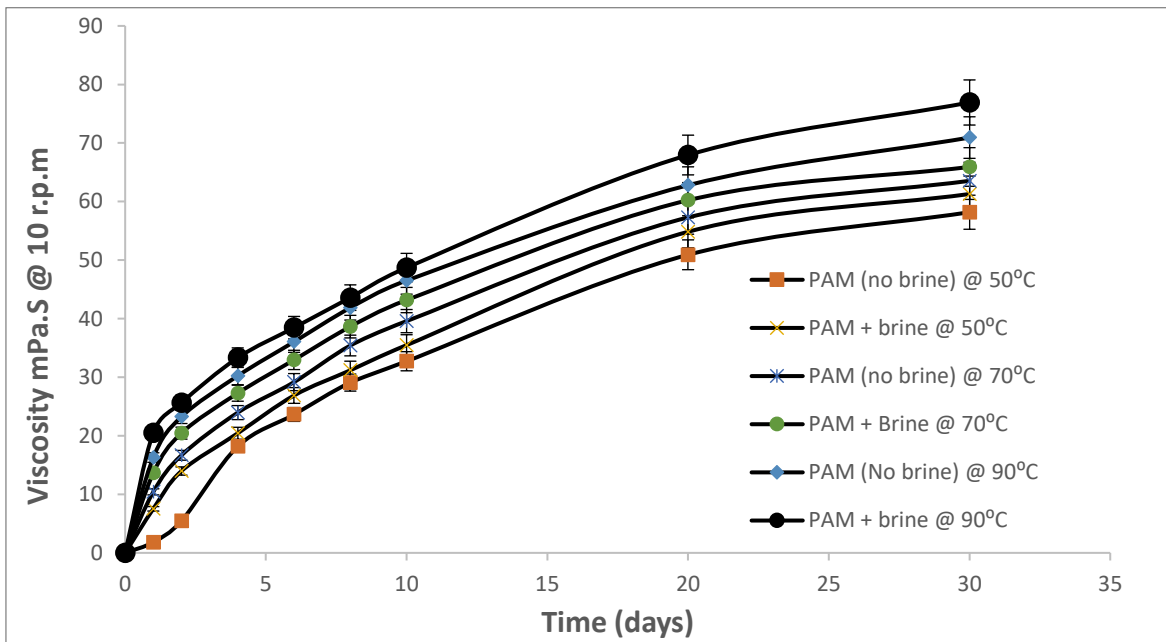


**Figure 5.8:** Percentage loss of viscosity of PAM in pure water and in the presence of brine at temperatures of 50, 70 and 90°C at rotational speeds of (a) 10 rpm, and (b) 30 r.p.m.

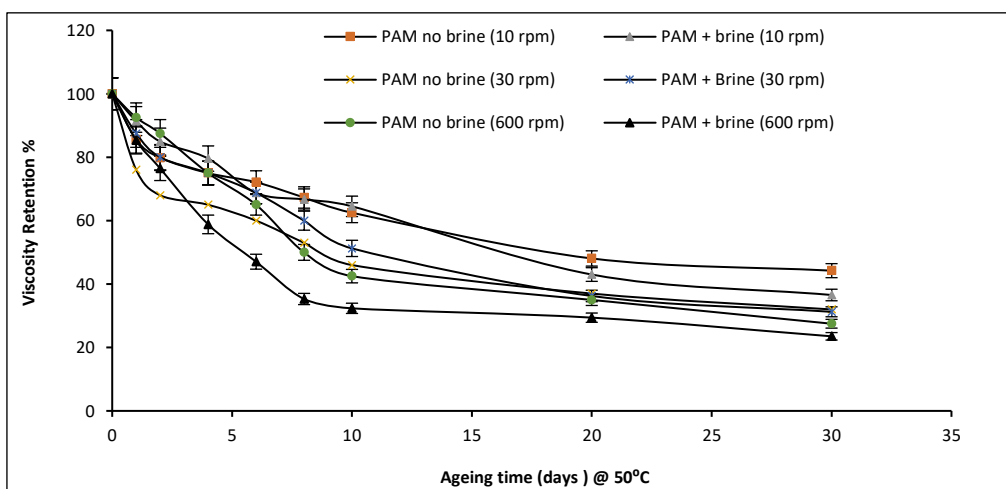
### 5.3.3. Efficiency of PAM performance

To investigate the efficiency of PAM performance at different operational conditions, the shear rate dependence of viscosity retention needed to be checked. Tests were conducted at shear rates of 17, 51 and 1021 s<sup>-1</sup> for temperatures of 50, 70 and 90°C and analysed using equation 5.5.

$$\text{viscosity retention (\%)} = \frac{V_t}{V_0} * 100 \quad 5.5$$

where  $V_0$  = initial viscosity, and  $V_t$  = viscosity at each time interval

The viscosity retention of PAM under studied conditions are presented in **Figure 5.9** at 50 °C, 70°C, and 90°C for both PAM mixed with pure water and PAM mixed with brine. The highest degree of viscosity retention is observed for 50°C followed by 70 °C and 90°C. The lower the shear rate of the PAM, the better the retention of the viscosity in the solution. The polymer solution with brine affected retention, where adding brine to the solution decreased the retention of viscosity. The minimum retention arises in the case where PAM is mixed with brine and has experienced the highest shear rate of 600 rpm for the longest ageing time of 30 days at higher temperature.



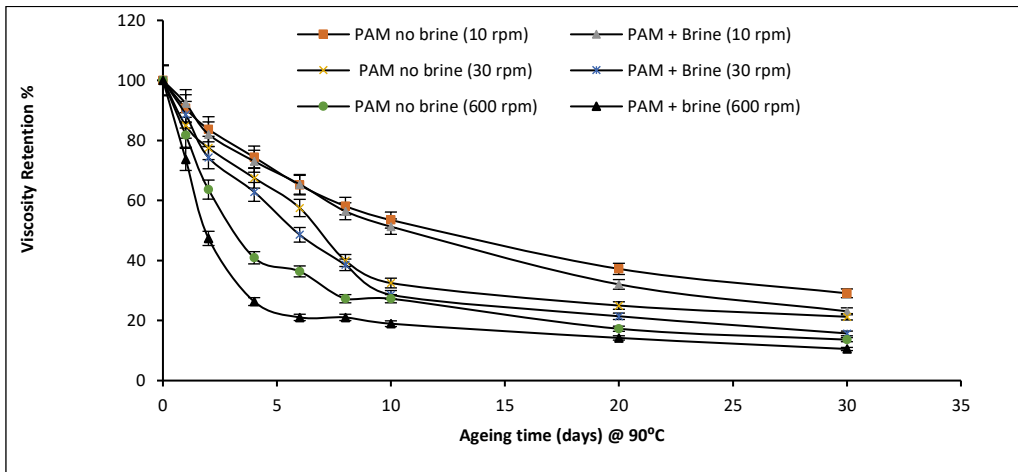
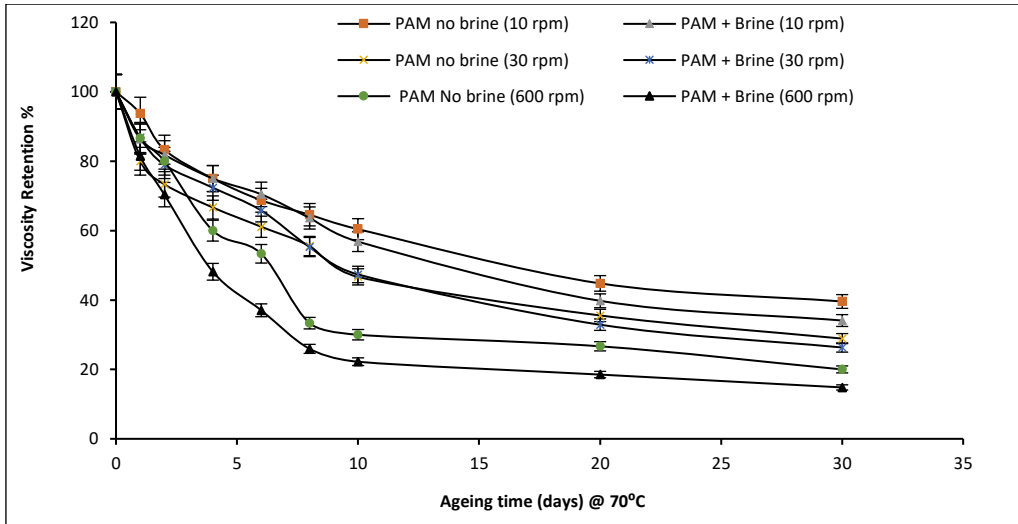


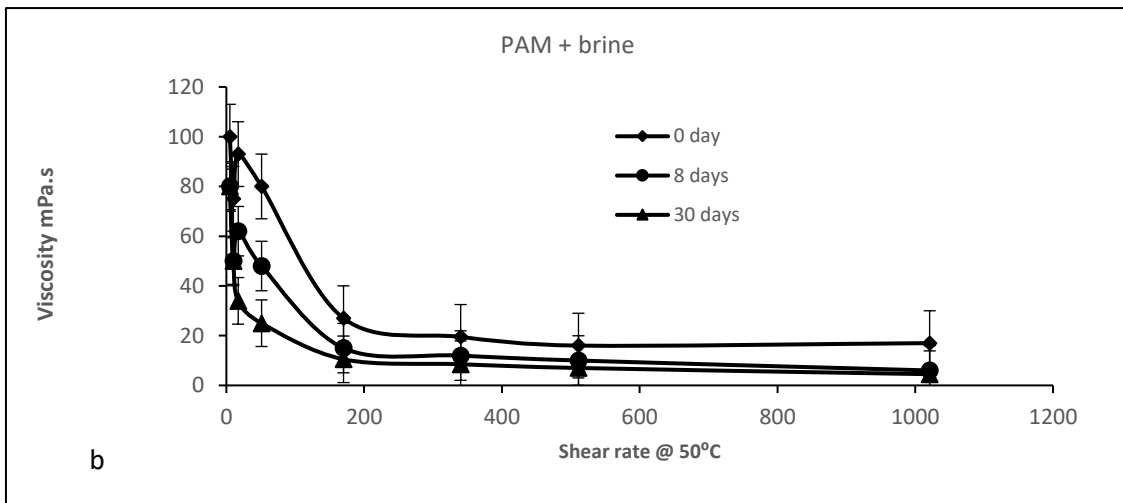
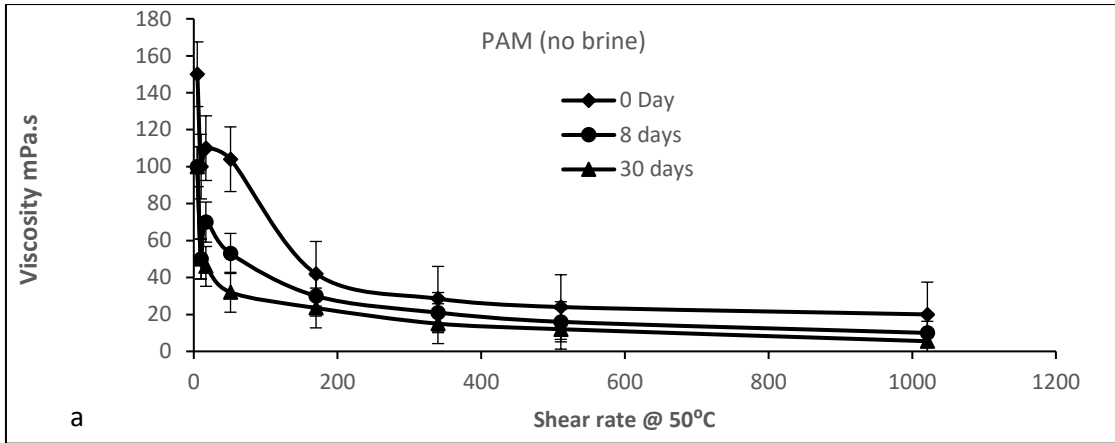
Figure 5.9: Evaluated viscosity retention of PAM solutions at 50°C (a), 70°C (b), and 90°C (c).

### 5.3.4 Shear degradation on PAM solution

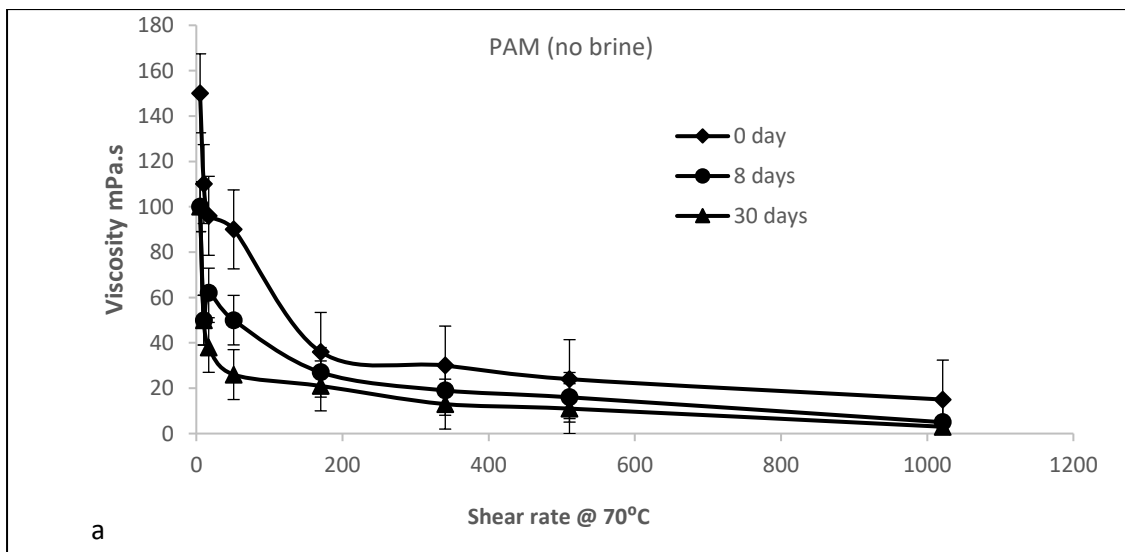
Viscosity of polymer solution depend strongly on shearing. Shearing process breakdown the molecules in the high flow rate region close to a well, as a result of high mechanical stresses on the macromolecule and it is describes as mechanical degradation. Mechanical degradation can lead to significant reductions in viscosity and most time could be describe as to a reversible decrease in viscosity with increasing shear rate generally called shear thinning [17, 90]. This imply that shearing process polymer flooding degrades the solution viscosity. This behaviour

of polymer gel is known as pseudo-plastic behaviour and it can occur when PAM solutions are injected into a reservoir from the injection well [89]. The flow regime usually changes as the solution flows first through the wide wellbore and finally to the reservoir. Because fluid viscosity is a function of shear rate, the solution's viscosity will also change from near the wellbore to the in-depth of a reservoir. PAM's pseudo-plastic behaviour may also occur in pipes and through chokes, valves or pumps.

To determine the effect of shear on viscosity of PAM solution when the polymer is added to a water-flooding operation, tests were conducted at 50, 70 and 90°C and at shear rates of 5, 10, 17, 51, 170, 340, 510 and 1021 s<sup>-1</sup>. The results are shown in detail in **Figures 5.10 - 5.12**. At low shear rates, the viscosity of PAM solution is reduced less compared to a high shear. However, the reduction in viscosity at different shear rates proved to be affected by ageing time as well as temperature. Even at low temperatures and low shear, the rate of viscosity reduction was slower in contrast to at higher temperature and higher shear rate. Therefore from the rheological measurements of fluid flow described above, it is recommended that polymer flooding is performed under laminar flow conditions and at a lower operational temperature, since shearing forces and elevated temperature may degrade the polymer and hence suppress its performance.



**Figure 5.10:** shear degradation of PAM presented as viscosity versus shear rate at 50°C: (a) in the absence of brine; and (b) with the presence of brine.





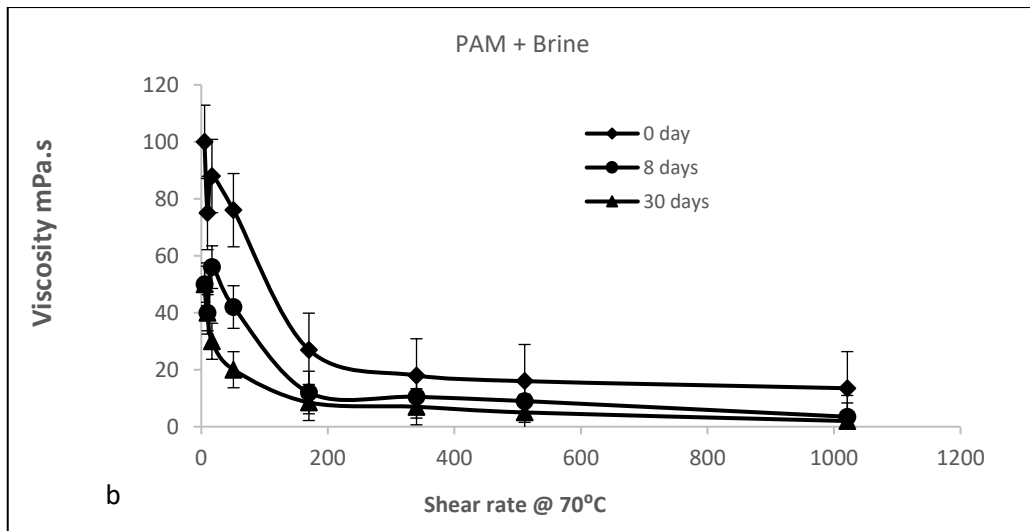


**Figure 5.11:** shear degradation of PAM presented as viscosity versus shear rate at 70°C: (a) in the absence of brine; and (b) in the presence of brine.

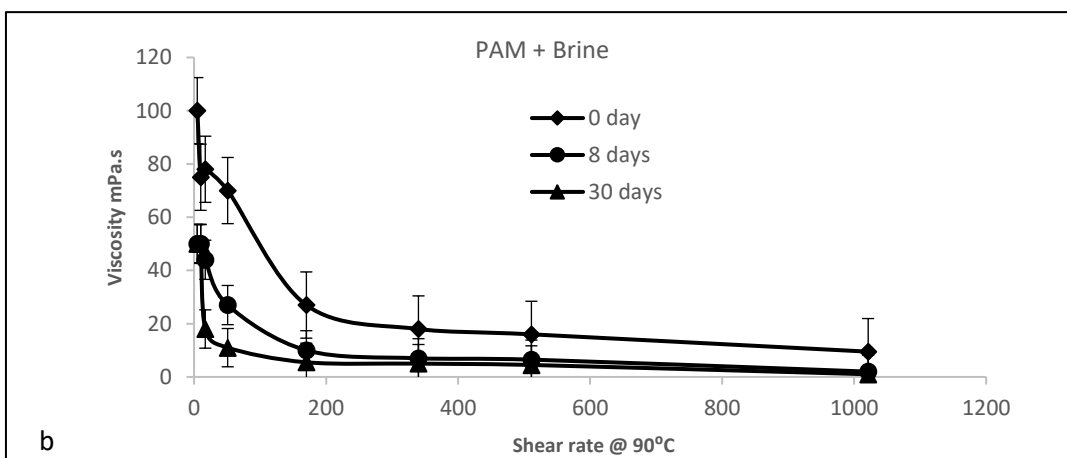
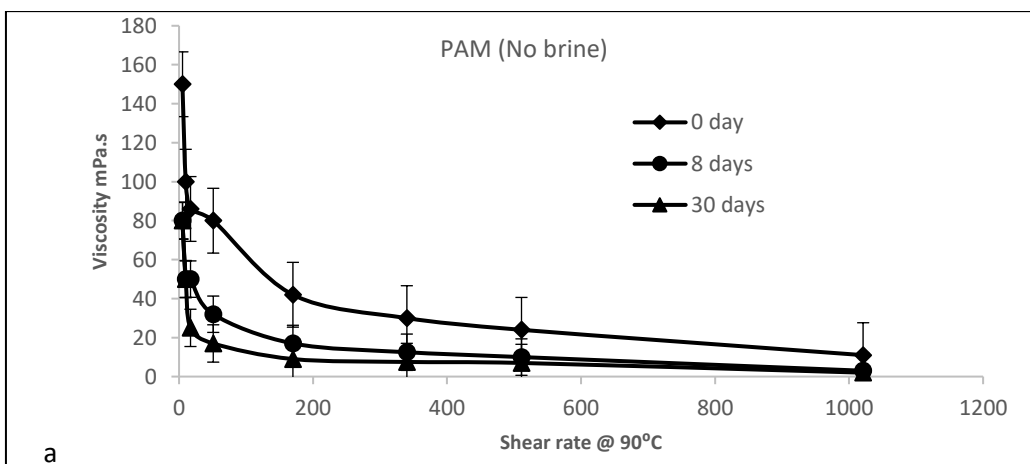


**Figure 5.12:** shear degradation of PAM presented as viscosity versus shear rate at 90°C: (a) in the absence of brine; and (b) in the presence of brine.

The experiments conducted to investigate the polymer solution (PAM) performance under the influences of moderate and high temperature, shearing and brines. Shows that PAM rheological viscosity measurement experienced high degradation. Accordingly, temperature is behind the extensive amide group hydrolysis, at moderate and high temperature of 50, 70 and 90°C, It is deduced that PAM dissolved in 42380 ppm TDS and in pure water. Showed an increasing degree of hydrolysis as the temperature increases and viscosity of PAM solution decreases. At high temperature 90°C, high extensive thermal hydrolysis up to 74% were observed for brine solution with high decrease in polymer viscosity solution. To achieve allowable PAM solution during EOR operation, there is need to improve PAM performance by stabilizing the degree of hydrolysis of PAM within 30% to 40% for longer stability. The challenging effect of high degree of hydrolysis resulting from high temperature caused polymer solution viscosity instability. Improving the polymer performance, the primary approach is developing better polymers through integration and optimization of PAM performance in high temperature reservoirs discussed in Chapter 6.

## CHAPTER 6: INTEGRATION AND OPTIMIZATION OF PAM PERFORMANCE IN HIGH TEMPERATURE RESERVOIRS

The instability in PAM performance at reservoir conditions such as high temperature and brine happens as a result of hydrolysis of the amide functional groups as studied in chapter 5. A synthetic approach called the polymer integrated technique (PIT) was adopted and is defined as a process of combining high molecular weight polymer with other polymers to meet the stability limitations or degradation of high molecular weight polymer at reservoir conditions of high temperature and high brine. The synthetic approach followed has been to modify polyacrylamide (PAM) with Polyvinylpyrrolidone (PVP). PVP is non-toxic, eco-friendly water soluble polymer that is resistant to thermal degradation [126, 133]. The monomer (PVP) provides protection to hydrolysis at elevated temperatures [124, 127, 133]. Although, Davison, Mentzer [124] and Doe et al., [127] reported that despite PVP's thermal stability capacity, the polymer cannot be applied alone because it is not a good viscosifier but capable development maybe needed to combine PVP with more viscosifying water soluble polymer like polyacrylamide as to have an optimized good enough viscosity and criteria acceptable for degree of hydrolysis. To accelerate this, detailed practical characterization ranges from degree of hydrolysis in high temperature of 90°C aged sample to the viscosity of the polymer solution as regards shearing time and shear rate, which form the rheological behavior.

### 6.1 Hydrolysis of PAM and PVP mix polymer at 90°C aged samples

One of the criteria in improving the performance of water-soluble polymers during EOR polymer flooding applications is to keep the degree of hydrolysis below 33% [13]. Above this level, degradation or precipitation may occur [21, 13]. This is due

to a consequences of interaction between the hydrolysed amide group and the salinity of formation water containing divalent cations. This chemical transformation in PAM could cause significant losses in solution viscosity and separation could eventually occur in extreme conditions of high degrees of hydrolysis or extreme concentrations of formation salinity [16]. The primary mechanism behind polyacrylamide degradation has been found to be the hydrolysis of amide groups. Moreover, the hydrolysis level is a function of temperature [4, 15]. A high degree of hydrolysis leads to the high adsorption of hydrolysed PAM in porous rock [86]. Therefore, the level of hydrolysis of amide groups in the structure of mixed water-soluble polymers of PAM and PVP needs to be determined. However, FTIR and NMR spectroscopy were utilised to determine the degree of hydrolysis of the integrated PAM and PVP polymer solution

### 6.1.1 FTIR analysis of PAM and PVP mix polymer

FTIR determined the change in absorbance associated with the stretching of the amide ( $\text{CONH}_2$ )  $\text{C}=\text{O}$  to finally give the absolute degree of hydrolysis of the amide functional group. Accordingly, the FTIR spectrum of pure PAM, PVP and PAM: PVP samples was analysed and the outcome indicates that the observed absorption peaks correspond to the characterised chemical bonds presented in **Table 6.0**.

Table 6.0 shows FTIR spectra of pure PAM and pure PVP. For pure PAM spectrum, the peaks corresponding to primary amide  $\text{NH}_2$  asymmetric and symmetric stretching were assigned to  $3347\text{-}3331\text{ cm}^{-1}$  and  $3190\text{-}3170\text{ cm}^{-1}$  respectively. However, the peaks at  $3300\text{-}3250\text{ cm}^{-1}$  correspond to secondary amide N-H stretching. A noticeable peaks at  $1680\text{-}1630\text{ cm}^{-1}$  and  $1629\text{-}1603\text{ cm}^{-1}$  correspond to primary amide and secondary amide  $\text{C}=\text{O}$  stretching respectively. The peaks at

1603-1330  $\text{cm}^{-1}$  correspond to the  $\text{COO}^-$  group asymmetric stretching, while the peaks at 1329-1300  $\text{cm}^{-1}$  were assigned to C-N stretching, those at 1299-1000  $\text{cm}^{-1}$  to C-O-H bending, and those at 900 - 992  $\text{cm}^{-1}$  to C-C symmetric-asymmetric stretching. Whereas for pure PVP spectrum, the peaks at 3380-3320  $\text{cm}^{-1}$  and 2186-2143  $\text{cm}^{-1}$  were assigned to primary C-H asymmetric stretching and C-H symmetric stretching respectively, peaks at 2956 -2223  $\text{cm}^{-1}$  were assigned to secondary C-H stretching. Apparently a noticeable Peak at 1644-1642 and 1634-1630  $\text{cm}^{-1}$  were assigned to primary amide and secondary amide C=O stretching respectively, and those at 1461-1422  $\text{cm}^{-1}$  correspond to the C-N-C group asymmetric stretching, while peaks at 1320-1286  $\text{cm}^{-1}$  were assigned to C-N stretching, those at 1127-1094  $\text{cm}^{-1}$  to C-O-C bending and those at 994-871  $\text{cm}^{-1}$  to C-C symmetric-asymmetric stretching.

**Table 6.1** presents the variations in blend ratio for PAM: PVP and their correspondence peaks. The primary amide  $\text{NH}_2$  asymmetric and symmetric stretching showing peak at 3361 – 3298  $\text{cm}^{-1}$  and 2984 – 2219  $\text{cm}^{-1}$ . Peaks at secondary amide N-H stretching were assigned to 2984 – 2219  $\text{cm}^{-1}$ . The primary amide and secondary amide C=O stretching show a prominent peak at 1680-1630  $\text{cm}^{-1}$  and 1629-1603  $\text{cm}^{-1}$  respectively, this peak can be investigated to explore the interaction between PAM:PVP amide group hydrolysis. Furtherance is the peaks at 1496 -1492  $\text{cm}^{-1}$  correspond to the C-N-C group asymmetric stretching, whereas the peak at 1492 -1420  $\text{cm}^{-1}$  is corresponding to the  $\text{COO}^-$  group asymmetric stretching. Then the peaks at 1320-1293  $\text{cm}^{-1}$  were assigned to N - C stretching while peak at 1108-1098  $\text{cm}^{-1}$  assigned to C-O-C bending and those at 996-896  $\text{cm}^{-1}$  assigned to C-C symmetric-asymmetric stretching. In line with **Table 6 and 6.1**, **figures 6 (a and b)** presents a plots evidence of FT-IR absorbance spectra for

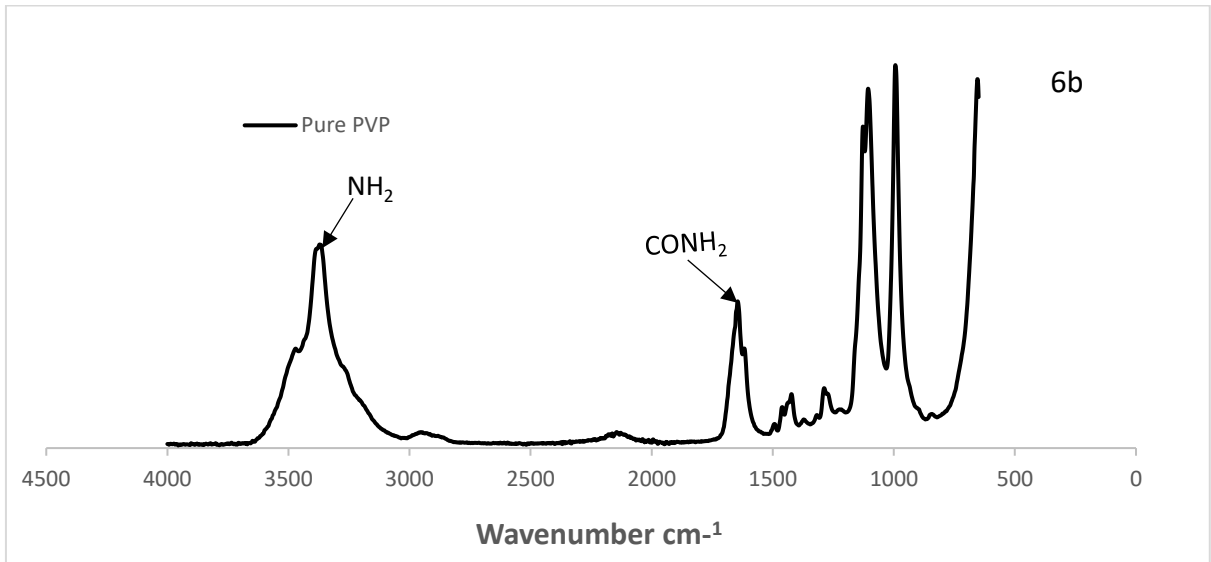
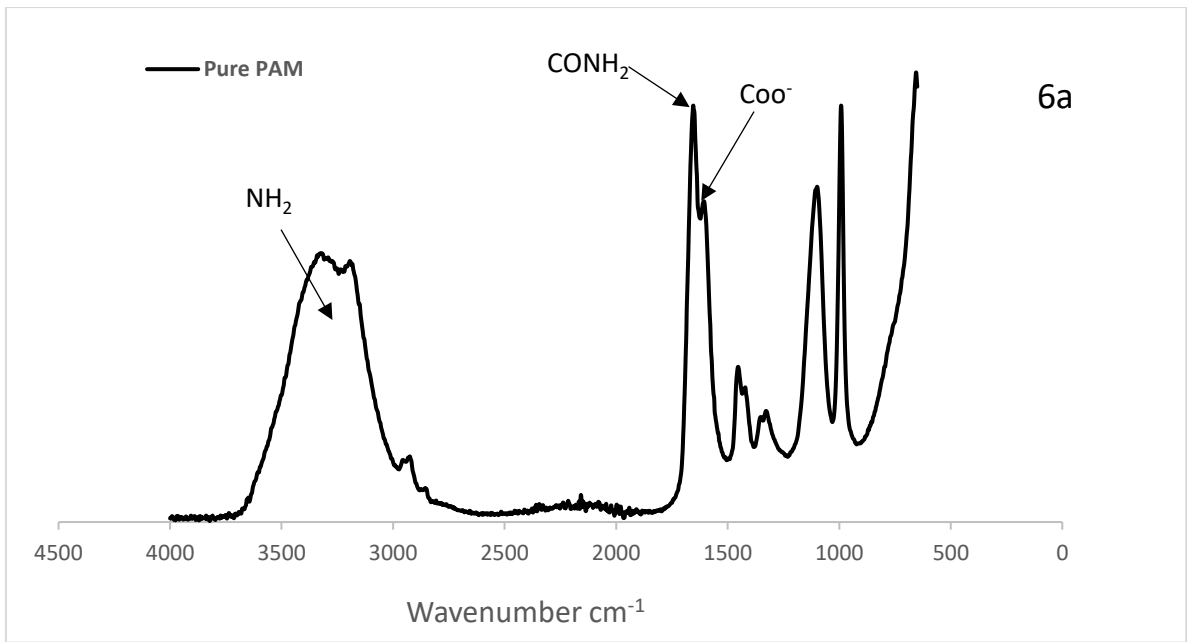
PAM, PVP and AMPS and comparative plot of PAM, PVP and AMPS mix samples at time 0 and 30 days respectively. However, at time zero in day, absorbance

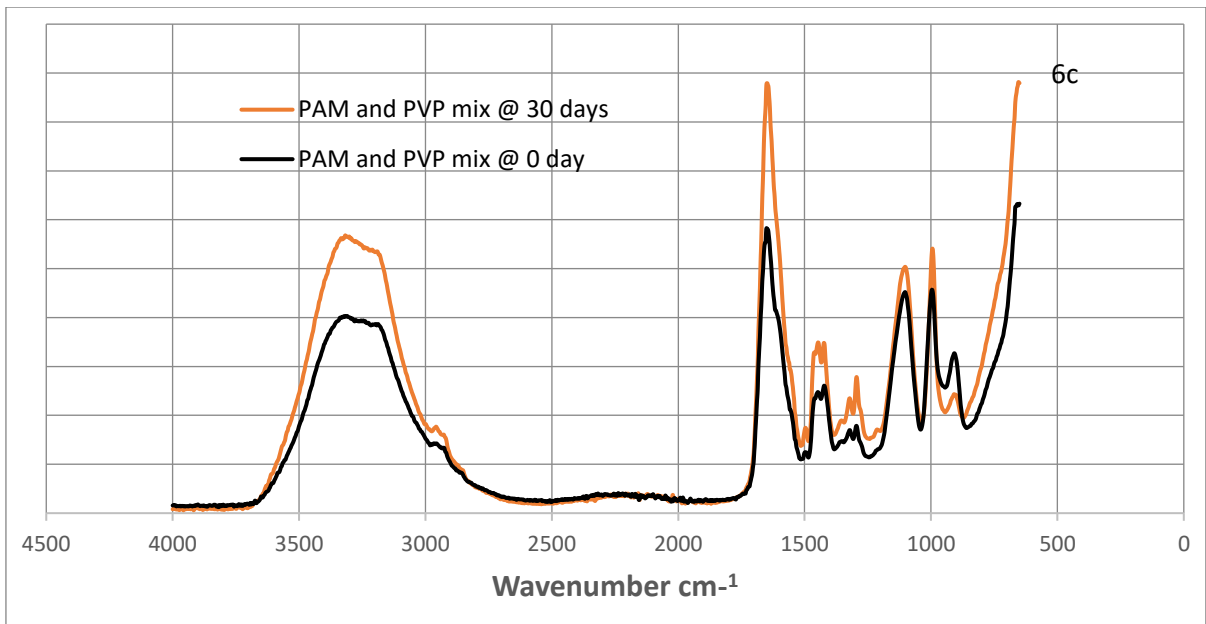
Table 6.0: Assignment of FT-IR characterization bands ratio for pure PAM and pure PVP after ageing at 90oC

<b>Peak Assignment</b>	<b>PAM (wavenumber cm<sup>-1</sup>)</b>	<b>PVP (wavenumber cm<sup>-1</sup>)</b>
Primary amide NH <sub>2</sub> asymmetric stretching	3347 - 3331	3380 - 3320
Secondary amide N - H stretching	3300 - 3250	2956 -2954
Primary amide NH <sub>2</sub> symmetric stretching	3190 - 2298	2186 - 2143
Primary Amide C=O Stretching	1680 - 1630	1644 - 1642
Secondary amide C =O Stretching	1629 - 1603	1634 - 1630
COO- Stretching	1603 - 1330	1461 - 1422
C - O Stretching	1329 - 1300	1320 -1286
C - O-H in plane bending	1299 - 1000	1127 - 1094
C - O - H out plane bending	900 - 992	994 - 871

Table 6.1: Assignment of FT-IR characterization bands ratio for PAM: PVP

<b>Peak Assignment</b>	<b>Weight proportion of PAM:PVP (wavenumber cm<sup>-1</sup>)</b>
Primary amide NH <sub>2</sub> asymmetric stretching	3361 - 3298
Secondary amide N - H stretching	2984 - 2219
C - H Stretching	2159 - 2189
Primary Amide C=O Stretching	1650 - 1642
Secondary amide C =O Stretching	1639 - 1629
C-N-C Stretching	1496 -1492
COO- Stretching	1492 - 1420
N - C Stretching	1320 -1293
C - O-C Stretching	1108 -1098
C - C symmetric - Asymmetric stretching	996 -896

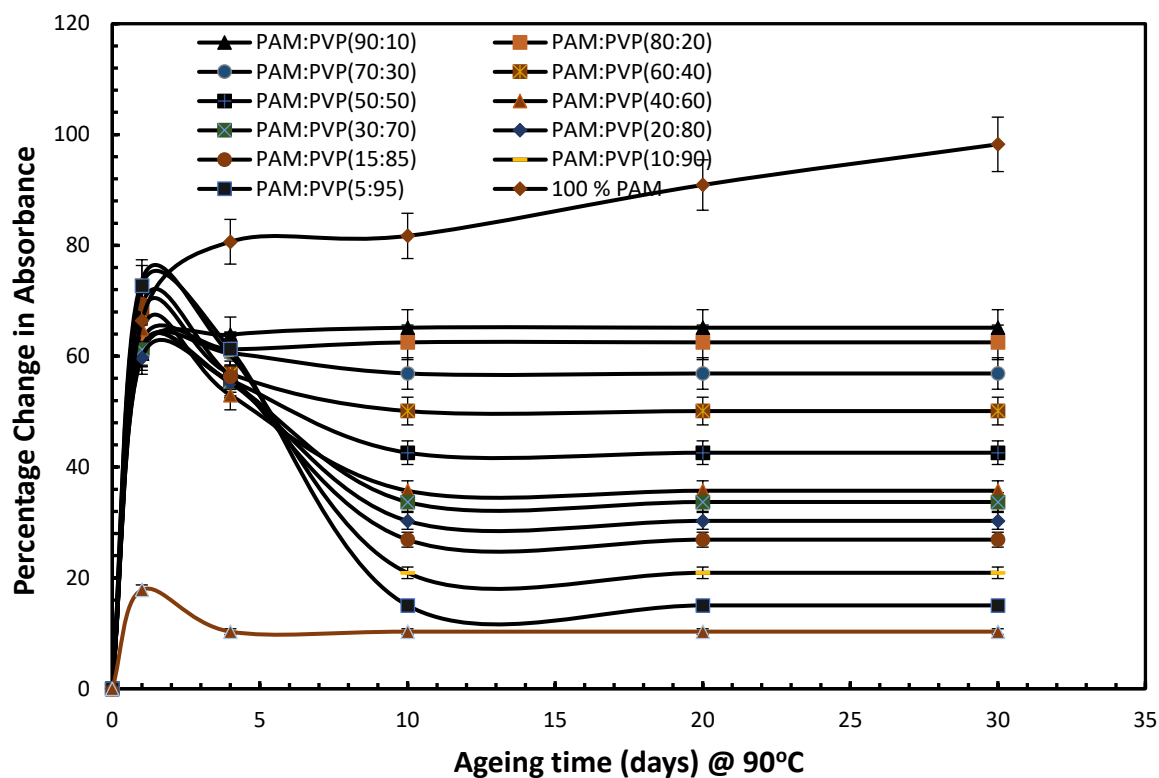




**Figure 6.0:** FT-IR absorbance spectra (6a) pure PAM, (6b) pure PVP and (6c) PAM and (6c) Comparative PAM and PVP mix samples at time 0 and 30 days after aging at 90°C

To determine if the degree of hydrolysis is suppressed and gel stability is maintained by mixing the PAM with Polyvinylpyrrolidone (PVP). **Figure 6.1** indicates the percentage change in absorbance of the CONH<sub>2</sub> amide group on integrated polymer solutions of PAM: PVP against ageing time at 90°C and a salinity of 43,280 ppm. The weight ratios with high proportions of PVP in the solution showed lower percentages of amide absorbance, which could result in less hydrolysis, whereas weight ratios with high PAM percentages exhibited high amide group absorbance, which could result in more hydrolysis. For instance, 63% absorbance was recorded for 80:20 PAM: PVP at 30 days of ageing, compared to 30% absorbance for 20:80 PAM: PVP.

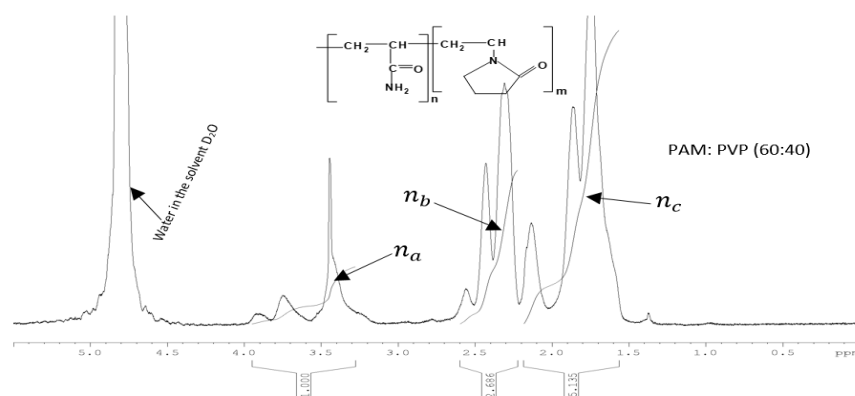




**Figure 6.1:** Percentage change in amide absorbance of PAM, PVP and integrated polymers at 90 °C and 43,280 ppm TDS

### 6.1.3 NMR analysis of PAM and PVP mix polymer hydrolysis

To finally determine the degree of hydrolysis of PAM and PVP integrated polymer solution. Figure 6.2 illustrate the  $^1\text{H}$  NMR spectra for integrated polymers of PAM and PVP at 90°C in moderate salinity of 43,280 ppm TDS, more structures are shown in figure 6.2b under appendix B.



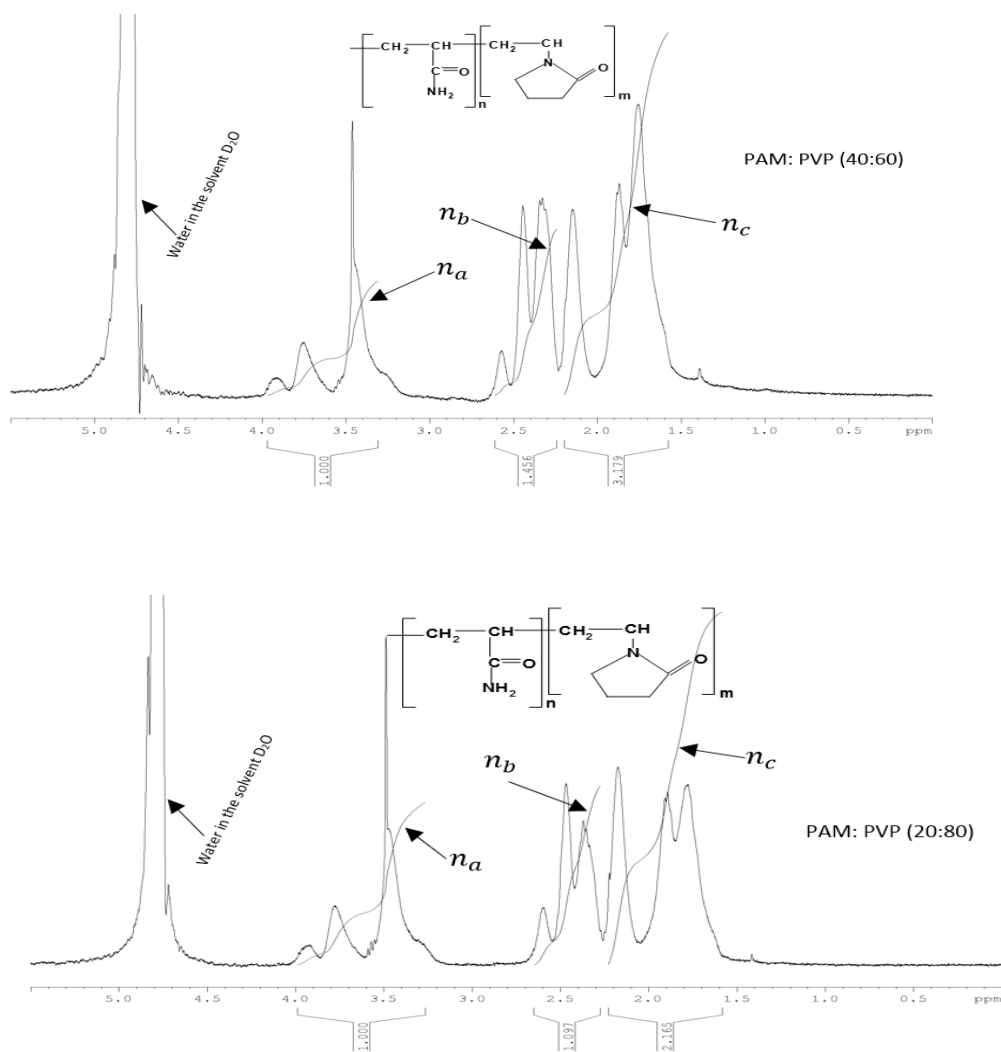


**Figure 6.2:**  $^1\text{H}$  NMR spectra for integrated polymers of PAM: PVP at  $90^\circ\text{C}$  and TDS 43,280 ppm.

Evidence from figures 6.2 is the  $^1\text{H}$  NMR spectrum of the PAM and PVP mix Samples showing a prominent peak that is positioned at 4.8 ppm. The peak represents a water content in the deuterium oxide solvent. Accordingly, the amount of proton atom (H) within a peak area were further calibrated. The calibrated point at each area identify the amount of the proton atom (H) in the carbon skeleton that is bonded to methine (CH), methylene ( $\text{CH}_2$ ) and methyl ( $\text{CH}_3$ ) or equivalent H atoms corresponding to the sample chemical structure as seen in figure 3.3.  $^1\text{H}$

NMR spectrum of the PAM: PVP shown in figure 4 has a peaks at 3.4-3.8 ppm representing the proton (H) atom in functioning group of methine (CH) that is bonded to amide group in PVP as represented in  $n_a$  whereas the peak at 2.00-2.5 ppm represent the methylene amide group (C=O) in PVP and the methine (CH) bonded to amide group (C=O) in PAM as represented in  $n_b$ . The peak at 1.50-1.90 ppm represents the methylene (CH<sub>2</sub>) group in PAM and PVP as represented in  $n_c$  [125 – 126]. Accordingly, a three-step approach to the analysis of the initial degree of hydrolysis ( $DH_i$ ) using proton NMR was adopted as shown in equations 5a, b and c:

$$\text{Average peaks shift } (N_{avg}) = \frac{1}{n} \sum_{i=1}^n N_i = \frac{1}{n} (N_a + N_b + N_c + \dots N_n) \quad (5a)$$

$$\text{Proton and Equivalent H atom total series} = Na + \frac{N_b}{N_{avg}} + \frac{N_c}{N_{avg}} \quad (5b)$$

$$DH_i (\%) = \frac{\frac{N_b}{N_{avg}}}{Na + \frac{N_b}{N_{avg}} + \frac{N_c}{N_{avg}}} \times 100 \quad (5c)$$

where,  $n_a$  is the calibration point for methine (CH) proton in PVP,  $n_b$  is methylene (CH<sub>2</sub>) proton bonded to amide group in PVP and the methine (CH) bonded to amide group (C=O) in PAM and  $n_c$  is the equivalent H atoms in the peak integration of the methylene (CH<sub>2</sub>) proton in PAM: PVP solutions. The initial degree of hydrolysis of the integrated PAM: PVP polymers dissolved in brine are recorded in **Table 6.2**.

**Table 6.2:** Initial degree of hydrolysis (DH<sub>i</sub>) for time zero ageing and brine sample of 43,280 ppm salinity at 90°C.

Sample No:	PAM wt%	PVP wt%	DH <sub>i</sub>
1	100	0	38 %
2	90	10	27%
3	80	20	26%
4	70	30	25%
5	60	40	25%
6	50	50	25%
7	40	60	24%
8	30	70	24%
9	20	80	24%
10	15	85	24%
11	10	90	24%
12	5	95	23%
13	0	100	23%

The results indicate that at the rate of initial degree of hydrolysis decreases with the weight ratio of PVP in the integrated polymer solutions. For the initial samples at time zero, it is clear that the degree of hydrolysis rises when the weight proportion of PAM is higher than that of PVP. For instance, at 90:10 PAM: PVP, the initial degree of hydrolysis is 27%, whereas for 10:90 PAM: PVP it is 23%. According to **Uranta et al., [103]**, to convert the percentage absorbance change into degree of

hydrolysis, the percentage increases in amide groups and the initial degree of hydrolysis (DH) are combined and the final equation is expressed in equation 6.3.

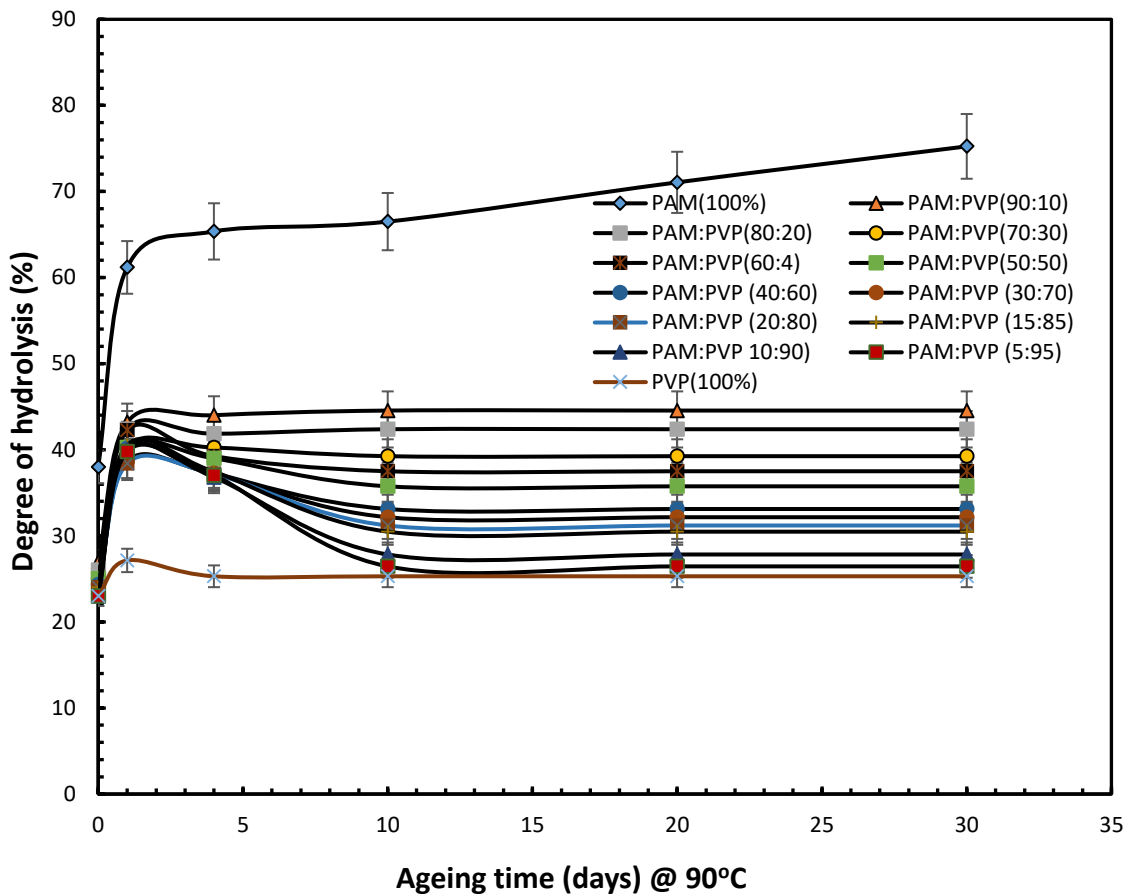


**Figure 6.3:** Extent of degree of hydrolysis of PAM: PVP solutions at different PAM: PVP weight ratios with respect to ageing time at 90°C and salinity of 43,280 ppm.

From **figure 6.3** is the degree of hydrolysis of pure PAM and PAM and PVP mix together with their different weight ratios against ageing time up to 30 days in a moderate salinity of 43,280 ppm TDS. The results show that a high weight proportion of PVP in the mixed solution has experienced less hydrolysis compared to PAM. The stability of the integrated polymer is exhibited from 4 days of ageing and continues until 30 days. The extent of the degree of hydrolysis of pure aged PAM after 30 days was reduced significantly from 74 % by adding 10 wt% of PVP

and the reduction continued linearly down to 44.55 % at 90:10 wt % PAM: PVP. Further addition of PVP had no impact on PAM hydrolysis. This weight ratio is less susceptible to hydrolysis compared to 100% PAM.

## **6.2 Stability of PAM and PVP integrated polymer**

Earlier stability test results on PAM solution in subsection 5.2.1 shows a steady decrease in viscosity at high temperature 90°C in each shearing. But incorporation of Polyvinylpyrrolidone (PVP) to PAM maintained high gel stability. From **figures 6.4 and 6.5** is a plot evidence of viscosity of PAM and PVP integrated polymer at rotational speeds of 10 and 30 rpm against ageing time s on various weight ratios in presence of 43,280 ppm TDS and temperature of 90°C. The figure shows that incorporation of PVP to PAM solution enhanced resistance to hydrolysis by maintaining stability. Irrespective of rotational speed of 10 and 30 rpm or shearing, the viscosity decreased at first day of ageing and started building up or increasing until 10 days. From 10 days stability began and continue till 30 days of ageing. That proved that PAM solution viscosity on addition of PVP showed high improvement in gel performance compare to 100 wt % PAM solution with high decrease as the ageing time increases. It is also noticed that weight ratio with more PAM and less PVP have high viscosity compare to more PVP less PAM. However, it is due to the fact that PAM is a better viscous polymer compare to PVP, but there is tendency that in a long run PAM may exhibit or suffer degradation because PAM is acrylamide based polymer. Optimizing to have weight ratio more PVP and less PAM could be a better option as to maximize performance.

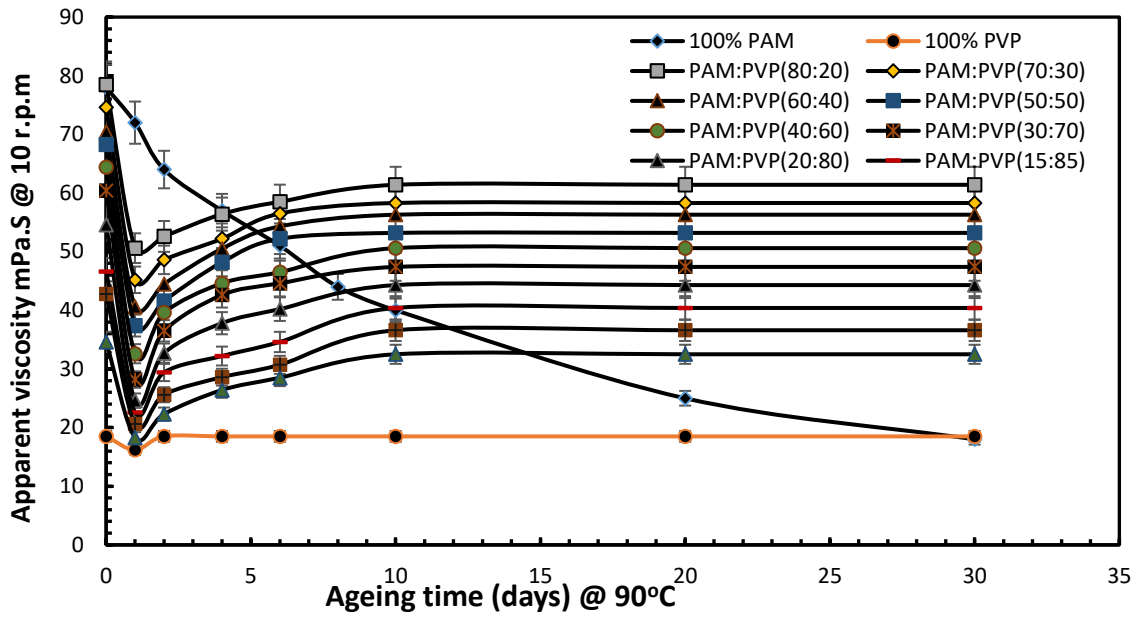


**Figure 6.4:** Viscosity of PAM and different weight ratios of integrated polymer at 90°C and 43280 ppm TDS for a rotational speed of 10 r.p.m.

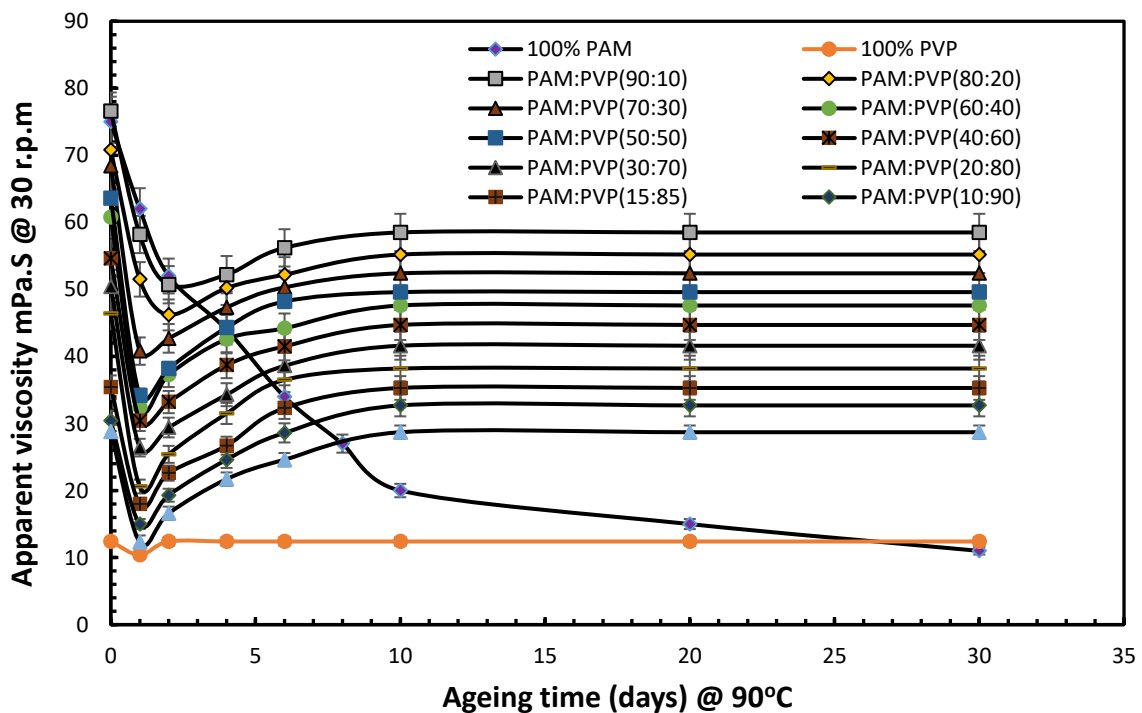


**Figure 6.5:** Stability of PAM and different weight ratios of integrated polymer at 90°C and 43280 ppm TDS for a rotational speed of 30 r.p.m.

### 6.3 Optimization of PAM and PVP mix solution at High temperature

To optimize and maximize the efficiency of integrated polymers of PAM and PVP solution performance at elevated temperature in salinity of 43,280 ppm TDS solution. Three important factors was considered; polymer solution viscosity, degree of hydrolysis, ageing time and the PVP concentration. **Figures 6.6** and **6.7** plot integrated polymer solution viscosity and degree of hydrolysis against integrated polymer (PAM: PVP) concentration at rotational speeds of 10 and 30 rpm in 30 days. Both plots show similar trends. For viscosity measurements we see a rapid increase in viscosity from pure PAM to 10% PVP and then a linear drop on viscosity from 10% PVP to 80% PVP. Above 80% PVP the drop in viscosity increases with composition. The hydrolysis results mirror those seen for viscosity. A rapid decrease in degree of hydrolysis is seen between pure PAM and 10 % PVP followed by a much slower linear reduction for PVP concentrations greater than 10%. 80 wt% PVP and 20 wt % PAM is considered to be the optimal point for effective application in reservoir temperature 90°C and formation water salinity of 43280 ppm.



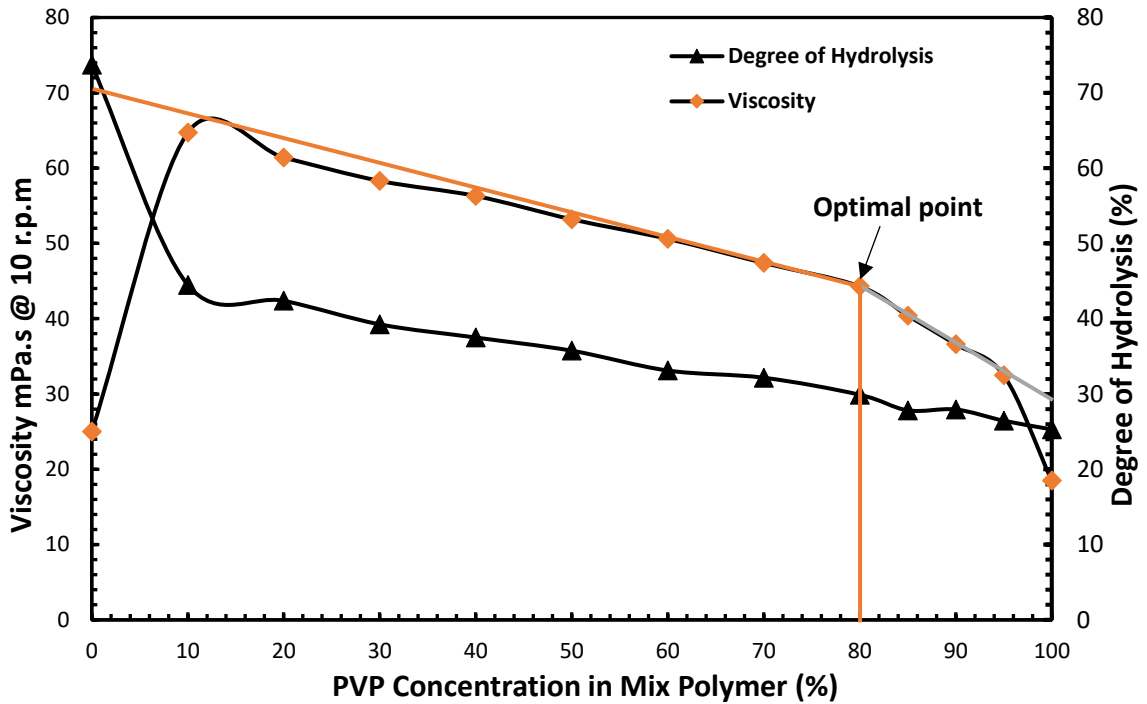


**Figure 6.6:** Determination of optimum concentration of PVP in integrated polymers of PAM: PVP at 90°C and a salinity of 43,280 ppm for a rotational speed of 10 rpm.

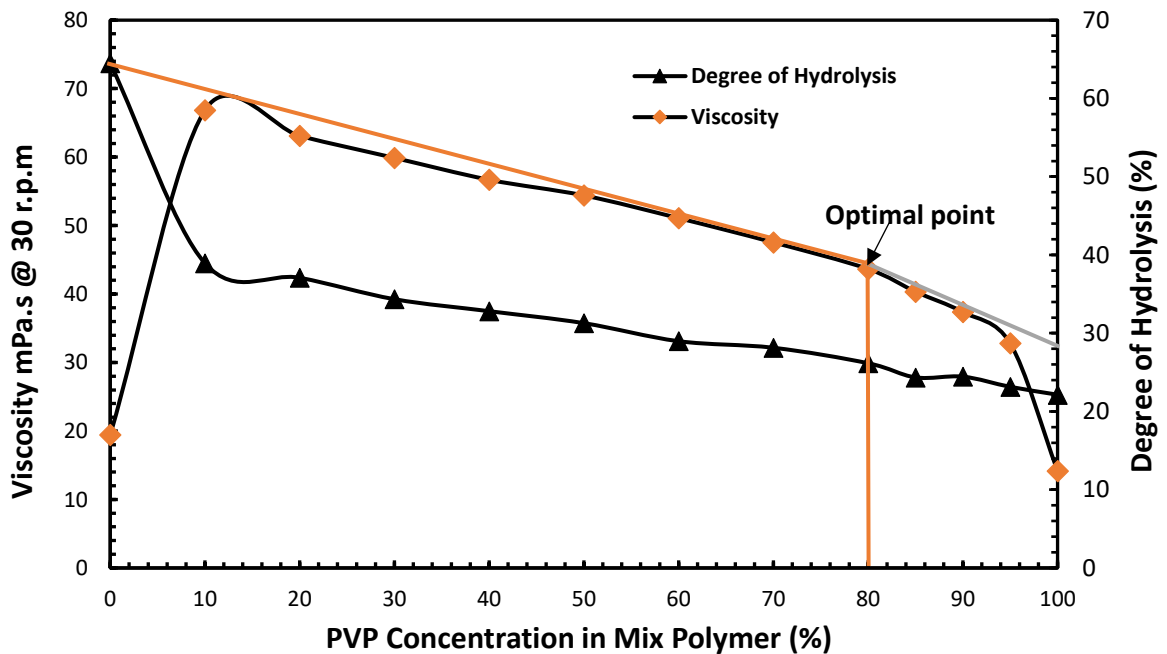


**Figure 6.7:** Determination of optimum concentration of PVP in integrated polymers of PAM: PVP at 90°C and a salinity of 43,280 ppm for a rotational speed of 30 rpm.

#### 6.4 Impact of Salinity on high temperature optimized PAM and PVP integration

The incorporation of Polyvinylpyrrolidone (PVP) effectively protects the polyacrylamide (PAM) against thermal hydrolysis in the presence of moderate salinity of 43280 ppm TDS and temperature of 90°C as discussed in section 5.2 and 5.3. To further investigate the stability of the optimised mix of PAM and PVP in presence of increased salinity of 20000 ppm TDS. **Figure 6.8** is a comparative plot evidence of viscosity and degree of hydrolysis of the optimised integrated polymer solution (20:80 wt % PAM: PVP) against total dissolved salts (TDS) at 30 days. The figure shows that at comparative total dissolved salts (TDS) of 43280 ppm and 20000 ppm, the degree of hydrolysis increased considerably from 30 to 47%, while viscosity decreased sharply from 44 to 38.4 mPa.s respectively at 10 rpm. At 30 rpm, there exists same degree of hydrolysis with 10 rpm but the viscosity drop from 38.6 to 28.6 mPa.s. It is clear that an extreme increase of total dissolved salts in the reservoir from 43280 to 200000 ppm affected the performance of the combined polymer by increasing the degree of hydrolysis and decreasing the viscosity.

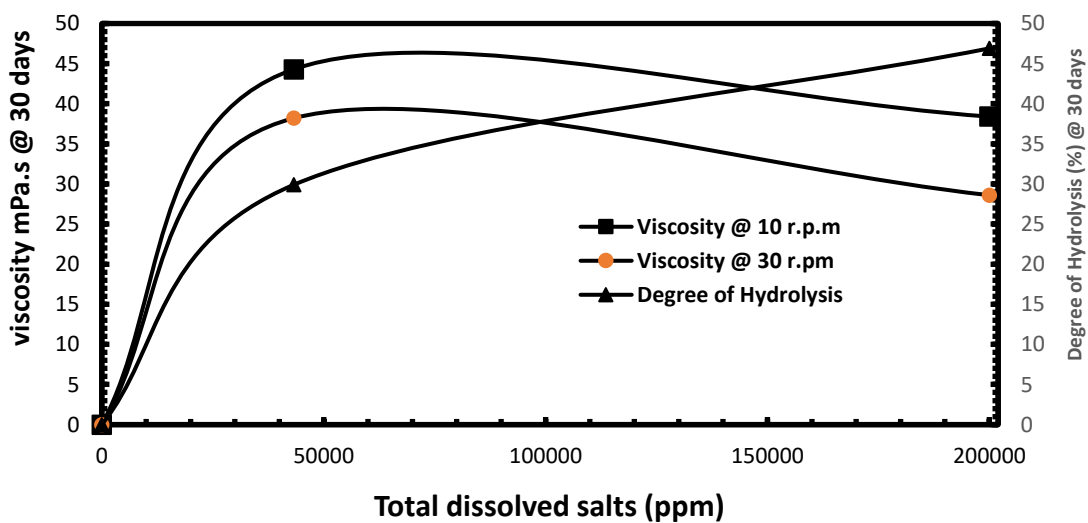


**Figure 6.8:** Effect of salinity concentration on optimized integration of 20 wt % PAM and 80 wt % PVP

In summary, a synthetic approach called the polymer integrated technique (PIT) adopted in facing the challenging reservoir conditions of high temperature 90°C and moderate salinity of 43,280 ppm. This work added polyvinyl Pyrrolidone (PVP) to modify the PAM performance against the behavior of high degree of hydrolysis and degraded viscosity at 30 days of ageing. Chemical modification of PAM solution shows that optimized polymer mixture of 80 wt% PVP and 20 wt % PAM reduced the degree of hydrolysis from 74% to 29.9% and the viscosity increased to 44.3 and 38.2 mPa.s on a corresponding 10 and 30 rpm respectively.

Extending the optimized mixture of 20 wt % PAM and 80 wt % PVP found on operational conditions of 43,280 ppm salt concentration and temperature 90°C to extreme high salinity of 200,000 ppm TDS. The results shows increasing degree of hydrolysis of 46.9% as compare to 29.9% with decreasing viscosity of 38.6 to 28.6 mPa.s on a corresponding 10 and 30 rpm respectively. It becomes clear that extending the optimized mixture to extreme high salinity of 200,000 ppm at temperature of 90°C, affected the performance of the optimized integrated polymer mixture. To improve and stabilise the polymer performance in presence of extreme high salinity of 200,000 ppm and temperature of 90°C, 2-acrylamido-2-methylpropanesulphonic acid (AMPS) was added to the optimized integrated polymer mixture as to remediate high salinity instability during EOR polymer flooding operations and are discussed in Chapter 7.

## **CHAPTER 7: APPLICATION OF PIT TO OPTIMIZE PAM PERFORMANCE AT HIGH TEMPERATURE AND HIGH SALINITY MEDIUM**

The optimized point of 20 wt % PAM and 80 wt % PVP found on operational conditions of 43,280 ppm salt concentration and temperature 90°C, were extended to extreme high salt concentration of 200000 ppm TDS on same temperature to see if polymer solution could withstand stability. The result as discussed in section 6.4 shows that the degree of hydrolysis increases with decreasing viscosity, which is contrary to standard specification of low degree of hydrolysis and relatively high viscosity stability during polymer flooding EOR applications [10].

To improve the performance of the polymer solution and stabilize optimize fit at reservoir conditions of 200000 ppm TDS and temperature 90°C. 2-acrylamido-2-methylpropanesulphonic acid (AMPS) were incorporated to optimized polymer solution mix of 20 wt % PAM and 80 wt % PVP [146]. Accordingly, In 2014 Gao, confirmed that technical gap still exist extending chemical EOR precisely polymer solution to reservoir conditions of 100000 to 200000 ppm TDS at 90°C [147]. Although Chinese researchers found KYPAM as a modified HPAM, the product indicated good stability in high salinity of 160000 ppm TDS on temperature of 180°F (82°C) at Shengli field [86]. This work AMPS addition were screened at weight percentages (wt %) of 90, 50, 10, 5 and 0. The three combination of PAM, PVP and AMPS is termed as the polymer integrated Technique (PIT).

### **7.1 Hydrolysis of the PIT solution**

Apparently, the level of hydrolysis of amide groups in the structure of mixed water-soluble polymers of PAM: PVP: AMPS needs to be determined. FTIR and NMR spectroscopy were utilised.

### 7.1.1 FTIR Analysis of PIT solution

FTIR spectra identified the peak as assigned to the various weight ratios of PIT (PAM: PVP: AMPS) as shown in **table 7.0**. Though in **tables 7.1** is also the peaks for 100 wt % AMPS. From **table 6.0**, the peak at  $1638-1631\text{ cm}^{-1}$  could be assigned to the C=O stretching vibrations of CONH<sub>2</sub>. Apparently, peaks between  $3356$  to  $3349\text{ cm}^{-1}$  represents the primary amide NH<sub>2</sub> and OH asymmetric stretching vibrations of CONH<sub>2</sub>, while the peaks at  $1463-1553\text{ cm}^{-1}$  are assigned to CH<sub>3</sub> and CH<sub>2</sub> group stretching. Those peaks in the range of  $1294-1296\text{ cm}^{-1}$  are assigned to C-N-C stretching, and those between  $1115-1188\text{ cm}^{-1}$  to C-N stretching. However, **Tables 7.0 and 7.1** show the AMPS structure, with the bands for the sulfonate (SO<sub>3</sub>,) functional groups and their stretching appearing in the range  $1043-1044\text{ cm}^{-1}$  [88, 134] whereas those for C-C symmetric asymmetric stretching are at  $995-996\text{ cm}^{-1}$ . In line with **Table 7.0 and 7.1 figures 7 (a and b)** presents a plots evidence of FT-IR absorbance spectra for PAM, PVP and AMPS and comparative plot of PAM, PVP and AMPS mix samples at time 0 and 30 days respectively. However, at time zero in day, absorbance shows less intensities compared to the absorbance at 30 days.

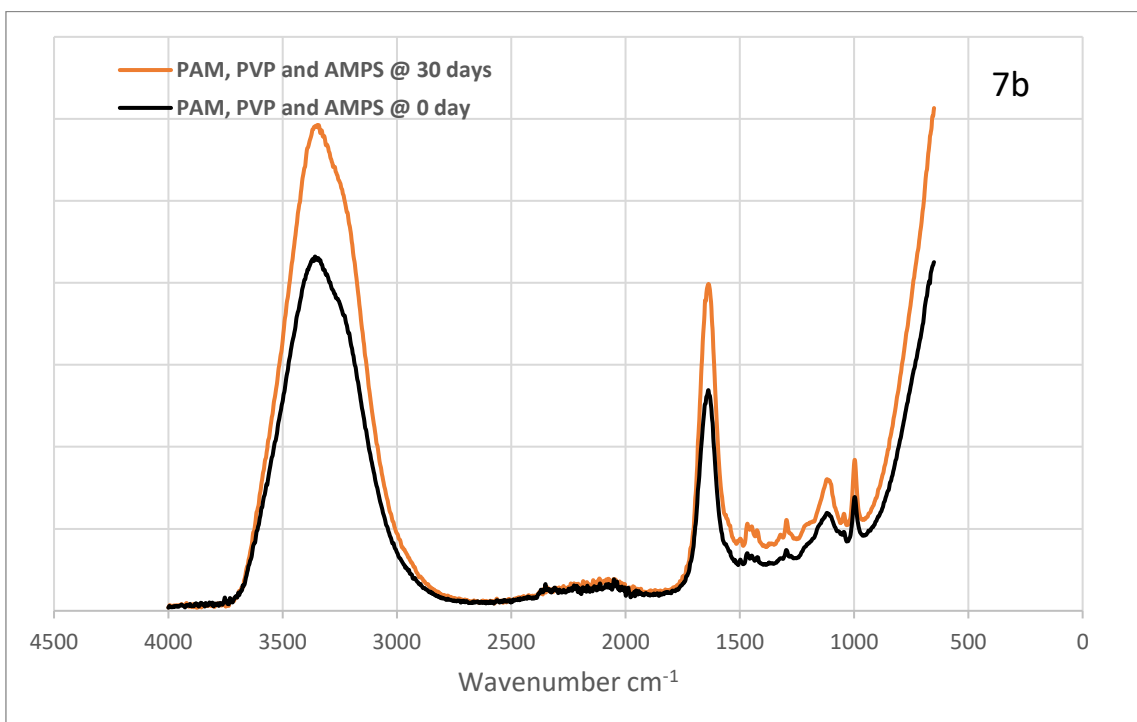
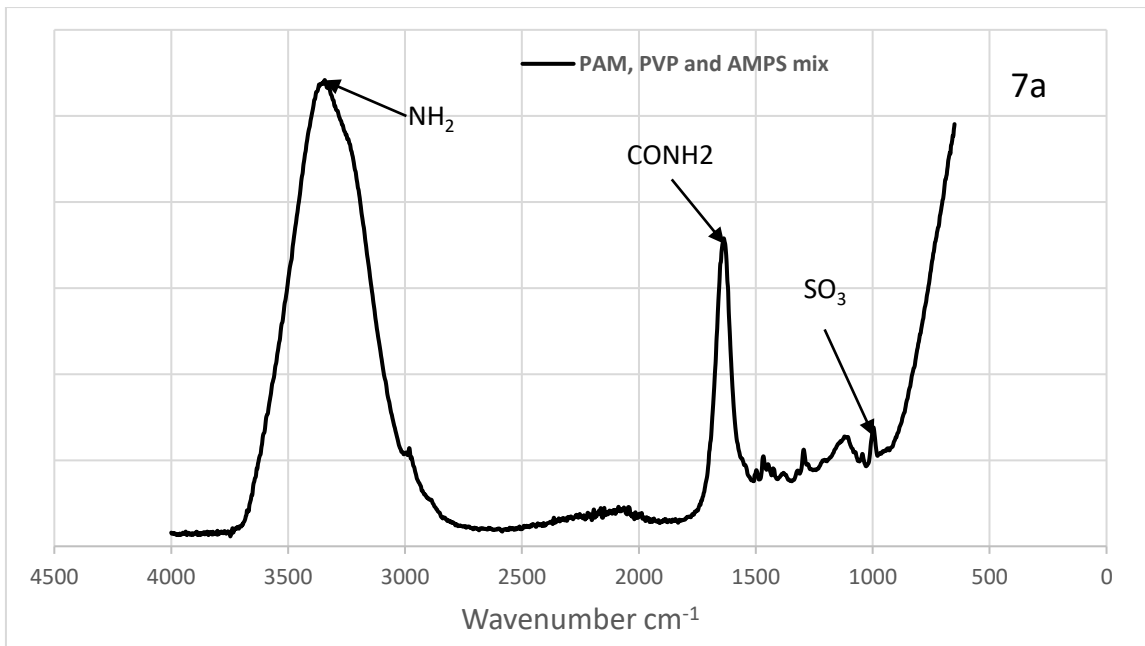


**Figure 7.0:** FT-IR absorbance spectra for (7a) PAM, PVP and AMPS (7b) Comparative PAM, PVP and AMPS mix samples at time 0 and 30 days

Table 7.0: FTIR Spectra or peak assignment for weight proportion of PAM: PVP: AMPS

Peak Assignment	Weight proportion of PAM:PVP:AMPS (wavenumber cm <sup>-1</sup> )			
	19:76:5	18:72:10	10:40:50	02:08:19
Primary amide NH <sub>2</sub> , and OH asymmetric stretching	3356	3333 - 3335	3349	3344 - 3354
Secondary amide N - H stretching	2022 - 2185	2038 - 2067	2039 2169	- 2032 -2089
Primary Amide C=O Stretching	1638 - 1645	1632 - 1638	1638 1551	1631 - 1644 -
CH <sub>3</sub> and CH <sub>2</sub> stretching	1466 - 1467	1465 - 1466	1553	1463 - 1467
C-N-C Stretching	1296	1295	1296 1187	1294 -
C - N Stretching	1116	1115 - 1119	1188	1118 - 1188
SO <sub>3</sub> Stretching	1044 - 1043	1044 - 1043	1044 -1043	1044 - 1043
C - C symmetric - Asymmetric stretching	996 - 997	991 - 996	995 - 997	996 - 997

**Table 7.1:** Peak assignment for 100 % AMPS at 200,000 ppm salinity.

Peak Assignment	100 % AMPS
Primary amide NH <sub>2</sub> , and OH asymmetric stretching	3358 - 3347
Secondary amide N - H stretching	2162
Primary Amide C=O Stretching	1636 - 1638
CH <sub>3</sub> and CH <sub>2</sub> stretching	1551 - 1553
C-N-C Stretching	1296
C - N Stretching	1187 - 1189
SO <sub>3</sub> Stretching	1044
C - C symmetric - Asymmetric stretching	995 - 997

From **figure 7.1** is the pilot evidence that represent the percentages change in amide absorbance for both 20:80 PAM: PVP mix solution and the PIT (PAM: PVP with AMPS) mix solution at different weight percentages (wt %) and also pure AMPS dissolved in water with extremely high salinity at 200,000 ppm. High percentages of amide absorbance were observed of up to 58 and 56% respectively after the second and fourth days of ageing; however the levels declined gradually with ageing until 10 days and subsequently remained stable. The integration of PAM: PVP with 90% by weight of AMPS reduced amide absorbance significantly from 30% down to 9 % after 30 days of ageing.

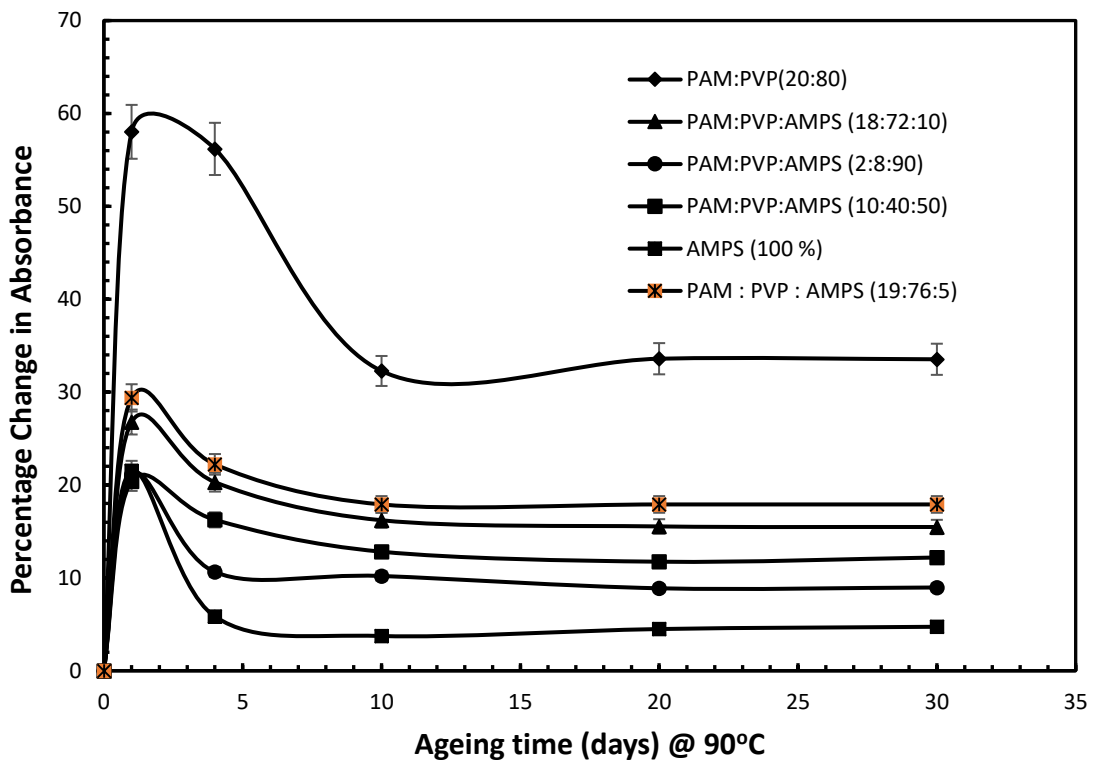
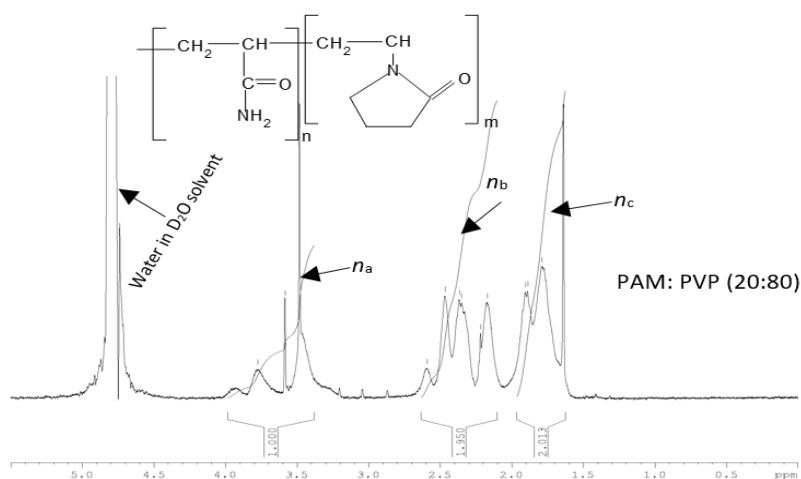


**Figure 7.1:** Percentage change in amide absorbance of PAM and integrated (PAM: PVP polymers at 90 °C and 200,000 ppm TDS.



### 7.1.2 NMR Analysis of PIT solution

Determining the degree of hydrolysis of PIT solution. **Figure 7.2a** presents the  $^1\text{H}$  NMR spectra for integrated polymers of PAM: PVP (20:80) and different weight ratios of PAM: PVP: AMPS at  $90^\circ\text{C}$  and salinity 200,000 ppm, more of different weight ratio of PAM: PVP: AMPS are shown in figure 7.2b. The peak at 4.8 ppm represents water content in the deuterium oxide ( $\text{D}_2\text{O}$ ) solvent. However, the peak observed between 3.4-3.2 ppm could be attributed to the equivalent hydrogen (H) atom of the CH group bonded to  $\text{SO}_3$  in AMPS and the amide group ( $\text{C}=\text{O}$ ) in the PVP structure [88, 126, 134]. The peaks between 2.20-2.40 ppm and 1.60-1.90 ppm are assigned to the equivalent hydrogen (H) atom of the CH group bonded to the amide group ( $\text{CONH}_2$ ). The peaks measured at 1.60-1.90 ppm represent the equivalent atom of the  $\text{CH}_2$  group in PAM, PVP and AMPS respectively. In these set of results  $n_a$ ,  $n_b$  and  $n_c$  are defined as equivalent H atom in peak integration for CH group for PVP and AMPS bonded to amide group ( $\text{C}=\text{O}$ ), equivalent H atoms in peak integration for CH group bonded to amide group ( $\text{C}=\text{O}$ ) combined PAM and PVP, and equivalent H atoms in peak integration for  $\text{CH}_2$  group for PAM and PVP, respectively.



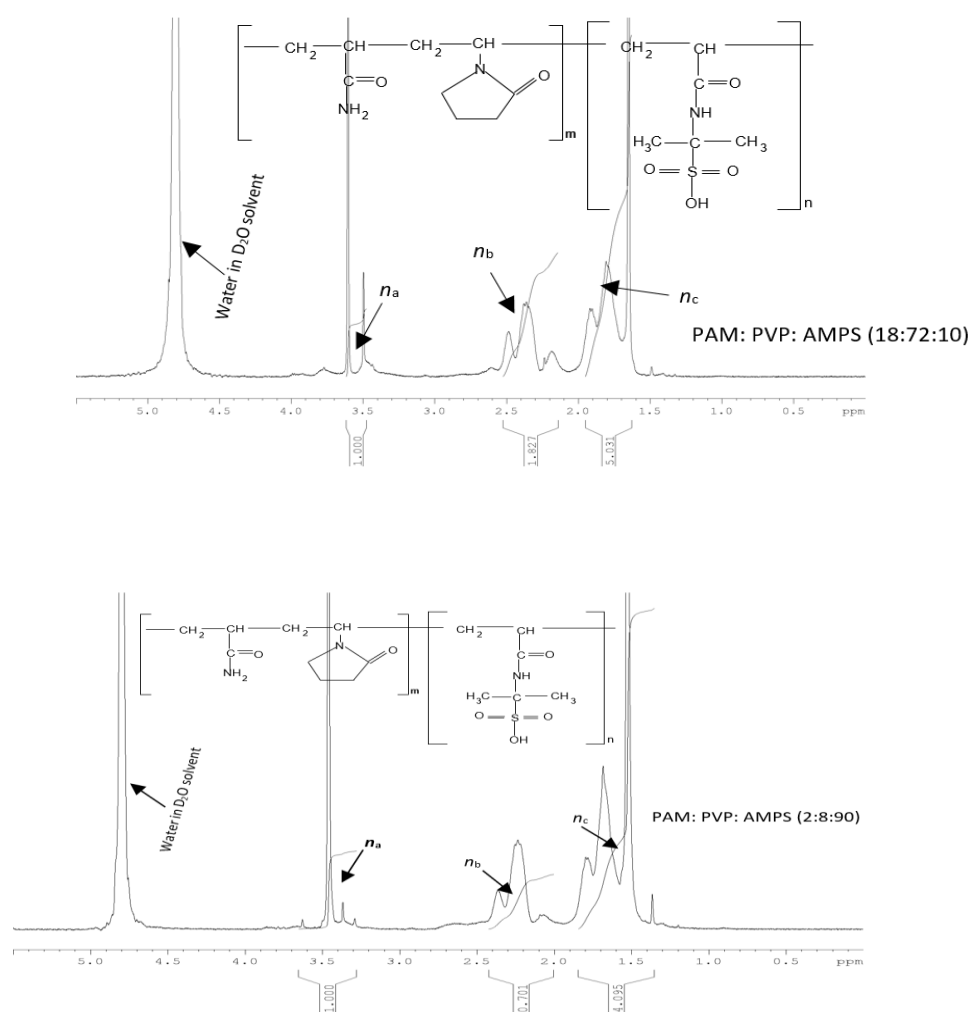


Figure 7.2a: <sup>1</sup>H NMR spectra for integrated polymers of PAM: PVP (20:80) and different weight ratios of PAM: PVP: AMPS at 90°C and salinity 200,000 ppm.

The initial degrees of hydrolysis for integrated polymer solutions were evaluated using Buker Topsin 3.5 software and results are presented in **Table 7.3**. As can be seen from the table, the higher the weight proportion of AMPS, the lower the initial degree of hydrolysis ( $DH_i$ ). The weight proportion of AMPS at 5 % in the integrated polymer solution shows an initial degree of hydrolysis ( $DH_i$ ) of 20% compared to 18% for the 90 wt % AMPS mixture.

**Table 7.3:** Initial degree of hydrolysis ( $DH_i$ ) for brine samples of 200,000 ppm at 90°C.

	<b>PAM</b>	<b>PVP</b>	<b>AMPS</b>	
<b>Sample No:</b>	<b>wt%</b>	<b>wt%</b>	<b>wt%</b>	<b><math>DH_i</math></b>
1	20	80	0	35
2	19	76	5	20
3	18	72	10	19
4	10	40	50	18
5	2	8	90	18

In determining the degree of hydrolysis over the designated ageing times, the percentage absorbance needs to be converted into degree of hydrolysis. This is accomplished by combining the percentage increase in amide groups and the initial degree of hydrolysis ( $DH_i$ ) as given in **equation 4.3 [103]**. **Figure 7.3** shows the degree of hydrolysis for integrated polymer solutions in high temperature and high salinity conditions. As can be deduced from this figure, the integrated PAM:PVP:AMPS polymers exhibit lower degrees of hydrolysis of about 22% compared to 46% for PAM:PVP solutions when dissolved in extremely high salinity formation water of 200000 ppm, with a stabilised degree of hydrolysis of 46.2%.

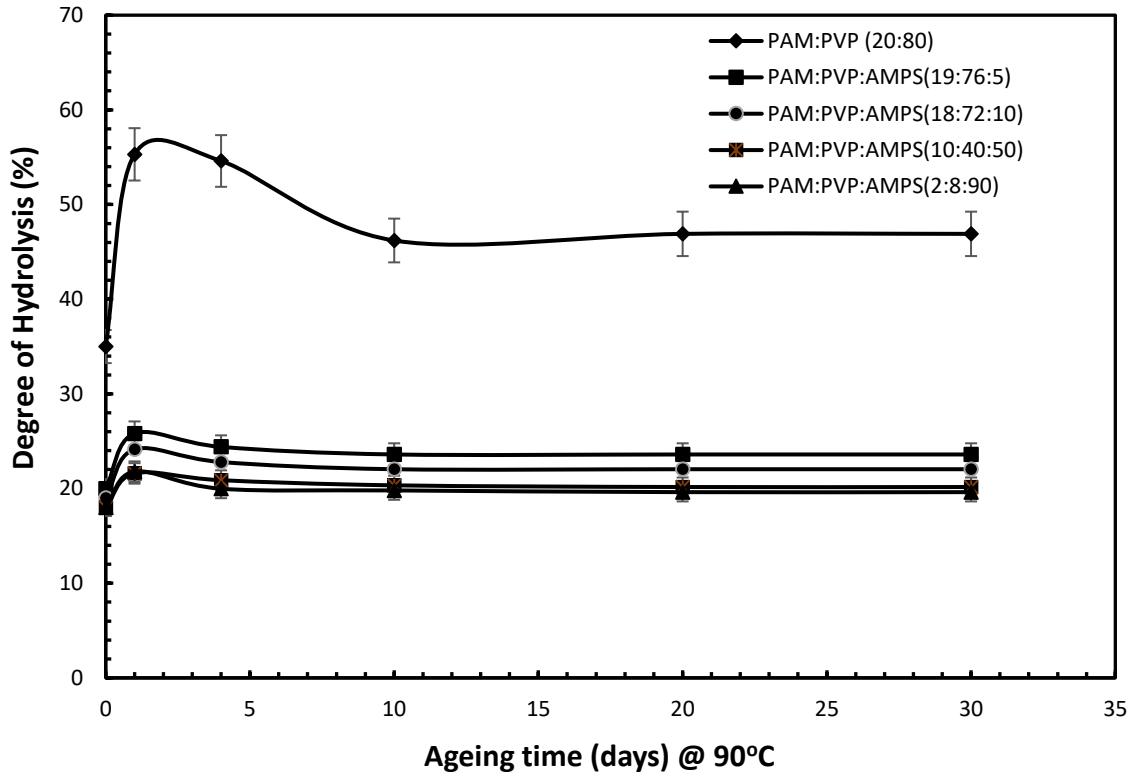
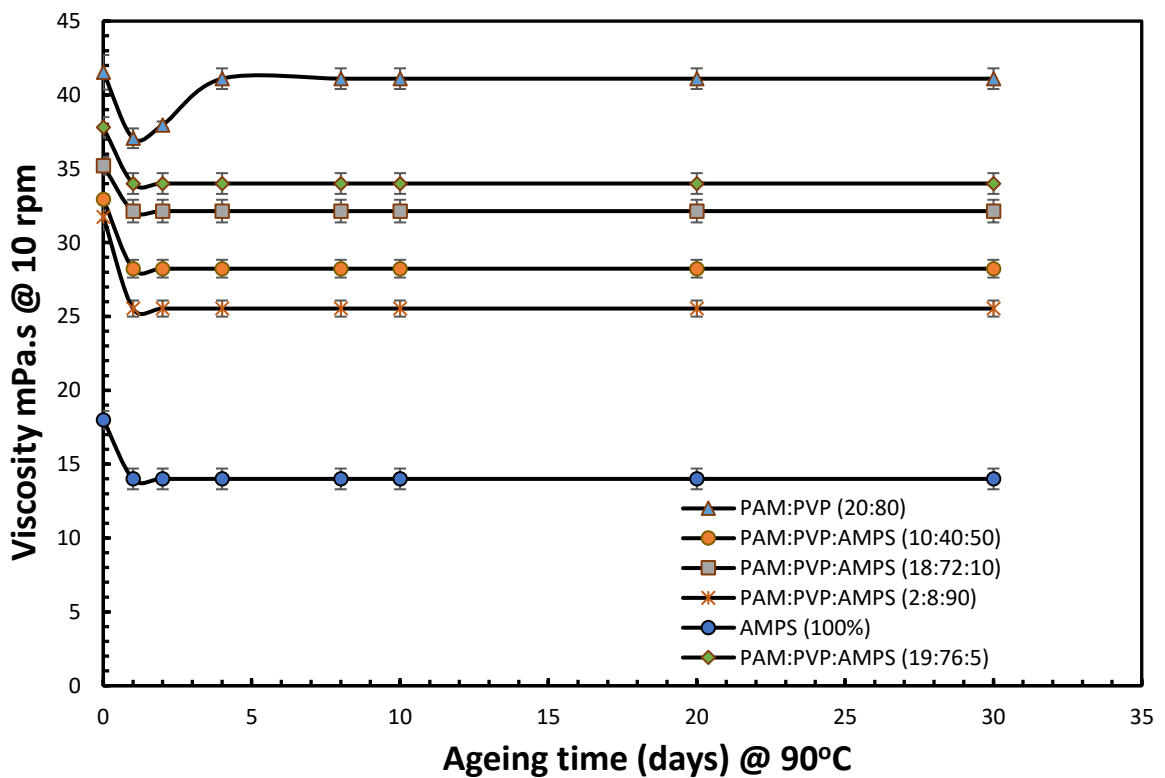
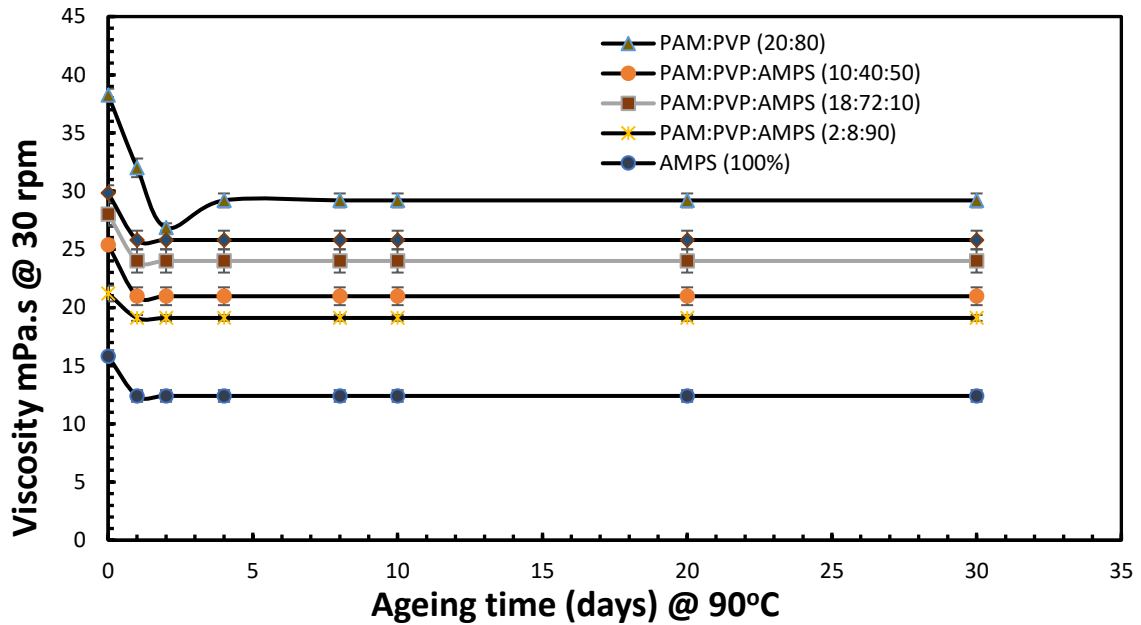


**Figure 7.3:** Extent of degree of hydrolysis of 20:80 PAM: PVP and different weight ratios of PAM: PVP: AMPS at 90°C and 200,000 ppm salinity.

## 7.2 Stability of integrated polymers extreme reservoir conditions

High gel stability and high viscosity are the two main requirements in the selection of suitable polymer solutions under the influences of extremely high salinity formation water and high temperature. **Figure 7.4** illustrates changes in viscosity against ageing time for three rotational speeds of 10, 30 and 600 rpm, accordingly, the viscosity test for each weight composition was conducted three times and the mean of the three viscosity measurements presented as final viscosity error bars calculated based on test repeatability. The figure shows stability in the polymer solution from 4 to 30 days of ageing. Although the weight proportion of 20:80 PAM: PVP copolymer shows greater viscosity, it exhibits a high degree of hydrolysis at 54.6% before stabilising at 46.2%, and it seems obvious that this level of hydrolysis

might cause degradation. A comparison of the viscosity results obtained for different weight proportions of PAM: PVP: AMPS ter-polymers with those for the copolymer PAM: PVP shows that more solutions with more PAM: PVP and less AMPS have higher viscosity compared to those with less PAM: PVP and more AMPS.



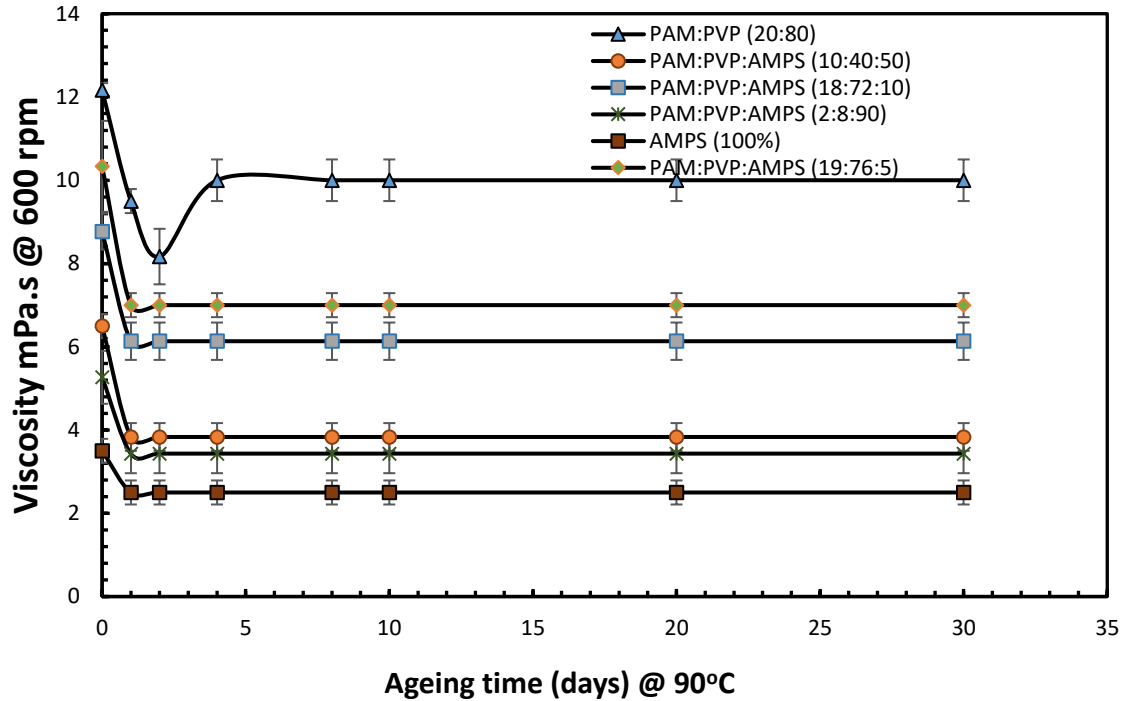


**Figure 7.4:** The viscosity of PAM: PVP: AMPS at 90°C in salinity of 200,000 ppm TDS at (a) 10 rpm and (b) 30 rpm and (c) 600 rpm.

### 7.3 Optimized integrated polymer solution at extreme reservoir conditions

The ter-polymer of PAM, Polyvinylpyrrolidone and 2-Acrylamido-2-Methylpropane Sulfonic acid (AMPS) produced high stability and could be effective for mobility control in EOR applications. Optimization of the weight ratio composition of the PAM: PVP: AMPS (PIT) polymer mixture will provide more sweep in enhanced oil recovery process, especially in terms of the economic evaluation and feasibility of the process. **Figure 7.5** demonstrates how the optimised concentration of AMPS in the integrated polymer for 30 days ageing time was selected. From the figure, an AMPS weight proportion of 10 wt % was found to be optimum, resulting in the overall optimum composition of the ter-polymer of PAM: PVP: AMPS at the weight percentages of 18:72:10 for use in a temperature of 90°C and a salinity of 200000 ppm.

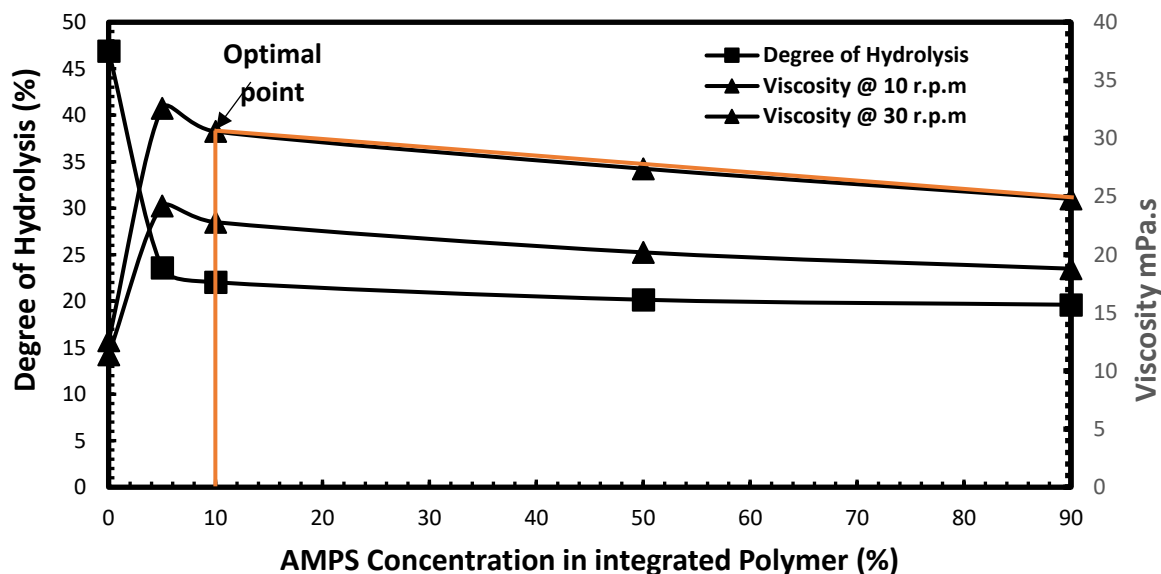


**Figure 7.5:** Optimized weight proportion of PAM: PVP: AMPS at 90°C and 200,000 ppm TDS.

In summary, **Gao et al., [86]** reported on the specifications used for the application of hydrolysed PAM based on experience at the Shengli Company. They stated that hydrolysed PAM product should go through screening tests before being deployed in the field and that two criteria should be met: (1) the degree of hydrolysis should be < 25%; and (2) the hydrolysed solution must maintain good stability and viscosity > 11.5 mPa.s against the influence of shearing, temperature and water salinity. However, the results in figure 7.5 show that the polymer mixture proposed in the present work has surpassed the criteria by achieving a degree of hydrolysis of 22.04% with good stability and viscosity maintained at 30.6 mPa.s at the low shearing rate of 10 rpm ( $17 \text{ sec}^{-1}$ ) in the presence of extremely high salinity at 200,000 ppm and a temperature of 90°C.

## 7.4 PIT shear behaviour

The Fann and Palmer viscometer studies in section 4.4 on polymer degradation shows that polyacrylamide solutions are pseudo plastic (shearing thinning solution). In pseudo plastic or shear thinning behaviour, the viscosity of the polymer solution decreases as the shear rate increases [102,135]. However, for polymer integration technique (PIT) shear test, the flow characterization were determined through studying the relationship between the effective viscosity and shear rate. The method utilised for effective viscosity and shear rate relationship are expressed from equation 3.0 to 3.2. The results in **figure 7.6** demonstrated that effective viscosity of PIT solution increases as the weight proportion of PAM, PVP and AMPS in the overall solution composition increases. This imply that the pseudo plasticity behaviour of the solutions increases as each component solution increases. From the figure, it is also noticed that the degree of shear degradation was found to depend on the proportion of the polymer concentration in the PIT mix solution.



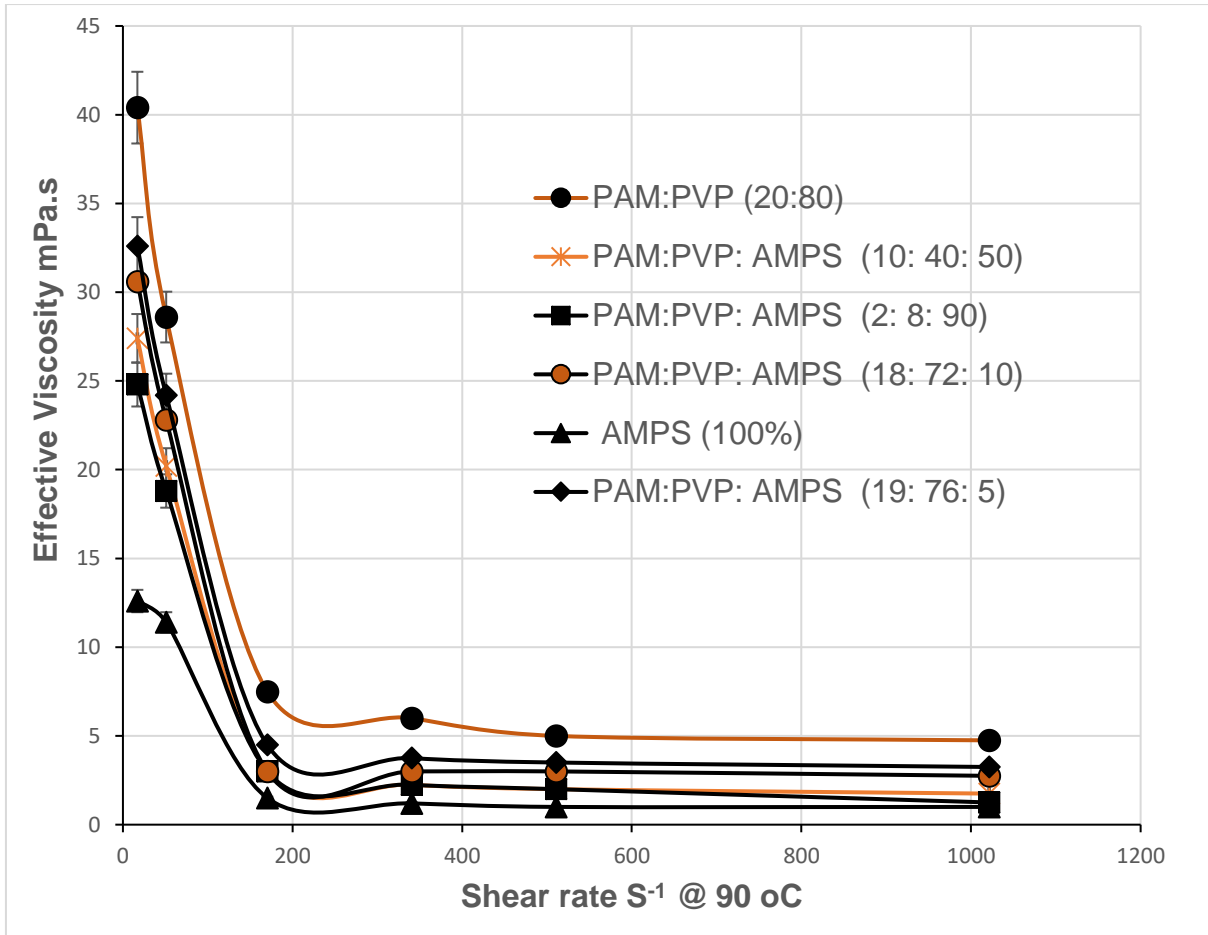


**Figure 7.6:** PIT Shearing at the salinity of 200000 ppm TDS and 90°C

Comparatively, from **figure 7.7** is effective viscosity of polymer solution between PAM mixed with brine (43280 ppm) and that of 80 wt% PVP and 20 wt % PAM at salinity of 43280 and 200000 ppm TDS against the shear rate. From the figure, the composition of 80 wt % PVP and 20 wt % PAM mixed with salinity of 43280 ppm TDS, the plot demonstrated a shear thinning or pseudo plastic behaviour where the viscosity decreases as the shear rate increases. High effective viscosity loss was observed as the shear rate increases for PAM mixed with brine (43280 ppm) compare to the PAM: PVP

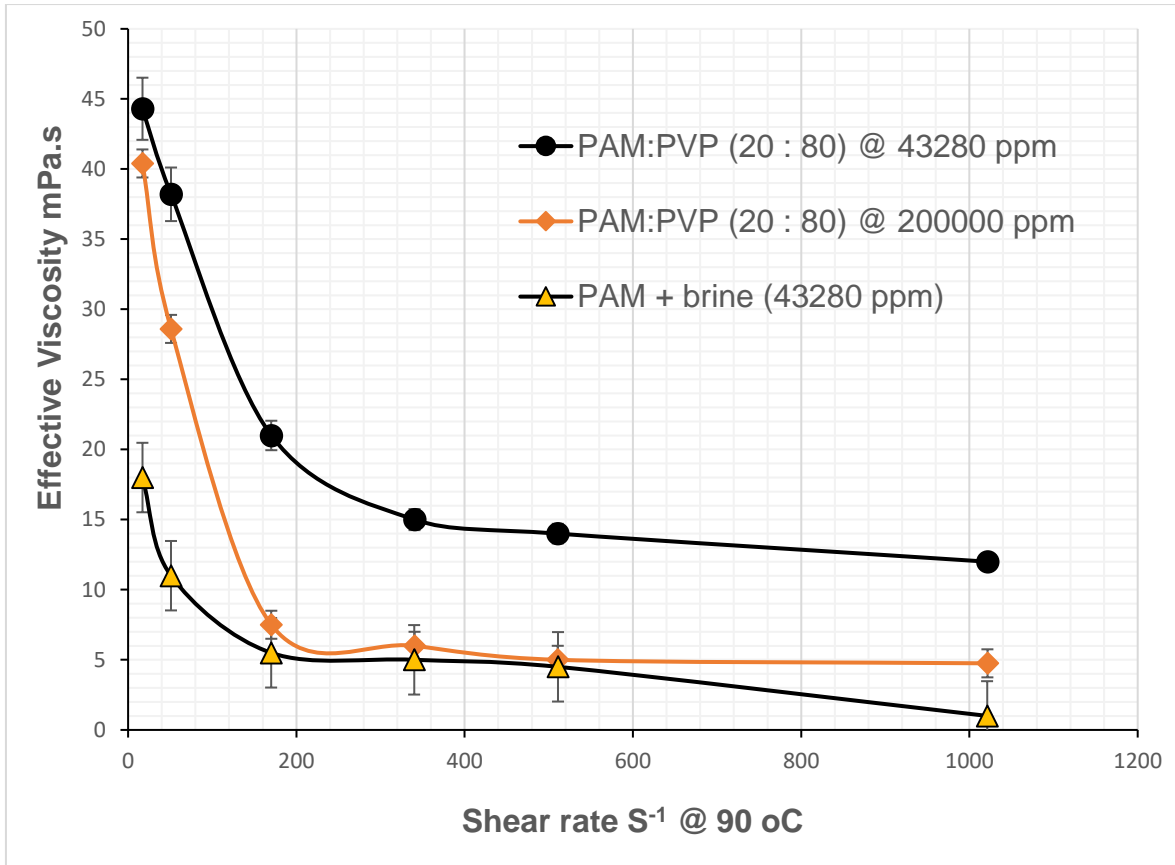


**Figure 7.7:** Shearing and mechanical degradation at different PAM and salinity concentration.

### 7.5 Stability of PIT

Significant research effort made on this work to identify and develop a new synthetic polymers with improved stability and increases viscosity of injection water. The approach focuses on meeting the criteria of inactivity or insensitivity on high temperature in the phase of brines. This is to remediate thermal degradation by resistant to hydrolysis and improving the rheology of the polymer solution. The synthetic approach called the polymer integrated technique (PIT) adopted to face the challenging reservoir conditions of high temperature 90°C and moderate salinity of 43,280 ppm. Shows high thermal stability on addition of PVP to PAM solution in the phase of high temperature and as well reducing the degree of hydrolysis from 74% to

29.9%. In rheology phase the viscosity increased to 44.3 and 38.2 mPa.s on a corresponding 10 and 30 rpm respectively at optimized polymer mixture of 80 wt% PVP and 20 wt % PAM.

Extending the optimized mixture on operational conditions of 43,280 ppm salt concentration and temperature 90°C to extreme high salinity of 200,000 ppm TDS. The results shows increasing degree of hydrolysis of 46.9%, the polymer solution viscosity degraded from 44.3 and 38.2 mPa.s to 38.6 and 28.6 mPa.s on a corresponding 10 and 30 rpm respectively. The degradation occurs because of increases in salinity concentration from 43,280 ppm to 200,000 ppm in phase the temperature of 90°C. To remediate, stabilise and improve the polymer performance in presence of extreme high salinity of 200,000 ppm and temperature of 90°C, 2-acrylamido-2-methylpropanesulphonic acid (AMPS) was added to the optimized integrated polymer mixture as to remediate the degradation and thermally stabilise the polymer solution for effective EOR polymer flooding operations.

The AMPS addition as shown in figure 7.5 shows reduced degree of hydrolysis to 22.04% and viscosity at 30.6 mPa.s at the low shearing rate of 10 rpm ( $17 \text{ sec}^{-1}$ ) in the presence of extremely high salinity at 200,000 ppm and a temperature of 90°C.

## CHAPTER 8: CONCLUSIONS AND RECOMMENDATIONS

### 8.1 Conclusions

The water-soluble polymer PAM (polyacrylamide) and its derivative HPAM is applied in enhanced oil recovery (EOR) operations when mobility ratio of a waterflood is unfavorable ( $M > 1$ ) causes viscous fingering and reservoir heterogeneity. To control these challenging situations and improve the sweep efficiency, polymer solution (PAM and HPAM) is pumped into water injection wells to increase the viscosity of the injected water and in turn push or divert more oil towards production wells. Accordingly, PAM and HPAM solution proven to be sensitive to reservoir conditions, such as high temperature and high salinity. These challenging effects drove this research in improving the polymers performance by developing better polymers and optimizing to fit reservoirs. Before the improvement and optimizing polymer solution, a correlation analysis was conducted to determine the safe maximum temperature point (SMTP) from previous published data. The correlation analysis proved that different saline solutions like NaCl, CaCl<sub>2</sub> and NaHCO<sub>3</sub> contain different SMTP as in chapter 4. Proceeding is synthetic experimental approach on studying the effectiveness of polyacrylamide (PAM) at different operational conditions in chapter 5.

From the results obtained in chapter 5, temperature acted as the major cause of PAM and HPAM degradation by increasing the hydrolysis of the amide functional group when the polymer sample is being aged at temperatures of 50, 70 and 90°C. The increasing effects of degree of hydrolysis took place from moderate to high temperature. At 30 days ageing, the increase in hydrolysis took place in two stages. In stage one, a quick rise in hydrolysis is seen over the first day. In stage two, the rate of hydrolysis is reduced and the increase is a linear function of time. Beside

the temperature, the brine favoured more increase in the degree of hydrolysis, with the addition of brine a similar pattern is seen, but the rate of hydrolysis in the first stage is increased.

Accordingly, the dependence of degree of hydrolysis on temperature affected the performance of viscosity of the polymer solution and the viscosity retention. The lower temperature have higher viscosity and higher the viscosity retention compared to higher temperature having lower viscosity and lower viscosity retention.

The effects of shearing on the viscosity of the polymer solution (polyacrylamide) caused high decrease in viscosity on high shear rates compared to low shear rate with low decrease in viscosity. This suggests that the nature of the gel changes after 10 days and the gel collapses. Even the shearing effect work concurrently with the temperature.

Finally in chapter 5, at higher temperature of 90°C, the onset of the collapse of the gel occurs at lower shear rates. The degree of hydrolysis occurs faster than the reduction in viscosity.

To make the polymer solution maintain a relatively high viscosity under the influences of high temperature of 90°C and moderate and high salinity. The synthetic approach followed has been to modify polyacrylamide (PAM) with Polyvinylpyrrolidone (PVP) as seen in chapter 6. In chapter 6 after various polymers mix screening, a non-extant Polyvinylpyrrolidone (PVP) weight proportion of 80 wt % was found to be the optimum concentration of the composition resulting to overall optimum composition of copolymer PAM: PVP (20:80) wt % with low degree of

hydrolysis of 29.9% for use in temperature of 90°C and high salinity of 43,280 ppm. Hydrolysis herein were suppressed and viscosity maintained stability.

To further investigate the stability of the optimised mix of PAM and PVP in presence of increased salinity of 200,000 ppm. Comparatively at total dissolved salts (TDS) of 43280 ppm and 200,000 ppm, the degree of hydrolysis increased from 30 to 47%, while viscosity decreased sharply from 44 to 38.4 mPa.s respectively at 10 rpm. Same experience were duplicated at 30 rpm the viscosity drop from 38.6 to 28.6 mPa.s. Increasing the salinity from 43280 to 200,000 ppm TDS affected the performance of the optimised mix of PAM and PVP polymer solution by increasing the degree of hydrolysis and decreasing the viscosity.

To face the challenge of extreme high salinity of 200,000 ppm at 90°C, 2-Acrylamido-2-MethylpropaneSulfonic acid (AMPS) were incorporated to the optimised mix of PAM and PVP. The results at chapter 6 indicated a reduction of initial degree of hydrolysis (DH<sub>i</sub>) to 22.2%, of the system. A novel AMPS weight proportion of 10 wt % was found to be the optimum concentration to overall optimum composition of 18:72:10 ter polymers of PAM: PVP: AMPS to enhance the performance of polymer application at temperature of 90°C and salinity of 200000 ppm.

Finally, substantial effort has been made on this research in improving the performance of polyacrylamide and the new synthetic polymers known as polymer integrated technique (PIT) shown to improve stability and maintain viscosity of the solution. This research novel synthetic approach met the criteria of inactivity or insensitivity to salt concentration at high temperature and resistance to hydrolysis. These chemical modifications named polymer integrated technique (PIT) constitute

an important technique for polymer flooding during EOR applications in improving the polyacrylamide and HPAM performance for reservoirs with hostile conditions.

## **8.2 Recommendations**

On completion of this study, there are some areas that the author could like to recommend as focuses for future research work or for further investigation.

- The properties or data from laboratory experiments of the optimised polymer integration technique (PIT) should be use for rheology characterization through laboratory core flooding experiment in a porous media. For the sole aim of measuring the permeability (mD) by flowing a fluid known viscosity of core sample using Berea sandstone or carbonate in porous media on characterization in extremely high permeability water cut above 65% of known dimensions at a set fluid flowrate and measuring the pressure drop across the core or setting the fluid to flow at a set pressure difference, and measuring the flow rate produced.
- Simulation model based on simple rig and modify model to use new properties Speculative of real data from well (s): (a) using real data for well and (b) then stimulate with new properties.
- The economical evaluation to demonstrate that the polymer flooding increased oil production and increased ultimate recovery by certain percentage level. The cash flow determined by generating the revenues by combining the oil production profile with the oil price profile. The revenues and cost are combined to yield a net cash flow, or net present value of the project. Accordingly, as regarding the verification of laboratory results for comparative simulation and modelling on polymer flooding brief information highlighted in the appendix supported with main figures as preliminary analysis.

## References:

1. Lake LW., Schmidt RL., Venuto PB. A Niche for Enhanced Oil Recovery in the 1990s. *Oilfield Review*, January, 1992. 55 -61p.
2. Al-Mutairi, SM., Kokal SL. EOR Potential in the Middle East: Current and Future Trends.SPE143287. In proceedings of the SPE EUROEC/EAGE Annual Conference and Exhibition held in Vienna, Austria 23 – 26 May 2011; 1 -11p.
3. Wei B. Advances in Polymer Flooding.INTECH Open science/Open minds 2016. Pp 1 – 17p. <http://dx.doi.org/10.5772/64069>.
4. Vermolen, E.C.M., Van Haasterecht, M.J.T., Masalimeh, S.K., Faber, M.J., Boersma, D.M., Gruenenfelder M. Pushing the envelope for polymer flooding towards high-temperature and high-salinity reservoirs with polyacrylamide based ter – polymers. SPE 141497. In *Proceedings of the SPE Middle East Oil and Gas Show and Conference*, Manama, Bahrain, 25-28 September 2011.
5. Craft BC., Hawkins M. *Applied Petroleum Reservoir Engineer*.1<sup>st</sup> edition. Published by Pearson Education, Inc Westford Massachusetts, 2015.
6. Sandiford B. Laboratory and field studies of water floods using polymer solutions to increase oil recoveries. *Journal of Petroleum Technology*, 1964. 16(08), 917–922p.
7. Mungan N. Shear viscosities of ionic polyacrylamide solutions. *Society of Petroleum Engineers Journal*. 1972; 12(6):469–473.
8. Gogarty W.B. Mobility control with polymer solutions. SPE 1566B, Paper presented at 41<sup>st</sup> Annual fall meeting held in Dallas, Texas. 1967; 161 – 173p.
9. Jennings RR, Rogers JH, West TJ. Factors influencing mobility control by polymer solutions. *Journal of Petroleum Technology*, 1971; 23(03), 391–401.
10. Gao, C., Shi, J., Zhao, F. Successful polymer flooding and surfactant – polymer flooding projects at Shengli Oilfield from 1992 and 2012. *Journal of Petroleum Exploration and Production Technology* 2014; 4, 1-8p.
11. Li X., Xu Z., Yin H., Feng Y., Quan, H. Comparative studies on enhanced oil recovery: thermoviscosifying polymer versus polyacrylamide. *Energy and Fuels* 2017; 31 (3), 2479-2487p.
12. Muller G, Fenyo JC, Seleny E. High molecular weight hydrolysed polyacrylamides. III. Effect of temperature on chemical stability. *Journal of Applied Science*. 1980; 25, 657–633p.
13. Zaitoun A, Potie B. Limiting Conditions for the use of Hydrolysed Polyacrylamides in Brines Containing Divalent Ions. SPE 11785, paper presented at the *International Symposium on Oilfield and Geothermal Chemistry* held in Denver, Colorado, June 1–3. 1983; 143–150p.
14. Moradi–Araghi, A, Doe, PH. Hydrolysis and precipitation of polyacrylamides in hard brines at elevated temperatures. *SPE Reservoir Engineering*. 1987; 189–198p.
15. Ryles R.G. Chemical stability limits of water-soluble polymers used in oil recovery processes. SPE (13585) *Reservoir Engineering*. 1988: 3(01): 23 – 34p.



16. Albonico P., Lockhart T.P. Divalent ion-resistant polymer gels for high-temperature applications: syneresis-inhibiting additives. SPE-25220. In *Proceedings of the SPE International Symposium on Oilfield Chemistry*. New Orleans, Louisiana, USA, 2-5 March, 1993.
17. Sheng James J. *Modern Chemical Enhanced oil recovery*. 1<sup>st</sup> edition. Gulf Professional Publishing imprint of Elsevier Inc. Kidlington Oxford UK. 2011.
18. Thomas A, Gaillard N, Favero C. Some Key Features to Consider When Studying Acrylamide – Based Polymers for Chemical Enhanced Oil Recovery. *Oil & Gas Science and Technology – Rev. IFP Energies nouvelles*, 2012. 67(6): 887 – 902p.
19. Zaitoun A., Makakou P., Blin N., Al-Maamari RS., Abdel-Goad M., Al-Sharji HH. Shear Stability of EOR Polymers. In proceeding of SPE International Symposium on oilfield Chemistry in woodlands, Texas USA, 11 – 13 April 2011.
20. Data M.J., Milanesio J.M., Martini R., Miriam S. Synthesis techniques for polymers applied to enhanced Oil Recovery. *MOJ Polymer Science*. 2018. 2(1) 17 – 20p.
21. Sorbie, KS. *Polymer-Improved Oil Recovery*. 1<sup>st</sup> Ed. Blackie and Son Glasgow, Scotland, 1991. 28(3): 2 – 206p.
22. Dang C., Nghiem L., Nguyen N., Yang C., Chen Z., Bae W. Modelling and optimization of alkaline – surfactant – polymer flooding and hybrid enhanced oil recovery process. *Journal of Petroleum Science and Engineering*, 2018. 169; 578 – 601p.
23. Green DW., Willhite GP. *Enhanced Oil Recovery*. 1<sup>ST</sup> edition. Society of Petroleum Engineers Inc. United State of America 1998.
24. Algharaib M., Alajimi R., Gharbi R. Improving polymer flood performance in high salinity reservoirs. *Journal of Petroleum Science and Engineering (Elsevier)* 2014. 115; 17 – 23.
25. Rellegadla S., Prajapat G., Agrawal A. Polymer for enhanced oil recovery: Fundamentals and selection criteria. Article in *applied Microbial Biotechnology + Springer (cross mark)*. 2017.
26. Lake, Larry W. *Enhanced Oil Recovery*, Prentice – Hall, Inc., New York (1989), 195 – 196p.
27. Stosur GJ., Hite RJ., Carnahan NF., Miler K. The Alphabet Soup of IOR, EOR and AOR: Effective Communication Require a Definition of Terms. SPE 84908. In proceeding of SPE International Improved of Recovery Conference in Asia Pacific Kuala Lumgur Malaysia, 20 – 21 October, 2003.

28. Al – Bahar M.A., Merrill R., Peake W., Jumaa M., Oskui R. Evaluation of IOR Potential within Kuwait. SPE 88716. In proceeding of 11<sup>th</sup> Abu Dhabi International Petroleum Exhibition and Conference held in Abu Dhabi, U.A.E., 10 – 13 October, 2004. 1 – 9p.
29. Haynes H.J., Thrasher W.L., Katz M.L., Eck T.R. Enhanced oil Recovery (EOR): An analysis of the Potential for Enhanced Oil Recovery from Known Fields in the United States – 1976 – 2000. National Petroleum Council (NPC), Washington DC, December, 1976.
30. Singh SP., Kiel OG. Waterflood Design (Pattern, Rate, and Timing). SPE 10024. In proceeding of SPE International Petroleum Exhibition and Technical Symposium Beijing China, 18 – 26 march, 1982.
31. Alvarez JM., Sawatzky RP. Waterflooding: Same old, Same Old. SPE 165406. In proceeding of SPE Heavy Oil Conference Canada in Calgary, Alberta Canada, 11 – 13 June, 2013.
32. United oil & Gas Corporation. United oil & Gas Corp. Acquires 5 new oil leases. Online available @ <https://uogcorp.com/united-oil-amp-gas-corp-acquires-5-new-oil-leases>. 2018. Accessed 17/12/18.
33. Craig Forrest F., Jr. The Reservoir Engineering Aspects of Water flooding. SPE Monograph series, printed in United States of America. 1993.
34. Romero – Zeron L. Advances in Enhanced Oil Recovery Processes, Introduction to Enhanced Oil Recovery (EOR) processes and Bioremediation of Oil – Contaminated sites. INTECH open science/open minds, 2012.
35. Lyons W. & Plisga B.S, (eds). Standard Handbook of Petroleum & Natural Gas Engineering (second edition). Published by Elsevier Inc, Burlington, USA. 2005.
36. Sun Y, Saleh L, Bai B. Measurement and impact factors of polymer rheology in porous media. InTech Open Science/Open Mind. 2012.187–188p.
37. Leverett, M.C. Capillary Behaviour in Porous Solids, Trans., AIME 1941. 142 152 – 169p.
38. Buckley, S.E., and Leverett M.C. Mechanism of Fluid Displacements in Sands. Trans., AIME 1942 .146, 107 – 116p.
39. Ahmed T. Reservoir Engineering. 2<sup>nd</sup> edition. Published by Gulf Professional Company, Houston, Texas USA, 2001. 880 – 920p.
40. Prasad GR. Enhanced Oil Recovery by Using Polymer Flooding in Oil and Gas Industry in Tertiary Recovery Process. International Journal for Research in Applied Science & Engineering Technology (IJRASET), 2018: 9(1), 2146 – 2153p.

41. Baker Richard. Reservoir Management for Waterfloods – Part II. Journal of Canadian Petroleum Technology, January, 1998. 37(1) 1 – 17p.
42. Araktingi, U.G., Orr Jr, F.M. Viscous Fingering in Heterogeneous Porous Media. SPE Advanced Technology Series, 1993. 1 (01), 71 – 80p.
43. Xu F., Kim J., Lee S. Particle – induced Viscous Fingering. Elsevier Journal of Non – Newtonians Fluids Mechanics. 2016. (238) 92 – 99p.
44. Malhotra S., Sharma MM. Impact of fluid elasticity on miscible viscous fingering. Elsevier Journal of Chemical Engineering science 2014. 117, 125 – 135p.
45. Erandi DI., Wijeratne N., Halvorsen BM. Computational study of fingering phenomenon in heavy oil reservoir with water drive. Elsevier Journal of Fuel 2015. 158, 306 – 314p.
46. Doorwar, S., Mohanty K.K. Fingering Function for Unstable Immiscible Flows. SPE – 173290. In proceeding of SPE Reservoir Simulation Symposium, 23 – 25 February, Houston, Texas USA. 1 – 14p.
47. Luo H., Mohanty K.k., Delshad M., Pope G.A. Modelling and Upscaling Unstable Water and Polymer floods: Dynamic Characterization of the effective Finger zone. SPE – 179648. In proceeding of SPE International of SPE Improved Oil Recovery Conference in Tulsa, Oklahoma, USA, 11- 13 April, 2016.
48. Bonn D., Kellay H., Braunlich M., Ben Amar M., Meunier J. Viscous Fingering in complex fluids. Elsevier Journal of Physica A. 1995. 220, 60 – 73p.
49. Mora S., Manna M. From Viscous Fingering to Elastic instabilities. Elsevier Journal of Chemical Engineering science 2012. 73 (174) 30 – 39p.
50. Homsy GM. Viscous Fingering Porous Media. Annual Review Fluid Mechanics. 1987.19, 271 – 311.
51. Kumar M., Hoang V., Satik C., Rojas DH. High Mobility Ratio water flood performance Prediction: Challenges and new insights. SPE 97671. In proceeding of SPE International Improved Oil Recovery Conference in Asia Pacific Kuala Lumpur Malaysia 5 – 6 December 2005.
52. Sharma T, Suresh Kumar G, Sangwai JS. Enhanced oil recovery using oil-in-water (o/w) emulsion stabilized by nanoparticle, surfactant and polymer in the presence of NaCl. Geosystem Engineering (Taylor & Francis), 2014: 17(3) 195 – 205p.
53. Udy J., Hansen B., Maddux S., Petersen D., Heilner S., Stevens K., Lignell D., Hedengren J.D. Review of Field Development Optimization of Waterflooding, EOR, and Well Placement Focusing on History Matching and Optimization Algorithms. Process MDPI, 2017. 5(34), 1 – 25p.

54. Lyons Williams. Working Guide to Reservoir Engineering. 1<sup>st</sup> edition. Published by Elsevier Inc. 2011.
55. Selby R., Alikhan A.A., Farouq S.M. Potential of Non – Thermal Methods for Heavy Oil Recovery. Petroleum Society of Canada (JCPT), 1989. 28(04); 45 – 59p.
56. El – hoshoudy A.N., Desouky S. CO<sub>2</sub> Miscible Flooding for Enhanced Oil Recovery. A chapter page on Carbon Capture, Utilization and Sequestration, Published by IntechOpen, 2018. <http://dx.doi.org/10.5772/intechopen.79082>.
57. Hawez H., Ahmed Z. Enhanced oil Recovery by CO<sub>2</sub> injection in Carbonate Reservoirs. WIT Transaction on Ecology and The Environment, 2014. (186), 547 – 558p.
58. Brailovsky, I., Babchin, A., Frankel M., Sivashhinsky, G A. Fingering Instability in Water - Oil Displacement. Transp. Porous Media 2006, 63, 363 – 380.
59. Brailovsky, I., Babchin, A., Frankel M., Sivashhinsky, G A. Reduced Model for Fingering Instability in Miscible Displacement. Phys. Let. A 2007. 369, 212 – 217p.
60. Verma K. Mahendra. Fundamental of Carbon Dioxide – Enhanced Oil Recovery (CO<sub>2</sub> – EOR) – Supporting Document of the Assessment Methodology for Hydrocarbon Recovery Using CO<sub>2</sub> – EOR Associated with Carbon with Carbon Sequestration. Published by USGS Science for a challenging world, Reston, Virginia, 2015.
61. Lastra Y., Moulton L., Anazco R., Kondic L. The Hele – Shaw Cell/ Saffman Taylor Instability: Theoretical and Experimental Comparison of Newtonian Fluids. Online-available@- [https://web.njit.edu/~kondic/capstone/2015/2014\\_final\\_reports/451FinalReport.pdf](https://web.njit.edu/~kondic/capstone/2015/2014_final_reports/451FinalReport.pdf). 2014. 25/11/18.
62. Yernazarova A., Kayirmanova G., Baubekova A., Zhubanova A. Microbial Enhanced Oil Recovery. Published by INTECH (open science/ open minds) 2016.
63. Portwood J.T. A commercial microbial enhanced oil recovery technology: Evaluation of 322 projects, In proceedings of SPE production operations symposium, Oklahoma USA 2 – 4 April, 2007. 693 – 709p.
64. Fan Z., She Y-H., Hua –Min L., Xiao – Tao Z., Fu – Chang S., Zheng – Liang W., Long –Jiang Y., Du – Jie H. Impact of an indigenous microbial enhanced oil recovery field trial on microbial community structure in a high pour – point oil reservoir. Applied Microbiology and Biotechnology, 2012. 95, 811 – 821p.
65. Bekbauov B., Berdyshev A., Baishemirov Z. Numerical Simulation of Chemical Enhanced Oil Recovery Processes. DOOR, Vladivostok, Russia, 2016. 654 – 676p.

66. Thomas S.M., Farouq A. Micellar Flooding and ASP – Chemical Methods for Enhanced Oil Recovery. The Petroleum Society Calgary Alberta Canada 14 – 18 June 1999.
67. Sedaghat M. H., Ahadi A., Kordnejad M., Borazjani Z. Aspects of Alkaline Flooding oil Recovery Improvement and Displacement Mechanism. Middle – East Journal of Scientific Research, 2013. 18(2), 258 – 263p.
68. Sheng James.J. Status of Alkaline Flooding Technology. Journal of Petroleum Engineering & Technology 2015; 5(1) 44 – 50p.
69. Mayer E.H., Berg R.L., Carmicheal JD. Alkaline Injection for enhanced oil recovery – a status report. JPT. 1983. 35(1): 21 – 209p.
70. Nwadee, L.N., Barifcani A., Maxim L., Sarmadivaleh, M., Iglauer, S. A realistic look at nanostructured material as an innovative approach for enhanced oil recovery process upgrading. Recent insights in petroleum science and engineering. InTechOpen 2018. 155 – 188p.
71. Al – Anssari., Arif M., Wang S., Barifcani A., Lededev M. Wettability of Nanofluid – modified oil – wet calcite at reservoir conditions. Fuel (Elsevier) Journal 2018. 405 – 414p.
72. Peng B., Zhang L., Luo J., Wang P., Ding B., Zeng M., Cheng Z. A review of Nanomaterials for Nanofluid enhanced oil recovery. Royal Society of Chemistry (RSC) Advances, 2017. 7 32246 – 32254p.
73. Chung Lau H., Yu M., Nguyen P. Nanotechnology for Oilfield Applications: Challenges and Impact. SPE – 183301. In proceeding Abu Dhabi International Petroleum Exhibition & Conference in Abu Dhabi, UAE, 7 – 10 November 2018. 1 – 18p.
74. Poettman, F.H. Microemulsion flooding, Secondary and Tertiary Oil Recovery Processes. Oklahoma, OK: Interstate Oil Compact Commission.
75. Salih T.A., Hussain S., Hameed O.K. Rheological Evaluation of Polymer (Sav 10) for polymer flooding Applications. IJCPE 2016. 17(1); 37 – 46p.
76. Sheng James J. Enhanced oil recovery Field Case Studies. 1<sup>st</sup> edition. Gulf Professional Publishing imprint of Elsevier Inc, Kidington Oxford UK. 2013
77. Al-Hajri, N.F. Screening Criteria for Enhanced Oil Recovery in Carbonate Reservoirs. 2010 (A PhD thesis at Imperial College).
78. Bedaiwi, E, Al-Anazi BD, Al-Anazi, AF, Paiaman, AM. Polymer injection for water production control through permeability alteration in fractured reservoir. *NAFTA* 2009. 60(4) 221-231p.

79. Sun Y, Saleh L, Bai B. Measurement and Impact factors of polymer rheology in porous media. *INTECH open Science / Open Mind* 2012. 187 – 188p.
80. Levitt, D.B, Pope, G. A, Jouenne, S. Chemical degradation of polyacrylamide polymers under alkaline conditions. SPE 129879. In *Proceedings of the SPE improved oil Recovery Symposium*, Tulsa, USA, April, 2011. 24-28p.
81. Stahl G.A., Schulz D.N. *Water Soluble Polymers for Petroleum Recovery*. 1<sup>st</sup> edition, Springer Science and Business Media, New York, 1987.
82. Demin W., Huifen X., Zhongchun L., Quingyan A.Y. Study of the Mechanism of Power Solution with Visco – Elastic Behavior Increasing Microscopic Oil Displacement Efficiency and the Forming of steady “oil Thread” Flow Channels. SPE 68723. In *Proceeding of the SPE Asia Pacific; Oil and Gas Conference and Exhibition in Jakarta Indonesia 2001*. 1 – 9p.
83. Choi B., Sik Jeong M., Sang Lee. (Polymer Degradation and Stability) Temperature – Dependent Viscosity Model of HPAM Polymer through High – Temperature Reservoirs. Elsevier Science direct, 2014. 110(1) 225 – 231p.
84. Uranta, K.G, Gomari, S.R, Russel, P.A, Hamad F. Determining safe maximum temperature point (SMTP) for polyacrylamide polymer (PAM) in saline solutions. *Journal of Oil and Gas Petrochemical Science* 2018. 1(1) 26-33p.
85. Martin FD, Sherwood NS. The Effect of Hydrolysis of Polyacrylamide on Solution Viscosity, Polymer Retention and Flow Resistance Properties. SPE 5339 paper presented at Rocky Mountain Regional Meeting of the society of Petroleum Engineers of AIME. Denver, USA April 7-9, 1975.
86. Gao C. Viscosity of partially hydrolysed polyacrylamide under shearing and heat. *Journal of Petroleum Exploration Production Technology* (2013). 3:203 – 206p.
87. Luo J, H., Bu, R.Y., Wang P, M., Bai, F, L., Zhang, Y., Yang, J, B. Properties of KYPAM, a salinity – resistant polymer used in EOR. *Oilfield Chem* 2002. 19(1), 64 – 67p.
88. Jamshidi H., Rabiee A. Synthesis and characterization of acrylamide-based anionic copolymer and investigation of solution properties. *Advances in Materials Science and Engineering* 2014. (1) 1-6. <http://dx.doi.org/10.1155/2014/728675>.
89. Kavanagh GM, Ross–Murphy SB. Rheological Characterization of Polymer. *Pergamon paper of prog. Polymer Science*, 1998. (23), 533 – 562p.
90. Barnes HA., Hutton JF., Walters K. An introduction to Rheology. 1<sup>st</sup> Edition. Elsevier Science Publishing Co, Amsterdam Netherland, 1989.
91. Barnes, H.A. A handbook of elementary rheology, Institute of Non – Newtonian Fluid Mechanics, University of Wales, Aberystwyth, U.K. (2000).

92. Bird, R.B., Armstrong, R.C., Hassager, O. Dynamics of polymeric Liquids. Vol 1. Fluids mechanics 2<sup>nd</sup> edition, Wiley, Chichester 1987.
93. Carreau, P.J. Rheological equations from molecular network theories. Trans. Society of Rheology, 19 (1) 99 -127.1972. (Ph.D. Dissertation University of Wisconsin Madison 1968).
94. Lam C., Jefferis. Interpretation of Viscometer Test Results for Polymer Support fluids. Process, sessions of Geo Shanghai Inter Conference GSP 242, ASCE Reston VA, 2014. 439 – 449p.
95. Meyer Jr B. *Polymer Science Textbook*. 1<sup>st</sup> edition, New York: John Wiley & Sons, 1971.
96. Fann Instrument Company. Model 35 Viscometer instruction Manual. Published by Fann Instrument Company Houston Texas, USA, 2016. 33p.
97. Sochi Taha. Non – Newtonian flow in porous media. Polymer (Elsevier at Science direct), 2010. 51, 5007 – 5023p.
98. Bonnier J., Gathier R.F., Quillien B., Thomas A. Inline Viscosity Monitoring of Polymer Solutions Injected in Chemical Enhanced Oil Recovery Processes. SPE 165249. In proceeding of SPE enhanced oil recovery Conference in Kuala Lumpur, Malaysia 2 – 4 July 2013.
99. Moukhtari F.E., Lecampion B. A semi – infinite hydraulic fracture driven by a shear – thinning fluid. Journal Fluid Mechanic © Cambridge University Press 2018. 838, 573 – 605p.
100. Wang D., Seright RS., Shao Z., Wang J. Key Aspects of Project Design for Polymer flooding at the Daqing Oil Field. SPE 109682. In proceeding of SPE Reservoir Evaluation and Engineering, December, 2008.
101. Xiaoqing Z., Feng P., Wenting G., Dan Li., Songlin G. A Novel Method of Optimizing the Molecular Weight of polymer Flooding. SPE 144252. In proceeding of SPE enhanced oil Recovery Conference in Kuala Lumpur, Malaysia, 19 – 21 July 2011. 1 – 4pp
102. Seright RS. The Effects of Mechanical Degradation and Viscoelastic Behaviour on Injectivity of Polyacrylamide solutions. Society of Petroleum Engineers of AIME, 1983
103. Uranta K.G, Gomari, S.R, Russel, P.A, Hamad F. Studying the effectiveness of polyacrylamide (PAM) application in hydrocarbon reservoirs at different operational conditions. *Energies* (2018) 11, 2201.

104. Sheng, James J, Leonhardt, Bernd, Azri, Nasser. Status of polymer flooding technology. *Journal of Canadian Petroleum Technology*. (2015): 116 – 126.
105. SNF Floerger. Petroleum Geology Petroleum Systems. Online available @ <http://www.oilproduction.net/files/EOR%20Handbook.pdf.2016>. Accessed 16<sup>th</sup> August, 2018.
106. Shupe Russell D. *Chemical Stability of Polyacrylamide Polymers*. SPE 9299 paper presented at the 55<sup>th</sup> Annual Technical Conference and Exhibition held in Dallas. 1981. 1513 – 1529p.
107. Crees O.L, Whayman E, and Willersdorf AL. The degradation of high molecular weight flocculants. Paper made available from Sugar Research Institute, Mackay, Queensland, Australia. 1973. 263 – 266p.
108. Levitt D.B., Slaughter W., Pope G.A., Jouenne S. The Effect of Redox Potential and Metal solubility on Oxidative Polymer Degradation. SPE Reservoir Evaluation & Engineering. 2011
109. Fenton H.J.H., Oxidation of tartaric acid in presence of iron. *Journal of the Chemistry Society*. <http://www.geocleanse.com/chemical-remediation/reagents/catalyzed-hydrogen-peroxide/>, 24/7/17. (1894):1 – 6p.
110. Haber F., and Weiss, J. Hydroperoxide. *Naturwissenschaften*. 1932. 20 (51): 948-950p.
111. Yang S.H., Treiler L.E. Chemical Stability of Polyacrylamide under simulated field conditions. SPE 14232, in proceeding at the SPE Annual Technical Conference and Exhibition Las Vegas, 22 – 26 September, 1985.
112. Maerker J.M. Shear Degradation of Partially Hydrolysed Polyacrylamide Solutions. SPE 5101, in proceeding of SPE – AIME 49<sup>th</sup> Annual Fall Meeting held in Houston August, 1975.
113. Khan, Y.M., Samanta A., Ojha K., Mandal A. Design of Alkaline/Surfactant/Polymer (ASP) Slug and its use in Enhanced Oil Recovery. *Petroleum Science and Technology* 2009. 27, 1926 – 1942p.
114. Lewandowska K. Comparative studies of rheological properties of polyacrylamide and partially hydrolyzed polyacrylamide solutions. *Journal of Applied Polymer Science*, 2007. 103(4), 2235 – 2241p.
115. Albonico P, Lockhart T. Stabilization of polymer gels against divalent ion-induced syneresis. *Journal of Petroleum Science and Engineering*. 1997. 61 – 71p.
116. Dovan H T. Hutchins R D. Sandiford, B.B. Delaying gelation of aqueous polymers at elevated temperatures using novel organic cross-linkers. SPE 37246, Paper presented at the *SPE International Symposium on Oilfield Chemistry*, Houston, Texas, U.S.A., February 18 -21. 1997. 361 – 371p.
117. Borling Daniel, Chan Ken., Hughes Trevor, and Sydansk Robert. Pushing out the oil with conformance control. *Oilfield Review*. (1994): 44 – 58p.
118. Cheremisinoff, Nicholas. P. *Handbook of Engineering Polymeric Materials*. 1<sup>st</sup>



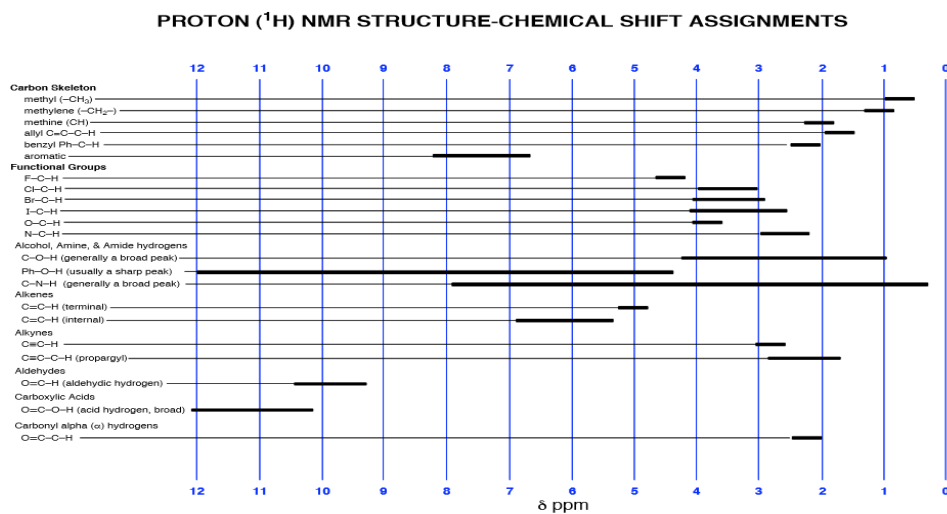
- edition. New York: Marcel Dekker. 1997, 61 – 65p.
119. Karimi, S, Kazemi, S, Kazemi, N. Syneresis measurement of the HPAM-Cr (III) gel polymer at different condition: an experimental investigation. *Journal of Natural Gas Science and Engineering*. (2016): 34: 1027-1033p.
  120. Mohammad S, Mohsen V, and Ahmad KD, Reza H. Polyacrylamide gel polymer as water shut-off system: preparation and investigation of physical and chemical properties in one of the Iran oil reservoirs condition. *Iranian Journal of Chemistry and Chemical Engineering (IJCCE)*, 2007. 26(4), 99 – 108p.
  121. Kelland Malcolm. *Production Chemicals for the Oil and Gas Industry*. 2<sup>nd</sup> edition, CRC Press Taylor & Francis Group London. 2009. 23 – 36p.
  122. Bryant, SL, Rabaioli, MR, Lockhart, TP. Influence of syneresis on permeability reduction by polymer gels. SPE 35446 paper presented at SPE/DOE Symposium on improved oil Recovery held in Tulsa OK April 21 - 24. 1996. 209 – 215p.
  123. Zhu, D., Zhang, J., Han, Y., Wang, H., Feng Y. Laboratory study on the potential EOR use of HPAM/VES hybrid in high Temperature and high salinity. *Journal of Chemistry* 2013, (1) 1-8p. <http://dx.doi.org/10.1155/2013/927519>
  124. Davison P., Mentzer E. Polymer Flooding in North Sea Reservoirs. SPE of AIME, June 1982. 353 – 362p.
  125. Anasuya K.V., Veeraiah M.K., Hemalatha P., Manju M. Synthesis and characterisation of poly (vinylpyrrolidone) nickel (II) complexes. *Journal of Applied Chemistry (IOSR – JAC)* 2014. 7(8), 61-66p.
  126. Anasuya K.V., Veeraiah M.K., Hemalatha P. Synthesis and characterisation of poly (vinylpyrrolidone)-copper (II) complexes. *Research Journal of Chemical Sciences* February 2015; 5(2), 64-69p.
  127. Doe H.P, Moradi-Araghi, A., Shaw E.J, Stahl A.G. Development and evaluation of EOR polymers suitable for hostile environments: Part 1: copolymers of vinylpyrrolidone and acrylamide. *SPE Reservoir Engineering*. 1987. 2(04), 461-467p.
  128. Glover, P. Reservoir Fluids. 2012. Available online:[http://homepages.see.leeds.ac.uk/~earpwjg/PAGE\\_EN/CD%20Contents](http://homepages.see.leeds.ac.uk/~earpwjg/PAGE_EN/CD%20Contents) (Accessed on 10 February, 2017)
  129. Potter MC., Wiggert DC., Ramadan BH. *Mechanics of Fluids*. 5<sup>th</sup> edition. Published by Cengage Learning United States of America. 2017.
  130. Hu Y., Wang SQ., Jamieson AM. Rheological and Rheoptical Studies of Shear – Thickening Polyacrylamide Solutions. *Macromolecules* 1995. (28) 1847 – 1853p.
  131. Friebolin Horst. *Basic one and Two – Dimensional NMR Spectroscopy* 4<sup>th</sup> edition. Published by Wiley – VCH Verlag GmbH & Co.KGaa, Weinheim Germany, 2005.

132. Stuart Barbara H. Infrared Spectroscopy Fundamentals and Applications. 1<sup>st</sup> edition, John Wiley & Sons Ltd, The Atrium, Southern Gate, Chichester, West Sussex England, 2004.
133. Fernandez, I.J. Evaluation of cationic water-soluble polymers with improved thermal stability. SPE 93003. In proceedings of the *SPE International Symposium on Oilfield Chemistry*, Houston, Texas, USA, 2-4 February, 2005; pp 1 – 13p.
134. Akbari S., Mahmood M.S., Tan I.M., Hosein G, Ling O.L. Assessment of polyacrylamide based co-polymers enhanced by functional group modifications with regards to salinity and hardness. *MPDI Journal of Polymers* 2017. 9(12), 647, 1-16p.
135. Zhang R., He X., Cai S., Liu K. Rheology of diluted and semi – diluted partially hydrolysed polyacrylamide solutions under shear: Experimental studies. *Ke Ai Advancing Research Evolving Science (Petroleum 3, (2017) 258 – 265p.*
136. Vulin D., Gacina M., Borovina A., Bosnjak I., Smajla I. Sensitivity Tests of Parameters in Laboratory Polymer Flood Analysis. *Petroleum & Petrochemical Engineering Journal* 2017, 1(3): 1 – 8p.
137. Kim C., Lee J. Experimental study on the variation of relative permeability due to clay minerals in low salinity water flooding. *Journal of Petroleum Science and Engineering* 2017; 1(151) 292 – 304p.
138. Miller M.A., Ramey H.J. Effect of Temperature on oil/water Relative Permeabilities of Unconsolidated and consolidated sands. SPE 12116-PA. In proceeding of *SPE Symposium on Oilfield Chemistry*, Austin, Texas 1985. 06(25); 945 – 953p.
139. Miller M.A. Effect of Temperature on oil – water relative permeabilities of Unconsolidated and Consolidated sands. Stanford Geothermal Program Interdisciplinary Research in Engineering and Earth Sciences, California, 1983.
140. Hamouda A.A., Karoussi O., Chukwudeme E.A. Relative Permeability as a Function Temperature, Initial water saturation and flooding fluid compositions for modified oil – wet chalk. *Journal of Petroleum Sciences and Engineering* 2008. 63, 61 – 72p.
141. Algharaib M., Alajmi A., Gharbi R. Improving polymer flood performance in high salinity reservoirs. *Journal of Petroleum Sciences and Engineering* 2014. 115, 61 – 72p.
142. Nazari J., Nasiry F., Seddiqi N., Honma S. Influence of Relative permeability and viscosity ratio on oil displacement by water in petroleum reservoir. *Proc. Schl. Eng. Tokai University, Ser, 2015. 40 15 – 20p.*
143. Cole – Parmer Rotational Viscometers. Accurate Measurements at the push of a-button. Available online <https://pim-resources.coleparmer.com/literature/3542-rotaviscom.pdf>. Accessed 20<sup>th</sup> March, 2019.
144. Teesside University Laboratory Equipment. Analytical chemistry Laboratory snaps photos
145. Fulcher R.A., Ertekin T., Stahl CD. Effect of Capillary Number and its Constituents on two – phase Relative Permeability Curves. *Journal of Petroleum Technology*, February, 1985. 249 - 260p.
146. Uranta K.G., Gomari SR., Russell P., Hamad F. Application of Polymer Integration Technique for Enhancing Polyacrylamide (PAM) Performance in High Temperature and High Salinity Reservoirs. *Elsevier Heliyon* 2019. 5(02113): 1 – 14p

147. Gao G. H. Experiences of Polymer Flooding Projects at Shengli Oilfield. In proceedings of the SPE EOR Conference at Oil and Gas West Asia held in Muscat, Oman, 31 March, 2 April 2014: 1 – 13p

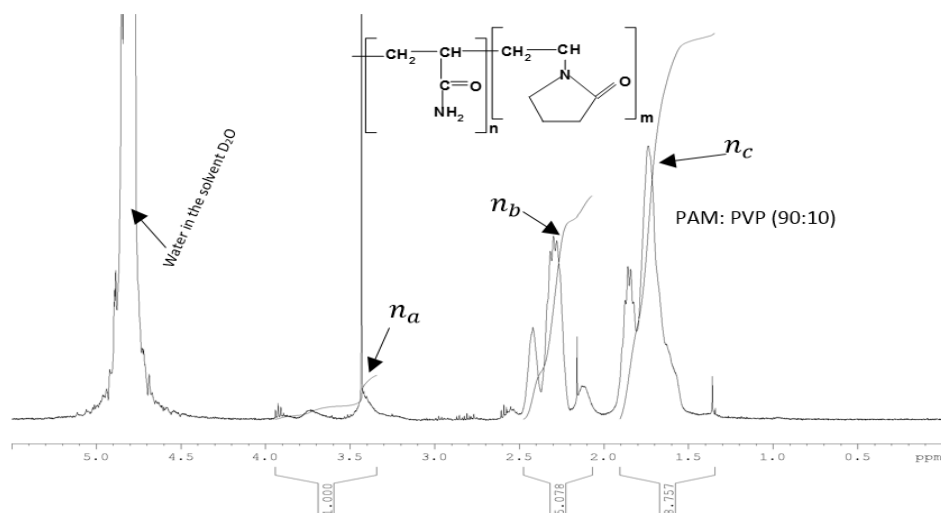
## APPENDICES

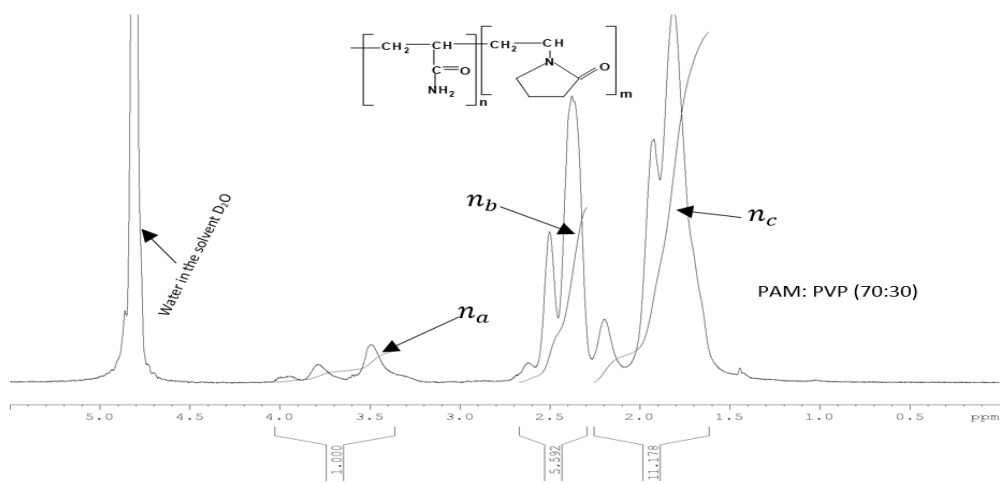
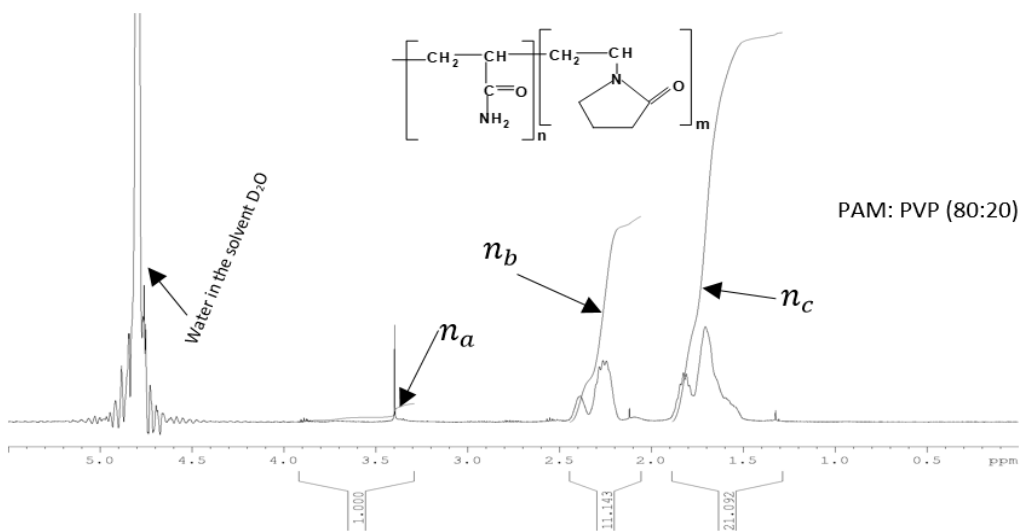
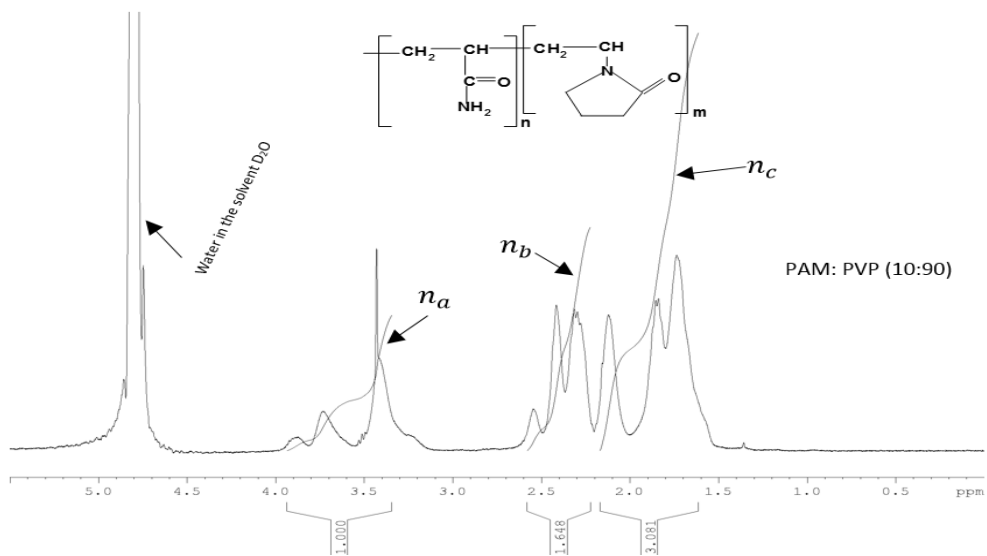
### Appendix A: NMR Techniques

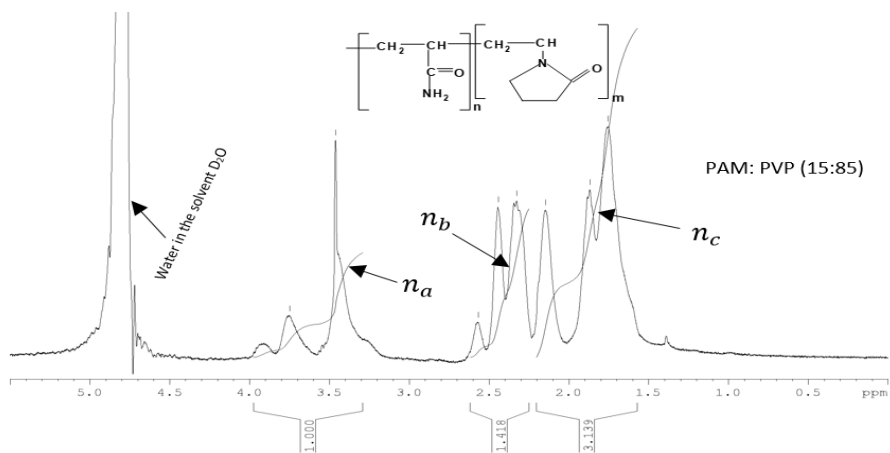
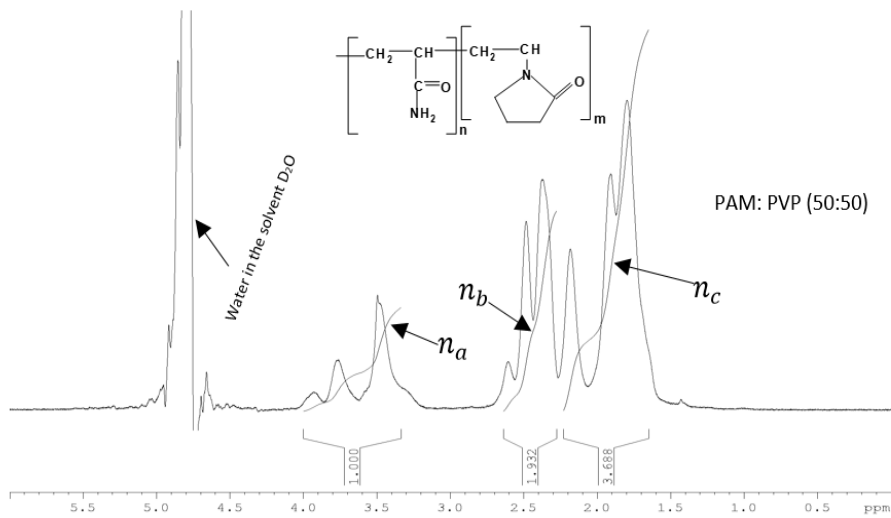
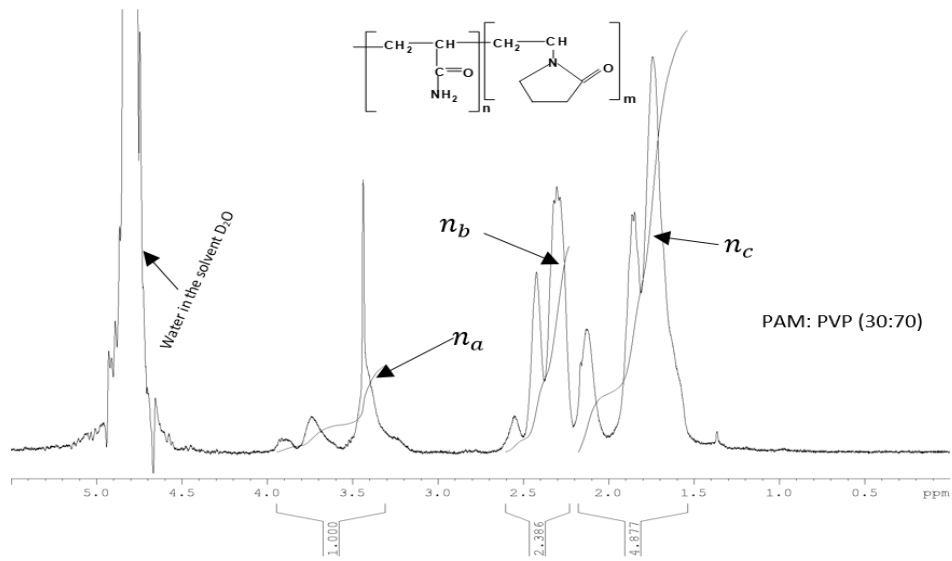


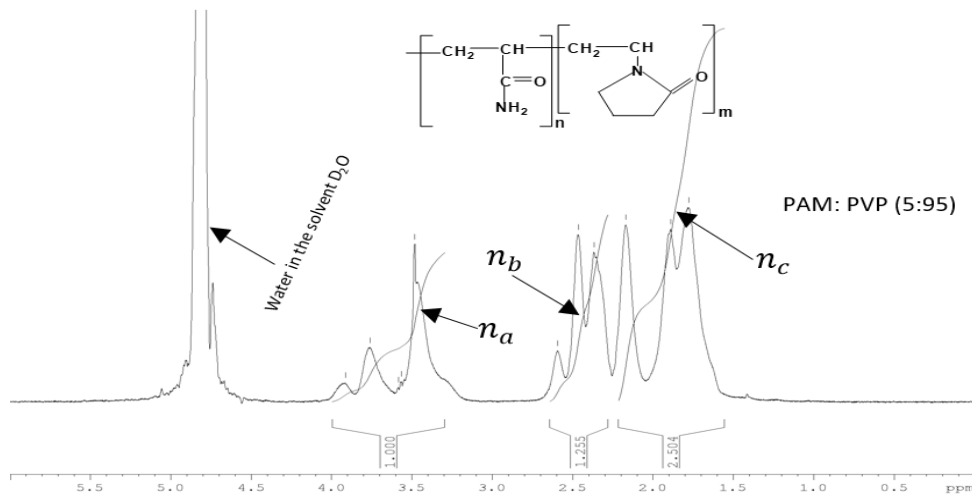
**Figure 3.5b** Chemical shift assignment for protons (<sup>1</sup>H) ([https://www2.onu.edu/~b-myers/organic/2511 Files/NMR structure assignments.pdf](https://www2.onu.edu/~b-myers/organic/2511%20Files/NMR_structure_assignments.pdf))

### Appendix B: Integration and Optimization of PAM Performance in High Temperature Reservoirs



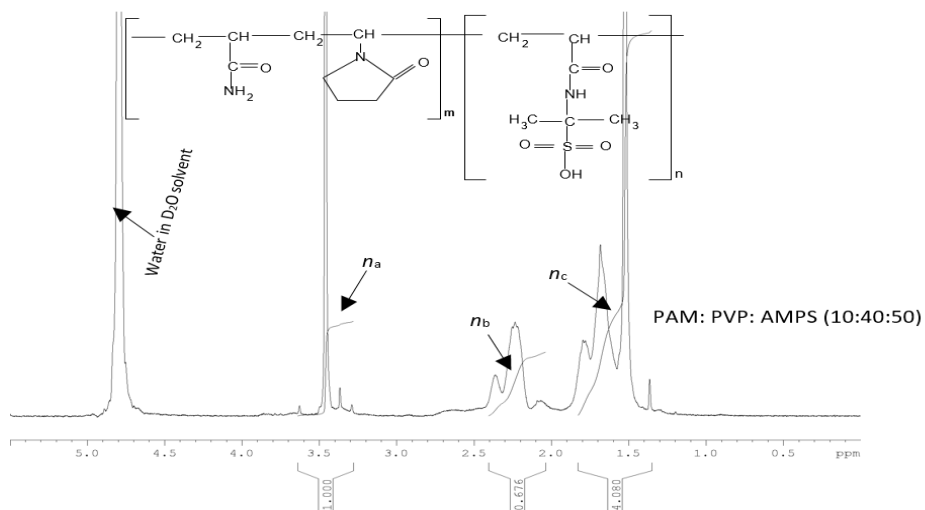






**Figure 6.2b:**  $^1\text{H}$  NMR spectra for integrated polymers of PAM: PVP at  $90^\circ\text{C}$  and TDS 43,280 ppm.

### Appendix B: Application of PIT to Optimize PAM Performance at High Temperature and High Salinity Medium



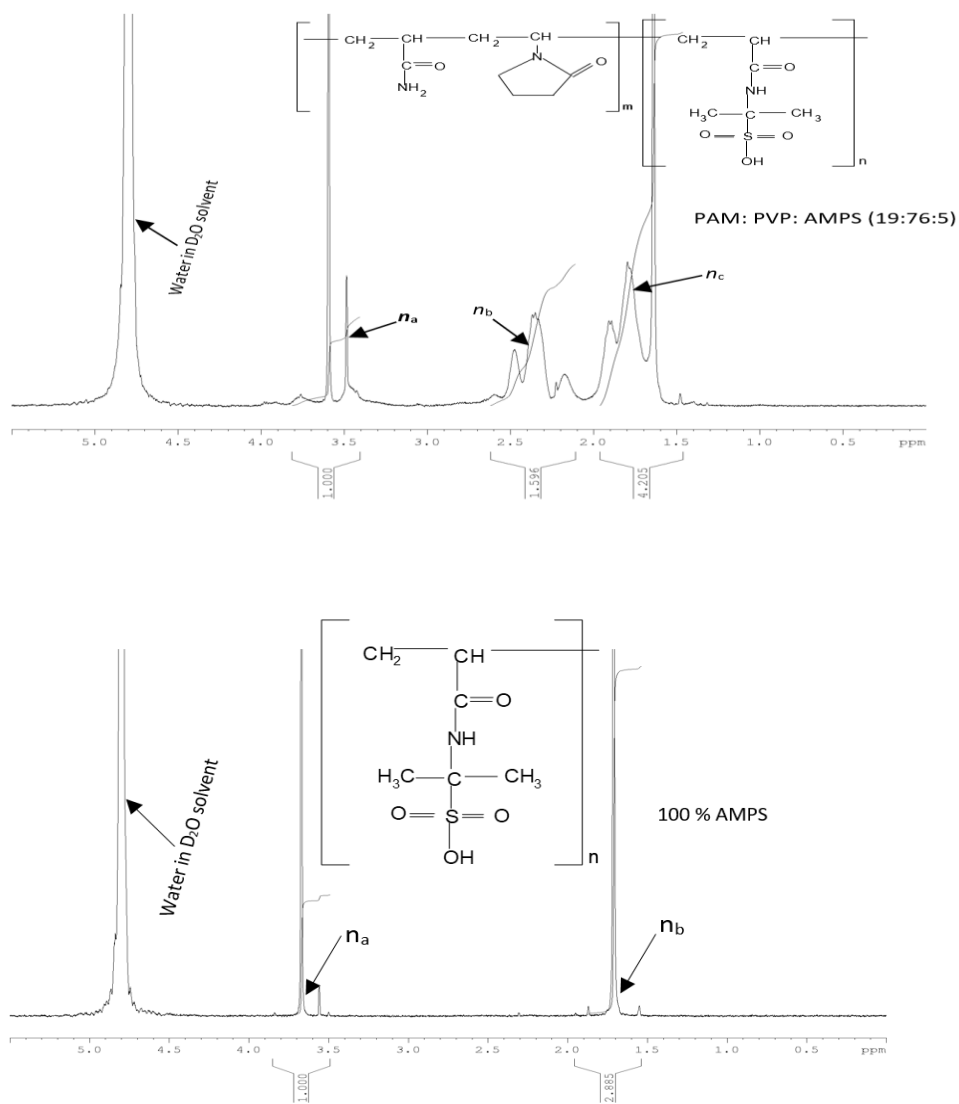


**Figure 7.2b:**  $^1\text{H}$  NMR spectra for integrated polymers of PAM: PVP (20:80) and different weight ratios of PAM: PVP: AMPS at  $90^\circ\text{C}$  and salinity 200,000 ppm.



## Appendix C: Verification of Lab results for Comparative Simulation and Modelling on Polymer Flooding

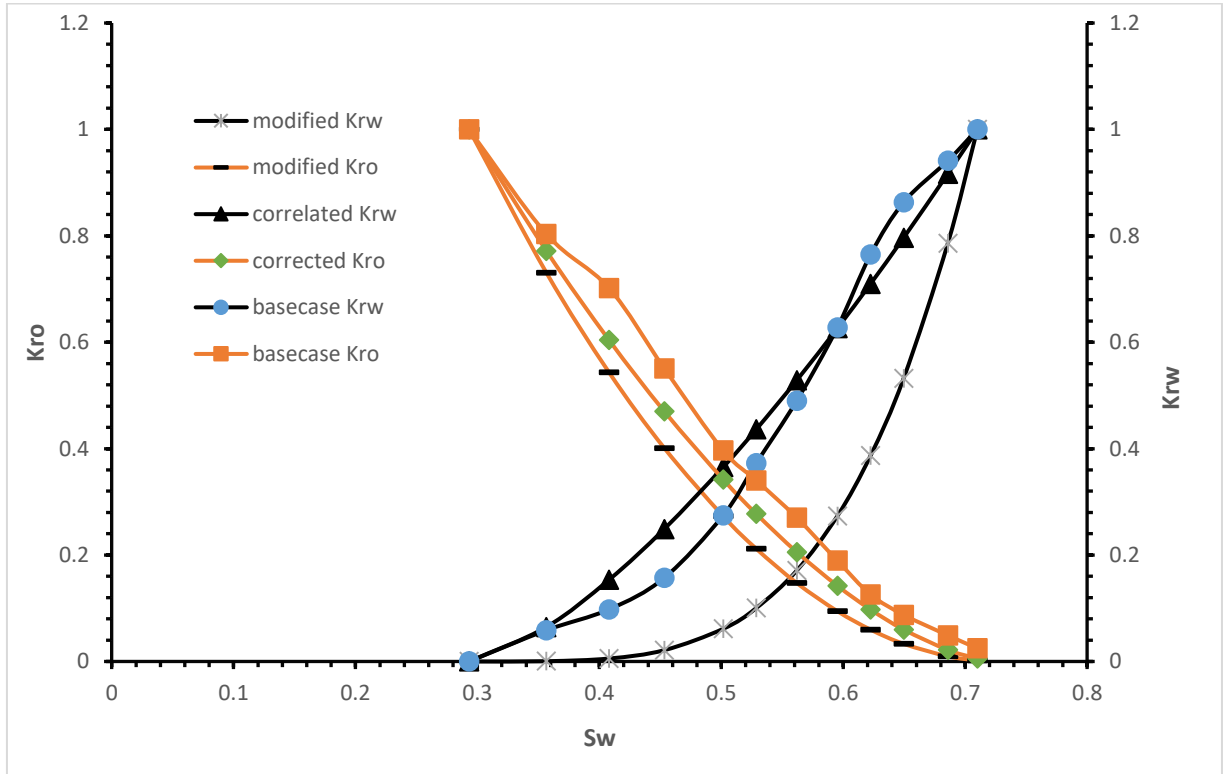


**Figure 8.2a:** The normalised endpoint permeabilities of the oil and water against water saturation.

### 8.3 Corey equation for estimating the endpoint modified Relative permeabilities.

$$k_{ro} = k_{ro(S_w \min)} \left( \frac{S_w \max - S_w - S_{orw}}{S_w \max - S_{wi} - S_{orw}} \right)^{c_{oe}} \quad 8.2a$$

$$k_{rw} = k_{rw(S_{orw})} \left( \frac{S_w - S_{wcr}}{S_w \max - S_{wcr} - S_{orw}} \right)^{c_{we}} \quad 8.2b$$

Where  $S_{w \min}$  is the minimum salt saturation,  $S_{wcr}$  is the critical saturation,  $S_{wi}$  initial water saturation,  $S_{orw}$  is the residual oil saturation to water,  $k_{rw(S_{orw})}$  water relative permeability at residual oil,  $k_{ro(S_w \min)}$  is the water relative permeability at maximum water saturation,  $c_{oe}$  Corey oil exponent,  $c_{we}$  Corey water exponent.

#### 8.4 Equation for estimating the endpoint correlated Relative permeabilities.

Developing a relative permeability model based on the rheological (viscosity) experiment results, the Minitab II statistical computation system was used.

$$k_{ro(dr)} = AS *^{B+C} \ln y \left( \frac{\mu_w}{\mu_o} \right)^D \quad 8.2c$$

$$k_{rw} AS *^{[B+D \ln(\frac{\mu_w}{\mu_o}/y)]} \quad 8.2d$$

Table 8.2 Reservoir properties used for Simulation and model

Reservoir properties utilised in model and simulation			
Recovery Technique	Viscosity (mPa.s)	Water Salinity (ppm)	Temperature
Water flooding	1.5	43280	90°C
<b>Polymer Flooding</b>			
(a) PAM	11	43280	90°C
(b) PAM:PVP	38.2	43280	90°C
(c) PAM:PVP	28.6	200000	90°C
(d) PAM:PVP:AMPS	22.8	200000	90°C

#### 8.5 Sensitivity Analysis of the Experimental

In sensitivity analysis, waterflooding injection improved the process by increasing the simulation run to 4% oil recovery efficiency on injecting time of 600 days (280 TSTEP). Continuous improvement yielded 3% addition on PAM injection and further improvement on PAM injection 3%. Field oil Efficiencies (FOE) = field OIP (initial) – OIP (original) / OIP (initial). On PAM: PVP injection 25% incremental was achieved. Below are figures 8.2 (b – f), showing incremental recovery polymer flooding and increasing water cut for water flooding and PAM.

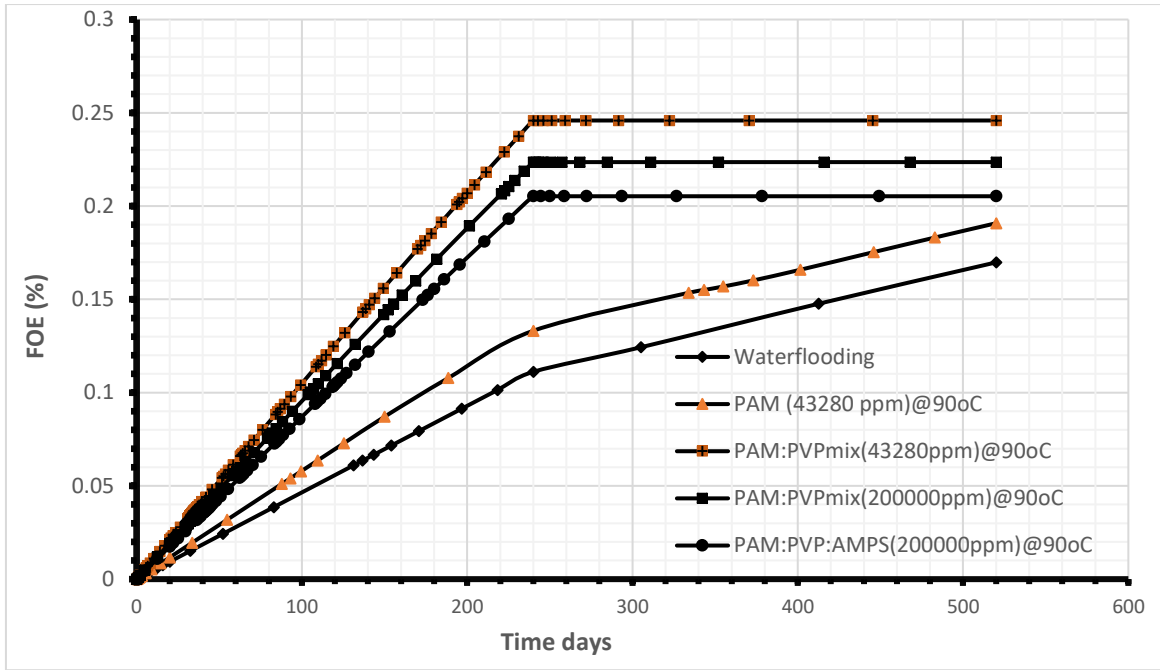


Figure 8.2a: Recovery vs time graphs for incremental recovery estimate.

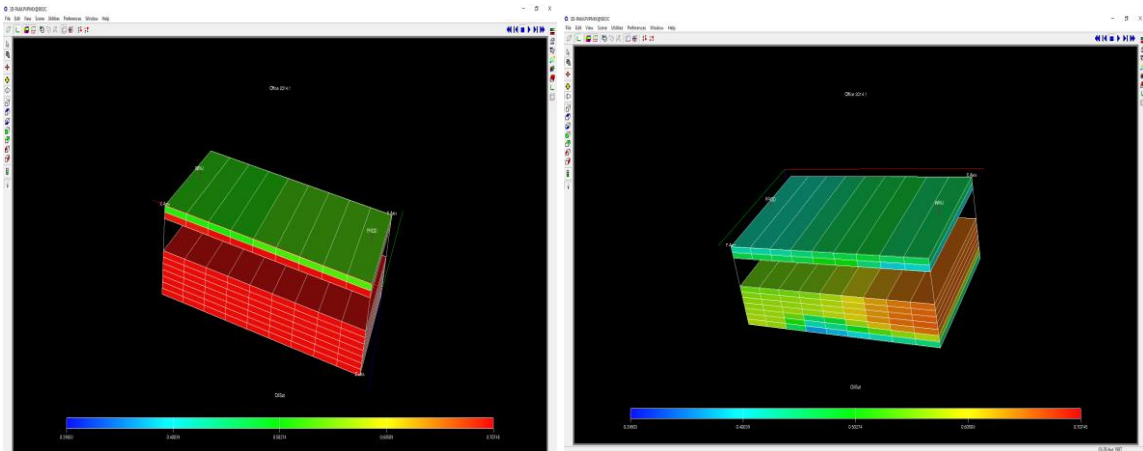


Figure 8.2b: Grid section of the PAM/PVP mix @ 90°C

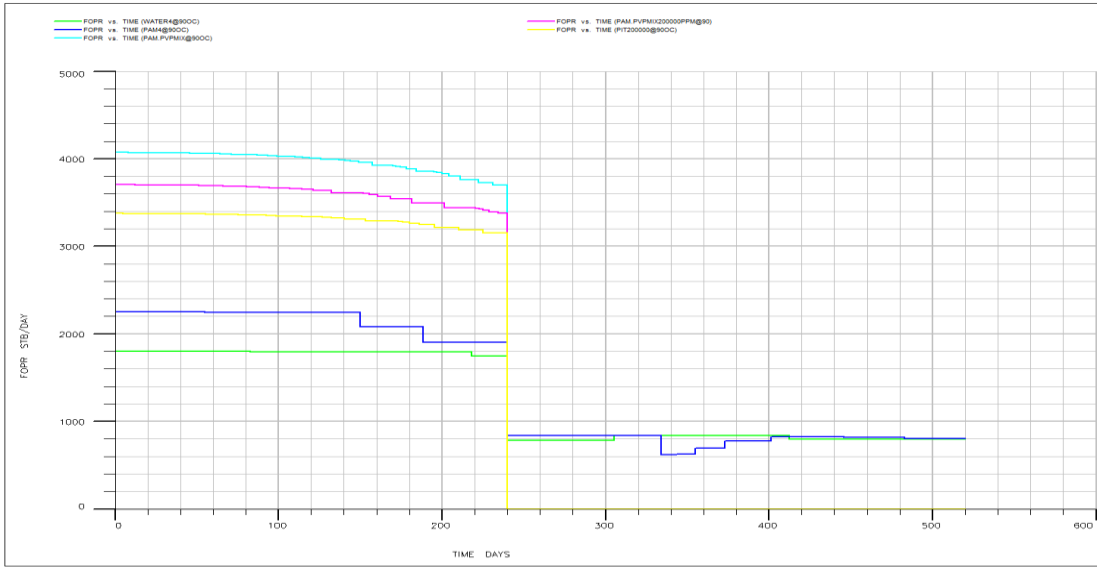


Figure 8.2c: Field oil production rate vs time

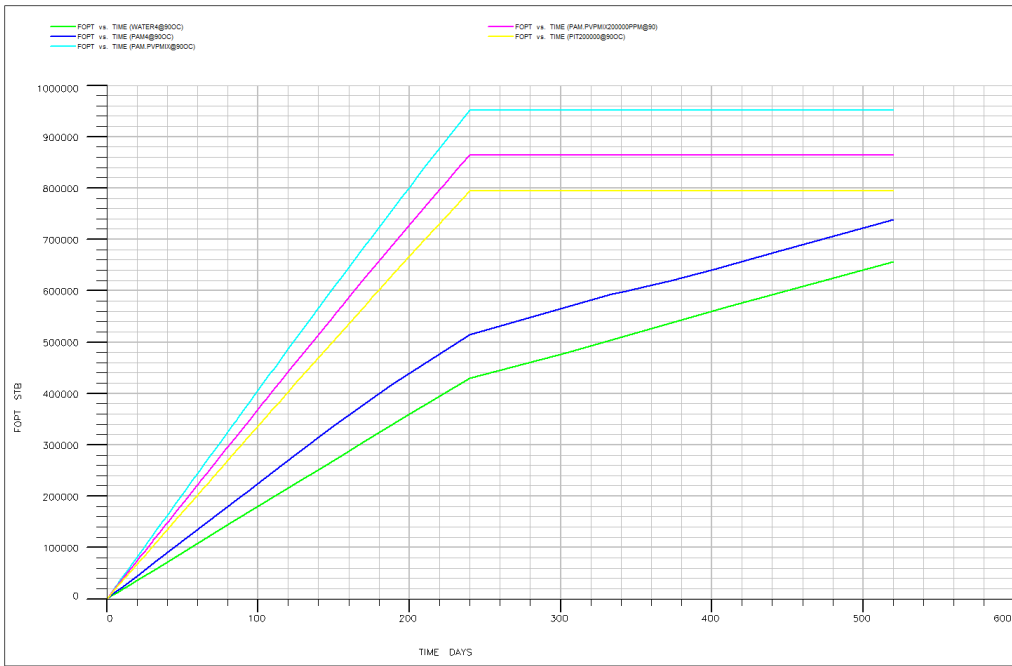


Figure 8.2d: Field oil production total Vs time

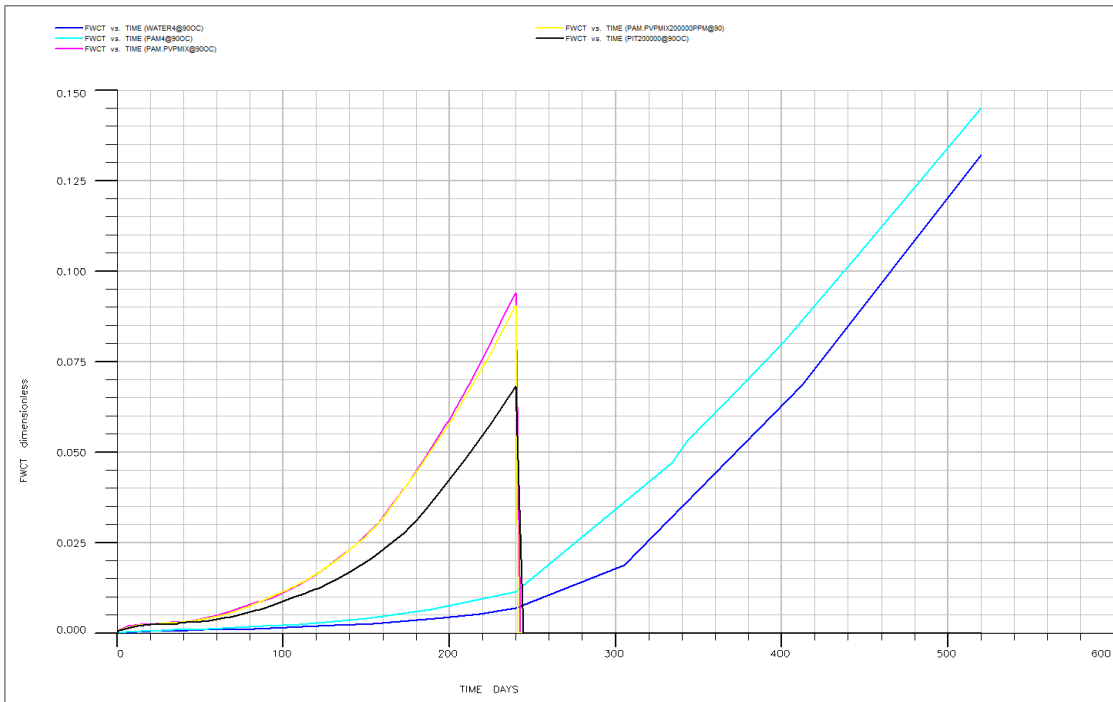


Figure 8.3e: Field water cut Vs time

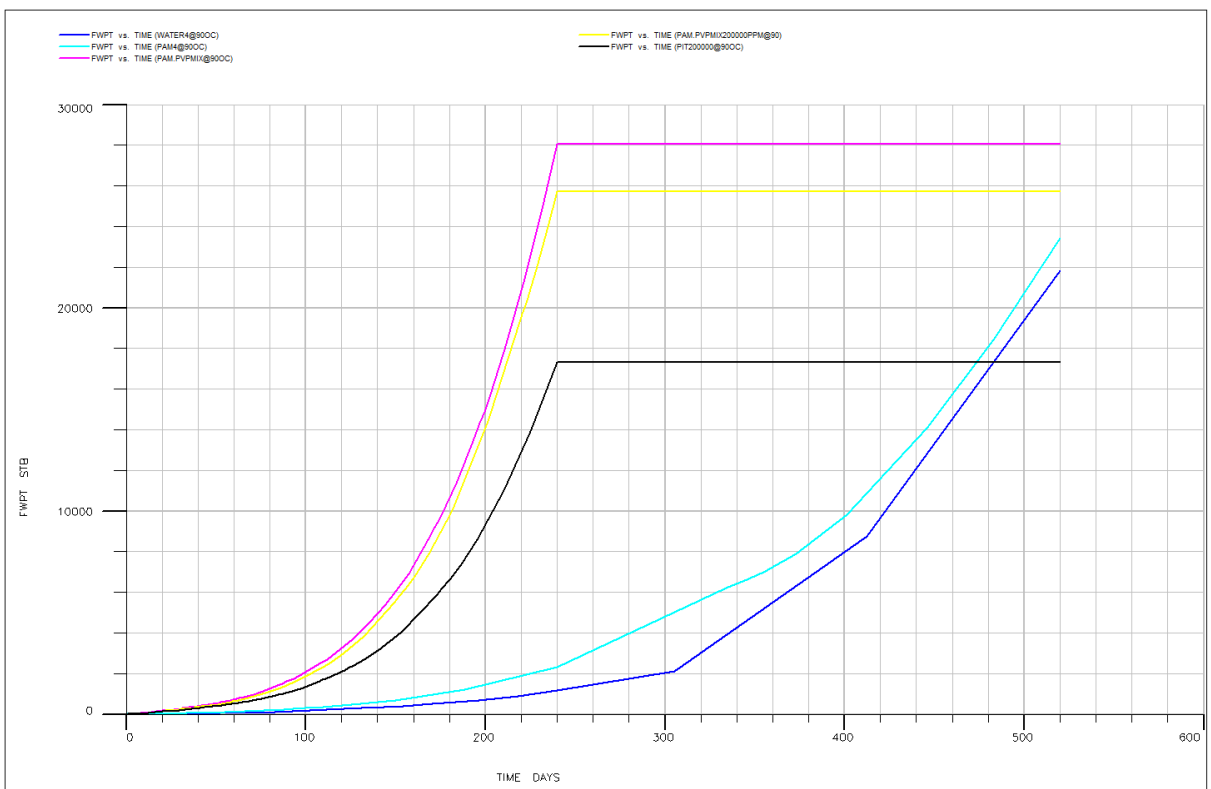


Figure 8.3f: Field water production total Vs time

**Modified Model data used for the Simulation (extracted from Schlumberger model data 1997)**

RUNSPEC

TITLE

A MULTI-LATERAL PRODUCER AND INJECTOR - MULTI-SEGMENT BRANCHES WITH POLYMER

DIMENS

9 1 10 /

OIL

WATER

GAS

DISGAS

POLYMER

BRINE

TEMP

FIELD

TABDIMS

1 1 15 15 2 15 /

EQLDIMS

2 /

WELLDIMS

3 20 1 3 /

VFPPDIMS

6 3 3 3 1 1 /

VFPIDIMS

6 3 2 /

WSEGDIMS

2 30 4 /

START

1 'JAN' 1997 /

GRID =====

EQUALS

'DX' 100 /

'DY' 500 /

'PERMX' 25 /

```

'PERMZ' 5 /
'DZ' 20 /
'PORO' 0.4 /
'TOPS' 7000 19 11 11 /
'DZ' 100 19 11 33 /
'PORO' 0.0 19 11 33 /
/
RPTGRID
-- Report Levels for Grid Section Data
-- 24*0
'PORO'
'PORV'
/
PROPS =====
SWFN
-- Sw Krw Pcow
0.293 0.000 0.544
0.357 0.0834 0.456
0.408 0.1825 0.365
0.453 0.2830 0.298
0.502 0.4007 0.245
0.529 0.4711 0.200
0.562 0.5606 0.100
0.595 0.6539 0.090
0.622 0.7327 0.050
0.650 0.8132 0.030
1.0 1.0 0.000 /
SGFN
-- Sg Krg Pcgo
0.0 0.000 0.000
0.08 0.0004 0.200
0.11 0.00204 0.500
0.14 0.00559 1*
0.17 0.01159 2.250

```

0.23 0.02023 3.200  
0.26 0.04700 4.100  
0.29 0.06531 5.050  
0.32 0.08702 6.020  
0.35 0.11035 7.010  
0.40 1.0 8.000 /

SOF3

-- So Krow Krog

0.000 0.0000 0.0  
0.290 0.0045 0.0  
0.314 0.0191 0.0  
0.351 0.0548 1\*  
0.378 0.0905 0.02  
0.404 0.1336 1\*  
0.438 0.1952 0.3  
0.471 0.2659 1\*  
0.499 0.3305 0.8  
0.547 0.4588 1\*  
1.000 1.000 1.00 /

PVTW

3000 1.00341 3.0D-6 1 0 /

ROCK

3000 4.0D-6 /

DENSITY

45 63.02 0.0702 /

PVDG

400 5.9 0.013  
800 2.95 0.0135  
1200 1.96 0.014  
1600 1.47 0.0145  
2000 1.18 0.015  
2400 0.98 0.0155  
2800 0.84 0.016  
3200 0.74 0.0165



3600 0.65 0.017  
4000 0.59 0.0175  
4400 0.54 0.018  
4800 0.49 0.0185  
5200 0.45 0.019  
5600 0.42 0.0195 /

PMAX

10000 /

PVCO

400 0.165 1.012 1.17 5.0E-5 1\*  
800 0.335 1.0255 1.14 2\*  
1200 0.500 1.038 1.11 2\*  
1600 0.665 1.051 1.08 2\*  
2000 0.828 1.063 1.06 2\*  
2400 0.985 1.075 1.03 2\*  
2800 1.130 1.087 1.00 2\*  
3200 1.270 1.0985 0.98 2\*  
3600 1.390 1.11 0.95 2\*  
4000 1.500 1.12 0.94 2\*  
4400 1.600 1.13 0.92 2\*  
4800 1.676 1.14 0.91 2\*  
5200 1.750 1.148 0.9 2\*  
5600 1.810 1.155 0.89 2\*

/

PLYVISCS

0.0000 1.0

1.0

/

10.0 38.2

1.0

/

/

SALTNODE  
 0.0  
 43.280 /  
 PLYROCK  
 0.16 1.5 1000.0 1 0.005 /  
  
 PLYADS  
 0.0 0.000  
 20.0 0.010  
 70.0 0.010 /  
 PLYMAX  
 10 43.280 /  
 PLMIXPAR  
 1.0 /  
 RTEMP  
 194 /  
 SPECHEAT  
 0.00 0.5 1 0.5  
 363.0 0.5 1 0.5  
 /  
 SPECROCK  
 0.00 30  
 363.0 30 /  
 0.00 30  
 363.0 30 /  
 RPTPROPS /  
 REGIONS =====  
 FIPNUM  
 18\*1 72\*2 /  
 EQLNUM  
 18\*1 72\*2 /  
 RPTREGS  
 0 0 0 0 0 /  
 SOLUTION =====

EQUIL

7020.00 2700.00 7990.00 .00000 7020.00 .00000 0 0 5 /

7200.00 3700.00 7300.00 .00000 7000.00 .00000 1 0 5 /

RSVD 2 TABLES 3 NODES IN EACH FIELD 12:00 17 AUG 83

7000.0 1.0000

7990.0 1.0000

/

7000.0 1.0000

7400.0 1.0000

/

SALTV

7000.0 43.280

10000.0 43.280 /

7000.0 43.280

10000.0 43.280 /

RPTSOL

0 /

SUMMARY =====

FOPR

FGPR

FWPR

FWIR

FOE

SOFR

'PROD' 1 /

'PROD' 4 /

'PROD' 5 /

'PROD' 6 /

/

SWCT

'PROD' 1 /

'PROD' 4 /

'PROD' 5 /

'PROD' 6 /

/

SGOR

'PROD' 1 /

'PROD' 4 /

'PROD' 5 /

'PROD' 6 /

/

SPR

'PROD' /

/

SPRDH

'PROD' 2 /

'PROD' 3 /

/

SPRDF

'PROD' /

/

SWFR

'WINJ' 1 /

'WINJ' 4 /

'WINJ' 5 /

'PROD' 9 /

'PROD' 18 /

'PROD' 10 /

/

SCFR

'PROD' 9 /

/

SCCN

'PROD' 9 /

/

SSFR

'PROD' 9 /

/  
SSCN  
'PROD' 9 /  
/  
SWCT  
'WINJ' 4 /  
/  
SGOR  
'WINJ' 4 /  
/  
SPR  
'WINJ' /  
/  
SOVIS  
'WINJ' /  
/  
SWVIS  
'WINJ' /  
/  
SEMVIS  
'WINJ' /  
/  
SGVIS  
'WINJ' /  
/  
SPRDH  
'WINJ' 2 /  
'WINJ' 3 /  
/  
SPRDF  
'WINJ' /  
/  
WCPC  
PROD /

```

WSPC
PROD /
WSIC
WINJ /
WCIC
WINJ /
RUNSUM
ALL
SEPARATE
MSUMLINS
MSUMNEWT
SCHEDULE =====
RPTRST
Basic=2 /
/
DRSDT
1.0E20 /
RPTSCHED
'PRES' 'SWAT' 'SGAS' 'RS' 'WELLS=2' 'SUMMARY=2'
'CPU=2' 'WELSPECS' 'NEWTON=2' /
NOECHO
--PRODUCTION WELL VFP TABLE 1

VFPPROD
1 7.0000E+03 'LIQ' 'WCT' 'GOR' 'thp' 'iglr' 'field' /
2.0000E+00 6.0000E+02 1.4000E+03 2.0000E+03
4.0000E+03 6.0000E+03
/
2.0000E+02 5.0000E+02 1.0000E+03
/
.0000E+00 4.0000E-01 8.0000E-01
/
1.0000E+00 2.0000E+00 4.0000E+00
/

```

.00000E+00

/

1 1 1 1 1.97594E+03 1.37517E+03 7.75232E+02 7.31301E+02  
8.63600E+02 1.07507E+03

/

2 1 1 1 2.24076E+03 2.05768E+03 2.00844E+03 1.95077E+03  
1.91803E+03 1.99808E+03

/

3 1 1 1 2.71295E+03 2.70532E+03 2.71278E+03 2.72263E+03  
2.78084E+03 2.87541E+03

/

1 2 1 1 2.34711E+03 1.96200E+03 1.80998E+03 1.63946E+03  
1.53864E+03 1.65905E+03

/

2 2 1 1 2.61779E+03 2.49181E+03 2.45750E+03 2.45608E+03  
2.49589E+03 2.53344E+03

/

3 2 1 1 3.09452E+03 3.09009E+03 3.09663E+03 3.10603E+03  
3.15875E+03 3.24354E+03

/

1 3 1 1 2.85373E+03 2.68696E+03 2.63428E+03 2.62542E+03  
2.66829E+03 2.70294E+03

/

2 3 1 1 3.14219E+03 3.09125E+03 3.08104E+03 3.08301E+03  
3.12402E+03 3.20092E+03

/

3 3 1 1 3.63367E+03 3.63377E+03 3.64044E+03 3.64886E+03  
3.69552E+03 3.76936E+03

/

1 1 2 1 1.90703E+03 4.23900E+02 4.91041E+02 5.61854E+02  
8.41860E+02 1.14254E+03

/  
2 1 2 1 2.13732E+03 1.51748E+03 1.10210E+03 1.13989E+03  
1.31168E+03 1.53169E+03

/  
3 1 2 1 2.52712E+03 2.36101E+03 2.32094E+03 2.26533E+03  
2.32880E+03 2.47300E+03

/  
1 2 2 1 2.24180E+03 1.37824E+03 7.45545E+02 7.21454E+02  
9.51216E+02 1.21802E+03

/  
2 2 2 1 2.47044E+03 2.06424E+03 1.91696E+03 1.78107E+03  
1.76738E+03 1.92943E+03

/  
3 2 2 1 2.87369E+03 2.74718E+03 2.72192E+03 2.72627E+03  
2.78577E+03 2.89035E+03

/  
1 3 2 1 2.75731E+03 2.35384E+03 2.23030E+03 2.18779E+03  
2.01332E+03 2.05525E+03

/  
2 3 2 1 3.02294E+03 2.83361E+03 2.77281E+03 2.76184E+03  
2.80340E+03 2.86235E+03

/  
3 3 2 1 3.47670E+03 3.41854E+03 3.40882E+03 3.41186E+03  
3.45913E+03 3.54604E+03

/  
1 1 3 1 1.87259E+03 3.91529E+02 5.70235E+02 7.19731E+02  
1.21992E+03 1.71171E+03

/  
2 1 3 1 2.11457E+03 8.41615E+02 9.39654E+02 1.03956E+03  
1.43521E+03 1.86682E+03

/



3 1 3 1 2.50409E+03 1.83217E+03 1.79926E+03 1.85238E+03  
 2.09347E+03 2.40294E+03  
 /  
 1 2 3 1 2.22684E+03 5.02107E+02 5.73039E+02 6.81812E+02  
 1.06856E+03 1.47815E+03  
 /  
 2 2 3 1 2.45705E+03 1.54829E+03 1.10263E+03 1.17176E+03  
 1.46382E+03 1.80211E+03  
 /  
 3 2 3 1 2.83378E+03 2.42600E+03 2.30007E+03 2.22995E+03  
 2.38437E+03 2.65017E+03  
 /  
 1 3 3 1 2.73870E+03 1.91960E+03 1.48679E+03 1.24203E+03  
 1.23967E+03 1.44955E+03  
 /  
 2 3 3 1 2.98935E+03 2.50931E+03 2.37089E+03 2.32059E+03  
 2.18865E+03 2.28214E+03  
 /  
 3 3 3 1 3.40018E+03 3.17167E+03 3.10777E+03 3.09743E+03  
 3.14591E+03 3.22270E+03  
 /

--INJECTION WELL VFP TABLE 1

VFPINJ

1 7.0000E+03 'WAT' /  
 2.00000E+00 6.00000E+02 1.40000E+03 2.00000E+03  
 4.00000E+03 6.00000E+03  
 /  
 5.00000E+02  
 /  
 1 3.49209E+03 3.48640E+03 3.46590E+03 3.44178E+03  
 3.30981E+03 3.10032E+03  
 /

--INJECTION WELL VFP TABLE 2

VFPINJ

2 6.90000E+03 'GAS' /  
1.00000E+00 3.00000E+02 7.00000E+02 1.00000E+03  
2.00000E+03 3.00000E+03

/

1.00000E+03 2.00000E+03 3.00000E+03

/

1 1.31963E+03 1.31781E+03 1.31049E+03 1.30133E+03  
1.24694E+03 1.15029E+03

/

2 2.73750E+03 2.73671E+03 2.73365E+03 2.72991E+03  
2.70847E+03 2.67303E+03

/

3 3.92693E+03 3.92631E+03 3.92396E+03 3.92110E+03  
3.90493E+03 3.87853E+03

/

ECHO

WELSPECS

'PROD' 'G' 1 1 7030 'OIL' /

'WINJ' 'G' 9 1 7030 'WATER' /

/

COMPDAT

'PROD' 1 1 2 2 3\* 0.2 3\* 'X' /

'PROD' 2 1 2 2 3\* 0.2 3\* 'X' /

'PROD' 3 1 2 2 3\* 0.2 3\* 'X' /

'PROD' 4 1 2 2 3\* 0.2 3\* 'X' /

'PROD' 5 1 2 2 3\* 0.2 3\* 'X' /

'PROD' 1 1 5 5 3\* 0.2 3\* 'X' /

'PROD' 2 1 5 5 3\* 0.2 3\* 'X' /

'PROD' 3 1 5 5 3\* 0.2 3\* 'X' /

'PROD' 4 1 5 5 3\* 0.2 3\* 'X' /

'PROD' 5 1 5 5 3\* 0.2 3\* 'X' /

'PROD' 1 1 8 8 3\* 0.2 3\* 'X' /  
 'PROD' 2 1 8 8 3\* 0.2 3\* 'X' /  
 'PROD' 3 1 8 8 3\* 0.2 3\* 'X' /  
 'PROD' 4 1 8 8 3\* 0.2 3\* 'X' /  
 'PROD' 5 1 8 8 3\* 0.2 3\* 'X' /

'WINJ' 9 1 2 2 3\* 0.2 3\* 'X' /  
 'WINJ' 8 1 2 2 3\* 0.2 3\* 'X' /

'WINJ' 9 1 10 10 3\* 0.2 3\* 'X' /  
 'WINJ' 8 1 10 10 3\* 0.2 3\* 'X' /  
 'WINJ' 7 1 10 10 3\* 0.2 3\* 'X' /  
 'WINJ' 6 1 10 10 3\* 0.2 3\* 'X' /  
 'WINJ' 5 1 10 10 3\* 0.2 3\* 'X' /  
 'WINJ' 4 1 10 10 3\* 0.2 3\* 'X' /

/

WELSEGS

-- Name Dep 1 Tlen 1 Vol 1

'PROD' 7010 10 0.31 'INC' HFA /

-- First Last Branch Outlet Length Depth Diam Ruff Area Vol

-- Seg Seg Num Seg Chang

-- Main Stem

2 12 1 1 20 20 0.2 1.E-3 1\* 1\* /

-- Top Branch

13 13 2 2 50 0 0.2 1.E-3 1\* 1\* /

14 17 2 13 100 0 0.2 1.E-3 1\* 1\* /

-- Middle Branch

18 18 3 9 50 0 0.2 1.E-3 1\* 1\* /

19 22 3 18 100 0 0.2 1.E-3 1\* 1\* /

-- Bottom Branch

23 23 4 12 50 0 0.2 1.E-3 1\* 1\* /

```

24 27 4 23 100 0 0.2 1.E-3 1* 1* /
/
COMPSEGS
-- Name
'PROD' /
-- I J K Brn Start End Dirn End
-- No Length Length Penet Range
-- Top Branch
1 1 2 2 30 1* 'X' 5 /
-- Middle Branch
1 1 5 3 170 1* 'X' 5 /
-- Bottom Branch
1 1 8 4 230 1* 'X' 5 /
/
WELSEGS
-- Name Dep 1 Tlen 1 Vol 1
'WINJ' 7010 10 0.31 'INC' /

-- First Last Branch Outlet Length Depth Diam Ruff Area Vol
-- Seg Seg Num Seg Chang
-- Main Stem
2 14 1 1 20 20 0.2 1.E-3 1* 1* /
-- Top Branch
15 15 2 2 50 0 0.2 1.E-3 1* 1* /
16 16 2 15 100 0 0.2 1.E-3 1* 1* /
-- Bottom Branch
17 17 3 14 50 0 0.2 1.E-3 1* 1* /
18 22 3 17 100 0 0.2 1.E-3 1* 1* /
/
COMPSEGS
-- Name
'WINJ' /
-- I J K Brn Start End Dirn End
-- No Length Length Penet Range

```

-- Top Branch

9 1 2 2 30 1\* 'X' 8 /

-- Bottom Branch

9 1 10 3 270 1\* 'X' 4 /

/

WEFAC

'\*' 0.68 /

/

WCONPROD

'PROD' 'OPEN' 'LRAT' 3\* 6000 1\* 1000 0.0 1 /

/

WCONINJE

'WINJ' 'WAT' 'OPEN' 'RESV' 1\* 2000 3500 1\* 1 /

/

WPIMULT

PROD 8 /

PROD 3 1\* 1\* 5 /

PROD 1.5 1\* 1\* 1\* 7 7 /

/

WVFPEXP

'\*' 'EXP' /

/

WPOLYMER

WINJ 10.0 43.280 /

/

WTEMP

WINJ 194 /

/

WRFTPLT

PROD REPT REPT REPT /

WINJ REPT REPT REPT /

/

TUNING

/  
/  
4\* 16 /  
TSTEP  
2 18 220  
/  
WELTARG  
'PROD' 'THP' 600 /  
'PROD' 'LRAT' 10000 /  
'WINJ' 'RESV' 5000 /  
'WINJ' 'THP' 500 /  
'WINJ' 'BHP' 4000 /  
/  
WPOLYMER  
WINJ 10.0 43.280 /  
/  
TSTEP  
280 /  
END